Identifying metabolic biomarkers of physiological adaptation to change in physical activity and age

Isabelle Jane Alldritt

Thesis submitted to the University of Nottingham for the degree of

Doctor of Philosophy

Abstract

Skeletal muscle is a significant contributor to maintaining health at a whole-body level. Loss of skeletal muscle mass and strength is associated with reduced reports of quality of life, increased mortality and morbidity rates, and increased healthcare spending. As traditional approaches have so far failed to identify effective interventions to treat or prevent loss of muscle mass and strength and key mechanisms in the development of muscle wasting remain unknown, this thesis adopts an untargeted metabolomics approach to examine the plasma metabolomic profile of volunteers in four studies associated with maintenance or loss of skeletal muscle health. Throughout this thesis an integrative approach combining metabolomics data with outcome measures that demonstrate adaptation at the whole-body level has been adopted to provide relevant physiological context for observed changes in the plasma metabolome.

In Chapter 3, untargeted metabolomics was used to assess the effect of sedentary behaviour induced by chronic bed rest on the plasma metabolome in healthy young men maintained in energy balance. Metabolites present at a significantly different plasma abundance relative to baseline following bed rest were linked to networks reflective of altered fat and carbohydrate utilisation, paralleling work which shows chronic bed rest blunts both the insulin mediated increase in carbohydrate oxidation and the suppression of fat oxidation. Correlation analysis found change in the plasma metabolome was most highly associated with rate of insulin mediated fat oxidation and glucose disposal following bed rest.

In Chapter 4, the plasma metabolome was compared between three age groups before and after 20 weeks of resistance exercise training. Plasma metabolites characteristic of age prior to training showed a high degree of similarity to the muscle metabolome at the same timepoint. However, the abundance plasma metabolites

characteristic of age at baseline were found to be unchanged by resistance exercise training in all ages. In addition, within group analysis found that no plasma metabolites were present at a significantly different abundance relative to baseline after resistance exercise training regardless of age.

In Chapter 5, the impact of aerobic exercise training and subsequent exercise withdrawal on the plasma metabolome in healthy young volunteers was assessed. Aerobic exercise was associated with a shift in lipid profile that can be linked to mitochondrial lipid oxidation. These results are in line with previous work reporting an increase in mitochondrial ATP production rates in response to palmitate. Associations were also found between lipid oxidation with respiratory exchange ratio and maximal oxygen uptake, providing further evidence to support mitochondrial adaptations in response to aerobic exercise training.

Finally, in Chapter 6 the impact of aerobic exercise and subsequent exercise withdrawal on the plasma metabolome in healthy older individuals and age matched COPD patients was assessed. Although there was an observable response to exercise in the healthy controls, no differences in the abundance of any plasma metabolites were found in COPD following 8 weeks of training. This parallels previous work demonstrating a lack of adaptation in respiratory exchange ratio, maximal oxygen uptake and mitochondrial ATP production in COPD patients. In the healthy control group, correlation analysis supported a link between lipid oxidation mechanisms and physiological adaptations to aerobic exercise training, suggesting mitochondrial adaptations are common between healthy young and older individuals in response to aerobic training.

Declaration

Plasma for experiments in this thesis was provided from several studies completed before I began my research. The contribution of others to the data presented is as follows:

Plasma samples for the study of chronic bed rest in Chapter 3 were collected at the Institute of Space Medicine and Physiology in Toulouse. Clinical measures of anthropometry and metabolism were provided by Dr Natalie Shur at the University of Nottingham. Data acquisition using mass spectrometry was conducted at the Phenome Centre, University of Birmingham. Plasma samples for the study of resistance exercise in older adults in Chapter 4 was provided from a previous study completed at the University of Nottingham by Professor Beth Phillips. The MATCH study which provided plasma for Chapter 5 and Chapter 6 was completed at the University of Leicester by Dr Lorna Latimer. Physiological measures of peak oxygen uptake and exercise steady-state respiratory exchange ratio were collected and provided by Dr Lorna Latimer. Supplemental plasma samples for Chapter 6 were provided from an inhouse biobank at the University of Nottingham and were originally collected by Dr Matthew Brook.

All data analysis and interpretation are entirely my own work. I confirm that this work was completed during the period of my registration and has not been submitted, in whole or in part, in any previous application for a degree.

Elements of this thesis have been published as a peer-reviewed paper:

Introduction

Alldritt, I., Greenhaff, P.L., Wilkinson, D.J., 2021. Metabolomics as an Important Tool for Determining the Mechanisms of Human Skeletal Muscle Deconditioning. Int. J. Mol. Sci, 22(24)

Acknowledgements

I would first like to thank my supervisors Dr Daniel Wilkinson and Professor Paul Greenhaff for giving me the opportunity to conduct this research and for their advice and guidance throughout.

I would also like to thank the members of the COMAP group at Derby, particularly those in the PhD office, for their support and assistance. I'll miss our lunch clubs.

Thanks to April, Ed, Eleanor, Emily, Lauren, and Lucy for keeping me sane on a (semi) weekly basis. Thanks to Jenny for being you. Without you all this thesis would never have been written and I'm incredibly thankful to have you in my life.

Finally, a massive thank you to my family. Tom and Shiki, thank you for the encouragement from near and far. Lynne, you're the cutest good luck charm in the world. Mum and Dad, thank you for everything. I will be eternally grateful for all the support you've given me.

Table of Contents

List of Figures

List of Tables

List of Abbreviations

Nuclear magnetic resonance	NMR
Mass spectrometry	MS
Matrix assisted laser desorption/ionisation	MALDI
Resonance ionisation	RIMS
Atmospheric pressure chemical ionisation	APCI
Gas chromatography	GC
Liquid chromatography	LC
Reverse phase	RP
Hydrophilic interaction chromatography	HILIC
Limit of detection	LOD
k-Nearest neighbours	kNN
Random forest	RF
Coefficient of variation	CV
Quality control	QC
Food and Drug Administration	FDA
Locally estimated scatterplot smoothing	LOESS
Probabilistic quotient normalisation	PQN
Variance stabilisation normalisation	VSN
Principal component analysis	PCA
Partial least squares discriminant analysis	PLS-DA
Principal component	PC
Sparse PLS-DA	sPLS-DA
Human Metabolome Database	HMDB
Kyoto Encyclopedia of Genes and Genomes	KEGG
Metabolite set enrichment analysis	MSEA
Peak oxygen uptake	VO2PEAK
Intramyocellular lipid	IMCL
European Working Group on Sarcopenia in Older People	EWGSOP
Asian Working Group for Sarcopenia	AWGS
International Working Group for Sarcopenia	IWGS
Cross sectional area	CSA
Branched chain amino acid	BCAA
Essential amino acid	EAA
Muscle protein synthesis	MPS
Muscle protein breakdown	MPB
Lysophosphatidylcholine	LPC
Tricarboxylic acid	TCA
Methanol	MeOH
Double distilled water	ddH2O
Chloroform	CHCl3
Methyl tert-butyl ether	MTBE
Isopropanol	IPA
Acetonitrile	MeCN
Robust spline correction	RSC
Generalised logarithm	glog

Resting energy expenditure	REE
Physical activity level	PAL
Dual energy X-ray absorptiometry	DEXA
Glucose disposal	GD
Non-esterified fatty acid	NEFA
Lean body mass	LBM
Variable importance in projection	VIP
Weighted correlation network analysis	WGCNA
Over representation analysis	ORA
Phosphatidylethanolamine	PE
Phosphatidylcholine	PC
Phosphatidylserine	PS
Superoxide dismutase 2	SOD2
Sarco/endoplasmic reticulum Ca2+ ATPase	SERCA
Extracellular matrix	ECM
Myostatin	MSTN
Resistance exercise training	RET
Mammalian target of rapamycin	mTOR
Repetition maximum	RM
Maximal voluntary contraction	MVC
Vastus Lateralis	VL
Homeostasis model of insulin resistance	HOMA-IR
Fractional synthetic rate	FSR
False discovery rate	FDR
Dehydroepiandrosterone	DHEA
13-L-hydroperoxylinoleic acid	13(S)-HPODE
Nicotinamide adenine dinucleotide	NAD+
Nicotinamide D-ribonucleotide	NMN
Aerobic exercise training	AET
Respiratory exchange ratio	RER
Chronic obstructive pulmonary disease	COPD
Cardiopulmonary exercise test	CPET
Healthy older	HO
Healthy younger	HY

Chapter 1. Introduction

1.1. OMICs approaches to the study of health, ageing and disease research

The use of OMICs in the study of health, ageing and disease has expanded rapidly in recent years (Borges et al., 2020). OMICs refers to technologies aimed at the detection of the complete complement of DNA, RNA, proteins/phosphoproteins and/or metabolites within a biological system/tissue or sample (Hasin et al., 2017). In contrast to beginning with a pre-determined hypothesis, as is common to many research problems, OMICs experiments adopt a holistic approach by focusing on understanding a complex biological system of cells, tissues and organs by looking at it as a whole and exploring the roles and relationships between molecules within that system (Hasin et al., 2017). OMICs experiments are often high-throughput and generate very large datasets with the premise being that if as much as possible is measured within a single system this may help highlight, through associations based on statistical interference, previously unknown biological factors important in the development of disease states or physiological phenotypes that can be used to define hypotheses which can be tested further (Kell and Oliver, 2004). A number of different OMICs techniques currently exist with the most commonly used being genomics, transcriptomics, proteomics, and metabolomics. Each provide a different level of information about the system under investigation and interact with each other to provide information predisposing a particular phenotype. An overview of the OMICs cascade is provided in Figure 1.1.

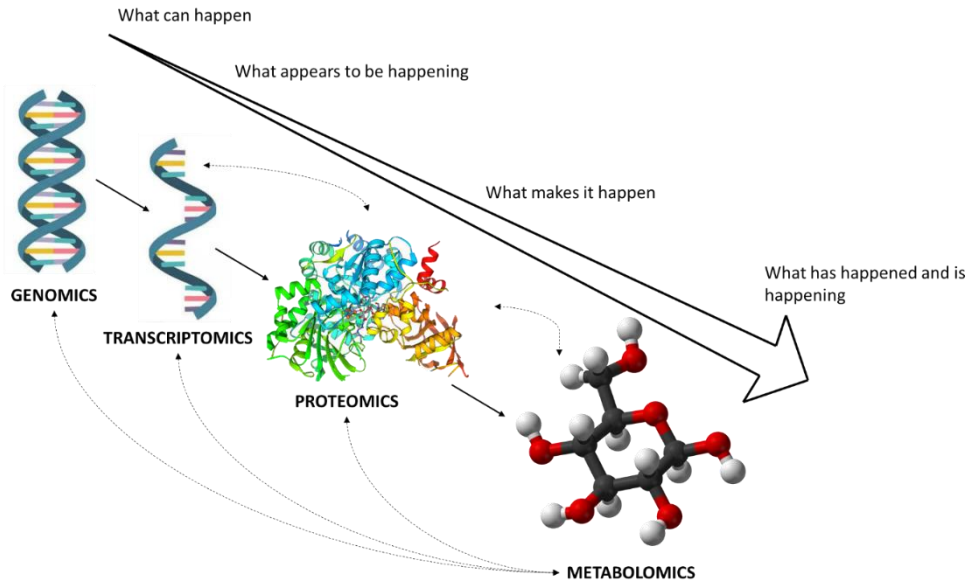

Figure 1.1 Overview of the omics cascade

Biological systems can be studied using different omics approaches which each interact with each other. Genes are transcribed to mRNA transcripts, which can be translated to proteins or themselves regulate expression of other genes. Metabolites are produced as substrates in protein-mediated reactions and can themselves act as signalling molecules for proteins in cellular events. Perturbations to the genome, transcriptome and proteome are reflected in the downstream metabolome. Unlike genomics, transcriptomics and proteomics, which predict how changes in their respective omes can affect what happens at a phenotypic level, metabolomics provides a direct chemical link between genotype and phenotype.

1.1.1. Genomics, proteomics and transcriptomics

The first OMICS technique to be developed was genomics, the study of an organism's complete set of genetic information, which emerged in the 1990s as a result of the Human Genome Project and has since been commonly used in the study of relationships between genes and protein functions as well as to identify variations within the gene loci (Horgan and Kenny, 2011). Thousands of genomic variations have been associated with diseases and some have gone on to have translational benefits, for instance the identification of a t(9;22) translocation in chronic myeloid leukaemia by genomics enabled the therapeutic use of a BCR-ABL tyrosine kinase inhibitor that improved prognosis (Druker et al., 2001) and 5 year survival rate (Jain et al., 2017) in

leukaemia patients. However there are some limitations to genomics. Firstly, genome wide studies can identify the same genetic variants which contribute to different final outcomes depending on environmental factors (for example the differences in prevalence of Parkinson's disease (Tanner et al., 1999), multiple sclerosis (Baranzini et al., 2010) or asthma (Sarafino and Goldfedder, 1995) in genetically identical twins) and, although many variants have been identified, associations with disease are often weak (Johnson and Donnell, 2009). To account for multiple test correction genome wide studies must adopt a level of significance of approximately $7.2x10^{-8}$ (Dudbridge and Gusnanto, 2008) therefore for a genomics experiment to be appropriately powered very large sample sizes are often required. For complex phenotypes with multiple identified loci variations that must all be accounted for, such as those associated with health, ageing, disease and the loss of muscle mass, this can be prohibitively expensive and difficult to accomplish (Visscher et al., 2012).

Transcriptomics, the study of the total RNA content of a cell, is most often used to measure the active expression of gene transcripts but can also measure the expression of non-coding RNAs that do not translate to active genes but instead control DNA expression (de Goede et al., 2021). Transcriptomics approaches have been successful in finding prognostic and diagnostic markers of breast cancer which have been successfully translated with clinical benefit (Aarøe et al., 2010). However a major limitation of transcriptomics is that mRNA transcripts are not necessarily directly proportional to protein level. High expression of some mRNA transcripts is not correlated with subsequent protein expression while relatively small changes in the expression level of others result in large changes of the total amount of corresponding protein (Schwanhäusser et al., 2011) therefore important changes in RNA expression may be missed in transcriptomics experiments as they may not reached the statistical cut-offs required in large data sets and as a result transcriptomics can provide non-

representative data. The benefit of transcriptomics in early intervention for cancer patients is established but potential markers for other diseases such as potential miRNA diagnostic markers of Alzheimer's disease (Keller et al., 2014) or Parkinson's disease (Youdim et al., 2007) have yet to reach the clinic. Additionally, as with genomics, sample size and reproducibility is an important factor in transcriptomics to overcome underpowered studies (Button et al., 2013).

Finally, proteomics is the study of the full complement of proteins in a cell, tissue, or organism. Proteomics can also be used to characterise protein pathways and networks to understand their functional relevance. Proteomics is also a popular technique in biomarker research as proteins are likely to be affected by disease. For example, proteomics approaches enabled the development of a diagnostic kit for use in detecting soluble CD19 present in cerebrospinal fluid as a biomarker of lymphomas (Muniz et al., 2014). Proteomics has also been applied in musculoskeletal research in an attempt to identify molecular mechanisms of muscle mass loss in sarcopenia and cachexia however a robust protein signature of muscle mass loss has not yet been identified (Ibebunjo et al., 2013; Ebhardt et al., 2017; Ubaida-Mohien et al., 2019). Furthermore, while a number of candidate biomarkers for other diseases, such as cancer (Kwon et al., 2021), have been identified in clinical studies many have not yet reached clinical translation (Diamandis, 2012) and, as in transcriptomics, there is no simple relationship between protein expression and functional changes (Yu et al., 2017).

1.1.2. Metabolomics

While genomics, transcriptomics and proteomics can be very powerful techniques that have enabled significant advances in the field of biomedical science, data gathered from such experiments only represent alterations that predispose an organism's phenotype so findings do not always correlate directly with the phenotype or any

changes to this phenotype in response to intervention or perturbation by disease (Horgan and Kenny, 2011; Hasin et al., 2017). For example, one pleiotropic gene can impact on multiple proteins to affect more than one phenotypic trait. A specific example can be found when looking at mutations in the *Mc1r* gene locus, which can influence rates of melanoma (Shuyang Chen et al., 2019) due to the role of MC1R in controlling skin pigmentation but are also associated with sepsis (Seaton et al., 2017) and rates of developing cancer unrelated to skin pigmentation (Feller et al., 2016).

Metabolomics is a comparatively new field, first described in 1998 as an approach to measure the "change in the relative concentrations of metabolites as the result of the deletion or overexpression of a gene" (Oliver et al., 1998), that studies the metabolome, the full complement of small molecules (usually less than 1500 Da) present in a cell that represent the key intermediaries and/or endpoints in all metabolic reactions, and that are required for the normal growth, maintenance and function of a cell (Fiehn, 2002; Færgestad et al., 2009). Changes in this "metabolome" are directly responsive to stimuli (such as intracellular signalling triggered by disease (Mavers et al., 2009) reflecting the current status of an organism and, most importantly, any perturbations to the upstream genome, transcriptome or proteome should be reflected through concomitant changes in the downstream metabolome making it a vital and strong link between genotype and phenotype (Bujak et al., 2015). The metabolome in theory should carry an imprint of all genetic, epigenetic and environmental factors impacting on a system and as a consequence the majority of biological and medical perturbations can be expected to be visible in the metabolome making metabolites the ideal biomarkers of disease mechanisms and development.

A key principle in metabolomics is that certain diseases or conditions that impact phenotypic change have effects on normal physiological processes within a system

which translate to visible differences in the metabolome of individuals with and without this condition or change. Untargeted metabolomics analyses the full set of measurable metabolic features within a sample, including uncharacterised metabolites, in an unbiased way allowing for the identification of consistent relative differences in groups of metabolites between individuals with or without a particular condition or phenotypic change (Schrimpe-Rutledge et al., 2016). These changes act as biomarkers, allowing the stratification of individuals into groups based on their metabolic profile, and can be used to infer prognostic or diagnostic markers of disease, the mechanism of disease progression and identify possible therapeutic targets by studying alterations in metabolic pathways and the molecular or cellular functions regulating them (Zhang et al., 2017). Metabolomics therefore has the ability to detect changes before they are measurable within the phenotype. This is particularly important in helping to understand non-communicable diseases with complex pathologies.

The use of untargeted metabolomics in the clinical study of complex diseases has been growing over the past 20 years (Tolstikov et al., 2020). For example, reduced levels of dehydroascorbic acid and increased levels of fructose, mannose and threonic acid in cerebrospinal fluid were indicative of early-stage Parkinson's disease (Trezzi et al., 2017). Ten plasma phospholipids predicted preclinical Alzheimer's disease in cognitively normal individuals with a 90% degree of accuracy (Mapstone et al., 2014). Differences in plasma metabolite abundance in ALS patients compared to controls were used to identify novel pathways which were highly correlated with known ALS pathology (Goutman et al., 2020). Finally, a panel of 31 urinary metabolite biomarkers suggestive of abnormal amino acid and pentose phosphate metabolism pathways were closely associated with nonalcoholic fatty liver disease (Dong et al., 2017). However none of these potential markers have been translated for clinical application.

The number of features able to be measured by metabolomics techniques is key to the strength of this approach. Current metabolomics techniques are able to detect tens of thousands of metabolites in human studies (Patti et al., 2012), comparable to high-throughput proteomics (Low et al., 2013) or whole-transcriptome panels (Moses and Pachter, 2022). While number of features are comparable between omics approaches, transcript expression does not necessarily equal functional changes, as discussed above, and therefore may be relaying information not directly related to the biological question at hand. By measuring large numbers of metabolites per sample, a greater sensitivity to identify clear signatures is achieved which allows biological insights into changes underlying complex conditions as, unlike mRNA transcripts or proteins, differences relative metabolite concentrations must complement each other (Lu et al., 2017) and therefore provide direct information about changes within each impacted pathway.

In contrast to the hypothesis generating approach of untargeted metabolomics there is an alternative and complimentary approach called targeted metabolomics which involves verification and validation of pre-defined metabolites or metabolite groups across samples provided through hypotheses generated using prior knowledge of conditions or previous untargeted experiments. While untargeted metabolomics studies relative changes within samples, targeted metabolomics provides a more precise and quantitative approach often involving semi-quantitative or quantitative measures of absolute concentrations of the defined groups of metabolites (Roberts et al., 2012). By its nature targeted metabolomics limits the coverage of the metabolome to a few known groups which in turn limits the discovery of novel metabolic responses, however it may reveal new associations between the defined metabolites (Lewis et al., 2010). As such, targeted analysis is well suited to hypothesis testing studies and can be used to validate the results of untargeted works and help with translation to

clinical application. Examples of this are evident from the as early as the late 90's, where conditions such as inborn errors of metabolism, disorders of fatty acid oxidation or phenylketonuria have been routinely screened for at birth using targeted tandem mass spectrometry (Wiley et al., 1999). This demonstrates the potential for application in clinical use of other metabolic biomarkers once investigations have progressed to the validation stage.

1.1.3. The metabolomic workflow for untargeted analysis

1.1.3.1. Experimental design

Metabolomics experiments generally have one of three desired outcomes: to identify clinically relevant diagnostic or prognostic markers (biomarker discovery); to uncover disease mechanism (pathogenesis studies); or to map associations between the metabolome and environmental factors, such as lifestyle (association studies) (Dunn et al., 2012). Regardless of intended outcome, careful experimental design is required to ensure that only biologically relevant variation is measured and confounding factors are accounted for in the analysis process. This involves the collection of metadata such as data related to physiology of the participants (for example, their age, gender, or BMI).

1.1.3.2. Sample collection and preparation

Having posed the research question and designed the study, the next consideration in the metabolomics pipeline is sample collection. Metabolomics can be used on a range of samples including biofluids (e.g. serum, plasma, urine or saliva), cells or tissues. With the exception of urine, which is considered to be metabolically inactive (Chetwynd et al., 2017) these sample types are considered to be metabolically active (i.e. metabolism is continuing within the sample even after collection). Samples must be quenched and stored immediately as metabolites are not stable at higher

temperatures (for example, plasma and serum concentrations of lysophospholipids underwent significant changes during storage at 4°C (Yang et al., 2013)).

The collection of blood samples is further complicated by clotting. For serum collection, blood is allowed to be clotted before serum is removed however time and temperature of clotting can influence the serum metabolic profile. Extending clotting time was associated with a 9.08% increase in median absolute percent difference in level of metabolites (McClain et al., 2020) and pattern recognition showed clear differences in metabolic profile from serum clotted and room temperature and on ice from the same volunteers (Teahan et al., 2006). The collection of plasma does not involve a clotting process however the type of anticoagulant in blood tubes to prevent clotting can also have an impact on metabolic profile. For example, lipids were generally higher in abundance in tubes coated in EDTA than CPT and hierarchical clustering analysis showed clear differences in metabolic profile of plasma samples collected at the same time from the same donor depending on type of anticoagulant (Khadka et al., 2019). Blood tubes used in sample collection and clotting time and temperature must therefore be consistent across all samples.

Other factors to consider include nutrition and time of sample collection. Nutrition can provide signals which perturb the metabolome. For instance high and low fat diets have differential effects on abundance of amino acids and nucleotides in the liver and serum regardless of sample collection time (Abbondante et al., 2016). Therefore fasting samples are often collected in metabolomics studies to remove the potential effect of dietary habits when studying how metabolism differs between populations of interest (Chetwynd et al., 2017). Metabolite expression is also regulated by the diurnal cycle. 15% of identified metabolites in saliva and plasma were found to be under circadian rhythm (Dallmann et al., 2012). Time of sample collection should

therefore be homogenous between individuals and across collection days to reduce variability (Smith et al., 2020).

Having preserved as much true metabolic variation as possible at the same collection stage, the optimal method of sample preparation must simplify the processing stage as much as possible to avoid introducing error while also extracting the greatest number of metabolites representing the sample's phenotype possible without inducing degradation or contamination (Y. Chen et al., 2016). There is no universally accepted method of metabolite extraction therefore when designing a study the selected sample preparation method must be well documented to ensure consistency across all batches and to ensure the focus of the experimental outcomes are achieved. As with sample collection, this is particularly important in large scale studies where sample preparation may take place at multiple research sites as inaccuracies in processing and storage of samples may impact on the metabolic profile and prevent the identification of true metabolic variation (Smith et al., 2020).

1.1.3.3. Data acquisition

In metabolomics experiments metabolites are typically detected in samples though the use of either one or both of nuclear magnetic resonance (NMR) spectroscopy or mass spectrometry (MS) (Cambiaghi et al., 2017). NMR spectroscopy is a highly reproducible platform often used in metabolomic fingerprinting studies. Metabolites generate their own specific signal, referred to as resonance. Resonance of any particular proton is influenced by its chemical environment, and therefore the resonance obtained can be related to the relative position of chemical groups within the structure of the metabolite, and intensity is proportional to the number of nuclei under observation generating that specific resonance, and therefore to the molar concentration of the metabolite (Deidda et al., 2015; Tognarelli et al., 2015).

NMR is a non-destructive technique that can provide in-depth structural information and concentration of metabolites without the need for extensive sample preparation (Liu and Locasale, 2017) however NMR has a low sensitivity, typically only reaching around 100 μM (Lee et al., 2014). In contrast MS is a destructive method of acquisition that requires several stages of sample preparation and is not able to be used quantitatively in untargeted studies (Liu and Locasale, 2017) but enables the detection of metabolites at concentrations as low as the femtomolar range (Tsedilin et al., 2015). A single proton NMR spectrum can quantify up to approximately 200 metabolites while high resolution MS is capable of detecting tens of thousands of metabolites within a single sample (Ganna et al., 2016). NMR has a limited dynamic range, the ratio between maximum and minimum measurable values above background noise (Hung et al., 2013), spanning only two orders of magnitude (Suiter et al., 2014) while MS has an improved dynamic range of approximately 1:5000 in modern instruments (Kaufmann and Walker, 2016). Thus, while it is able to provide structural information about metabolites without extensive sample processing, the low sensitivity, resolution and dynamic range of NMR in comparison to MS limit the applicability of NMR in many metabolomics studies (Liu and Locasale, 2017). For these reasons the use of MS as a method of acquisition in metabolomics is more popular than NMR, with 16,207 non-review articles (per Web of Science) relating to the use of MS in metabolomics compared to 6,428 non-review articles for NMR.

MS converts analytes to an ionised state then detects molecules present in a sample by using their mass-to-charge (m/z) ratio such that each peak in the resulting chromatogram is associated with the mass spectrum of a specific metabolite, allowing its identification (Pitt, 2009) (Figure 1.2). While there are several examples of ionisation techniques in mass spectrometry including matrix-assisted laser desorption/ionisation (MALDI), resonance ionisation (RIMS) or atmospheric pressure

chemical ionisation (APCI) (Munson, 2006), one of the most popular methods in metabolomics experiments is electrospray ionisation which will be discussed here in more detail. First, the sample of interest is nebulised at the tip of a metal capillary which is receiving an electric charge typically between 3 and 5 kV (Kebarle, 2000) to create a spray of charged droplets in the ion source. Dry nitrogen is used as a flow of sheath gas around the capillary to improve nebulisation. In addition, the dry nitrogen facilitates the movement of droplets from the capillary into the mass spectrometer and, alongside the application of heat at temperatures of approximately 100-300°C (Banerjee and Mazumdar, 2012), causes the droplets to rapidly evaporate. As the droplets evaporate the charge on the outside is transferred to the analyte inside leaving the analyte ionised. Therefore, only charged analytes enter the mass analyser (Banerjee and Mazumdar, 2012).

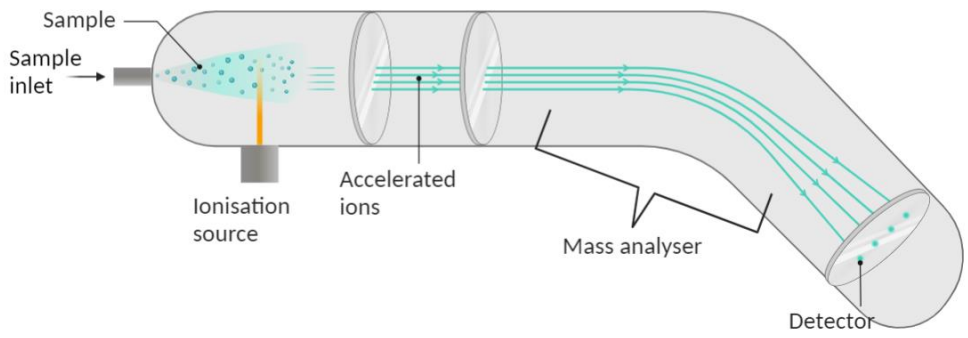

Figure 1.2 Schematic overview of the mass spectrometer

Samples enter the mass spectrometer via the sample inlet, after which they are converted into charged ions in the ionisation source. Ions are accelerated and propelled into the mass analyser, which separates ions based on their unique mass-to-charge (m/z) ratios. Finally, ions reach the detector which generates a signal for each ion, displayed as peaks on a chromatogram. Each peak represents a unique m/z ratio and retention time value.

In the mass analyser ions are separated using their unique m/z ratios. There are many types of mass analysers which each work slightly differently, including time of flight, ion trap or electrostatic sector analysers (de Hoffmann and Stroobant, 2001) but the orbitrap analyser is most relevant to this thesis and will be discussed in more detail. An orbitrap analyser typically has a working resolution of up to 1,000,000 (Eliuk and Makarov, 2015), higher than time of flight analysers which often operate at a resolution of around 60,000 (van der Heeft et al., 2009) or ion trap analysers which have a resolving power of 240,000 (Michalski et al., 2012), meaning there is a better separation of metabolite peaks with an orbitrap compared to alternative mass analysers. An orbitrap consists of 3 outer electrodes and 1 central electrode between which a voltage is applied. Ions are injected into the volume between the central and outer electrodes. The electric field created by the voltage between the electrodes combined with the tangential velocity of the ion keep the ion spiralling inside the orbitrap (Zubarev and Makarov, 2013). The specialised shape of the electrodes creates an axial electric field which pushes the ion towards the widest part of the orbitrap, where the outer electrodes are used as detector plates (Figure 1.3).

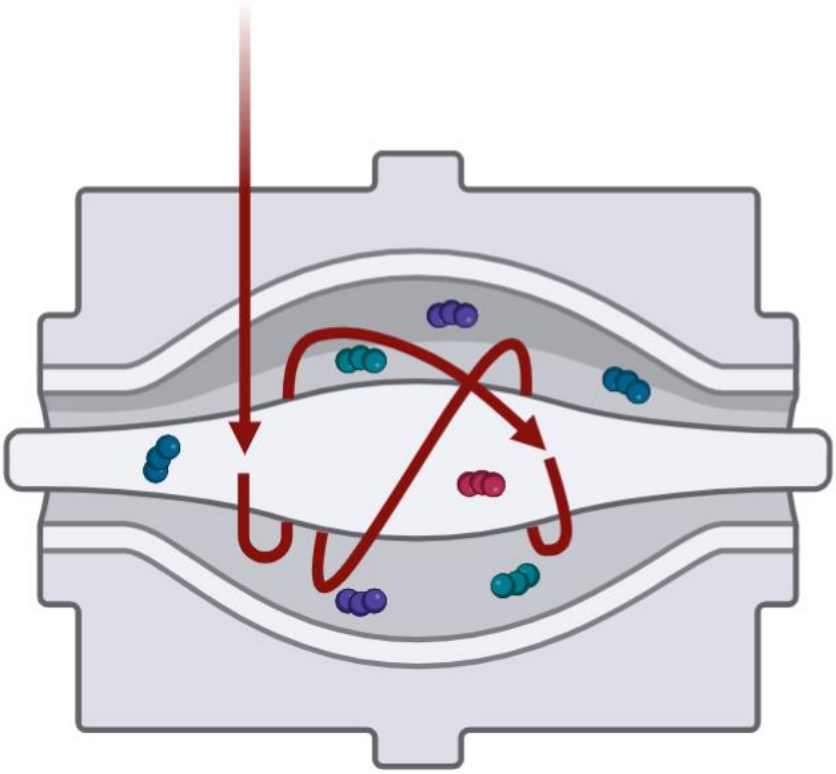

Figure 1.3 Illustrative example of orbitrap mass analyser used to separate ions by their m/z values

Three outer and one central electrode form a unique shape in the mass analyser to generate an axial electric field which pushes ions towards the widest part of the orbitrap where the three outer electrodes are used as detectors. Ions are injected in the space between the central and outer electrodes of the mass analyser. The electric field generated by the electrodes and the existing velocity of the ions cause ions to spiral inside the orbitrap. Image available at: https://biorender.com/

A signal is generated when each ion reaches the detector and is passed to a computer where it is registered as a peak on a chromatogram. Every detectable analyte in the sample will create their own unique peak associated with their unique mass spectrum allowing for metabolite identification. To further improve resolution an orbitrap analyser can be combined with a quadrupole mass filter (Michalski et al., 2011). In a quadrupole mass filter, 4 rods are held parallel to each other and ions travel down the quadrupole between the rods. A radio frequency voltage with a DC offset voltage is applied between one opposing rod pair and the other. For a given ratio of radio

frequency to DC offset voltage, certain ions will have stable trajectories based on their m/z values. Only these ions will reach the detector while others will have unstable trajectories and collide with the rods (Figure 1.4). This principle allows for the monitoring of ions based on their m/z value by varying the voltage ratio (de Hoffmann and Stroobant, 2001). A quadrupole orbitrap mass spectrometer (Figure 1.5) uses the quadrupole mass filter for the selection of ions in a defined m/z range (though this can be wide for untargeted studies) and only those ions are transferred on for orbitrap analysis (Michalski et al., 2011). This combined approach in the mass analyser is termed tandem mass spectrometry and reduces the complexity of the sample and the likelihood of matrix effects, where a co-eluting compound can suppress the signal from an analyte of interest (Panuwet et al., 2016), which can be a limitation on MS sensitivity.

To further reduce the likelihood of ion suppression, MS is commonly coupled to a chromatographic separation system (Cambiaghi et al., 2017). Chromatographic separation minimises signal suppression and provides a retention time identifier to further aid metabolite identification (Johnson et al., 2016). The most commonly employed methods for separation in metabolomics are gas chromatography (GC) and liquid chromatography (LC).

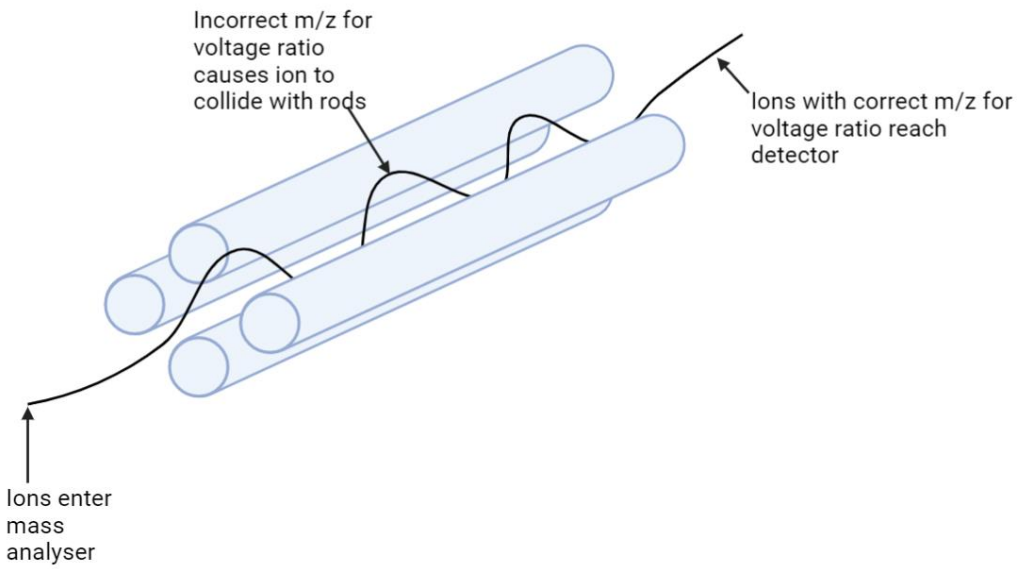

Figure 1.4 Illustrative example of the quadrupole mass analyser used to separate ions by their m/z values

Four rods are held parallel to each other and a radio frequency voltage with a DC offset voltage is applied between each opposing rod pair. Ions are injected into the space between the rods. The trajectory of the ions is determined by their m/z value and the ratio of the voltages. Only certain m/z values will allow ions to have a stable trajectory and reach the detector, while ions with other m/z values will have unstable trajectories and collide with the rods.

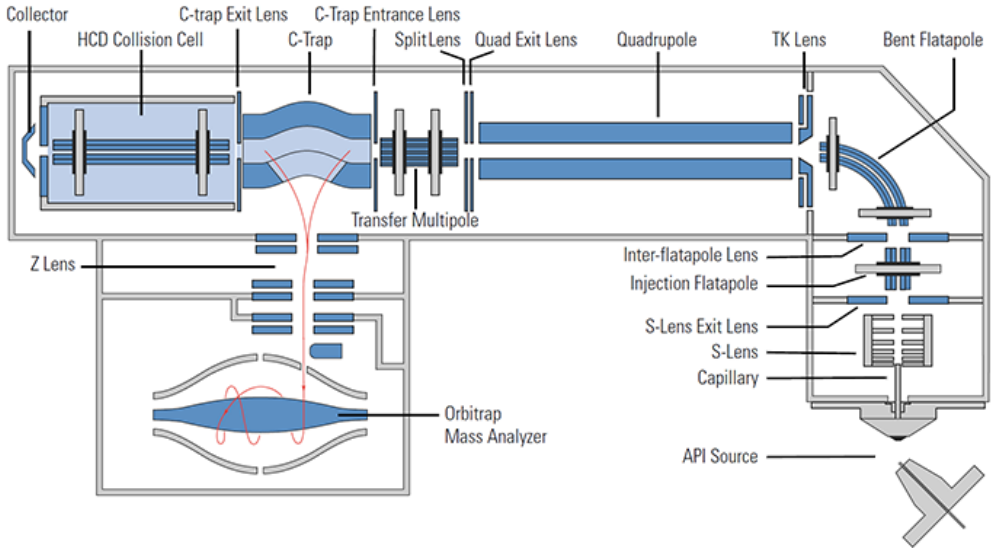

Figure 1.5 Schematic of quadrupole orbitrap mass spectrometer

Schematic of the Q-Exactive mass spectrometer produced by Thermo Fisher Scientific, a benchtop quadrupole orbitrap which can improve resolution of acquired data. The quadrupole mass filter is used to select ions in a defined m/z range. The selected ions are then passed to the orbitrap. Image from Thermo Fisher Scientifc UK: https://www.thermofisher.com/uk/en/home/industrial/mass-spectrometry/mass-spectrometry-learning-center/mass-spectrometry-technology-overview/mass-analyzer-technology-overview.html

1.1.3.3.1. Chromatographic separation techniques

GC-MS has historically been a popular choice in metabolomics. Samples are dissolved in a solvent and vaporised, then passed through a heated column by a chemically inert gas (Guiochon and Guillemin, 1990). In the column, the sample is repeatedly dissolved and vaporised in the stationary phase. The process of dissolving and vaporising depends on physiochemical properties of the column and the interaction with each metabolite, therefore the time of dissolving and vaporising is unique for each compound allowing metabolites to separate within the column. A mass spectrometer at the end of the column monitors the composition of the gas stream and converts it into signals which form chromatograms with peaks representing metabolites (Bartle

and Myers, 2002). GC-MS has clear chromatographic resolution, high reproducibility, and can provide detailed spectral information however it is limited by the size and type of metabolite that can be separated with GC (Ren et al., 2018). GC-MS is not suitable for larger compounds, or non-volatile or thermally unstable metabolites (Lei et al., 2011). It also requires extensive preparation of samples prior to analysis often including the derivatisation of non-volatile compounds to make them volatile, which is time consuming (Liu and Locasale, 2017). It can also be difficult to distinguish compounds with similar chemical properties or low molecular weights using GC resulting in low resolution of chromatograms and poorer reproducibility (Büscher et al., 2009). Due to these issues and limitations of GC and the rapid technical development in the field of LC over the past few decades, LC is becoming a more popular choice than GC in metabolomics studies.

LC separates molecules based on their physical and chemical properties, such as molecular size, charge, polarity, and affinity towards other molecules. It consists of a stationary and a mobile phase. The mobile phase comprises the solution containing the sample mixture and the solvent that moves the sample through the chromatographic column containing the stationary phase before it is injected into the mass spectrometer. Solvents in the mobile phase are typically a mix between non-polar solvents (most commonly water) and polar solvents such as methanol or acetonitrile (Rusli et al., 2022). Composition of the mobile phase must be considered so that it does not accidentally damage the stationary phase. The stationary phase in LC is composed of long chain alkyl groups attached to the surface of irregularly or spherically shaped porous particles (Dass, 2007) typically between 2 and 5 µm in diameter (Borges, 2015). Traditionally particles in the stationary phase have been silica and this remains a popular choice for LC, though more recently non-silica stationary phases are being explored (Borges, 2015) as different separation methods are suited

to varying classes of metabolites. Functional groups in the long chain alkyls attached to stationary phase particles interact with compounds through hydrogen bonding, dipole-dipole interactions (both examples of hydrophilic bonding) and London forces (hydrophobic interactions) (Rusli et al., 2022) leading to retention. Non-interacting compounds or compounds with weaker interactions are not retained and elute quickly from the column, exhibiting shorter retention times (Petrova and Sauer, 2017) (Figure 1.6).

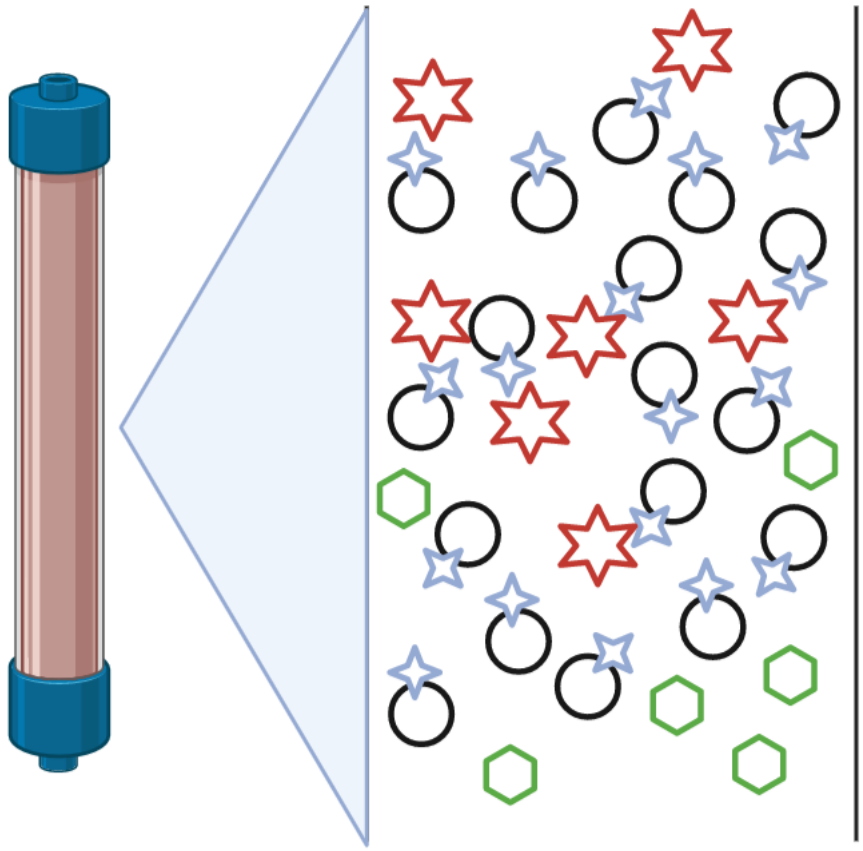

Figure 1.6 Schematic example of interactions between analytes and stationary phase in a liquid chromatography column

Silica stationary particles (black circles) are bonded to functional groups (blue stars) which form hydrophobic and hydrophilic interactions with analytes (red stars) in the sample mixture, resulting in these compounds being retained in the column. Compounds which do not interact with the functional groups of the stationary phase (green hexagons) are not retained by the stationary phase and elute quickly.

Reverse phase (RP) chromatography is the most commonly used technique in metabolomics. In RP columns, the stationary phase is composed of compounds with high numbers of carbon molecules such as octadecylsilane (C18) or octylsilane (C8). The mobile phase begins at a high polarity which when passed through the stationary phase makes the surface of the particles in the column non-polar and hydrophobic (Molnar and Horvath, 1976). The hydrophobic particles in the column have a higher affinity for non-polar molecules in the sample with higher hydrophobicity and retain them, while polar compounds do not form interactions and elute quickly (Shabir, 2010). The decreasing polarity of the mobile phase over the course of the separation reduces the hydrophobic interactions and allows non-polar compounds to elute at a later time point than polar compounds (Molnar and Horvath, 1976). However the quick elution of polar species of metabolites can increase ion suppression (Kloos et al., 2013). The relatively recent development of hydrophilic interaction chromatography (HILIC) columns which are well suited for polar metabolites but do not retain hydrophobic molecules well has enabled the separation of metabolites that are only retained minimally using RP chromatography (Theodoridis et al., 2008). HILIC uses a polar stationary phase which can be bare silica or silica modified by many polar molecules such as DIOL, amino or amide bonded phases (Buszewski and Noga, 2012) and an aqueous/organic mobile phase of which a large proportion (>60%) is an organic solvent, commonly acetonitrile (Periat et al., 2013). Water molecules are attracted by the polar groups of the stationary phase and form a semi-immobilised aqueous layer over the surface of the stationary phase. Polar analytes within samples become partitioned between the semi-immobilised layer and the mobile phase which contains some aqueous content. The more hydrophilic an analyte is the greater the partitioning equilibrium shifts towards the semi-immobilised layer and the stronger the retention of the analyte (Tang et al., 2016). Thus, polar metabolites are retained for longer while

non-polar metabolites elute quickly. HILIC is a variant of normal phase chromatography but uses less toxic solvents which make it an advantageous technique (Borges, 2015). HILIC has been continuously growing in popularity as a separation method (Buszewski and Noga, 2012) and it is now generally accepted that using both RP and HILIC separation techniques in LC-MS analysis maximises coverage of the metabolome (Gika et al., 2008; Lu et al., 2008; Engskog et al., 2016).

After metabolites have eluted from the chromatographic column they enter the source region of the mass spectrometer where they are ionised, as discussed in the previous section (Lu et al., 2008). The number and class of metabolites that can be detected depends on the ionisation mode of the mass spectrometer. No single mode can cover all the metabolome due to its complexity. As such positive and negative modes are often used in conjunction to maximise the number of detected metabolites (Emwas, 2015).

LC-MS is a highly sensitive, specific and reproducible technique that provides an unbiased method of identifying metabolites associated with a particular clinical condition or phenotype (Guijas et al., 2018). In a study comparing three commonly used separation techniques coupled to MS the use of an LC system was found to be superior in reproducibility, time efficiency, and coverage of multiple metabolite classes regardless of polarity (Büscher et al., 2009). In toxicology and forensic testing LC-MS was found to be comparable in detection capability to GC-MS but with the additional advantages of easier and faster sample extraction and shorter run times (Perez et al., 2016). LC-MS is also advantageous because it can simultaneously measure multiple analytes in complex biological samples, giving a wider metabolite coverage than GC-MS, and can be used for the analysis of non-volatile polar molecules

(Leung and Fong, 2014). Because of these advantages the use of LC-MS in metabolic profiling has become increasingly popular.

However LC-MS is not without its limitations. Analytical columns deteriorate over time resulting in retention time drifting that must be corrected computationally after data is acquired (Li and Li, 2020). Instability of signal can occur if the MS ion source becomes contaminated therefore a high level of maintenance is required for reproducible and accurate results. Finally despite some advances in this area the identification of metabolites remains a bottleneck in metabolomics research. While the hard electron ionisation of GC-MS produces a unique fragmentation pattern and reliably reproducible spectrum for each metabolite, spectra produced by LC-MS are variable between instruments (Gika et al., 2014) and the soft fragmentation produced by electrospray ionisation (commonly used in LC-MS) does not produce a unique fragmentation pattern for each ion. An additional step can be included in tandem mass spectrometry to select ions of a particular m/z ratio and increase their kinetic energy so they collide with neutral gas molecules and fragment further into unique fragment ions (Sleno and Volmer, 2004). In doing so, tandem mass spectrometry can separate ions with similar m/z ratios. Although freely available metabolite databases with information regarding m/z values and unique fragmentation patterns are growing in popularity there is still a large number of metabolites missing from their lists and matching metabolite features can be manually intensive and time consuming. An overview of the approaches required for data processing before analysis of eluted metabolites can be conducted is discussed in the following sections.

1.1.3.4. Data pre-processing

Metabolomics experiments generate large amounts of highly complex data. In order to produce a data matrix with the quantification of signals detected in a sample which

can be easily manipulated for further analysis the collected data must undergo a series of computational transformations, termed pre-processing. These involve detecting features present in the acquired spectra; performing correction to remove background noise that may impact signal intensity; alignment of peaks between samples; filtering of data and removal of low-quality features; and the removal of any differences between samples generated by technical, rather than biological variation (Katajamaa and Orešič, 2007).

1.1.3.4.1. Peak picking and alignment

The first step towards data analysis involves the generation of peak lists from raw LC-MS data. Peak picking methods detect peaks in the chromatogram and integrate their areas to provide quantitative information about the corresponding metabolite (Zhang et al., 2009). The chromatographic data is transformed into a two-dimensional matrix characterised by m/z value and retention time or scan number ((m/z)/retention time). Thousands of variables can be detected and transformed at this stage (Bijlsma et al., 2006). However, retention time drift, which can occur as a consequence of column degradation, unstable pH value of the mobile phase, and variations in column temperature and pressure, can result in the position of peaks which correspond to the same metabolic feature changing over the course of a single experimental run potentially resulting in the same feature being assigned a different identification between samples (Y. Wang et al., 2019). To counteract this, a peak alignment step is commonly included in the metabolomic pipeline. Although signal drift occurs along the retention time axis the high accuracy of modern MS technologies means shifts along the m/z axis are minimal (provided instruments are regularly calibrated) so data can be binned in m/z intervals. Peak alignment is then performed on each bin by the retention time axis. One commonly used method of peak alignment calculates retention time boundaries in the bin within which the observed peaks are understood

to represent the same feature across each of the samples (Alonso et al., 2015). However, some binned peaks may not be representative of the biological variation of interest and therefore filtering steps must be applied to ensure only relevant features are kept.

1.1.3.4.2. Feature filtering

Feature filtering is an important step in the metabolomic workflow to ensure subsequent statistical analysis is not impacted by low quality data (Schiffman et al., 2019). Low quality data may arise from degenerate features, high background noise, unintentional removal of relevant peaks with low signal-to-noise ratio (a setting within the MS that can be adjusted based on known abundances of metabolites), or the presence of contaminants/artifacts within the samples from impurities in extraction solvents, the mobile phase, or metabolites retained in the column or ion source from previous experiments (Smith et al., 2006; Verpoorte et al., 2022). When filtering, high quality, biologically meaningful features should be retained while low quality features and background noise that may cause false positives in analysis should be removed from the dataset. The filtering pipeline typically consists of removing features based on the ratio of biological signal to blank signal, percentage of missing features, and variability of features across samples (Schiffman et al., 2019).

Blank samples can be used to find background contaminating features contributing to increased technical variation. Median intensity of each feature in the biological samples is compared to the median intensity of the same feature in the blank samples and where the ratio of intensity is insufficient the feature is removed (Gadara et al., 2021). Typically, 20-30% of untargeted data from MS experiments is missing values affecting approximately 80% of measured compounds (Hrydziuszko and Viant, 2012). When a feature is missing in more than 20% of samples in any one sample class it is

removed from the dataset, the so-called “80% rule” (Yang et al., 2015), as the proportion of missingness is high and suggests the feature is truly missing from many samples. Although removing features can increase the sparsity of data it prevents skewing of the distribution. Aside from the metabolite being truly absent from the sample there are several reasons why missing values occur. Firstly, the metabolite may be present at a concentration lower than the instrument’s limit of detection (LOD). Secondly, co-eluting compounds and ion suppression may produce matrix effects which impede the detection and quantification of the metabolite (Redestig et al., 2011). A decline in the separation ability of the column or increasing contamination of the mass spectrometer may also affect quantification. Finally, limitations in upstream computational processing, such as poorly chosen peak picking or alignment parameters, may affect the detection of the compound across samples (Do et al., 2018). A complete data matrix is required for most downstream statistical analysis so missing values remaining after the 80% rule has been applied must be addressed before analysis can proceed. A commonly used strategy for missing values is imputation, replacing the missing value with an acceptable substitute value, but there are various methods to do so. For example, if the LOD is known it can be used as a replacement for the missing value (Wei et al., 2018). Alternatively, a replacement value is calculated using the available measurements for each variable such as k-nearest neighbour (kNN) where missing values are replaced by the average of the next closest non-missing values (Do et al., 2018), random forest (RF) where missing values are imputed based on a proximity matrix generated by RF classification of the remaining metabolites (Kokla et al., 2019), and mean or median replacement where the missing value is replaced by the mean or median of the remaining values for that metabolite (Hrydziuszko and Viant, 2012). Mean substitution may lead to inconsistent bias if values are missing not completely at random and increases sample size while

underestimating error (Kang, 2013) so is generally not recommended for high dimensionality data, but otherwise there is no consensus over which method is superior. Gromski et al. (2014) reported that RF outperformed kNN, median and zero replacement methods in clustering of samples and total explained variance after values were imputed, but Hrydrziuszko and Viant (2012) reported kNN was the superior method based on clustering of samples and spread of variance. More recently it has been suggested that selection of imputation method should depend on downstream analysis, with RF providing the best percentage variance for contribution to unsupervised analysis but kNN providing the most well fitted permutations in supervised analysis (Di Guida et al., 2016). More detailed explanations of statistical analysis techniques can be found later in section 1.1.3.5. As there is no current consensus over which method is optimal imputation technique should be selected under consideration of future analysis.

Finally, variability of features across samples is typically measured by the coefficient of variation (CV), calculated by pooling samples of interest into a quality control (QC) sample which is injected alongside experimental samples and measuring variability of each feature within the pooled QC across the run. Typically a CV of 20-30% is used as a cut off, removing features with high variability across technical replicates which are unlikely to be genuine features of interest (Want et al., 2010). This cut off was set following recommendations set by the US Food and Drug Administration (FDA) in their guidance for validation of drugs in industry (Dunn et al., 2011) and considers the intensity of ions of interest which may unfortunately be near or at the LOD (Sangster et al., 2006). An overly conservative cut off may remove genuine metabolites of interest.

1.1.3.4.3. Data treatments

After low quality data is removed, normalisation of the remaining data aims to remove unwanted systematic biases such that only biologically relevant differences remain in the data (Alonso et al., 2015). Methods which normalise data can generally be grouped into two categories: method driven normalisation approaches which extrapolate an external model for normalisation, or data-driven models which construct a model under the assumption that large numbers of metabolites remain constantly expressed throughout an experiment (Ejigu et al., 2013).

One commonly used method-driven normalisation approach is the use of QC samples injected periodically throughout an analytical run. The QC samples are then used to construct a signal correction parameter with respect to the order of injection which can be applied to the remainder of the dataset, typically by locally estimated scatterplot smoothing (LOESS) signal correction which corrects for drift across samples by observing change in signal for the a given metabolic feature in QC samples and applying the same temporal shift in signal in the experimental samples (Dunn et al., 2011; Rusilowicz et al., 2016). Normalising to QC can minimise technical variation over the run. Another popular method is the use of one or multiple internal standards. Reference material is spiked into all samples at a uniform concentration. Internal standards are either stable isotopes or analogues of compounds which do not occur naturally within the chosen tissue (Ejigu et al., 2013) but should be chemically similar to a metabolite class of interest (for example $^{13}C_6$ glucose is used as an internal standard for monosaccharides (Dunn et al., 2011)). However, this strategy is not always practical especially in large scale untargeted studies where it is difficult to include a relevant standard for all metabolites of interest (Thonusin et al., 2017).

Some argue that data driven normalisation methods are better choices for large scale untargeted experiments. Examples of popular data driven methods to normalise data include probabilistic quotient normalisation (PQN) (Dieterle et al., 2006), cyclic LOESS, and variance stabilisation normalisation (VSN) (Li et al., 2016). In PQN a mean response is calculated using QC samples, generating a reference vector. The median between the reference vector and every sample is computed which provides a vector of coefficients relating to each sample. Every sample is then divided by the median value of the vector of coefficients. PQN is therefore advantageous because it considers existing concentration changes between metabolite features (Dieterle et al., 2006; Di Guida et al., 2016). Cyclic LOESS applies a local normalisation curve to all possible pairs of samples, cycling through pairs several times (Bolstad et al., 2003). As every possible pair combination must be tested cyclic LOESS can be computationally intensive and slower than other methods of normalisation, however it can be applied to unbalanced data. VSN is a non-linear method of normalisation that aims to keep variance constant over the data range. A transformation is applied to the data which approaches the logarithm for large values, removing heteroscedasticity and decreasing coefficient of variation, while variance does not decrease as values approach the LOD variance, increasing the coefficient of variation for smaller values (Huber et al., 2002). VSN is not recommended for smaller sample sizes (Jauhiainen et al., 2014). Untargeted metabolomics data is often high dimensional data, thus limiting the applicability of VSN in untargeted studies. However, it should be noted that data driven methods of normalisation assume that a large number of metabolites experience the same pattern of drift over the course of the analysis which may not always be the case (Thonusin et al., 2017). Therefore, the selection of normalisation method should be carefully considered.

Scaling is a data treatment which aims to balance fold change differences between metabolites. Large differences in the fold changes of metabolite concentration mean that absolute abundance of some metabolites can vary over orders of magnitude from pM to mM within the same tissue (van den Berg et al., 2006). Scaling helps bring data within similar dynamic ranges while preserving relevant variability. Scaling methods adjust each metabolite using a unique scaling factor. Scaling factors can be determined based on data dispersion or by average value (van den Berg et al., 2006). However, scaling can also result in the undesirable inflation of large measurement errors, particularly for small values (Yang et al., 2015).

Transformation is a type of scaling that refers to nonlinear conversions of the data. It compensates for the heteroscedasticity of metabolomic data and improves the symmetry of skewed distributions (van den Berg et al., 2006). Transformation is a necessary step as many statistical methods used for metabolomic analysis assume data distribution is approximately normal. A commonly example is the use of logarithmic transformations. Logarithmic transformations reduce the influence of large data values, such as outliers, and are particularly useful when interactions between variables are both additive and multiplicative (Boccard et al., 2010). This method has some limitations, particularly when handling low value or zero value data, however it does allow the fit of linear models which are often used in metabolomic statistical analysis (Alghamdi et al., 2019).

1.1.3.5. Statistical analysis

Having prepared the data in an appropriate format for further analysis, the primary goal in all metabolomic studies is the identification of metabolite signatures characteristic of any given condition, such as treatment, genotype, or disease, to allow the stratification of samples. This is often achieved by selecting metabolites which

significantly differ in abundance between sample populations, either by exploring each variable in the dataset individually (univariate) or by the simultaneous analysis of multiple variables (multivariate). Each of these approaches will now be discussed in more detail to provide insight into the statistical approaches to metabolomics techniques.

1.1.3.5.1. Univariate analysis

Untargeted metabolomics data often contains thousands of detected metabolites. Univariate methods, such as t-tests and ANOVA or their non-parametric alternatives, are employed to reduce the number of metabolites in a dataset by analysing one variable at a time such that only those with the largest changes between sample classes remain (Saccenti et al., 2014). In univariate analysis significance is determined where the calculated p value is less than a given number, typically 0.05 to align with conventional scientific practice. As the chance of finding a discriminating variable increases in proportion of the number of independent tests made the risk of type 1 error, the false identification of non-discriminatory variables as discriminatory, also increases. Due to the high dimensionality of omics data, methods to correct for multiple testing are required to protect against type 1 errors, i.e. false positive results (Broadhurst and Kell, 2006).

However, multiple test corrections can also increase the risk of type 2 errors (i.e. false negative results) potentially removing biologically important information (Groenwold et al., 2021). Another drawback to traditional univariate methods is that, even if there are multi-molecule interactions which would separate groups on a systems level, if differences between groups are minor on a single molecule level univariate methods can fail to differentiate the groups (Bartel et al., 2013). In this case multivariate analytical methods are used to not only identify changes on a single molecule level but

also interactions between metabolites which allow discrimination of groups. Multivariate methods of analysis aim to reduce the dimensionality of data, reducing the number of observations from the thousands to tens or hundreds while retaining as much information in the original dataset as possible such that it is still possible to identify classifying features between sample populations. Multivariate methods therefore help to identify major trends and features within the data without increasing risk of type 1 or type 2 errors and allowing for the use of univariate tests thereafter.

There are many options for multivariate analysis (including but not limited to hierarchical clustering to examine relationships between samples (Pang et al., 2021) and support vector machines for classification of samples (Mahadevan et al., 2008)) however due to the relevance of methods chosen in the studies detailed in this thesis only principal component analysis (PCA), partial least squares discriminant analysis (PLS-DA) and RF classification will be discussed in more detail.

1.1.3.5.2. Principal component analysis

PCA is an unsupervised linear transformation of high dimensionality data that aims to preserve as much of the variance in the original data as possible in a lower dimensionality output (Figure 1.7). PCA is ubiquitous in metabolomics as it provides an easily understandable overview of the data. By simplifying the dataset but retaining variance relationships between samples and metabolites can be more easily understood (Worley and Powers, 2013). PCA requires a n x p data matrix, X, which has been standardised such that all variables are measured on the same scale (hence the importance of scaling data, discussed previously), where n represents samples and p represents measured variables. To identify correlations between variables, a covariance matrix is computed. The covariance matrix is a p x p symmetric matrix

containing all possible pairs of measured variables, where each element represents the covariance between two variables (Equation 1.1) (Jolliffe and Cadima, 2016).

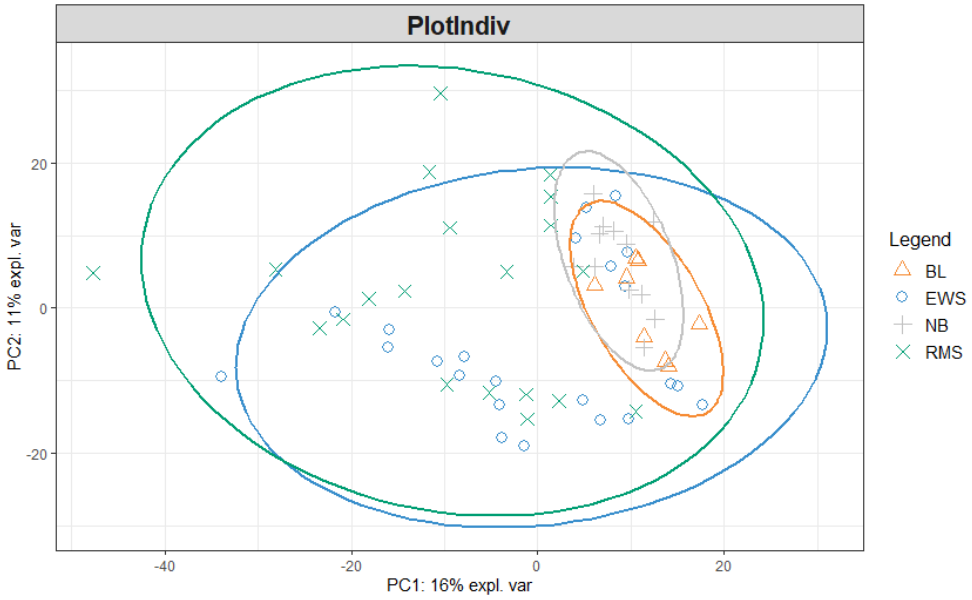

Figure 1.7 Example of principal component analysis (PCA) plot

Illustrative example of PCA plot using the small round blue tumours (SRBCT) dataset available in R package mixOmics (Le Cao et al., 2016). PCA clusters samples based on their similarity. It reduces the number of dimensions within the dataset by constructing principal components which convey maximum variation of the data and contain the minimum amount of error. A PCA plot is a projection of principal components where each dot represents one sample. Samples which are more similar are closer in proximity on the plot. This plot demonstrates similarity between samples from four types of cancer: 8 Burkitt Lymphoma (BL), 23 Ewing Sarcoma (EWS), 12 neuroblastoma (NB), and 20 rhabdomyosarcoma (RMS)

$$\begin{bmatrix} Cov(x,x) & Cov(x,y) & Cov(x,z) \\ Cov(y,x) & Cov(y,y) & Cov(y,z) \\ Cov(z,x) & Cov(z,y) & Cov(z,z) \end{bmatrix}$$

Equation 1.1 Example covariance matrix for 3-dimensional data with 3 variables, x, y and z

A principal component (PC) is a new variable constructed as linear combinations of the initial variables. PCs are constructed in a way that ensures the first PC accounts for the largest amount of variance possible, with each subsequent PC accounting for less variation (Figure 1.8). This method reduces dimensionality of the data without losing the large amount of information contained in the original data set. PCs are calculated using eigenvectors (the set of coefficients, also referred to as loadings or weights, appearing in each principal component which inform the direction of spread of the data) and eigenvalues (the variance of the principal component which gives the magnitude of the spread of the data) computed from the covariance matrix. Eigenvectors are ranked in descending order with respect to their eigenvalues. A d x k projection matrix, W, where d represents the number of original features and k represents the number of desired features based on the number of eigenvectors retained. The original matrix, X, is transformed via W to obtain a new n x k matrix, Y, where n is the number of observations and k is the number of desired features. The columns of matrix Y are the PCs (Alto, 2019). Therefore, the larger the eigenvalue, the greater the importance of the PC (Jolliffe, 1990).

PCA is an unsupervised method of separation which reduces dimensionality in an unbiased manner. However, it only reveals group structure in data when within-group variation is sufficiently smaller than between-group variation (Worley and Powers, 2013). For a greater understanding of variation which takes sample class into account, supervised multivariate methods can be utilised.

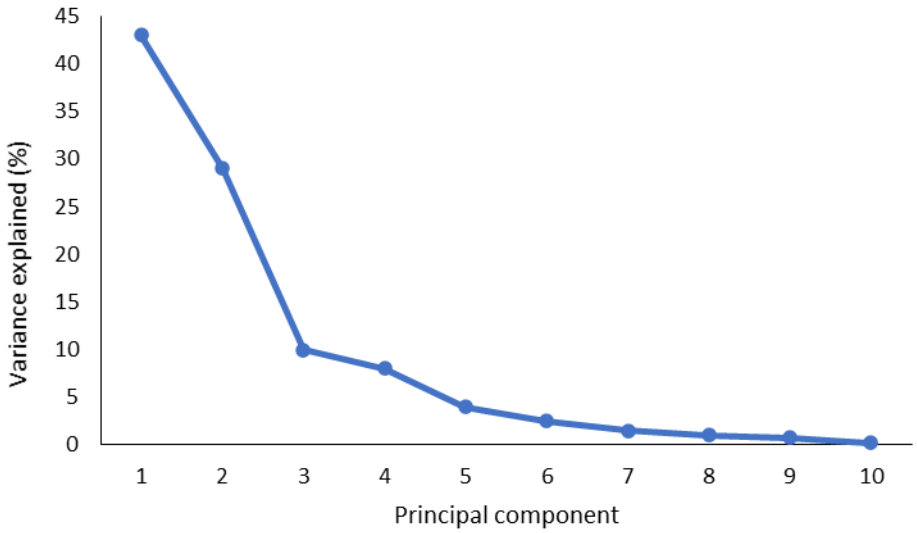

Figure 1.8 Example scree plot indicating variance explained for 10 principal components

Each principal component explains less variance than the previous component, with the majority of variance in the dataset explained by principal component 1

1.1.3.5.3. Partial least squares discriminant analysis

Partial least squares discriminant analysis (PLS-DA) is a method of supervised multivariate analysis which aims to reduce dimensionality of datasets with a separation model built with an awareness of class factors (Figure 1.9). Although originally developed for calibration and regression in chemometrics (Brereton and Lloyd, 2014), PLS-DA became a commonly used technique in metabolic analyses for classification and discrimination of data (Barker and Rayens, 2003). Like PCA, PLS-DA uses a *n* x *p* matrix, X, but also requires a *n* x *q* matrix containing sample class information, Y, where *q* represents class factors stored in numerical form (Figure 1.10). Instead of finding maximum variance between variables, as in PCA, PLS-DA aims to find the direction in the X space that explains the maximum variance direction in the Y space. This identifies fundamental relationships between the X and Y matrices.

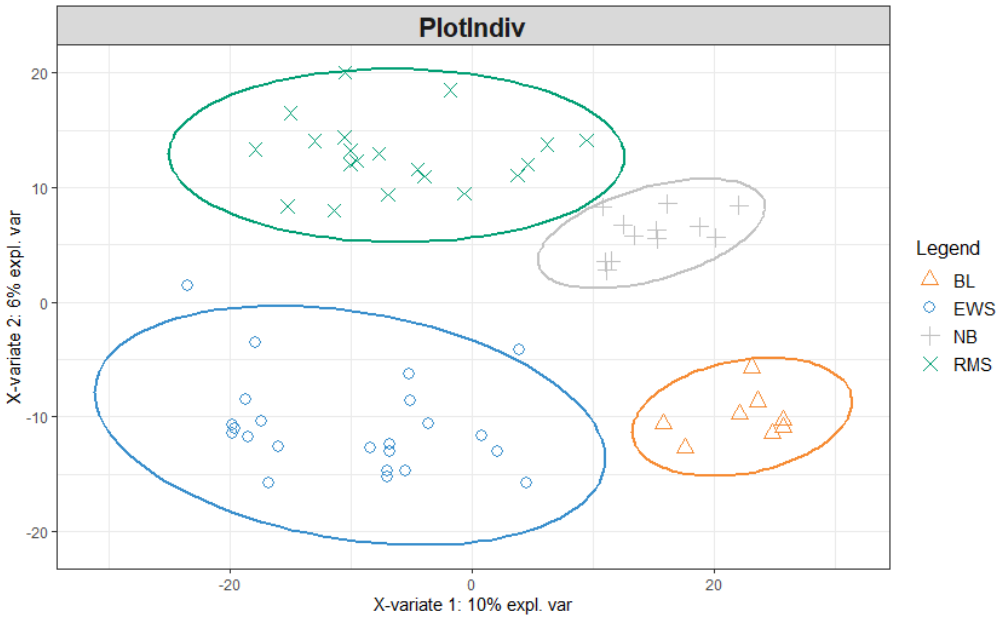

Figure 1.9 Example of partial least squares discriminant analysis (PLS-DA) plot

Illustrative example of PLS-DA plot using the small round blue tumours (SRBCT) dataset available in R package mixOmics (Le Cao et al., 2016). PLS-DA is a similar approach to PCA in that it also clusters samples based on their similarity, however PLS-DA links a matrix of raw data to a matrix of metadata such that sample class information is included in the separation model. This improves classification of samples, so samples cluster distinctly on plot based on their class. A PLS-DA plot is a projection of variance in components where each dot represents one sample. Samples which are more similar are closer in proximity on the plot. This plot demonstrates similarity between samples from four types of cancer: 8 Burkitt Lymphoma (BL), 23 Ewing Sarcoma (EWS), 12 neuroblastoma (NB), and 20 rhabdomyosarcoma (RMS)

$$\begin{bmatrix} \text{Old} \\ \text{Old} \\ \text{Old} \\ \text{Middle} \\ \text{Middle} \\ \text{Middle} \\ \text{Young} \\ \text{Young} \\ \text{Young} \end{bmatrix} \longrightarrow \begin{bmatrix} 1 & 0 & 0 \\ 1 & 0 & 0 \\ 1 & 0 & 0 \\ 0 & 1 & 0 \\ 0 & 1 & 0 \\ 0 & 1 & 0 \\ 0 & 0 & 1 \\ 0 & 0 & 1 \\ 0 & 0 & 1 \end{bmatrix}$$

Figure 1.10 Example Y matrix of multiclass data

Group information is recoded into dummy variables where 0 and 1 represent group status. 1 = 'in-group'; 0 = 'out-group'

The underlying model of PLS-DA can be written as:

$$X = \hat{X} + E = TP^T + E$$

$$Y = \hat{Y} + G = UC^T + G$$

Equation 1.2 Underlying model of partial least squares discriminant analysis

Where T and U are the scores for X and Y, P and C are the loadings for X and Y, and E and G are the residual errors of X and Y unaccounted for in the model, respectively (Worley and Powers, 2013). PLS aims to find a set of scores and loadings which summarize X and Y effectively, such that the U and T share maximum covariance.

To construct PLS components, the weight vector, W, is first calculated such that T and U, and therefore X and Y, share maximum covariance. Loading scores P and C are then determined sequentially. Lastly, W, P and C are used to estimate the regression coefficient and the first PLS component is established. E and G become the input matrices for the construction of the second PLS component and the procedure is repeated (L.C. Lee et al., 2018). PLS component construction is repeated as many times as required to build the number of components required for the optimal separation model.

However while PLS-DA has become a standard tool in metabolomic analysis it is known to be prone to providing an overly optimistic model of separation, termed 'overfitting'. Overfitted results suggest class differences where there are none. Overfitting in classical PLS-DA can be reduced by cross-validation. This typically involves splitting the dataset into a training and testing subsets. Analysis is performed on the training subset then validated on the testing subset. Multiple iterations of cross-validation are carried out to reduce variability using different subsets of the data (Figure 1.11). Two metrics

are used to evaluate the performance of the cross-validation algorithm: R2 and Q2 (Worley and Powers, 2016).

Figure 1.11 Example of k-fold cross validation used in PLS-DA with k = 10

Image from Karl Rosaen Log, http://karlrosaen.com/ml/learning-log/2016-06-20/

R2 provides a measure of the model fit to the original data, while Q2 is the R2 value when the PLS model built on the training subset is applied to the testing subset. R2 and Q2 are expressed on a scale of -1 to 1 with values closer to 1 indicating more PLS factors are incorporated in the fit and negative score showing clear overfitting (Golbraikh and Tropsha, 2002). For example, an R2 value of 0.9 means the PLS model accounts for 90% of variance in the training set while a value of 0.2 would imply only 20% of variance comes from the PLS model. In addition, the smaller the difference between R2 and Q2 the more robust the model. When R2 is substantially larger than Q2 the model parameters are being severely influenced by irrelevant information or noise, resulting in an overfitted model (Bevilacqua and Bro, 2020). In this case alternatives to traditional PLS-DA can be considered.

For instance, sparse PLS-DA (sPLS-DA) assumes that only a small number of features are responsible for driving an effect. As such, sPLS-DA performs variable selection on

the X matrix prior to classification in order to retain only informative variables in the model (Ruiz-Perez et al., 2020). Using lasso penalisation penalties are added to loading vectors to guide the feature selection and model fit processes (Jiang et al., 2013). sPLS-DA is particularly useful when the number of features greatly outnumbers the number of samples, which often occurs in metabolomic studies, as it overcomes the problem of data being affected by a large number of predictor variables (Chung and Keles, 2010).

1.1.3.5.4. Random Forest

Like PLS-DA, RF is a supervised machine learning form of classification and regression. RF can be used as an alternative to PLS-DA. This approach generates several decision trees, each of which is composed of different sets of randomly selected input variables (Figure 1.12). For each tree, input data is divided into training and testing sets using bootstrapping, a computational technique which resamples a single dataset to create multiple simulated samples (Figure 1.13) (Kulesa et al., 2015). On average, the training set will contain 63% of the samples from the original data, with the remaining 37% used in the testing set (Gromski et al., 2015). The trees start with root nodes, in which a few variables are randomly selected and evaluated for their ability to split the data. A common method of variable selection is to use as many as the square root of the number of variables. The variable resulting in the largest decrease in impurity is chosen to split the samples from the parent node into two subsets, producing two child nodes. The splitting process at each node is repeated until the nodes either contain a pre-determined number of samples, or, more commonly, samples from only one class (Touw et al., 2013).

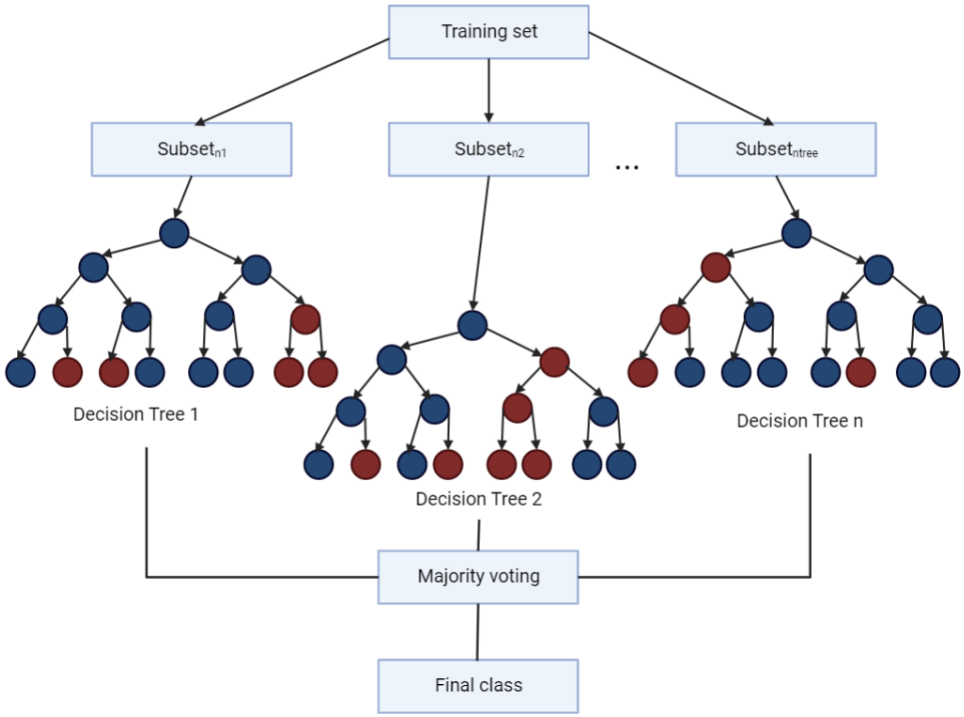

Figure 1.12 Example of a random forest decision tree

Schematic representing random forest decision tree used in classification of samples in metabolomics analysis. The data is divided into testing and training sets. The training set is split into nodes within which variables are randomly selected and evaluated for their ability to split data by decreasing impurity. The processing of splitting into nodes continues until the nodes are left with either a pre-determined number of samples from one class or only one class of samples.

RF has several advantages as a classification tool. Firstly, by constraining trees to a specified maximum depth and ensuring a minimum number of samples classified at each split, RF can avoid overfitting of data while remaining insensitive to noise within the dataset (Mendez et al., 2019). Like PLS-DA, RF provides an estimate of importance for variables within the data on the classification (Oza et al., 2019), however RF also contains a compensation mechanism within the model which avoids the need for cross-validation (Chen et al., 2013). As a result RF does not require additional steps for computational tuning of parameters in the same way as PLS-DA (Probst et al., 2018), decreasing processing time. RF does not require data to be on the same scale and can handle missing values in datasets better than PLS-DA further reducing the need for processing time (Gromski et al., 2015). Finally as a non-linear method of classification

RF can identify the covariance of non-linear data better than PLS-DA (Mendez et al., 2019), providing an advantage in metabolomics where data can often be non-linear.

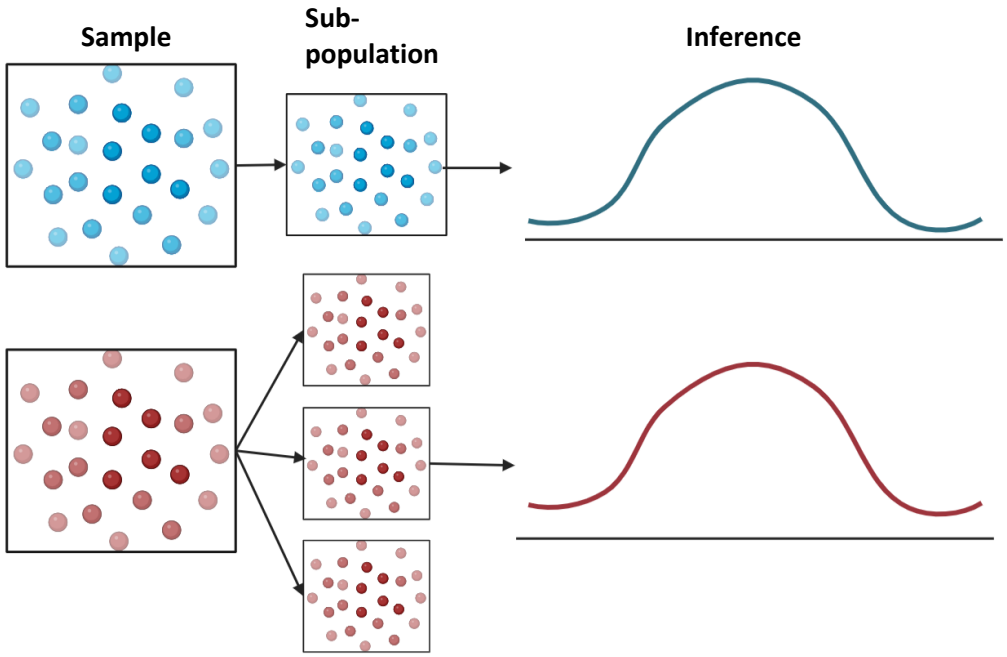

Figure 1.13 Bootstrap sampling of populations

Schematic representing normal (blue) and bootstrap (red) approaches to sampling. In normal sampling, one subset of a population is selected from which information is extrapolated to the whole population regarding sample distribution. In bootstrap sampling, several subpopulations are drawn from the original sample size by resampling observations with replacements from the original sample population. This achieves a better estimate of sampling distribution than traditional approaches.

1.1.3.6. Biochemical interpretation of metabolomics datasets

Following the selection of informative metabolites through multivariate or univariate techniques it is generally of interest to further investigate the biological roles of each of these metabolites and how they interact within the human body in an attempt to provide biological insight into these detected changes. Placing metabolites in their biological context can be achieved by mapping metabolites to pathways and networks in which they play a role. This enables a reliable interpretation of biological disturbances. There are several publicly available websites which permit users to upload their own data for pathway analysis, including MetaboAnalyst (Pang et al.,

2021) and Reactome (Fabregat et al., 2017), and an increasing number of local computational packages are becoming available, including but not limited to FELLA (Picart-Armada et al., 2018), metPath (Shen, Yan, et al., 2022), CePa (Gu and Wang, 2013) and pathwayPCA (Odom et al., 2022).

Biological interpretation is often performed via metabolite pathway enrichment analysis, also referred to as pathway over representation analysis, which allows for the visualisation of metabolomic changes at a systems level (Kamburov et al., 2011; Kankainen et al., 2011). Metabolite set enrichment analysis (MSEA) is based on the similar technique used in transcriptomics of gene set enrichment analysis. A defined list of metabolites is created from the output of multivariate and univariate statistical analysis, these are then tested against lists of pathways from publicly available databases such as the Human Metabolome Database (HMDB) (Wishart et al., 2022) or the Kyoto Encyclopedia of Genes and Genomes (KEGG) (Kanehisa and Goto, 2000) to determine which pathways are present more than would be expected, relative to chance, within the data (Reimand et al., 2019). From this, the overly expressed metabolites are expressed within the pathways and can be related to the functional activity of enzymes or other proteins, gene expression and expression of other metabolites to gain a greater understanding of metabolite-gene, metabolite-protein and metabolite-metabolite interactions within the cell which may contribute to explaining what exactly is changing in the cell in response to a particular stimulus (such as disease).

Another alternative to MSEA is topology based enrichment, which uses knowledge of network interactions derived from public databases to further test the likelihood of predicted metabolite interactions between and within pathways and is becoming increasingly popular (Canzler and Hackermüller, 2020). However, there are a number

of limitations to be considered when placing metabolites into a biological context. Notably, there is a knowledge gap when relating a metabolite's changed concentration to its physiological role which is exacerbated by the difficulty in comparing studies and poor linkage of metabolomics data with subject metadata or specific adaptations in physiology (Scalbert et al., 2009).

1.1.4. Advantages to metabolomics as an analytical tool

Metabolomics has several advantages as a tool in studying non-communicable conditions such as the loss of muscle mass. Firstly, advances in the field of LC-MS/MS technologies permit the collection of high-resolution data at a sensitivity level greater than that of conventional metabolic assays such as enzymatic photometry (Rohen et al., 1990) or scintillation counting (Nassar et al., 2004). Metabolic markers of complex conditions and diseases may be present at too low a concentration to be detected by these conventional assays but could be highly informative of the presence or prognosis of the disease or condition of interest. Metabolomics is therefore extremely beneficial in the search for specific markers of complex conditions and diseases (Zhang et al., 2015). Secondly, unlike conventional metabolic assays which can be limited in their scope of metabolism assessed, modern MS technology can detect thousands of metabolic features from a small biological sample which is of great benefit when searching for as yet unknown diagnostic or prognostic markers of disease (Gonzalez-Covarrubias et al., 2022). Finally, the increasing popularity of metabolomics as an analytical approach in biology and physiology has led to the increased availability of specialist software for analysis of data which permits the mapping of metabolites to their biological roles and provides potential for physiological integration and may allow for novel insights into multifactorial pathophysiological mechanisms. The examples in the following chapters of this thesis demonstrate the utility of

metabolomics as an analytical tool in the study of skeletal muscle wasting and associated conditions.

1.2. Current limitations to metabolomics approaches

However despite the potential of metabolomics as a tool in physiology there are some limitations that must be considered in metabolomics approaches. For example, compared to our understanding of the upstream genome or proteome, our knowledge and annotation of the metabolome is still relatively limited (Johnson and Gonzalez, 2012) and although advances in technology are being made rapidly the identification of novel metabolites remains a bottleneck in the workflow of discovery metabolomics (Zamboni et al., 2015). The diversity and size of the metabolome can also be a challenge. Firstly, the metabolome is much larger than the upstream genome, transcriptome or proteome. As of 2022 HMDB contains 220,945 entries (Wishart et al., 2022) although it is likely that the presence of currently unannotated metabolites within the metabolome means that its true size is much greater. Secondly, there is great variation in metabolite polarity and chemical structure which make it impossible to achieve complete coverage in one experiment. Metabolomics studies must instead aim for the highest possible fraction of coverage to get the best metabolomic profile (Clish, 2015). Furthermore, due to influence of genetic and environmental factors (for example, gender, BMI or smoking) on the metabolome, there can be large interindividual variation in relative metabolite variation over several orders of magnitude (Dunn et al., 2015) which must be controlled for in experimental design (Johnson and Gonzalez, 2012). Moreover, it is difficult to compare metabolomics data across laboratories and studies due to differences in experimental protocol and machinery, however the development of recommended protocols and establishment of quality control standards (Evans et al., 2020) can help to mitigate this problem.

Finally, a major limitation is that metabolomics analysis is often conducted in isolation from physiological data relating to the condition being explored that may provide insight into mechanisms leading to difficulty in the biological interpretation of metabolomics data (Scalbert et al., 2009). For example, very few studies link change in metabolite abundance with disease severity, morbidity or mortality rates when investigating metabolomics in chronic diseases. Lack of integration between physiological and metabolomic data may account for the general failure to translate metabolomics analysis to clinical use. There is growing interest in a 'multiomics' approach, the combination of metabolomics with output from transcriptomics, genomics or proteomics profiling (Hasin et al., 2017), however the collection of relevant phenotypic data which may be used to validate observed changes in the metabolome is still lacking, limiting the potential for metabolomic and physiological integration.

Despite these limitations, metabolomics has been gaining interest as an analytical technique due to its ability to add insight into disease aetiology and identify metabolic signatures which can act as prognostic or diagnostic tools for complex conditions.

1.3. Factors affecting skeletal muscle mass and function in health and disease

1.3.1. Exercise

1.3.1.1. Resistance exercise

Resistance exercise training (RET) provides skeletal muscle with anabolic signals that stimulate muscle protein synthesis and lead to hypertrophy (Miller et al., 2005). Resistance exercise is also associated with increases in measures of muscle strength, such as isometric (Hong et al., 2014) and eccentric contraction torques (Sato et al., 2022) in young individuals. Although ageing is accompanied by a blunting of the

magnitude in the exercise training response (Phillips et al., 2017), improvements in skeletal muscle strength (Lai et al., 2021), performance (such as increased gait speed, decreased sit to stand time or improved balance) (Keating et al., 2021), and mass (Bieler et al., 2022) are seen in older adults following resistance training. RET is also associated with improved metabolic health in older individuals and in patients with chronic illness. For example, older men with type 2 diabetes reported significantly lower HbA1c values after 10 weeks of resistance training relative to baseline (Bweir et al., 2009), suggesting improvements in insulin sensitivity are related to RET. This demonstrates the utility of resistance exercise in the maintenance of skeletal muscle mass and whole-body health regardless of age.

1.3.1.2. Aerobic and submaximal steady-state exercise

While not typically associated with hypertrophy to the same extent as resistance training, submaximal steady-state exercise is associated with well-defined benefits in the metabolism of skeletal muscle under healthy conditions and in chronic disease, for instance the amelioration of reductions in skeletal muscle metabolism induced by health problems such as obesity (Pérez-Martin et al., 2001) or heart failure (Esposito et al., 2018), which emphasise the importance of exercise in maintaining normal muscle metabolism. A predominant metabolic benefit associated with submaximal steady-state exercise is the increase in the oxidative capacity of skeletal muscle (Noonan and Dean, 2000). Although there are concurrent increases in the rates of fat and carbohydrate oxidation (Romijn et al., 1993), in submaximal exercise up to an intensity of approximately 65% of peak oxygen uptake (VO_2^{PEAK}) fat oxidation is favoured (Venables et al., 2005). It has been suggested that this shift towards greater fat utilisation in oxidation underpins improvements in muscle oxidative capacity (Gollnick and Saltin, 1982; Overmyer et al., 2015). Submaximal steady state exercise is also linked with improved glucose homeostasis. After submaximal exercise, glucose

uptake in skeletal muscle increases, resulting in lower blood glucose concentrations (Brun et al., 1995) which are maintained for up to 48 hours (Hawley and Lessard, 2008). Consequently, submaximal exercise is often included in healthcare treatment plans for chronic diseases associated with increased insulin resistance (Chodzko-Zajko et al., 2009).

1.3.2. Physical inactivity

Conversely to the benefits of increased activity, sedentary behaviour is associated with detrimental effects in skeletal muscle and whole-body health. Reduced physical activity is strongly correlated with prevalence non-communicable disease (Lee et al., 2012) and is associated with increased risk of early mortality regardless of age, ethnicity or sex and independent of adiposity (Roux et al., 2021). Within skeletal muscle inactivity is associated with the rapid atrophy of fibres and significant reductions in muscle cross sectional area (Inns et al., 2022) alongside significant reductions in force output representing a loss of muscle strength (Kawakami et al., 2001). Historically the accumulation of intramyocellular lipid (IMCL) content have been reported following periods of inactivity (Bergouignan et al., 2009; Pagano et al., 2018), however more recent evidence suggests that IMCL accumulation is not a direct adaptation of skeletal muscle to reduced physical activity per se but is instead simply reflective of excess energy balance. When individuals are maintained in energy balance IMCL content does not increase after acute (Dirks et al., 2016) or chronic (Shur et al., 2022) periods of bed rest despite the impairment of other metabolic processes, including the development of insulin resistance and failure to stimulate carbohydrate oxidation.

Impairments in metabolic flexibility, the ability to switch from fat to carbohydrate oxidation in response to changes in metabolic or energetic demand such as in the transition from the fasted to the fed state (Galgani et al., 2008; Goodpaster and Sparks,

2018; Smith et al., 2018), are strongly associated with low physical activity and sedentary behaviour (Kelley et al., 1999) even when energy balance is maintained (Rudwill et al., 2018). Several mechanisms likely underlie metabolic inflexibility in skeletal muscle including reduced glucose disposal rate, mitochondrial dysfunction, and subsequent accumulation of free fatty acids leading to lipotoxicity (Smith et al., 2018). Such disturbances to cellular homeostasis can cause disruption to insulin signalling networks and as a consequence lead to dysregulation in the balance of protein turnover and therefore further loss of skeletal muscle mass and function (Muoio, 2014), suggesting an association between skeletal muscle metabolism and the maintenance of muscle mass. This association is further emphasised by the decline in normal skeletal muscle metabolism and loss of muscle mass in ageing.

1.3.3. Diet

Nutrient availability is a primary determinant of skeletal muscle proteostasis (Atherton and Smith, 2012) and therefore also of muscle mass. The anabolic impact of nutrients is primarily driven by essential amino acids (EAAs) derived from protein in the diet (Smith et al., 1992). In the postprandial state, EAA signalling causes an increase in muscle protein synthesis (MPS) rates approximately 45 to 90 minutes after ingestion, with a peak after 1.5 to 2 hours. Following this peak, MPS rates rapidly return to postabsorptive levels regardless of substrate availability (Atherton et al., 2010). Furthermore, ingestion of a subset of EAAs termed branched chain amino acids (BCAAs) following resistance exercise can enhance the resistance exercise-induced increase in rate of MPS (Jackman et al., 2023) which are sustained for up to 48 hours (Churchward-Venne et al., 2012). Thus, skeletal muscle mass is increased. Conversely, failure to consume the adequate amount of dietary protein can contribute to loss of skeletal muscle mass (Huh and Son, 2022).

Other components of the diet can also impact skeletal muscle mass and function. For instance, diets containing high proportions of fat or caloric intake over the amount required to maintain BMI can lead to increased IMCL content (Ahmed et al., 2018). Thus, dietary regulation is an important aspect of maintaining skeletal muscle mass and function.

1.3.4. Ageing

Older individuals lose muscle mass at a proposed rate of 0.64-0.7% per year in women and 0.8-0.98% per year in men while muscle strength is lost at a much more rapid pace of 2.5-3% per year in women and 3-4% per year in men (Mitchell et al., 2012). The number of adults over 60 is estimated to increase worldwide from 962 million in 2017 to 2.1 billion by the mid-century (Granic et al., 2019). Sarcopenia is defined by the European Working Group on Sarcopenia in Older People (EWGSOP) as the unintentional loss of muscle mass and quality, strength or physical performance (for example, gait speed less than 0.8 m/s or a poor score on the short physical performance battery test) to two standard deviations below the mean of healthy young adults (Cruz-Jentoft et al., 2019).

While there is currently no clinically relevant consensus definition of sarcopenia, most research defines sarcopenia by the criteria set by either the EWGSOP, Asian Working Group for Sarcopenia (AWGS) or the International Working Group for Sarcopenia (IWGS) and estimates that between 10 and 20% of individuals are sarcopenic (Shafiee et al., 2017), rising to approximately 50% and 43% in men and women older than 80, respectively (Iannuzzi-Sucich et al., 2002).

Sarcopenia is characterised by morphological changes within muscle that contribute to loss of muscle mass and strength which are responsible for increased likelihood of falls, loss of autonomy (Landi et al., 2012) and increased mortality risk (J.H. Kim et al., 2014; Vetrano et al., 2014) compared to non-sarcopenic counterparts. The

preferential atrophy of type II muscle fibres is a defining feature of sarcopenia (Brown and Hasser, 1996), likely due to a failure in the denervation and reinnervation cycle of muscle fibres (Piasecki et al., 2018). Individuals with sarcopenia often gain visceral adipose tissue (Li et al., 2022), termed sarcopenic obesity. Differences between sarcopenic and non-sarcopenic obesity can be observed within the muscle. While in non-sarcopenic obesity, individuals usually have greater muscle mass and strength than lean counterparts, potentially due to higher muscle workload required for daily activities (Murton et al., 2015), sarcopenic obesity is associated with increased infiltration of muscle by fat and the increased deposition of intramuscular lipids (Choi et al., 2016) which in turn is associated with reduced muscle cross sectional area (Lang et al., 2010). However, the extent to which infiltration of fat is a causative factor in sarcopenia is unclear. Ageing is associated with reduced physical activity (Suryadinata et al., 2020) and therefore elevation in IMCL content may simply be reflective of a positive energy balance.

In parallel with the physical changes in muscle there is a decrease in muscle mitochondrial content and respiratory activity, reflected in lower phosphocreatine recovery rates (Andreux et al., 2018), lower maximal aerobic capacity and decreased activity of mitochondrial respiration complexes (Grevendonk et al., 2021), and the concurrent decrease in abundance of mitochondrial DNA and ATP production rates in skeletal muscle (Short et al., 2005) with advancing age.

Ageing is also associated with the development of anabolic resistance, the blunted response of muscle to contractive or nutritive stimuli such as those received from essential amino acid ingestion (Cuthbertson et al., 2005) or resistance exercise (Kumar et al., 2009) which may contribute to further loss of muscle mass or the blunting of hypertrophic responses following RET (Phillips et al., 2017). The inhibitive effect of

insulin on muscle protein breakdown (MPB) is also blunted in older adults, both of which point to dysregulation of protein turnover in skeletal muscle that may contribute to the aetiology of sarcopenia (Fry and Rasmussen, 2011).

1.3.5. Disease

Whilst there are clear factors contributing to muscle loss and deconditioning in health, the impact of disease can lead to additional burden as greater amounts of muscle mass loss in disease are associated with worse clinical outcomes. Patients with chronic heart failure and muscle loss had a significantly higher in-hospital mortality rate than age matched counterparts who did not experience loss of muscle mass (Attaway et al., 2021). Cancer patients with cachexia, a multifactorial condition characterised by rapid and unintentional loss of muscle mass and adipose tissue (Evans et al., 2008), had worse clinical outcomes and increased mortality rates (Dewys et al., 1980; Skipworth et al., 2007) than non-cachectic counterparts, regardless of disease progression or tumour type. In ICU patients, muscle mass declines at a rate of up to 2% a day, which effects recovery time and rehabilitation, and acts as an independent risk factor for mortality (Wandrag et al., 2019).

Skeletal muscle metabolism appears to be impacted by disease. Abnormal mitochondrial structure and increased mitochondrial area are found in the muscle of cachectic cancer patients (de Castro et al., 2019), pointing to mitochondrial dysfunction which may even precede muscle atrophy (Brown et al., 2017), although further validation is required. Loss of muscle mass and strength appears to be related to insulin sensitivity, potentially through impairment of protein turnover regulation, as type 2 diabetes is inversely associated with muscle strength (Hong et al., 2017) and mass (Tajiri et al., 2010) and cancer patients with cachexia report a higher degree of insulin resistance than those without (Jasani et al., 1978; Norton et al., 1984), although as cachexia was determined by weight loss alone the specific contribution of skeletal

muscle in the loss of insulin sensitivity is unclear. Nevertheless, disturbances to normal metabolism within skeletal muscle are associated with worse clinical outcomes and increased mortality rate in chronically ill individuals (Skipworth et al., 2007; Arthur et al., 2014; Tantai et al., 2022), demonstrating the importance of skeletal muscle in whole-body health.

1.4. Metabolomics as a tool to study adaptations in muscle

Despite an appreciation for the importance of muscle in maintaining whole-body health (Bhatheja and Bhatt, 2006; Stump et al., 2006; Wischmeyer et al., 2017) as of yet traditional analytical approaches have not fully defined the role metabolic dysregulation has played in skeletal muscle wasting and there are currently no effective interventions for treating or reversing muscle wasting in either health or disease (Garber, 2016; Aversa et al., 2017) despite growing interest and heavy investment in studying morbidities associated with poor skeletal muscle health and the subsequent loss of muscle mass over recent years (Yuan et al., 2022). This is in part due to the complexity of wasting conditions and difficulty in identifying patients most at risk of muscle mass loss, as the development of molecular and cellular adaptations which lead to a decline in muscle health must be detected prior to physiological changes for interventions to be successful (Bland et al., 2022). However, as metabolomics is capable of detecting small molecule changes in advance of observable physiological adaptations (Wishart, 2019) there is growing interest in the use of both untargeted and targeted metabolomics in musculoskeletal research to evaluate the role of different classes of metabolites across wasting conditions. The current findings will be discussed in more detail in the sections below.

1.4.1.1. Amino acids

Several metabolomics studies have highlighted abnormal amino acid level in deconditioned and wasting muscle. For example, circulating plasma concentrations of seven BCAAs and BCAA-related metabolites were found to be significantly associated with both muscle cross-sectional area (CSA) and fat free mass index in functionally limited older adults, indicating a role for these metabolites in sarcopenia (Lustgarten et al., 2014). Of these, four compounds (leucine and its metabolite α-hydroxyisocaproate, and two tryptophan-related metabolites, C-glycosyltryptophan and indolepropionate) accounted for 21% of variability in muscle CSA, suggesting these metabolites in particular could be important in classifying changes in CSA. BCAAs were also among the 10 metabolites found to be most associated with muscle mass in middle aged women (Korostishevsky et al., 2016). These studies do not link amino acids to muscle function, a key component of sarcopenia, and therefore clear links between amino acid metabolism and decline in muscle function cannot be established. However, when muscle quality (another key component used to define sarcopenia), determined by the ratio of quadriceps strength to thigh CSA, was assessed, leucine, isoleucine, and tryptophan were all found to be present at significantly higher plasma concentrations in participants with low muscle quality than their age-matched controls (Moaddel et al., 2016). Targeted studies support these findings. Low concentrations of serum BCAA and EAA have been linked to both lower skeletal muscle index and functional ability in older adults (ter Borg et al., 2019), and fasting BCAA plasma concentrations were significantly lower in sarcopenic women with poor physical performance than sarcopenic women with higher performance metrics or non-sarcopenic women (Yamada et al., 2018). However, neither of these studies recorded participants' daily protein intake (ter Borg et al., 2019; Yamada et al., 2018), and therefore it is possible that BCAA level simply reflects differences in habitual

protein consumption or energy balance. Non-fasting BCAA plasma concentrations were also significantly lower in sarcopenic than non-sarcopenic individuals, however no specific data was collected regarding the last meal eaten before the blood sample was taken and two general dietary recalls found absolute protein intake was lower in sarcopenic participants (Ottestad et al., 2018). Therefore, lower amino acids could simply be reflective of the reduced protein content of the last meal. The authors argue that non-fasting concentrations reflect the postprandial response to protein intake, but this could be better assessed by using a standardised and controlled diet.

Other non-BCAA or EAA related metabolites have also been linked to decline in skeletal muscle health with age. One study identified proline as an independent risk factor for sarcopenia (Toyoshima et al., 2017), while another identified nine metabolites significantly associated with both muscle mass and function, including aspartic acid and glutamate, which were both negatively associated with grip strength and appendicular lean mass (Zhao et al., 2018). Eight pathways were significantly associated with the loss of muscle mass and function, of which seven involved glutamic acid and/or aspartic acid. Of these pathways, the majority related to amino acid metabolism, supporting a role for aberrant amino acid metabolism in sarcopenia (Zhao et al., 2018), although the study only recruited young women and so potential further dysregulation of these pathways in ageing was not assessed. However, targeted analysis also identified significantly increased serum concentrations of glutamic acid, asparagine and aspartic acid in elderly individuals with sarcopenia (Calvani et al., 2018). Moreover, in severely frail elderly patients, significant differences in the plasma concentration of 11 amino acids was also identified (Adachi et al., 2018). EAAs were present at a significantly lower concentration in the plasma, with a 20.2% reduction in total EAA level in the frail group compared to a non-frail control. In addition, EAA, BCAA and tryptophan levels were strongly correlated with BMI in the frail group.

Although this study focused on frailty, which is distinct from sarcopenia, it further supports that amino acids provide a signature for low physical function and suggests that dysregulated amino acid metabolism may be common across conditions associated with the loss of muscle mass with age.

Dysregulated amino acid metabolism has also been noted in cachexia. For example, in cancer patients the most prominent metabolic alteration associated with cachexia was found to be a decrease in the plasma concentration of amino acids, particularly arginine, tryptophan, and threonine, which had a 0.4-fold reduction compared to non-cachexic cancer controls (Cala et al., 2018). Urinary metabolomics was able to effectively discriminate between cachectic and non-cachectic groups, and metabolites which differed between groups were largely involved in ketone body and amino acid metabolism pathways (Ose et al., 2019). However, as measures of muscle mass were not correlated with metabolite abundance and no measures of muscle strength or functional ability were carried out in these studies (Cala et al., 2018; Ose et al., 2019), associations between metabolite abundance and change in muscle health cannot be validated. As cachexia is a multi-organ syndrome and adaptations in amino acid metabolism were not confirmed to be correlated with loss of muscle mass, it is possible that these changes are not specific to skeletal muscle. Furthermore, differences in metabolite concentration did not remain significant after adjusting for multiple testing (Ose et al., 2019), and therefore further validation of these findings is required. Finally, Yang et al. identified 15 metabolites to be distinct biomarkers for cancer cachexia, including increases in the levels of lysine, isoleucine and tyrosine and decreases in leucine (Yang et al., 2018). The metabolic pathways most disturbed in cachexia included the metabolism of several amino acids, and the synthesis and degradation of BCAAs. However, as cachexia was defined based on weight loss alone and no assessment of muscle strength, functional ability or mass were included in the

study, further validation of these findings is required to confirm the association of BCAAs and loss of muscle mass in cancer.

Likewise, amino acid metabolism is clearly affected by daily energy expenditure. One study noted an inverse association between BCAA concentration and physical activity alongside lower plasma concentrations of several intermediates of BCAA metabolism in more active subjects (Xiao et al., 2016), while another found BCAA plasma concentration decreased in highly active individuals compared to their sedentary counterparts (Fukai et al., 2016), which suggests BCAA plasma concentration is linked in some way to muscle function. Additionally, in older adults, two weeks of step reduction resulted in a significant increase of plasma glutamine (1.3-fold) and methionine (1.2-fold) which did not return to baseline values following a recovery period of increased physical activity (Saoi et al., 2019). Proline has also been highlighted as a marker for both physical inactivity and cachexia. Reductions in plasma proline concentration were associated with higher physical activity and shorter sitting times (Fukai et al., 2016), and significant increases in proline concentrations were observed in COPD patients with cachexia (Ubhi, Cheng, et al., 2012). Proline is a glycogenic amino acid, providing a possible link between dysregulated skeletal muscle metabolism and glucose homeostasis in wasting.

While metabolomics studies investigating the effects of mechanical unloading in humans are lacking, a key limitation in this area, these results from healthy ageing and cachexia provide preliminary evidence that amino acid metabolism is dysregulated in skeletal muscle following periods of disuse, and perhaps a link in terms of metabolic disturbances within the regulation of amino acid metabolism. These observations of dysregulated amino acid metabolism could be related to a number of known metabolic disturbances present in muscle wasting conditions or could be indicative of

an as yet unknown mechanism common across wasting conditions. For example, ageing and physical inactivity are associated with the development of anabolic and insulin resistance in skeletal muscle. BCAAs are instrumental in driving MPS (Atherton and Smith, 2012) and increase following MPB proportional to fat free mass (Jourdan et al., 2012). The observed signatures of altered AA metabolism may therefore be indicative of a lack of incorporation after feeding leading to low MPS rates, or of increased MPB rates in muscle. Alternatively, the increased presence of BCAAs may promote insulin resistance through increased mTOR activation (Yoon, 2016). Abnormal glutamic acid metabolism and associated AA's may be reflective of depressed energy metabolism pathways in muscle, as skeletal muscle acts as a major sink for glutamic acid where it plays a central role in energy provision (Rutten et al., 2005). Although glutamine does not appear have a stimulatory effect on MPS under healthy conditions (Garlick and Grant, 1988), following surgery skeletal muscle levels of glutamine are depleted (Blomqvist et al., 1995) and administration of glutamine can increase MPS rates (Blomqvist et al., 1995). Glutamine therefore appears to have a role as a regulator of MPS under stressful conditions. Abnormal plasma levels of glutamine may therefore reflect a dysregulation to protein turnover not seen in healthy skeletal muscle which provides a mechanism driving early muscle mass loss (Xi et al., 2011).

However, the cross-sectional nature of many metabolomics studies prohibits causal links between abnormal amino acid metabolism and the aetiology of muscle atrophy from being established. As such, the precise role of amino acids in the wasting process remains unclear.

1.4.1.2. Lipids

An advantage to untargeted metabolomics is its unbiased nature, allowing a range of metabolite classes to be identified from a single sample. Although whether the increased presence of IMCL in ageing and disease is a driver of pathophysiology in the loss of muscle mass or simply a consequence of changes in habitual energy intake and physical activity levels is unknown, a few metabolomics studies suggest there is an impact on lipid metabolism within skeletal muscle.

Total abundance of major phospholipid classes in skeletal muscle was increased in sarcopenic elderly when compared to their healthy counterparts (Hinkley et al., 2020). Total phosphatidylcholine and phosphatidylethanolamine levels were negatively associated with muscle volume and peak power, suggesting they may be related to impaired muscle function and loss of muscle mass, however validation in a larger cohort is required to confirm the metabolic signature. Forty metabolites were identified as being strongly associated with cancer cachexia, most of which were classed as lipids or fatty acids, and six metabolites, including two phospholipids and two fatty acids, formed a distinct metabolic signature for cachexia (Miller et al., 2019). Two of the most abundant compounds in both the cachexia and non-cachexia groups, lysophosphatidylcholine (LPC) 16:0 and LPC 18:2, increased 1.34-fold and 1.75-fold with cachexia, respectively, indicating a significant shift in lipid metabolism. LPC has been implicated in inflammation, facilitating the release of proinflammatory cytokines (Law et al., 2019). Given that one important feature of cachexia is chronic systemic inflammation (Deans and Wigmore, 2005), increased LPC may be a key factor in its development. If validated in a larger cohort of patients, this signature may identify those at risk of developing cachexia, however it should be noted that the metabolites may be solely indicative of adipose tissue wasting and not muscle loss, as no assessment of skeletal muscle was performed. Loss of white adipose tissue before

reductions in skeletal muscle content have previously been observed in cachexia (Dalal, 2019). Additionally, increased IMCL content was linked to increasing lipolysis in other compartments of the body in cachexia patients (Stephens et al., 2011). In cancer patients with cachexia, mRNA expression of hormone sensitive lipase (HSL), a lipase protein present in adipose tissue, was approximately 50% higher than non-cachectic counterparts and HSL protein expressed increased 2-2.5-fold between cachectic and non-cachectic cancer groups (Cao et al., 2010). Similar increases were seen between patients with cachexia and cancer patients who had lost weight due to other factors, such as malnutrition, indicating a unique role for lipolysis in cachexia-associated weight loss (Agustsson et al., 2007). Loss of adipose tissue therefore appears to be a critical component in early-stage cachexia and such metabolites may provide evidence of a unique aetiology, perhaps distinguishing it from other diseases associated with the loss of muscle mass.

Changes in lipid metabolism as a result of disuse are less well studied. Although both short- and long-term bed rest studies have reported increased IMCL content similar to that observed in ageing disuse (Pagano et al., 2018; Cree et al., 2010; Bergouignan et al., 2009), as discussed previously it is unclear whether this accumulation is simply due to excess energy balance (Dirks et al., 2016). A key limitation in this area is the lack of metabolomics studies investigating lipid metabolism in relation to decreased energy expenditure.

Thus far, metabolomics has identified common lipid signatures in several states associated with a reduction in skeletal muscle health or the loss of muscle mass, with a particular focus on phospholipids. However more research is needed in this area to validate this signature and to provide mechanistic insight into potential aetiologies.

1.4.1.3. Metabolites produced by energy and fuel metabolism pathways

Mitochondrial adaptation to loss of muscle mass is reflected in the plasma metabolome. For example, following 7 days of post-surgery bed rest 557 metabolites were changed significantly. Notably, short-chain acylcarnitines and derivatives of fatty acid dicarboxylates were elevated immediately following surgery and circulating expression remained high after bed rest (Kemp et al., 2020). Acylcarnitine is involved in the transport of fatty acids into the mitochondria for oxidation, so increased circulating levels of acylcarnitine have previously been suggested as a marker of mitochondrial dysfunction (McGill et al., 2014). Importantly, this study did involve the correlation of metabolomics data with clinical parameters of handgrip and quadriceps strength, and muscle cross sectional area determined by ultrasound (Kemp et al., 2020). Changes in plasma levels of acylcarnitine and dicarboxylate were strongly associated with loss of muscle strength and size following bed rest, pointing to mitochondrial dysfunction as a contributing factor to loss of muscle mass associated with physical activity. Supporting this, plasma concentration short-chain dicarboxylic and hydroxylated acylcarnitines were inversely associated with a decline in hand grip strength with age in men over a period of 18 months and accounted for 16% of total variability in hand grip strength (Ng et al., 2021). As this study took a targeted approach, other markers of mitochondrial adaptation, such as change in plasma abundance in phospholipids or pyruvate (Finsterer and Zarrouk-Mahjoub, 2018), remain undetected, and because only old men were assessed the difference in acylcarnitine concentration between young and older individuals, which may provide insight into the progressive loss of muscle mass with age, was not evaluated.

A comprehensive profiling of frail elderly versus healthy elderly and healthy young individuals found clear differences in the muscle metabolome, including lower levels

of metabolites involved in the tricarboxylic acid (TCA) cycle in older participants (Fazelzadeh et al., 2016a). Metabolite expression was correlated with expression of genes related to mitochondrial function and oxidative phosphorylation, with similar declines in gene and metabolite expression seen across ageing, suggesting impaired mitochondrial function or lower mitochondrial content with age (Fazelzadeh et al., 2016b). Importantly, acylcarnitine levels decreased significantly after RET in both frail and healthy elderly, further supporting a role for dysfunctional mitochondrial bioenergetics in deconditioned muscle. However, it should be noted that as body composition was not accounted for in these measurements, this may simply be a consequence of muscle mass loss rather than a causative factor.

Metabolomics studies investigating changes to energy metabolism associated with muscle loss in ageing or disease are lacking, but several studies do show positive changes relating to energy metabolism in sedentary individuals following increased physical activity. For example, urinary metabolomics profiling revealed short term intensive exercise alters mitochondrial bioenergetics assessed by respiratory exchange rate and maximal oxygen uptake, particularly those relating to glycolytic systems (Enea et al., 2010). As only young women were assessed, the potential impact of the age-related blunting of the exercise response on metabolites associated with mitochondrial function was not explored.

Likewise, sprint training induces changes in the urinary metabolome relating to bioenergetic pathways including TCA cycle intermediates and products of ATP degradation (Pechlivanis et al., 2010). In particular, 2-oxoglutarate, a component of the TCA cycle, was elevated following physical activity alongside increases in metabolites released during its synthesis. Similar metabolic alterations are seen in the plasma metabolome (Lewis et al., 2010). Exercise induced the rapid upregulation of

metabolic pathways responsible for substrate utilisation and increases in intermediate metabolites from adenine nucleotide catabolism and the TCA cycle. However, these changes only reflect acute metabolic adaptations to exercise. It is unclear whether similar positive changes are reflected in chronic metabolic responses, and therefore how important these metabolites are in the exercise adaptation response is yet to be determined. Additionally, without corroboration to assessment of physiological adaptations, it is not possible to fully determine the association between muscle mitochondrial adaption and the metabolome.

1.4.1.4. Neuromuscular junctions and wider metabolic changes

Metabolic dysfunction in skeletal muscle extends past dysregulation of amino acids and lipids. For example, several aspects of the neuromuscular system are suggested to contribute to the loss of muscle strength in sarcopenia (Rygiel et al., 2016). Degradation of motor neurons and the subsequent denervation of muscle fibres may account for loss of muscle strength associated with increasing age, such as the decrease in doublet discharges from ~46% of motor units in younger individuals to ~25% in older individuals (Christie and Kamen, 2006), or the decreased maximal firing rate and decline in maximal voluntary contraction observed with increasing age (Ling et al., 2009). Denervation may be compensated for by the branching of surviving motor neurons resulting in increased motor unit size, as seen in healthy ageing where motor unit potential in non- and pre-sarcopenic men was larger than young men by 26 and 41%, respectively (Piasecki et al., 2018). However in sarcopenic men the motor unit potential was significantly smaller than the pre-sarcopenic group, suggesting failure to expand motor units and reinnervate muscle fibres plays a role in sarcopenic muscle and could provide a distinction between healthy ageing and the development of sarcopenia. Neuromuscular instability has also been associated with unloading with both 3 and 14 days of bed rest resulting in significant increases in the number of NCAM

positive fibres (Demangel et al., 2017; Arentson-Lantz et al., 2016). Additionally, markers of denervation were observed in individuals with an inactive lifestyle, with a significantly higher percentage of denervated muscle fibres in sedentary seniors than both young and active older individuals (Mosole et al., 2014). In contrast, denervation does not appear to be a driver of cachexia. A recent study found that despite muscle fibre diameter being reduced by nearly 15% in cachectic patients, the morphology of neuromuscular junctions remained conserved across cachectic and non-cachectic individuals, with no evidence of pathology or denervation (Boehm et al., 2020). As such, investigating changes to the neuromuscular system may provide a distinction between cachexia and other muscle wasting conditions that represent unique aetiologies.

However, metabolomics studies investigating such disturbances are lacking. Murine models have been used to show the potential of untargeted analysis in this area, such as the identification of a 1.8-fold increase in acetylcholine in aged mice, likely representing a compensatory mechanism for the degeneration of neuromuscular junctions (Uchitomi et al., 2019), or large-scale changes to cell metabolism identified in models of cachexia (Pin et al., 2019) or unloading (Chakraborty et al., 2020), but whether these findings translate to human cohorts is unknown. Metabolic disturbances contribute significantly to muscle loss, therefore validating these signatures is essential in attempting to understand the mechanisms that drive physiological adaptations in skeletal muscle.

1.4.1.5. Current limitations of metabolomics research

Despite clear interest in the use of metabolomics to study muscle wasting in a range of conditions, the key limitation to the current literature is that many metabolomics studies lack relation to the decline in relevant parameters of health associated with

wasting conditions or measures of muscle mass and strength. For instance, while many studies propose associations between metabolite expression and mitochondrial respiration, only one study provided evidence of correlation between metabolites indicative of mitochondrial function and reduction in muscle strength (Kemp et al., 2020). Therefore associations between metabolite abundance and known physiological adaptations in muscle wasting conditions cannot be validated. The associations discussed thus far are therefore highly speculative and the extent of the relationship between changes in the metabolome and adaptations to low muscle health cannot be fully comprehended. This may be a significant contributing factor in explaining why, despite targeted efforts, advancements in clinical biomarkers of wasting conditions have not been made. To fully comprehend the relationship between adaptations in the metabolome and the development of wasting conditions, physiological outcome measures of clinically relevant parameters including measures of muscle metabolism (for example, oxidative capacity) and function, strength and mass should be included in study designs.

The cross-sectional nature of many metabolomics studies further limits the establishment of causal links between metabolite level and disease. Cross-sectional studies are only able to establish differences in metabolite level between study populations at one timepoint and therefore cannot assess metabolic change over time, which may be key in the development of slow onset wasting conditions such as sarcopenia which develops over a period of years, nor can they identify where in the metabolic pathway dysregulation occurs, preventing effective interventions from being developed. In addition, although there is recent evidence from murine models to suggest metabolic disturbances beyond that of amino acid or lipid metabolism are associated with a decline in skeletal muscle health and the subsequent loss of muscle

mass across wasting conditions there is little focus in this area allowing potential key insights into the aetiology of muscle wasting to go undetected.

There is some disagreement on how accurately plasma metabolites reflect tissue metabolomic profiles, with some arguing that plasma is an inappropriate proxy for studying metabolism in muscle tissue (Fazelzadeh et al., 2016b) while others suggest the plasma metabolome has a high concordance with skeletal muscle metabolism with similar directional changes in metabolic profile (Dutta et al., 2012; Wu et al., 2022). Developing a full understanding of the link between plasma and muscle metabolomic profiles would be highly beneficial in identifying markers of metabolic dysregulation in sarcopenia and cachexia. Finally, differences in operational definitions of sarcopenia and cachexia (Cruz-Jentoft et al., 2019; Fielding et al., 2011; Evans et al., 2008; Morley et al., 2011; Chen et al., 2014; Fearon et al., 2011; Bijlsma et al., 2013; Van Ancum et al., 2020; Vanhoutte et al., 2016) have led to discrepancies in classification of disease between studies, hindering the ability to make accurate comparisons across studies and between different states of muscle wasting. This thesis aims to address these limitations in relation to the study of muscle wasting.

1.5. Thesis aims

Despite the recent advancements in this field the key gaps in the current literature relate to the lack of integration between physiological outcomes and metabolomics data and poor cohesion across study cohorts which limits ability to identify similarities and differences between the aetiologies underlying different states of muscle mass loss. Identifying potential universal mechanisms of muscular adaptations would be of great benefit in the development of successful therapeutics, but this requires a much greater understanding of the common links between conditions. In this thesis, I will explore differences in the plasma metabolomic profile of several cohorts of well

characterised participants with defined adaptations in skeletal muscle physiology relating to loss of muscle mass and strength, with correlation to relevant physiological parameters associated with declines in muscle health including lean mass, rate of oxidation, and insulin sensitivity to gain greater understanding of into the relationship of phenotypic changes in muscle and the plasma metabolome.

Additionally, although measuring metabolite profiles in muscle directly allows for clear links between metabolite expression and phenotypic changes to be established, the collection of muscle tissue is difficult and highly invasive. It would be more beneficial to develop alternative approaches to assess changes in the muscle indirectly through measurements of plasma metabolite level. In this thesis, in addition to identifying markers of wasting and their biological relevance, I will test associations between the plasma and muscle metabolomes.

The aims of this thesis are therefore as follows:

1. To use untargeted metabolomics to fully characterise the plasma metabolome in several conditions associated with adaptations in skeletal muscle leading to poorer muscle metabolic health and mass loss
2. To identify disrupted metabolic pathways in these conditions in order to understand the underlying mechanisms leading to metabolic dysregulation of skeletal muscle and their role in the loss of skeletal muscle mass
3. To compare the plasma metabolome of different study cohorts to investigate whether there is a universal mechanism underlying the loss of muscle mass

Chapter 2. General methods

This chapter describes the method development performed to find the optimal extraction method for untargeted metabolomics analysis of human plasma by mass spectrometry, in addition to the general methods and materials used across experimental Chapters 4, 5 and 6. Sample preparation and analysis by mass spectrometry in Chapter 3 was performed as part of a collaborative study at the Phenome Centre, University of Birmingham using different methods which are described in detail in the relevant chapter.

2.1. Consumables and equipment

2.1.1. Solvents and reagents

The following solvents and reagents were used in preparation of plasma samples and separation of metabolites within samples by liquid chromatography:

Table 2.1 Solvents and reagents used in sample preparation and liquid chromatography separation of metabolites in method validation and experimental method protocols

Solvents and reagents	Manufacturer	Location
^{2}H3-Caproate	QMX Laboratories	Thaxted, UK
^{2}H31-Palmitate	Sigma Aldrich	Gillingham, UK
^{2}H2-Glucose	Sigma Aldrich	Gillingham, UK
Nortestosterone	Sigma Aldrich	Gillingham, UK
Methanol (MeOH)	Thermo Fisher Scientific	Hemel Hempstead, UK
Double distilled water (ddH_2O)	Sigma Aldrich	Gillingham, UK
Chloroform ($CHCl_3$)	Thermo Fisher Scientific	Hemel Hempstead, UK
Methyl tert-butyl ether (MTBE)	Thermo Fisher Scientific	Hemel Hempstead, UK
Ethanol (EtOH)	Thermo Fisher Scientific	Hemel Hempstead, UK
Proteinase K	New England Biolabs	Hitchin, UK
Isopropanol (IPA)	Thermo Fisher Scientific	Hemel Hempstead, UK
Acetonitrile (MeCN)	Thermo Fisher Scientific	Hemel Hempstead, UK
Ammonium formate	Thermo Fisher Scientific	Hemel Hempstead, UK
Formic acid	Thermo Fisher Scientific	Hemel Hempstead, UK

2.1.2. Laboratory equipment

The following equipment was used in preparation of plasma samples, separation of metabolites in samples by liquid chromatography, and acquisition of metabolomics data by mass spectrometry:

Table 2.2 Laboratory equipment used in sample preparation, separation of metabolites by liquid chromatography, and acquisition of metabolomics data by mass spectrometry in method validation and experimental method protocols

Equipment	Manufacturer	Location
Heraeus Fresco 17 centrifuge	Thermo Fisher Scientific	Hemel Hempstead, UK
VXR Vibrax Shaker	IKA	Staufen, Germany
TurboVap	Biotage	Hengoed, UK
Ultimate 3000 UHPLC system	Thermo Fisher Scientific	Hemel Hempstead, UK
InfinityLab Poroshell 120 HILIC-Z column	Agilent	Cheadle, UK
Modus C18 column	Chromatography Direct	Runcorn, UK
Q-Exactive Hybrid Quadrupole-Orbitrap Mass Spectrometer	Thermo Fisher Scientific	Hemel Hempstead, UK
Accela UHPLC pump and autosampler	Thermo Fisher Scientific	Hemel Hempstead, UK
Zorbax SB-Aq RRHD column	Agilent	Cheadle, UK

2.2. Method validation

2.2.1. Comparison of extraction methods for metabolites in plasma

To assess the effectiveness of different sample preparation methods in the extraction of plasma metabolites three popular extraction methods were identified from the literature and selected for testing (Bligh and Dyer, 1959; Sostare et al., 2018; Wawrzyniak et al., 2018). For all methods pooled, fasted plasma from healthy adults provided from an inhouse biobank was first thawed at room temperature and centrifuged at 17,000 xg for 2 minutes at room temperature to pellet the fibrin clot. 50 µl of plasma was pipetted to a clean Eppendorf/Microcentrifuge tube. ^{2}H31-caproate, ^{2}H31-palmitate, ^{2}H2-glucose and nortestosterone (10µl of each) were

pipetted into each sample for use as internal standards. The same procedure was performed for each of the methods described below.

2.2.1.1. Method 1: The modified Bligh & Dyer method

First 5.5 µl of ice cold MeOH per µl plasma and 0.9 µl ddH_2O per µl plasma were added to each tube. The samples were then vortexed for 10 seconds. Two µl $CHCl_3$ per µl plasma was added to each tube and samples were shaken on a VXR Vibrax shaker for 2 minutes at 2,000 rpm. Samples were then centrifuged at 2,500 xg for 10 minutes at 18°C to remove cellular debris and the supernatant was transferred to a fresh tube. Two µl $CHCl_3$ per µl plasma and 2.27 µl ddH_2O per µl plasma were added to aid phase separation, then samples were shaken at 2,000 rpm for 2 minutes and left at room temperature for 10 minutes to allow for phase separation to complete followed by centrifugation at 2,500 xg for 20 minutes at 18°C. Following phase separation 300 µl of the upper, polar phase, and 300 µl of the lower, non-polar phase were each carefully removed into clean 1.5 ml autosampler vials. Both phases were then dried at 30°C under N_2 for 40 minutes.

2.2.1.2. Method 2: The modified Matyash method

First 5.5 µl ice cold MeOH per µl plasma and 0.9 µl ddH_2O per µl plasma were added to each sample and tubes were vortexed for 10 seconds. Two µl MTBE per µl plasma was added and samples were shaken on a VXR Vibrax shaker for 3 minutes at 2,000 rpm. Following this, 3.2 µl MTBE per µl plasma and 3.42 µl ddH_2O per µl plasma were then added to samples to aid phase separation and tubes were shaken at 2,000 rpm for 1 minute. Samples were then incubated at room temperature for 10 minutes, followed by centrifugation at 2,500 xg for 10 minutes at 18°C.

When following the protocol described above the polar and non-polar phases failed to separate on addition of MTBE and ddH_2O so different solvent ratios were tested.

Internal standards were added to 50 µl plasma as above, then 3.87 µl MeOH per µl plasma and 12.9 µl MTBE per µl plasma were added to each sample and tubes were vortexed for 10 seconds and shaken for 3 minutes at 2,000 rpm. Next 3.3 µl ddH_2O per µl plasma was added then samples were briefly vortexed and left at room temperature for 10 minutes. Samples were centrifuged at 2,500 xg for 10 minutes at 18°C. Finally, 300 µl of the upper, polar phase, and 300 µl of the lower, non-polar phase, were each carefully removed into clean 1.5 ml autosampler vials. Both phases were then dried at 30°C under N_2 for 40 minutes.

2.2.1.3. Method 3: A single phase Methanol:Ethanol solvent extraction method

Three µl ice cold MeOH:EtOH (1:1, v/v) per µl plasma was added to the plasma and the samples were vortexed for 10 seconds. Samples were stored at -20°C for 60 minutes followed by centrifugation at 2,500 xg for 15 minutes at 4°C. The supernatant was removed to a clean 1.5 ml autosampler vial and dried under N_2 at 30°C for 40 minutes.

2.2.1.4. Methods 4, 5 and 6: Addition of proteinase K

Evidence in the literature suggested that the addition of proteinase K (PK), a serine protease enzyme, improved metabolome coverage and reproducibility in both single- and dual-phase extraction protocols (Wawrzyniak et al., 2018; Zhang et al., 2019). Therefore for each protocol tested above 0.02 µl PK per µl plasma was added to the plasma after the addition of the internal standards. Samples were then incubated at 37°C for 15 minutes before the ice-cold solvents were added and Methods 1, 2 and 3, respectively, were then followed as detailed above.

2.2.1.5. Resuspension of samples

For methods 1, 2, 4 and 5, the polar phase was resuspended in 100 µl 80:20 MeOH:ddH_2O with 0.25% formic acid. The non-polar phase was first resuspended in 50 µl 60:30:4.5 $CHCl_3$:MeOH:ddH_2O and then vortexed for 10 seconds after which 50 µl 2:1:1 IPA:MeCN:ddH_2O was added to the resuspension. For methods 3 and 6, all samples were resuspended in 100 µl 80:20 MeOH:ddH_2O.

2.2.2. Separation of metabolites by liquid chromatography

Samples were separated using an UltiMate 3000 UHPLC system. For HILIC chromatography, an InfinityLab Poroshell 120 HILIC-Z column (2.1mm x 150mm x 2.7µm) was used with mobile phase A 10mM ammonium formate in 90% acetonitrile with 0.1% formic acid and mobile phase B 10mM ammonium formate in 50% acetonitrile with 0.1% formic acid. Mobile phase A increased from 1% to 95% over a gradient with total run time of 28 minutes. For reverse phase (RP) chromatography, a Modus C18 column (30mm x 3.0mm x 1.6µm) was used with mobile phase A 100% ddH_2O with 0.1% formic acid and mobile phase B 100% MeOH with 0.1% formic acid. Mobile phase B increased from 1% to 95% over a gradient with total run time of 21 minutes.

For each sample, 5 µl of suspension was injected. Injection order was randomised to avoid bias. A blank sample containing only the resuspension buffer was injected at the start of the run to assess systematic contamination. Eight pooled QCs were injected following the blank to condition the column. Pooled QCs were also injected every 10 experimental samples to assess sample drift within the acquisition (Figure 2.1). Due to technical error during the run, polar samples were run in two batches. The same pooled QCs were used across batches to allow for the correction of variation introduced by multiple acquisition batches.

Injection order	Sample type
1	Solvent blank
2	Conditioning QC 1
3	Conditioning QC 2
4	Conditioning QC 3
5	Conditioning QC 4
6	Conditioning QC 5
7	Conditioning QC 6
8	Conditioning QC 7
9	Conditioning QC 8
10	Pooled QC sample 1
11	Sample 3
12	Sample 5
13	Sample 9
14	Sample 12
15	Sample 2
16	Sample 7
17	Sample 4
18	Sample 8
19	Sample 14
20	Sample 15
21	Pooled QC sample 2
22	Sample 20
23	Sample 18
24	Sample 17
25	Sample 11
26	Sample 10
27	Sample 13
28	Sample 19
29	Sample 6
30	Sample 16
31	Sample 1
32	Pooled QC Sample 3

Figure 2.1 Example of sample injection order in LC run

A typical set up of samples for an LC run composed of blank samples, pooled QC samples and experimental samples. At the beginning of the run, a blank sample containing only the resuspension solvent is injected. Following the blank, 8 pooled QC samples are injected to condition the column before experimental samples are injected. The same pooled QC samples are then injected periodically throughout the run to assess sample drift over the course of the run. The experimental samples are given a number according to the order in which they were prepared but placed in a randomised order throughout the run to prevent bias.

2.2.3. Acquisition of data by mass spectrometry

Data was collected using the Q-Exactive Hybrid Quadrupole-Orbitrap Mass Spectrometer operated in both positive and negative ionisation modes for HILIC and RP chromatography (Table 2.3). Unless otherwise specified in the table, units of measurement are vendor specific Arbitrary Units.

Table 2.3 MS and MS/MS scan parameters for the acquisition of polar and non-polar metabolites in testing of extraction methods

Parameter	**HILIC**		**Reverse phase**	
Mode	Positive	Negative	Positive	Negative
MS scan parameters				
Scan type	Full MS		Full MS	
Scan range	70 – 1,050 m/z		70 – 2,000 m/z	
Fragmentation	None		None	
Resolution	70,000		70,000	
AGC target	1e6		3e6	
Maximum IT	100ms	200ms	100ms	250ms
Microscans	5		1	
Sheath gas flow	54		48	
Aux gas flow	13		11	
Sweep gas flow	0	3	5	
Spray voltage	4kV	3.5kV	3kV	3.5kV
Capillary temperature	260°C	320°C	300°C	320°C
S-lens RF level	50	60	60	
Aux gas flow heater temperature	430°C	320°C	300°C	
MS/MS scan parameters				
Resolution	17,500		17,500	
AGC target	1e6		1e6	
Maximum IT	50ms		50ms	
topN peaks	3		3	
Isolation window	1.5 m/z		1.5 m/z	
Normalised collision energy	25, 60, 100%		25, 60, 100%	

2.2.4. Pre-processing and filtering of acquired data

Raw data acquired from the mass spectrometer in both ionisation modes and polarities was converted to mzXML file format using MS Convert software (ProteoWizard, Palo Alto, USA) and imported into R (version 3.4) utilising the xcms (Smith et al., 2006) and CAMERA packages (Kuhl et al., 2012). Files were processed using inhouse R scripts provided in Appendix 1 (R Core Team, 2021).

Peak width was defined from the width of the narrowest and widest peaks, determined from manual inspection of the chromatograms. Parameters for peak detection were defined using the centWave algorithm with tolerance set at 20 ppm. Peaks were detected using the findChromPeaks function of xcms and aligned using the Obiwarp method and adjustRtime function to m/z bins of 0.6. Bin size was chosen to avoid signals from multiple compounds being converged into one signal by restrictions that were too lenient while also avoiding a signal from one compound being split by an overly conservative restriction. Peaks were grouped within bins using a bandwidth defined individually for each ion mode and polarity. Feature definitions for each metabolite were extracted to return a data frame containing the peak signal matched to m/z and retention time boundaries. The signal in areas of missing peaks was integrated from the m/z and retention time ranges defined in the data frame using the fillChromPeaks function. Finally, peaks were annotated with the CAMERA package (version 3.11) and data was exported as a data frame of metabolite feature vs sample ID with associated chromatographic peak areas for each detected metabolite.

As polar samples were run in two batches, datasets produced from peak picking were combined to produce a single merged dataset. Inter-batch alignment was performed using the MetaboAnalyst web platform 4.0 (available at https://dev.metaboanalyst.ca/MetaboAnalyst/upload/BatchUpload.xhtml) using the ComBat alignment method for both the positive and negative acquisition modes. Only

overlapping features across both batches were used. Intra-batch drift effect was corrected for using cyclic LOESS conducted using R package NormalyzerDE (version 1.6.0) (Willforss et al., 2019). The data were then filtered according to the following acceptance criteria: the signal from a blank sample was less than 5% of the mean biological signal, the feature was present in at least 80% of all samples, and coefficient of variation (CV) was less than 10% after normalisation. An overview of this process is provided in Figure 2.2.

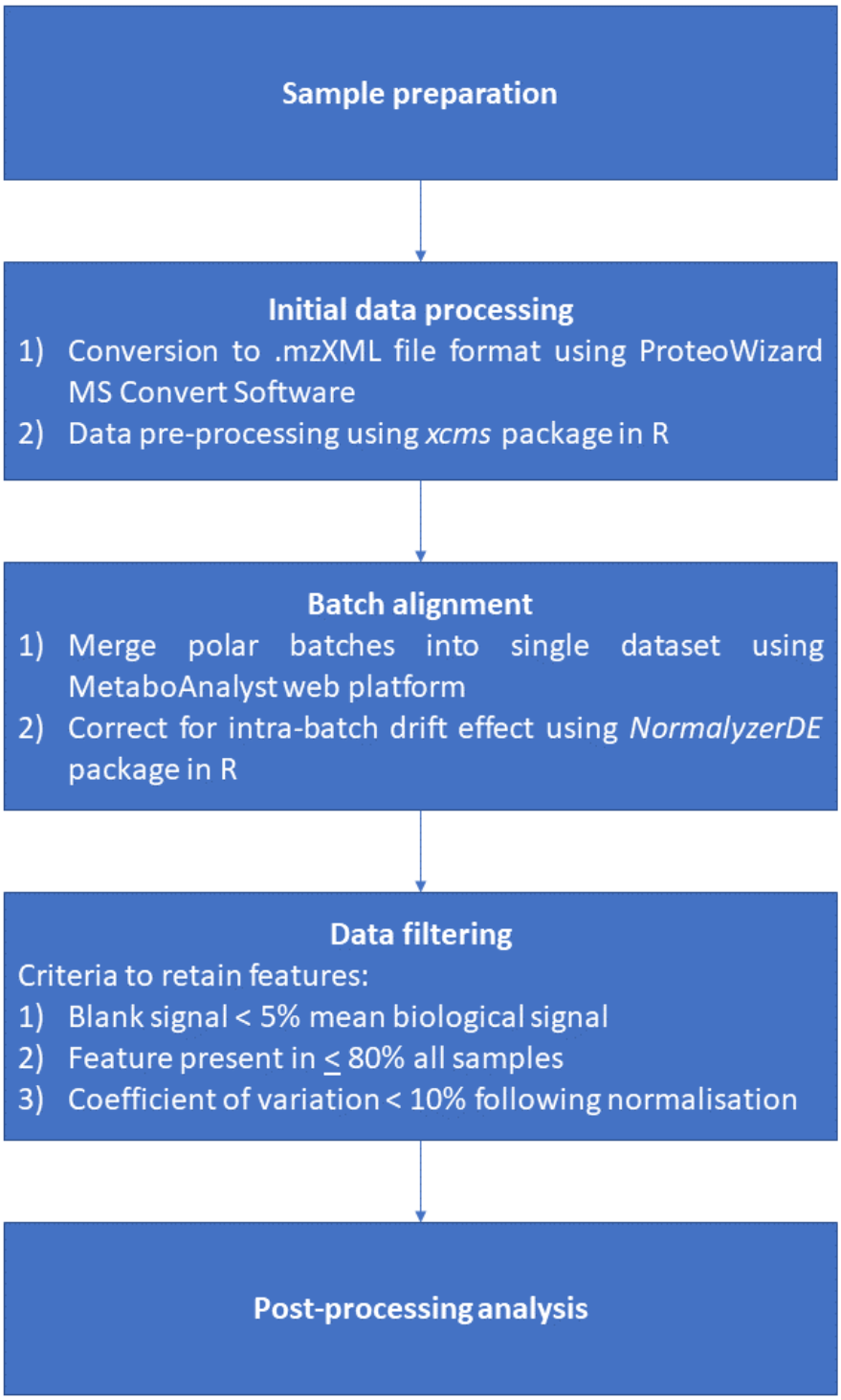

Figure 2.2 Workflow for pre-processing and processing of method validation samples

Raw data acquired by UHPLC-MS/MS was computationally processed to prepare it in appropriate format for subsequent data analysis. Processing output was a matrix of metabolite ID vs sample ID with chromatographic peak area for each detected metabolite

2.2.5. Data analysis

For each method, the total number of detected features in each polarity and ionisation mode that remained after processing and filtering were determined. From the total number of features, the percentage of features matching the acceptance criteria was calculated (Table 2.4). Reproducibility of the extraction methods was compared using the CV of all accepted features for each method (Figure 2.3). Incubation with PK generally increased the percentage of the accepted features relative to the same extraction method without PK, however it also increased variability in all methods. The Bligh and Dyer method had the most consistency of the percentage of accepted features across polar and non-polar samples. CVs across extraction methods were similar. Therefore, due to consistency across accepted features, the Bligh and Dyer method was selected as the most appropriate for use in future studies and was used for analyses in chapters 4, 5 and 6 with minor adaptions.

Table 2.4 Comparison of six extraction methods based on the total number of features detected and percentage of features accepted using filtering criteria from an extraction of human plasma

Method	**Polarity**	**Ion mode**	**Number of features detected**	**Features accepted (%)**
Bligh and Dyer	Polar	Positive	2153	48.68
		Negative	2828	46.78
	Non-polar	Positive	4584	25.41
		Negative	2592	35.65
Bligh and Dyer with enzyme	Polar	Positive	5294	72.25
		Negative	3627	57.29
	Non-polar	Positive	6935	47.27
		Negative	4031	2.431
Matyash	Polar	Positive	1671	33.81
		Negative	2198	26.43
	Non-polar	Positive	5698	45.05
		Negative	4119	12.84
Matyash with enzyme	Polar	Positive	4854	77.85
		Negative	3671	61.05
	Non-polar	Positive	7436	55.51
		Negative	5957	57.58
Single phase	Polar	Positive	1966	54.02
		Negative	3003	49.78
	Non-polar	Positive	3299	90.15
		Negative	3962	4.89
Single phase with enzyme	Polar	Positive	5698	80.13
		Negative	4401	68.28
	Non-polar	Positive	9683	69.85
		Negative	1732	1.27

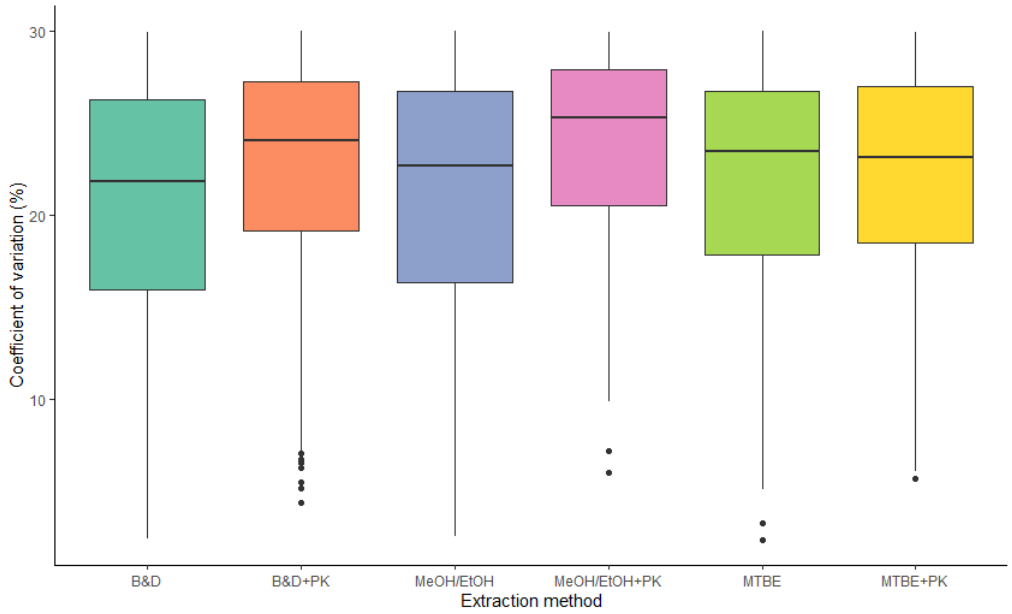

Figure 2.3 Representative example of comparison of six extraction methods based on reproducibility

Data from non-polar positive datasets. Boxplots representing coefficient of variation (CV) of all accepted features for each of the extraction methods tested. Reproducibility was similar across all methods but tended to be higher when proteinase K (PK) was added.

2.3. Metabolite extraction from plasma in studies

For all experiments where metabolite extraction from plasma samples was performed, metabolites were extracted from plasma according to the principles of the Bligh and Dyer method detailed in section 2.2.1.1. Further optimisation was performed following the method development work to ensure reproducible analyses across studies. The volumes of solvents and adaptations to the resuspension solvents used were based on work published by other groups which found the best metabolite yield and reproducibility (Southam et al., 2020). No benefit was found from including the internal standard mix for untargeted work, therefore internal standards were removed from the protocol to improve ease of workflow. The protocol described below is the final protocol used throughout experimental Chapters 4, 5 and 6 of this thesis.

First 320 µl ice-cold MeOH and 78 µl chilled ddH_2O was added to 50 µl plasma and vortex mixed for 10 seconds. Following this 320 µl ice-cold $CHCl_3$ and 160 µl ddH_2O was added to the same tube, vortex mixed for 10 seconds and shaken for 2 minutes at 2000 rpm. Samples were incubated at 4°C for 10 minutes, then centrifuged at 17,000 xg for 10 minutes at 4°C. Finally, 377 µl upper, polar phase and 273 µl lower, non-polar phase were each pipetted into clean autosampler vials. Both phases were dried at 30°C under N_2 and stored at -80°C until ready for analyses.

Prior to analysis, samples were suspended in 75:25 MeCN:ddH_2O and 75:25 IPA:ddH_2O for HILIC and RP chromatography, respectively. Ten µl was removed from each suspended plasma sample to a clean Eppendorf tube and briefly vortexed to create a pooled QC which acts as a representative sample and can be used in the evaluation of coefficients of variation for each metabolite (Beger et al., 2019). One hundred µl of the pooled QC was transferred into a new autosampler vial for analysis.

As the total number of samples in each study was larger than the maximum that could fit in the shaker and centrifuge at one time, samples were randomly assigned to equal sized batches for preparation such that each batch could fit in the equipment. Random assignment was chosen to reduce possible variation introduced by multiple sample preparations. A sample composed of fasted plasma from an inhouse biobank was prepared in each batch for use as an inter-batch QC to assess technical variation across batches. Additionally, a sample containing 50 µl ddH_2O was prepared alongside the plasma samples in an identical manner for use as an extraction blank to account for background noise from features in the extraction or suspension solvents.

2.4. Parameters for the separation of compounds by liquid chromatography

Further optimisation of the gradient methods was performed to provide the optimal throughput for large numbers of samples which reduced the run time from 28 minutes to 17.5 minutes for HILIC and 21 minutes to 15.5 minutes for RP. Improvement of sample throughput in RP was also achieved by using a different chromatographic column.

Samples from all preparation batches were combined in a single batch for data acquisition. Separation was performed on an Accela UHPLC pump and autosampler operated by Xcalibur software. For HILIC chromatography, an InfinityLab Poroshell 120 HILIC-Z column (2.1mm x 150mm x 2.7µm) was used with mobile phase A 10mM ammonium formate in 90% acetonitrile with 0.1% formic acid and mobile phase B 10mM ammonium formate in 50% acetonitrile with 0.1% formic acid. For RP, a Zorbax SB-Aq RRHD column (2.1mm x 100mm x 1.8µm) was used with mobile phase A ddH2O with 0.1% formic acid and mobile phase B methanol with 0.1% formic acid. Gradient programs are provided in Table 2.5. For each sample, 5 µl was injected. Injection order was randomised to avoid bias. A blank containing only the resuspension solvent was injected at the start of the run to assess systematic contamination. Eight pooled QCs were injected to condition the column followed by a pooled QC for MS/MS fragmentation to aid in metabolite annotation. Pooled QCs were also injected every 10 samples to assess drift effect and inter-batch QCs were injected every 20 samples to allow for the correction of variation introduced by different preparation batches (batch effect) if necessary. A second QC for MS/MS fragmentation was injected at the end of the run. Extraction blanks were injected after the MS/MS QC samples to assess for contamination introduced in the extraction process (Figure 2.4).

Table 2.5 Gradient elution programs for the separation of metabolites by ultra high performance liquid chromatography in each polarity

Time	Mobile Phase A (%)	Mobile Phase B (%)
Reverse phase (flow rate 400 µl/min)		
0.00	99.00	1.00
1.00	99.00	1.00
3.00	85.00	15.00
6.00	5.00	95.00
10.00	5.00	95.00
10.50	99.00	1.00
15.50	99.00	1.00
HILIC (flow rate 400 µl/min)		
0.00	99.00	1.00
0.50	99.00	1.00
2.00	50.00	50.00
10.00	1.00	99.00
12.00	1.00	99.00
12.50	99.00	1.00
17.50	99.00	1.00

Injection order	Sample type
1	Solvent blank
2	Conditioning QC 1
3	Conditioning QC 2
4	Conditioning QC 3
5	Conditioning QC 4
6	Conditioning QC 5
7	Conditioning QC 6
8	Conditioning QC 7
9	Conditioning QC 8
10	Pooled QC sample 1
11	Pooled QC MSn Sample 1
12	Extraction blank 1
13	Sample 3
14	Sample 5
15	Sample 9
16	Sample 12
17	Sample 2
18	Sample 7
19	Sample 4
20	Sample 8
21	Sample 14
22	Sample 15
23	Pooled QC sample 2
24	Sample 20
25	Sample 18
26	Sample 17
27	Sample 11
28	Sample 10
34	Pooled QC Sample 3
35	Pooled QC MSn Sample 2
36	Extraction blank 2

Figure 2.4 Example of sample injection order in LC run for experimental chapters

A typical set up of samples for an LC run composed of blank samples, pooled QC samples and experimental samples. At the beginning of the run, a blank sample containing only the resuspension solvent is injected. Following the blank, 8 pooled QC samples are injected to condition the column before experimental samples are injected. The same pooled QC samples are then injected periodically throughout the run to assess sample drift over the course of the run. 2 QC samples are injected for tandem mass spectrometry fragmentation (MSn samples) to aid in annotation of metabolites by generating fragmentation patterns. Extraction blanks are injected after each MSn sample for assessment of contamination introduced in the sample preparation stage. The experimental samples are given a number according to the order in which they were prepared but placed in a randomised order throughout the run to prevent bias

2.1. Parameters for acquisition of data by mass spectrometry

Acquisition of data was performed by a Q-Exactive Hybrid Quadrupole-Orbitrap Mass Spectrometer operated in both positive and negative acquisition modes for HILIC and RP chromatography (Table 2.6). The scan range parameter was adapted from section 2.1.3 after further optimisation for optimal data acquisition by mass spectrometry analysis. Unless otherwise specified in the table, units of measurement are vendor specific Arbitrary Units. Examples of chromatograms acquired by mass spectrometry are provided in the appendices.

Table 2.6 Final MS and MS/MS scan parameters for the acquisition of polar and non-polar metabolites for experimental chapters

Parameter	**HILIC**		**Reverse phase**	
Mode	Positive	Negative	Positive	Negative
MS scan parameters				
Scan type	Full MS		Full MS	
Scan range	70 – 1,050 m/z		150 – 2,000 m/z	
Fragmentation	None		None	
Resolution	70,000		70,000	
AGC target	1e6		3e6	
Maximum IT	100ms	200ms	100ms	250ms
Microscans	5		1	
Sheath gas flow	54		48	
Aux gas flow	13		11	
Sweep gas flow	0	3	5	
Spray voltage	4kV	3.5kV	3kV	3.5kV
Capillary temperature	260°C	320°C	300°C	320°C
S-lens RF level	50	60	60	
Aux gas flow heater temperature	430°C	320°C	300°C	
MS/MS scan parameters				
Resolution	17,500		17,500	
AGC target	1e6		1e6	
Maximum IT	50ms		50ms	
topN peaks	3		3	
Isolation window	1.5 m/z		1.5 m/z	
Normalised collision energy	25, 60, 100%		25, 60, 100%	

2.2. Pre-processing and filtering of acquired data

Data pre-processing was conducted in R using the same parameters as detailed in section 2.1.4. Due to updated software, version 1.4.1106 of R was used for pre-processing.

Filtering parameters varied from section 2.1.4 due to the release of new computational packages which allowed for filtering of data output from xcms pre-processing in R. Filtering of data was performed using the pmp R package (Jankevics et al., 2021). Following recommended guidelines for untargeted metabolomics (Broadhurst et al., 2018) metabolite features were retained when: peaks were present in at least 70% of pooled QC samples, relative standard deviation was less than 30%, and the extraction blank to mean QC peak area was less than 50%. PQN was applied to the remaining features, then missing values were imputed using the kNN algorithm. To correct for possible signal drift across the acquisition or batch effect, quality control robust spline correction (QC-RSC) was applied to the data matrix using inter-batch QCs and injection order of samples. Data were transformed using a variance stabilised generalised logarithm (glog) approach prior to analysis to correct heteroscedasticity of distribution and exported as a data matrix of metabolite ID vs sample ID with glog transformation of area of peaks that remained after filtering was applied for each detected metabolite. This finalised workflow is summarised in Figure 2.5. Following pre-processing data underwent statistical analysis which is detailed in subsequent chapters, although a general overview of the analytical pipeline is provided in Figure 2.6.

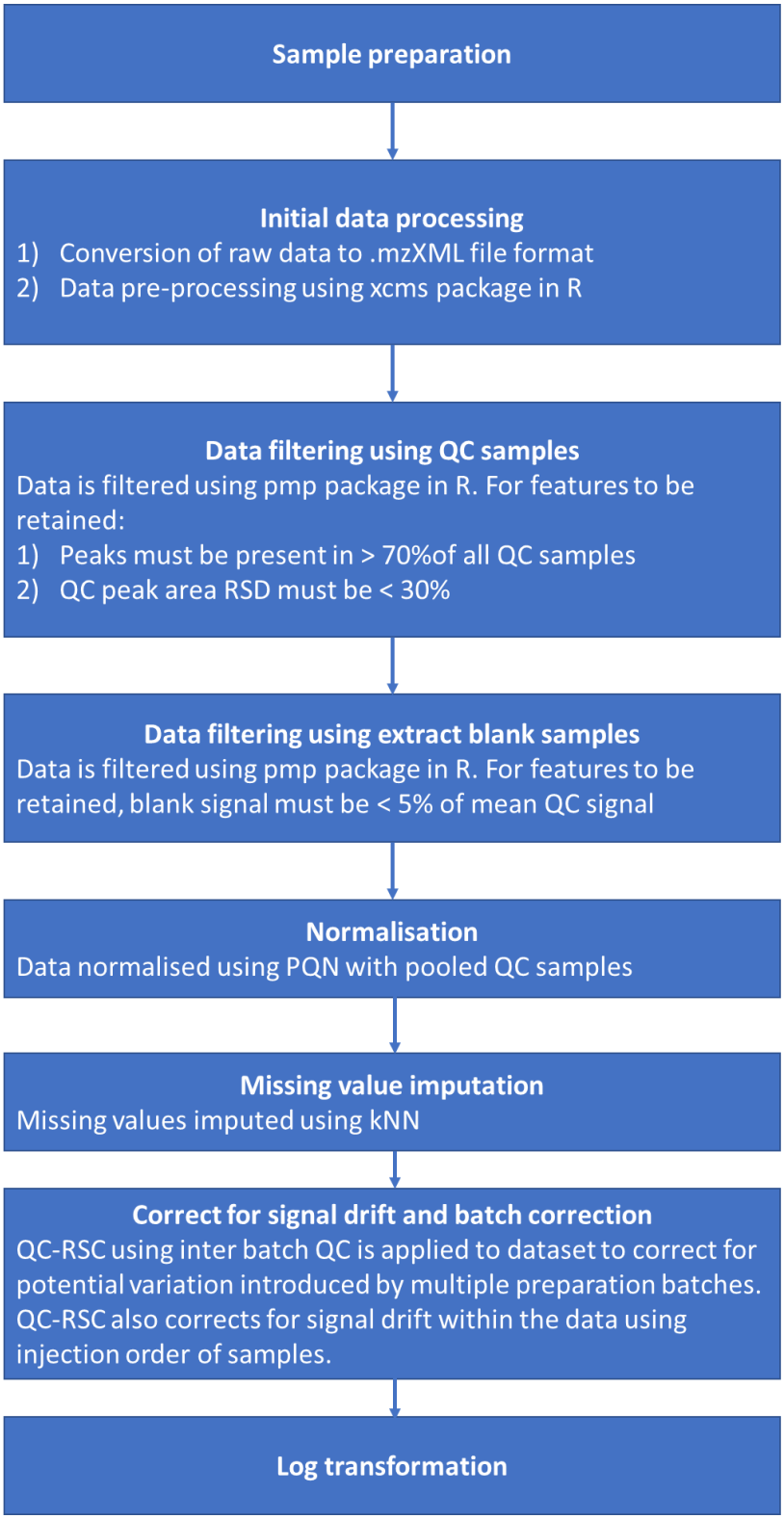

Figure 2.5 General workflow for pre-processing and processing of untargeted metabolomics data

Raw data acquired by UHPLC-MS/MS was computationally processed to prepare it in appropriate format for subsequent data analysis. Processing output was a matrix of metabolite ID vs sample ID with log transformation of chromatographic peak area for each detected metabolite.

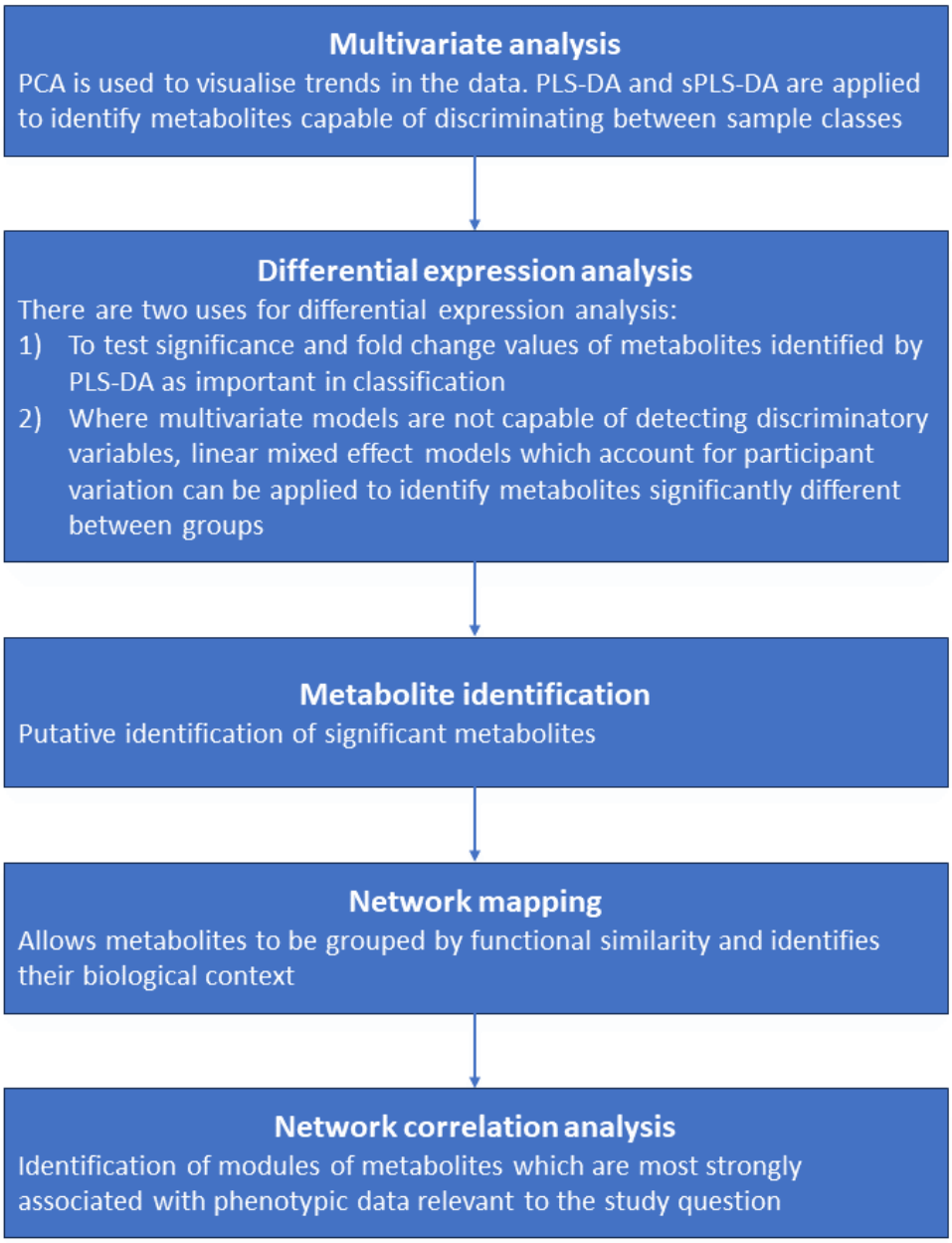

Figure 2.6 General workflow for statistical analysis of metabolomics datasets following sample pre-processing and processing steps

Chapter 3. Metabolomic analysis of plasma from healthy young men following chronic bed rest

3.1. Background

3.1.1. Skeletal muscle deconditioning following bed rest

Reduced mechanical loading of skeletal muscle due to prolonged periods of disuse, such as bed rest, immobilisation or spaceflight (Bowden Davies et al., 2019), is associated with the development of muscle level deconditioning, the process of physiological change that leads to a physical decline in locomotor function of skeletal muscle (Fovet et al., 2021). Deconditioning is believed to be underpinned by numerous metabolic changes, some of which are described in more detail below.

Firstly, skeletal muscle deconditioning associated with bed rest has well defined detrimental effects on skeletal muscle protein balance (Atherton et al., 2016; Rudrappa et al., 2016) and subsequently muscle mass and strength. These changes develop rapidly and are maintained as bed rest continues, for example one week of bed rest was associated with a 2.6% reduction in lean tissue mass, a 3.2% decline in quadriceps muscle cross-sectional area (CSA), a 6.9% reduction in leg press strength and a 8% reduction in leg extension strength (Dirks et al., 2016). Likewise, an earlier study demonstrated that 1 week of bed rest was associated with a 14% reduction in knee extensor strength (LeBlanc et al., 1992). Reductions continued after 17 weeks of bed rest when reductions in quadriceps (16-18%), ankle flexor (21%) and ankle extensor (30%) muscle volume were observed (LeBlanc et al., 1992). Similarly, 20 days of bed rest was associated with reductions in knee extensor (10%), knee flexor (11%), adductor (7%), and plantar flexor (12%) muscle groups (Akima et al., 2007), although changes in strength were not assessed.

Secondly, the development of insulin resistance, the impaired ability of any given blood insulin concentration to stimulate tissue glucose uptake (Wilcox, 2005) is a

common trait of metabolic dysregulation in deconditioning associated with bed rest regardless of duration. A 67% increase in the net serum insulin response over time to glucose loading via ingestion of 75g glucose, which is indicative of whole-body insulin resistance, was noted following 5 days of bed rest (Hamburg et al., 2007). Plasma insulin concentrations were greater after 7 days bed rest in the fasted state, and in response to infusion of glucose (Stuart et al., 1988), and whole-body and leg glucose uptake under euglycaemic clamp conditions decreased after 7 days of bed rest in healthy young volunteers (Mikines et al., 1991), which clearly demonstrates the development of both whole-body and peripheral insulin resistance with bed rest. Likewise, reduced muscle-level insulin sensitivity and the development of systemic glucose intolerance are reported following chronic bed rest (Rudwill et al., 2018). Data also demonstrates that bed rest has no effect on hepatic glucose utilisation or production (Stuart et al., 1988; Mikines et al., 1991), suggesting that of the development of insulin resistance during bed rest is reflective of changes in muscle glucose uptake.

In healthy conditions insulin promotes the uptake of glucose into skeletal muscle where it is stored in the form of glycogen (non-oxidative glucose disposal) or used as an energy substrate (oxidative glucose disposal) (Argilés et al., 2016). In addition, insulin has an anabolic role in skeletal muscle through its regulation of MPS and MPB. Firstly, insulin inhibits MPB in a dose dependent manner (Fukagawa et al., 1985). Secondly, in the postprandial state insulin signalling increases the transport of EAAs into skeletal muscle and positively regulates the mammalian target of rapamycin signalling pathway (Cynober, 2013), which increases the rate of MPS. Understanding the muscle centric mechanism that underlies the loss of insulin sensitivity may provide some insight into the aetiology of deconditioning and regulation of muscle protein turnover, however the precise causative mechanism is currently unclear.

Insulin resistance in bed rest has historically been linked to the accumulation of IMCL content which is commonly reported as a consequence of bed rest. For example, 28 days of bed rest increased intramyocellular triglyceride content by at least 20% in all participants in a cohort of healthy male volunteers (Cree et al., 2010) and total IMCL content increased 2.7% following 8 weeks bed rest in a group of healthy, young women (Bergouignan et al., 2009). Precisely how the accumulation of IMCL content and insulin resistance are related remains unknown although several mechanisms have been proposed. Initially it was suggested that the accumulation of IMCL content acted as a physical barrier to prevent insulin signalling thereby directly disrupting whole-body glucose homeostasis (Petersen and Shulman, 2006) but more recently it has been proposed that the coating of perilipins on the surface of the droplets influences droplet characteristics, such as inhibiting lipolysis, can induce morphological changes, including alterations to size and shape of the droplet, and affects the droplets' dynamic nature which modulates insulin sensitivity of skeletal muscle (Gemmink et al., 2017). This theory aligns with both changes in the size and shape of lipid droplets in poor quality muscle (Crane et al., 2010; Stephens et al., 2011) and the so-called athletes' paradox, the increase of IMCL content in insulin sensitive endurance trained athletes. Insulin sensitive, trained individuals and insulin resistant, non-trained individuals have similar muscle fat content but in trained muscle lipids are stored in small lipid droplets while in the untrained muscle lipids accumulate in large droplets (Nielsen et al., 2017).

However bed rest studies have historically been confounded by participants' dietary intake not being controlled. It is therefore unclear whether the observed rise in IMCL content is a direct consequence of inactivity or simply a side effect of excess energy. Recent research in which subjects are held in energy balance during bed rest suggest rapid changes in insulin metabolism occur without an increase in IMCL suggesting that

the development of insulin resistance is unrelated to gain in intramuscular fat. For example, IMCL content did not increase after one week of bed rest despite a 29% decrease in whole-body insulin sensitivity and a decline in muscle oxidative capacity when energy balance is maintained (Dirks et al., 2016).

Another possible mechanism underlying insulin resistance is the development of metabolic inflexibility of skeletal muscle. Metabolic inflexibility is defined as the lack of ability to switch from fat to carbohydrate oxidation in response to changes in metabolic or energetic demand such as in the transition from the fasted to the fed state (Galgani et al., 2008; Goodpaster and Sparks, 2018; Smith et al., 2018). Habitual physical activity levels predict metabolic flexibility of skeletal muscle, therefore impairments in metabolic flexibility are strongly associated with deconditioning induced by reduced physical activity and sedentary behaviour (Kelley et al., 1999). For example, 10 days of bed rest led to a decrease in the insulin-mediated suppression of fatty acid rate of appearance in individuals held in energy balance with no gain in fat mass (Coker et al., 2014) however the potential mechanisms underlying change in fatty acid appearance were not explored.

It has previously been suggested that metabolic inflexibility predisposes insulin resistance by the accumulation of incompletely oxidised lipid species in muscle which form as a consequence of higher rates of fat oxidation. The accumulated lipids are suggested to lead to muscle mitochondrial stress and subsequently insulin resistance (Palmer and Clegg, 2022). However it should be noted that while insulin resistance and metabolic inflexibility are clearly linked there is disagreement over whether insulin resistance is a consequence of metabolic inflexibility or a causative factor (Goodpaster and Sparks, 2018). The mechanism underlying development of insulin resistance in bed rest therefore remains unclear.

3.1.2. Metabolomics in the study of adaptations to bed rest

As discussed in Chapter 1, metabolites represent the endpoints of regulatory networks and provide a chemical link between changes occurring at the genomic and phenomic levels (Bujak et al., 2015). Adaptations in the metabolome during an intervention therefore reflect any observed physiological adaptations occurring in response to an internal or external stimulus which disrupts the normal biological state (Wishart, 2019). Undertaking a systems biology approach by adopting metabolomics techniques in traditional intervention studies can provide greater insight into complex physiological mechanisms (Bartel et al., 2015) including metabolic and physiological adaptations to physical inactivity, such as loss of muscle mass and strength or the development of metabolic inflexibility and insulin resistance.

Previous omics work in bed rest studies demonstrates the potential of such an approach. Lipidomics analysis of skeletal muscle tissue found total levels of cardiolipin significantly decreased with 10 days of bed rest (Standley et al., 2020) however given the great diversity of the metabolome there are likely to be wider effects of bed rest on metabolism which remain undetected by a lipid targeted approach. Forty five days of head down bed rest resulted in significant changes in the urinary excretion patterns of metabolites typically associated with muscle mass, such as lower levels of glutamine and guanidoacetate excretion and increased creatinine and glycine excretion, however association with physiological parameters was limited to bone mineral density and therefore the precise association of these metabolites with other physiological adaptations such as the loss of muscle mass remains unclear (P. Chen et al., 2016). Finally, 21 days of bed rest led to an enrichment in pathways involved in aminoacyl-tRNA biosynthesis, glycerophospholipid synthesis, and galactose metabolism, amongst others, but also caused a 2.5 fold reduction in urinary metabolite-metabolite interactions indicating a severe reduction in metabolic

diversity (Sket et al., 2020). However the study did not investigate the correlation between adaptations in the metabolome and physiological parameters representative of adaptation to bed rest.

The application of metabolomics in physiology can be limited by failure to collect physiological endpoint measures related to the study question which can be associated with metabolomic measurements to increase impact and meaningfulness of metabolomics data. Notably, there is a gap in the literature relating metabolite changes associated with bed rest with the known adaptations in insulin sensitivity and fuel substrate oxidation. The current literature also lacks associations between changes in metabolites and the loss of muscle mass in bed rest. The lack of research in this area presents an opportunity for generation of novel insight by employing an untargeted metabolomics approach to study the effects of bed rest on metabolism. Therefore, the aims of this chapter are as follows:

1. To investigate adaptations in the plasma metabolome under conditions of bed-rest induced decrements in insulin-mediated GD and changes in fuel oxidation, and to identify any specific pathways underlying this dysregulation of metabolism
2. To identify associations between specific metabolite changes and changes in GD and fuel oxidation and lean body mass during bed rest

3.2. Methods

3.2.1. Study design

This study utilised samples collected as part of a now published volunteer intervention study (Shur et al., 2022) which was conducted at the Institute of Space Medicine and Physiology, Toulouse, France (ClinicalTrials.gov Identifier: NCT03594799). The study was approved by the Toulouse ethics committee of the Rangueil University Hospital (Comite´ de Protection des Personnes Sud-Ouest outre-Mer I, France) in accordance with the Declaration of Helsinki and the French Health Authorities (Ethics reference 14-981). The study design is as follows:

Healthy, physically active males aged 20 to 45 (n = 20) were recruited to undergo 60 days of -6° head down tilt (HDT) bed rest. Prior to initiating bed rest participants underwent a 2-week run-in phase during which physical activity levels and diet were strictly controlled. During bed rest all activities including eating, washing and toileting were performed in the -6° HDT position. The sleep-wake cycle was controlled with wake up at 07:00 hours and lights out at 23:00 hours. Participants could move from side to side but were not permitted to sit up or stand at any time throughout the study.

Throughout the study period, diet was strictly controlled to keep participants in energy balance. Participants received three meals and one snack per day. Energy requirements were estimated from each participant's resting energy expenditure (REE) determined by indirect calorimetry multiplied by a physical activity level factor (PAL) of 1.2.

Dual energy X-ray absorptiometry (DEXA) scans (Hologic, QDR4500C, Massachusetts, USA) were performed on day -2 (prior to initiation of bed rest) and day 58 (following bed rest) to detect changes in lean body mass. In addition, two experimental visits were performed during the study on day -6 and day 56. Participants were provided a standardised meal the evening before and then fasted from midnight. A 3-hour

hyperinsulinaemic euglycaemic clamp (60 mU/m^2/min) was performed on both visits, and arterialised-venous blood samples were drawn for metabolomic analysis of plasma. On both visits, ventilated hood indirect calorimetry was performed immediately before and during the steady-state period of the insulin clamp to assess whole-body substrate oxidation. Arterialised-venous serum insulin and triglycerides and plasma non-esterified fatty acid (NEFA) concentrations were also measured before and every 15 minutes during the final hour of the clamp (steady-state). Bergström needle muscle biopsy samples were obtained from vastus lateralis before the clamp and at 180 min of the clamp. Two passes through the same entry site were made in each biopsy. The first pass was snap-frozen in liquid nitrogen. A portion of muscle from the second pass was imbedded in OCT mounting medium (361603E, VWR Chemical, Lutterworth, UK) and frozen in cooled isopentane (Thermo Fisher Scientific, Loughborough, UK) with the remaining tissue from the second pass frozen in liquid nitrogen. Muscle tissue was used to measure IMCL content and protein and gene transcripts.

3.2.2. Metabolite extraction from plasma

Preparation of plasma samples for metabolite extraction was performed at the Phenome Centre, University of Birmingham using established protocols (Dunn et al., 2011). 400µl plasma was mixed with 1,200µl MeOH. Samples were centrifuged at 15,800 xg for 15 minutes at room temperature to pellet the protein precipitate. 370µl aliquots of supernatant were lyophilized in a centrifugal vacuum evaporator for 18 hours. A saline blank consisting of 100µl 0.7% (wt/v) sodium chloride and a quality control (QC) plasma sample were prepared alongside the experimental samples. All samples were reconstituted in 100µl water, vortex mixed for 15 seconds and centrifuged at 15,800 xg for 15 minutes. 90µl supernatant was transferred to clean autosampler vials.

3.2.3. Separation of compounds by liquid chromatography and acquisition of data by mass spectrometry

Acquisition of data by UHPLC-MS/MS was conducted at the Phenome Centre, University of Birmingham. Analyses were performed with an Acquity UPLC system (Waters Ltd) coupled to a TOF mass spectrometer (LCT Premier, Waters Ltd). Chromatography was performed on a BEH column (C_{18}, 2.1 x 100mm, 1.7µm, Waters) operating at 50°C. Mobile phase A was ddH_2O with 0.1% (v/v) formic acid and mobile phase B was MeOH with 0.1% (v/v) formic acid. Data was acquired in 'V mode' as centroid data for an m/z range of 50-1,000. A scan time of 0.4s was applied. The mass spectrometer was operated in positive and negative ionisation modes.

3.2.4. Data pre-processing

Data pre-processing was conducted at the Phenome Centre, University of Birmingham. Data were deconvoluted using the xcms package (Smith et al., 2006) in R (R Core Team, 2021). The settings applied for deconvolution were set to default except for step (0.02), S/N threshold (3), mass limit (0.05 amu), bw (10) and mzwid (0.05). Preprocessed data was exported as a data frame of metabolite feature vs sample ID with associated chromatographic peak areas for each detected metabolite.

Per recommended guidelines (Broadhurst et al., 2018) metabolite features were retained when they met the following criteria: present in at least 70% of QC samples, QC relative standard deviation less than 30%, and blank signal of less than 5%. Remaining features were normalised by probabilistic quotient normalisation and log transformed to reduce heteroscedasticity of data.

3.2.5. Statistical analysis

After filtering, normalisation and missing value imputation steps were completed, multivariate statistical analysis was performed on the remaining metabolites. Data for each polarity and ionisation mode was analysed separately. Firstly, PCA was performed to assess data quality and identify trends within the data including

clustering of groups or outlying data points. PLS-DA was next used to assess group classification using pre-bed rest and post-bed rest as class labels for the model. PLS-DA assigns each feature a variable importance in projection (VIP) score summarising the contribution a variable makes to the separation model (Banerjee et al., 2013). If all variables have the same contribution to the model each would be assigned a VIP score of 1. A VIP score greater than 1 therefore indicates the variable is significant in distinguishing between classes. The model was validated by *k*-fold cross validation and accuracy was determined by Q2 and R2 values. All variables with a VIP score greater than 1 were extracted and formed a reduced dataset for further analysis. PCA and PLS-DA separation models were fitted using the statistics module in MetaboAnalyst 5.0 (Pang et al., 2021).

To determine significance of differential metabolite abundance between pre- and post-bed rest samples univariate analysis was performed on the reduced dataset. Firstly, normality of metabolite distribution between samples was assessed using frequency distribution. Based on this either a paired t-test or a Wilcoxon signed-rank test was used to determine the significance of each metabolite. Finally, the $\log_2$ transformed fold change of each metabolite feature between pre- and post-bed rest samples was obtained. This analysis was performed using the statistics module in MetaboAnalyst 5.0.

The returned p-values were then adjusted for false discovery rate using the Benjamini-Hochberg procedure using the R package sgof (Castro Conde and de Una Alvarez, 2020). The Benjamini-Hochberg adjustment is well suited to metabolomic studies where a large number of features are tested simultaneously as it is less stringent than other measures (Peluso et al., 2021), such as the Bonferroni adjustment which controls the number of false positives by testing each hypothesis the significance level of α/m

where α is the desired alpha level and *m* is the number of hypotheses, by applying stepwise adjustments to the significance level based on the ranked order of the p-values. As the Bonferroni adjustment method does not employ stepwise corrections, when there are a large number of hypotheses, it can be overly conservative. Adjustment methods which are too conservative may produce false negatives and discard truly significant observations. Significance was determined when FDR<0.05.

3.2.6. Prediction of functional activity of metabolomics data

Pathway enrichment analysis within the full dataset was performed using the Mummichog algorithm (Li et al., 2013). Mummichog is a freely available software developed for the annotation of metabolites and prediction of influential pathways without the need of definitive metabolite identifiers, in contrast to conventional metabolomics approaches. Mummichog utilises a user inputted list of significant metabolites ($p<0.05$) to compute all possible metabolite matches and searches a reference metabolic network for every module that could be formed by the tentative identifications. As false matches will distribute randomly through the network, local enrichment is used to identify true metabolite matches. Next, random m/z values from a list of all metabolic features detected in the study are drawn to estimate the null distribution of modular activities. The statistical significance of the identified modules is calculated based on this null distribution (Li et al., 2013). Mummichog has previously been used to study metabolic response to a range of stimuli, such as vaccination (Li et al., 2017), complex diseases (including chronic hepatitis B (Huang et al., 2016), nonalcoholic fatty liver disease (Jin et al., 2016), and Parkinson's disease (Ascenzo et al., 2022)), and age (Hoffman et al., 2014) amongst others. Network data output from mummichog analysis was reconstituted in Metscape 3 for legibility (Karnovsky et al., 2012).

3.2.7. Correlation of metabolomics data with physiological measures

Correlation of significant metabolite expression with outcome measures of total lean body mass (LBM), steady state GD normalised to LBM, and rates of fat and carbohydrate oxidation was assessed by weighted correlation network analysis (WGCNA) (Langfelder and Horvath, 2008) performed in R. WGCNA groups metabolites in modules based on hierarchical clustering. Each module is arbitrarily assigned a colour. Firstly, comparison of outcome measures and metabolite abundance at baseline was carried out. Next, change in outcome measures after 56 days bedrest was assessed against $\log_2$ fold change of metabolite abundance after bed rest. Metabolic modules with weak correlations ($r<|0.5|$) to outcome measures were discarded and further analysis was performed on the remaining metabolites.

3.2.8. Identification of metabolites important in correlation

Due to the smaller size of the remaining dataset after WGCNA, putative metabolite identification was performed using metID (Shen, Wu, et al., 2022) which utilises m/z and MS^2 spectra matching from public metabolomics databases (HMDB, KEGG, MoNA and MassBank) to identify metabolite features. Mass tolerance was set at 5ppm.

Common compound names of identified features were taken from HMDB and mapped to metabolic pathways by over representation analysis (ORA) using MetaboAnalyst (Pang et al., 2021). ORA analyses whether metabolites within a particular pathway are present at a higher rate than would be expected (i.e. over-represented) in an experimentally defined list (Khatri et al., 2012). ORA provides a pathway impact score which is calculated as the sum of the importance measures of the matched metabolites normalised by the importance measures of all matched and unmatched metabolites in each pathway (Xia and Wishart, 2011). Pathway impact score represents an estimate of the importance of each pathway relative to the global metabolic network (Liu et al., 2019). Pathways with impact score greater than 0.1 were

considered to be the most relevant in ageing, in keeping with current literature (Guo and Tao, 2018; Liu et al., 2019). ORA also provides a measure of importance for defined metabolites within the pathway allowing insight into which metabolites within each pathway are most expressed in the dataset.

3.3. Results

3.3.1. Changes in physiological end point measures of metabolism and lean mass

The physiological adaptations to bed rest including changes in GD and substrate oxidation are reported in Shur et al. (2022), however for clarity the main adaptations are presented here. REE decreased significantly ($p=0.027$) after bed rest. There was no lipid droplet density ($p=0.13$), droplet size ($p=0.38$), or percentage of IMCL relative to total tissue area ($p=0.6$), however LBM decreased significantly ($p<0.001$) showing loss of muscle mass without the accumulation of intramuscular fat. There was no difference in steady-state serum triglyceride concentration ($p=0.6$) or plasma NEFA concentration ($p=0.3$) before and after bed rest. There was a significant decline in whole-body GD, represented by a 22% reduction in insulin-mediated steady-state GD standardised to LBM, alongside a 19% blunting of the magnitude of increase in rate of carbohydrate oxidation and a 43% blunting of the magnitude of insulin-mediated inhibition of lipid oxidation during the steady state period of the insulin-clamp.

3.3.2. Multivariate analysis of plasma metabolite abundance

The metabolome reflects both transcriptional and physiological changes and modern metabolomics techniques are able to detect changes in metabolites at a much higher sensitivity than the assays used to assess serum triglyceride and plasma NEFA concentrations. The next aim of this study was therefore to define how the observed adaptations in transcription, metabolism and body composition were reflected in the plasma metabolome with an untargeted metabolomics approach. To do this, an untargeted metabolomics approach was taken to profile all plasma metabolites in the fasted, resting state. A total of 29,443 metabolites were detected in plasma by untargeted metabolomic profiling: 8513 polar positive, 4425 polar negative, 9542 non-polar positive and 9893 non-polar positive. After processing and filtering 16,462 total metabolites were retained.

PCA showed that there were no outlying data points and samples generally clustered well. However, there was no clear separation between pre- and post-bed rest samples. A PLS-DA separation model was able to classify samples as pre- and post-bed rest indicating clear differences occur in the fasting plasma metabolome as a consequence of chronic bed rest (Figure 3.1). K-fold cross validation found that the separation models were not overfitted and were accurate (Q2 > 0.4, R2 > 0.5 for all models).

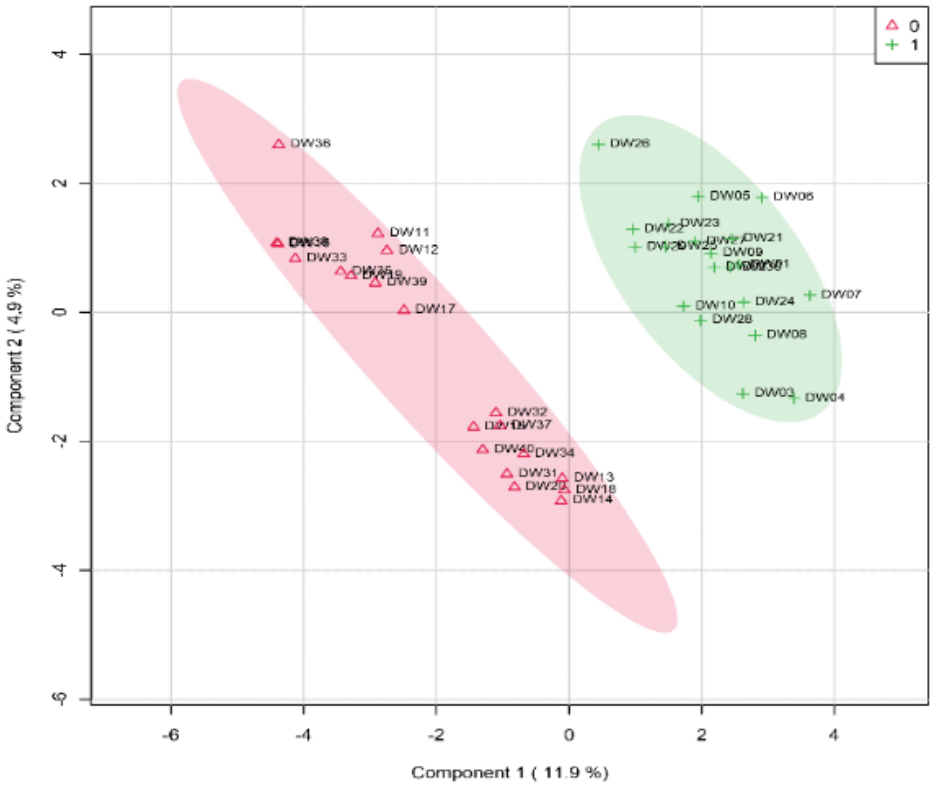

Figure 3.1 Separation of groups by timepoint using PLS-DA

Representative plot of partial least squares discriminant analysis (PLS-DA) separation model with 95% confidence intervals showing similarity in abundance of all metabolites detected in plasma before bed rest (red triangles) and after 56 days bed rest (green crosses) for healthy young men held in energy balance. Each point represents one participant. Data from the polar negative dataset. Classification of samples improved over PCA using a PLS-DA model.

Variables with a VIP score greater than 1 were selected as the most contributory factors in classification of samples by class and formed a reduced dataset for further analysis. A total of 3315 metabolites were deemed important in classification and

were retained for further analysis: 421 polar negative metabolites, 786 polar positive metabolites, 946 non-polar negative metabolites, and 1162 non-polar positive metabolites. Differential abundance of these metabolites between pre- and post-bed rest samples found that, of the 3315 metabolites assessed, 2835 were significantly different between the pre and post-bed rest timepoints following testing for FDR: 337 polar negative metabolites, 597 polar positive metabolites, 847 non-polar negative metabolites, and 1054 non-polar positive metabolites.

3.3.3. Metabolite identification and network analysis

Having formed a reduced dataset containing only metabolites important in classification of samples by timepoint the next step was to establish their physiological roles by placing metabolites in relevant networks and pathways. Mapping of metabolites deemed important in classification by VIP filtering to their predicted networks found that 25 unique pathways were significantly enriched ($p<0.05$) from pre- to post-bed rest across all ionisation modes and polarities. Notably, many of the disturbed pathways were found to be related to fat and carbohydrate oxidation pathways and metabolites involved in ATP generation. For instance, the purine metabolism pathway (Figure 3.2) was significantly impacted by bed rest in the polar positive and negative data sets ($p=0.016$ and $p=0.017$, respectively). Predicted interactions within the pathways suggested that differences in the plasma abundance of hypoxanthine, inosine, dAMP, xanthosine 5'-phosphate, L-aspartate, 5-hydroxyisoburate and 5-amino-4-imidazolecarboxyamide were most responsible for the change in this pathway.

Several amino acid metabolism pathways were also significantly affected by bed rest. Aspartate metabolism ($p=0.001$), arginine and proline metabolism ($p=0.005$) and lysine metabolism ($p=0.03$) were all significantly different after bed rest in the polar positive data set (Figure 3.3). Within these pathways there were differences in the

plasma abundance of three proteinogenic amino acids (L-methionine, L-proline, and L-aspartate), however most of the metabolites predicted to be influential in these pathways were intermediates of amino acid metabolism. L-pipecolate, L-citrulline, 5-oxo-L-proline, 4-guanidinobutanamide, L-3-amino-isobutanoate and 3-dehydroxycarnitine were the intermediate metabolites predicted to be the most influential in driving pathway change. Galactose metabolism was found to be significantly affected by bed rest ($p=0.018$), as were three pathways linked to the biosynthesis and oxidation of fatty acids ($p=0.006$, $p=0.018$, $p=0.02$) (Figure 3.4). Disturbances in galactose metabolism were mapped to differences in the plasma abundance of two precursors of galactose, melibiitol and 3-beta-D-galactosyl-sn-glycerol, as well as to difference in plasma abundance of lactose-6-phosphate.

Pathway analysis has shown that plasma metabolite abundance reflects the previously observed derangements to metabolism however it also demonstrates more widespread effects of bed rest on plasma metabolites which many not directly relate to insulin related changes in substrate oxidation or GD. For instance, significant differences in pathways relating to sialic acid ($p=0.017$), linoleate ($p=0.006$) and arachidonic acid ($p=0.018$) metabolism were also observed.

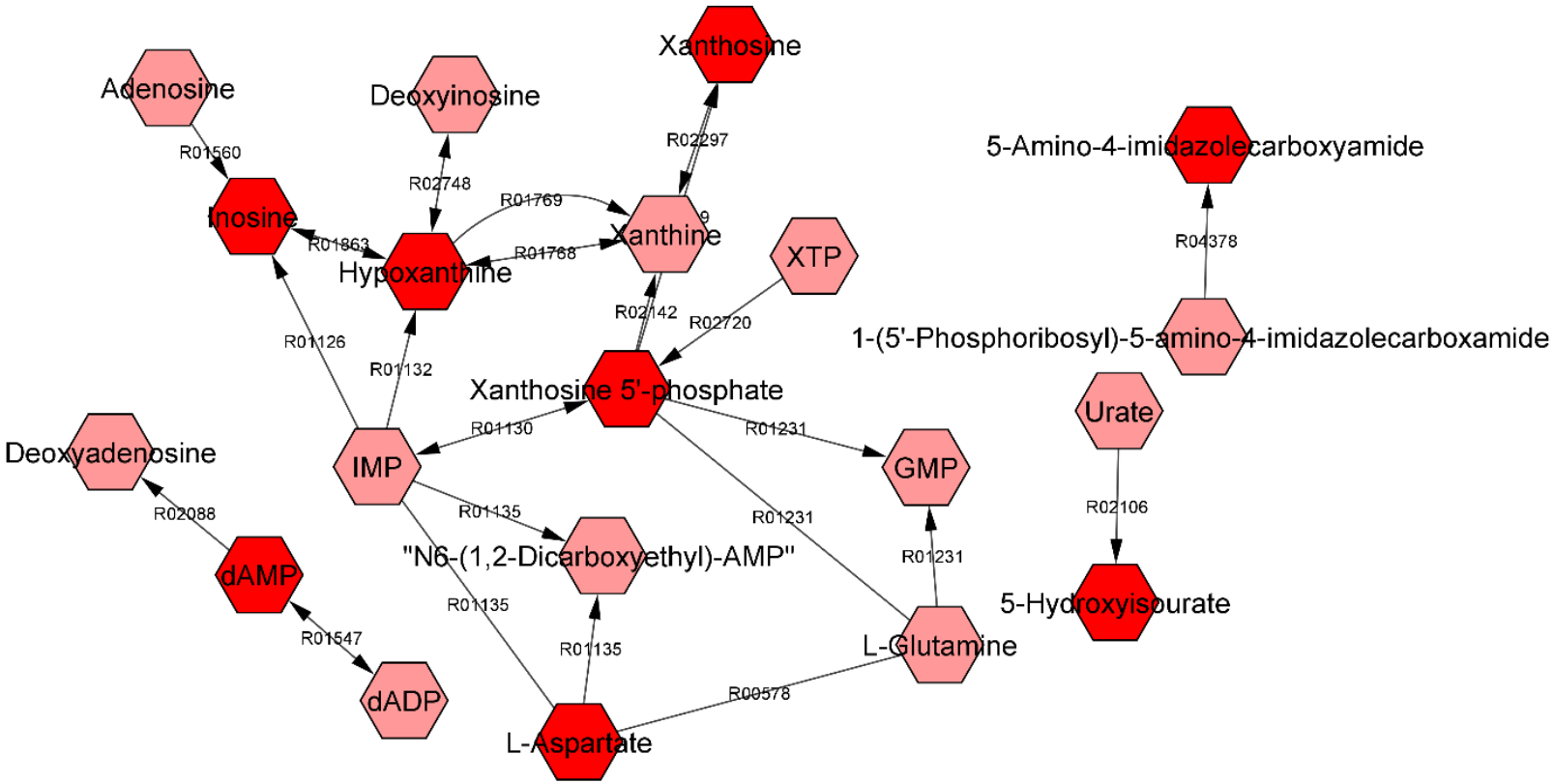

Figure 3.2 Network representation of purine metabolism pathways affected by chronic bed rest

Pathways relating to purine metabolism which were significantly impacted ($p<0.05$) by 56 days bed rest in healthy young, male volunteers. Metabolite identification and pathway analysis was performed using the mummichog server. Network data was reconstituted in MetScape for legibility. Metabolites suggested by mummichog to contribute to change in pathway significance are highlighted in dark red.

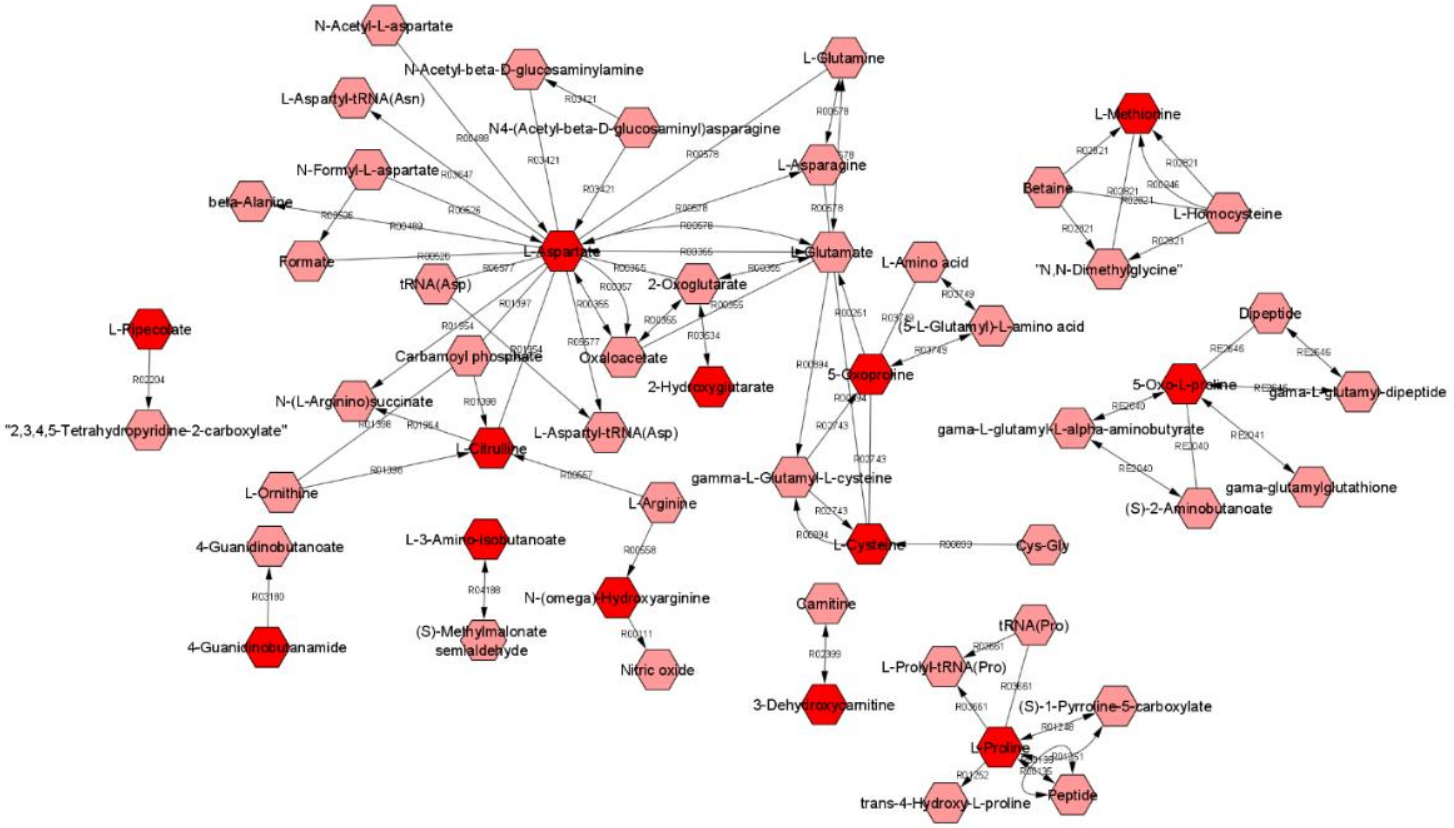

Figure 3.3 Network representation of amino acid metabolism pathways affected by chronic bed rest

Pathways related to metabolism of amino acids were significantly disturbed ($p<0.05$) by 56 days BR in healthy, young male volunteers. Metabolite identification and pathway analysis was performed using the mummichog server. Network data was reconstituted in MetScape for legibility. Metabolites suggested by mummichog to contribute to change in pathway significance are highlighted in dark red.

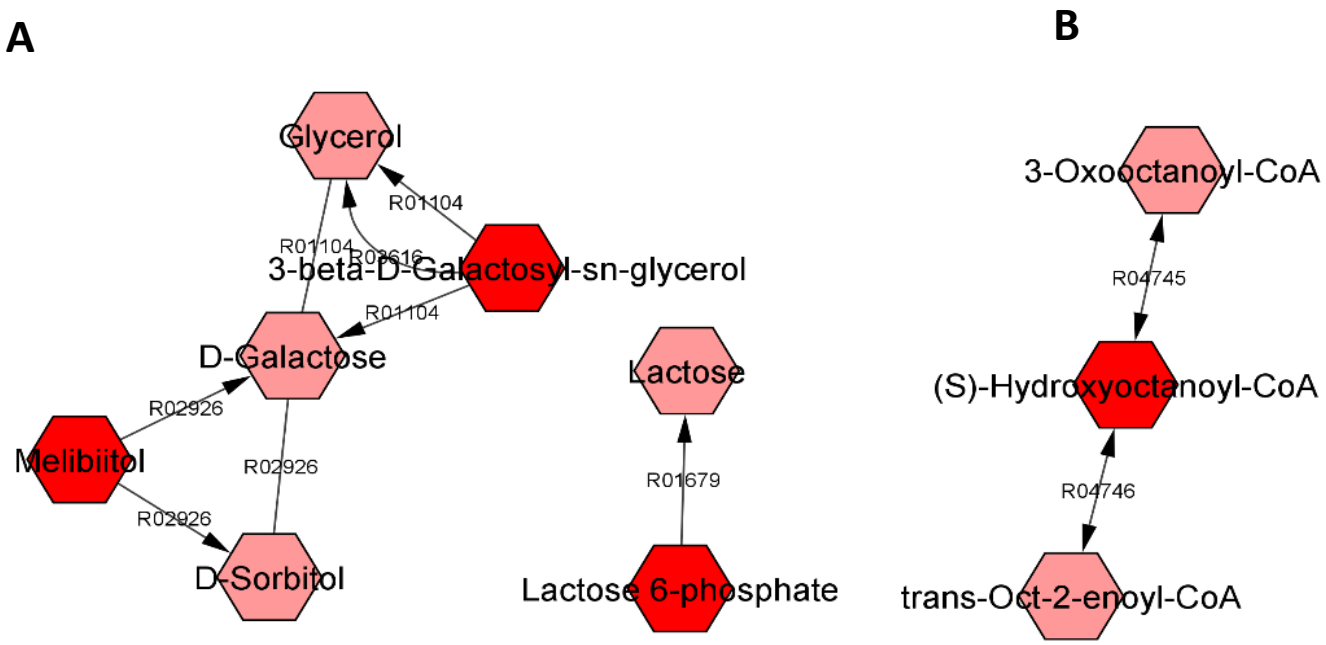

Figure 3.4 Network representation of galactose and fatty acid metabolism affected by chronic bed rest

Pathways relating to (A) galactose metabolism and (B) fatty acid biosynthesis and oxidation which were significantly disturbed ($p<0.05$) by 56 days BR in young, healthy male volunteers, reflecting disturbances to rates of carbohydrate and lipid oxidation. Metabolite identification and pathway analysis was performed using the mummichog server. Network data was reconstituted in MetScape for legibility. Metabolites suggested by mummichog to contribute to change in pathway significance are highlighted in dark red.

3.3.3.1. Association of metabolite abundance with physiological outcome measures at baseline

Profiling of metabolites using an untargeted approach provides insights into how the metabolome reflects physiological adaptations to chronic bed rest but does not provide key information regarding which metabolites and metabolic pathways are the most influential in driving these adaptations, if any. WGCNA allocates metabolites into modules based on topological overlap. Correlation of each module with relevant external traits can then be calculated to determine the relationship between metabolite abundance and phenotype data.

Prior to bed rest, only a few modules of metabolites were correlated ($r>|0.5|$ and $p<0.05$) with GD normalised to LBM, REE, rates of fat and carbohydrate oxidation, or LBM, providing insight into which metabolites are involved in maintaining metabolic homeostasis in healthy, young volunteers (Table 3.1). The strongest association at baseline was between the brown module of polar positive metabolites and GD normalised to LBM ($r=-0.75$, $p<0.001$). Within this module, the strongest associations were related to glycerophospholipid metabolism (impact score 0.20) which occurred due to plasma abundance of phosphatidylethanolamine (PE) and phosphatidylcholine (PC), and cysteine and methionine metabolism (impact score 0.12) with significant hits within the pathways mapped to plasma levels of L-cysteine and mercaptopyruvate.

Table 3.1 Table containing metabolic modules which are correlated (r>|0.5|, p<0.05) with measures of lean body mass (LBM), resting energy expenditure (REE), rate of fat oxidation, rate of carbohydrate (CHO) oxidation, or glucose disposal normalised to lean body mass (GD) prior to 56 days bed rest. Over representation analysis was applied to metabolites within each module to identify relevant metabolic pathways (impact score > 0.1)

Module	Outcome measure	Correlation coefficient	p-value	Pathway	Impact score
Blue	LBM	0.52	0.03	Terpenoid backbone biosynthesis	0.11
				Lysine degradation	0.14
				Biotin metabolism	0.2
				Sulphur metabolism	0.21
Yellow	REE	-0.59	0.009	Glycerophospholipid metabolism	0.26
				Biotin metabolism	0.2
Brown	GD	-0.75	0.0008	Glycerophospholipid metabolism	0.2
				Cysteine and methionine metabolism	0.12
Green	REE	-0.63	0.009	Glycerophospholipid metabolism	0.22
Red	GD	0.5	0.03	Glycerophospholipid metabolism	0.25
Tan	REE	-0.5	0.04	Glycerophospholipid metabolism	0.2
Red	LBM	0.5	0.03	Sphingolipid metabolism	0.27
	GD	-0.54	0.02		
	Fat oxidation	0.53	0.02	Glycine, serine and threonine metabolism	0.25
	CHO oxidation	-0.55	0.01	Glyoxylate and dicarboxylate metabolism	0.11

More moderate correlations between GD normalised to LBM and the red modules in the non-polar negative (r=0.5, p=0.03) and positive (r=-0.54, p=0.02) datasets were also observed. Metabolites in the non-polar negative red module were involved in glycerophospholipid metabolism (impact score 0.22), with PE and PC again matched within the pathway. Phosphatidylserine (PS) was also identified in the module. The non-polar positive red module was linked to sphingolipid metabolism (impact score 0.27), glycine, serine and threonine metabolism (impact score 0.25), and glyoxylate

and dicarboxylate metabolism (impact score 0.11) pathways. In both glycine, serine and threonine metabolism and glyoxylate and dicarboxylate metabolism pathways, plasma abundance of glycine was identified as influential in the pathway. In sphingolipid metabolism, sphingomyelin and ceramide were found to be important within the pathway. Rates of fat and carbohydrate oxidation during steady state in the insulin clamp at baseline were also found to be correlated with the non-polar negative red module (fat oxidation, r=0.53, p=0.02; carbohydrate oxidation, r=-0.55, p=0.01) and were therefore also linked to plasma levels of glycine, sphingomyelin and ceramide.

REE was negatively correlated with the yellow module in the polar negative dataset (r=-0.59, p=0.009), the green module in the polar positive dataset (r=-0.63, p=0.009) and the tan module of the non-polar negative dataset (r=-0.5, r=0.04). Metabolites in these modules were all involved in glycerophospholipid metabolism (for all, impact score > 0.1). The yellow module was also linked to biotin metabolism (impact score 0.2). Plasma abundance of biotin was found to be important in dictating the biotin metabolism pathway response. In the tan module, PE and PC were highlighted. PE and PC were also involved in the green module, alongside 1-acyl-Sn-glycero-3-phosphocholine. Likewise, in the yellow module, these metabolites were all highlighted alongside PS.

Finally, LBM was correlated with the blue module in the polar negative dataset (r=0.52, p=0.03) and the red module in the non-polar positive dataset (r=0.5, p=0.03), and was therefore linked to plasma levels of glycine, sphingomyelin and ceramide. In the blue module, metabolites were involved in terpenoid backbone synthesis (impact score 0.11), biotin metabolism (impact score 0.2), lysine degradation (impact score 0.14) and sulphur metabolism (impact score 0.21) pathways. Specific plasma metabolites

involved in these pathways were identified as mevalonic acid, biotin, 2-oxoadipate, and sulphate.

3.3.4. Associations between the change in metabolite abundance with bed rest from baseline and the change physiological outcome measures over the same period

Having established that metabolites can be associated with measures of metabolic function and lean body mass at baseline, the next aim was to investigate associations between the change in plasma abundance from baseline during bed rest of metabolites which were important in classifying samples as pre- and post-bed rest (VIP>1) and the change in physiological function with bed rest (Table 3.2).

Change in the rate of steady-state fat oxidation from baseline to day 56 of bed rest was moderately correlated with the brown module (r=-0.5, p=0.03) in the non-polar negative dataset. ORA found the metabolites within this module were linked to glycerophospholipid metabolism, with PE and 1-acyl-Sn-glycero-3-phosphocholine identified as most important within the pathway. All glycerophospholipids decreased in abundance following bed rest.

Relative change in GD normalised to LBM was correlated with the yellow (r=-0.55, p=0.02) and blue (r=-0.5, p=0.03) modules in the polar positive dataset. ORA found metabolites in both modules were linked to amino acid metabolism. Arginine and proline metabolism was affected in both the yellow (impact score 0.14) and blue (impact score 0.11) modules although influential metabolites within the pathway were different in each module. In the yellow module, hydroxyproline and L-proline were highlighted as most important while in the blue module putrescine was found to be the most important. All three metabolites increased in plasma abundance after bed rest. Metabolites within the blue module were also linked to tryptophan metabolism (impact score 0.10), with serotonin identified as important. In the yellow module,

metabolites were linked to alanine, aspartate and glutamate metabolism (impact score 0.22), tyrosine metabolism (impact score 0.29), and phenylalanine, tyrosine and tryptophan biosynthesis (impact score 0.5). Within these pathways, L-aspartate, dopamine, L-tyrosine, and tyramine were all identified as influential metabolites. Tyramine decreased in plasma abundance after bed rest, but all other metabolites increased in plasma abundance.

Table 3.2 Table containing metabolic modules which are correlated (r>|0.5|, p<0.05) with relative change in glucose disposal normalised to lean body mass (GD) or rate of fat oxidation after 56 days bed rest. Over representation analysis was applied to metabolites within each module to identify relevant metabolic pathways (impact score > 0.1)

Module	Outcome measure	Correlation coefficient	p-value	Pathway	Impact score
Yellow	Change in GD	-0.55	0.02	Phenylalanine, tyrosine and tryptophan biosynthesis	0.5
				Tyrosine metabolism	0.29
				Alanine, aspartate and glutamate metabolism	0.22
				Arginine and proline metabolism	0.14
Blue		-0.5	0.03	Arginine and proline metabolism	0.11
				Tryptophan metabolism	0.10
Brown	Change in fat oxidation	-0.5	0.03	Glycerophospholipid metabolism	0.11

3.4. Discussion

From untargeted analysis of the plasma metabolome 2835 metabolites were found to be significantly different from baseline after bed rest indicating that chronic bed rest induced large scale changes in the plasma metabolome.

3.4.1. Purine metabolism

Metabolites produced in the degradation of nucleotides were found to be responsible for the difference in purine metabolism between baseline and post-bed rest samples (Figure 3.11). Purine metabolism is responsible for maintaining cellular stores of nucleotides which are mediators of essential physiological processes including as an immediate source of energy for muscle contraction or as signalling molecules for myofiber hypertrophy (Berdeaux and Stewart, 2012). Increased adenine nucleotide degradation has previously been linked to murine models of skeletal muscle disuse although the role of purines in human inactivity is not currently well studied (Miller et al., 2020). Thus, the identification of purines as metabolites significantly impacted by bed rest provides novel insight into a role for purine metabolism in human inactivity.

3.4.2. Amino acid metabolism

Amino acid metabolism pathways were also disturbed between baseline and post-intervention samples (Figure 3.12) with many of the metabolites influential in the pathways identified as intermediates in amino acid metabolism rather than amino acids themselves. It is known that bed rest has a blunting effect on muscle sensitivity to EAA signalling and subsequently EAA induced protein synthesis (Biolo et al., 2004; Drummond et al., 2012) but these data suggest that wider changes in non-EAA metabolism also occur as a consequence of bed rest, potentially relating to the role of these metabolites as intermediaries in energy metabolism (Da Poian et al., 2010). Furthermore, the potential influence of L-aspartate as a driver of change in amino acid metabolism provides a possible mechanistic link between dysregulation of amino acid and purine metabolism pathways in the shift in metabolic health following bed rest.

3.4.3. Energy metabolism

Finally, galactose metabolism and three pathways involved in the biosynthesis and oxidation of fatty acids were found to be disturbed by bed rest (Figure 3.13). Cell culture models of myofibers suggest galactose improves oxidative capacity and enhances the inhibition of lipid oxidation in the fed state (Kase et al., 2013), although this has not yet been validated in humans, and it is therefore possible that the differences in plasma abundance of galactose-related metabolites are indicative of dysregulated galactose metabolism which contributes to the increased suppression of carbohydrate oxidation and reduced blunting of fat oxidation. Disturbances in de novo fatty acid biosynthesis and fatty acid oxidation and saturated fatty acid beta-oxidation were all mapped to differences in the plasma abundance of (S)-hydroxyoctanoyl-CoA, a metabolite involved in transferring fatty acids from the cytoplasm to the mitochondria for use in oxidation. Earlier transcriptomics analysis by Shur et al. (2022) showed the expression of muscle mRNA transcripts encoding the mitochondrial enzyme superoxide dismutase 2 (SOD2) increased after bed rest as part of transcriptional events that were collectively proposed to be causative of the shift in fuel oxidation. While SOD2 and (S)-hydroxyoctanoyl-CoA are not directly linked they both suggest mitochondrial adaptation may be linked to the blunted suppression of fat oxidation. Such as an association remains speculative without correlation to physiological measures.

3.4.4. Associations between metabolite abundance and outcome measures at baseline

A major strength of this study is the elucidation of relationships between the plasma metabolome and physiological outcome measures, which can identify which metabolites, among thousands, are the most associated with the development of insulin resistance and metabolic inflexibility during chronic bed rest. Thus, the primary aim of this chapter was to investigate whether these plasma metabolite changes with

bed rest reflected the changes in GD and rates of fat and carbohydrate oxidation with bed rest. Accordingly, preliminary metabolite annotation and network analysis suggested that plasma metabolites which were present at a significantly different abundance after bed rest played roles in metabolic networks reflective of fat and carbohydrate utilisation.

3.4.4.1. Phospholipids

It is well established that levels of PC and PE in skeletal muscle are associated with insulin sensitivity and GD (Clore et al., 1998; S. Lee et al., 2018). Total PC and PE content in skeletal muscle are positively correlated with insulin sensitivity and an elevated PC:PE ratio is found in type 2 diabetes patients (Newsom et al., 2016) indicating the importance of maintaining the balance of skeletal muscle phospholipids in mediating insulin action. Here, PC and PE were identified by network analysis as important metabolites in the correlation of glycerophospholipid metabolism and steady state GD even at baseline. Given the abundance of PE and PC as components in the mitochondrial membrane (Grapentine and Bakovic, 2020) this suggests a link between mitochondrial morphology and regulation of GD in healthy volunteers.

PC and PE were also identified as important in the correlation of glycerophospholipid metabolism with REE. It has previously been suggested that phospholipids are able to alter the activity of the sarco/endoplasmic reticulum Ca^{2+} ATPase (SERCA) in skeletal muscle to regulate energy expenditure (Verkerke et al., 2020). 1-acyl-Sn-glycero-3-phosphocholine was also selected as important in the correlation of glycerophospholipid metabolism and baseline REE. 1-acyl-Sn-glycero-3-phosphocholine is a constituent of plasma membranes (PubChem, 2022), and its role in the association of glycerophospholipid metabolism and REE suggests an association between membrane phospholipid composition and regulation of REE.

3.4.4.2. Amino acids

L-cysteine and its metabolite mercaptopyruvate were also identified as important in the association between GD with metabolite abundance. In agreement, supplementation with L-cysteine increases insulin sensitivity in a cell culture model (Achari and Jain, 2017), while patients with type 2 diabetes have reduced plasma cysteine levels (Jain et al., 2014). It has been suggested that the mechanism by which cysteine regulates insulin-mediated GD occurs through the degradation of cysteine to hydrogen sulphide (Carter and Morton, 2016). Plasma levels of hydrogen sulphide are negatively correlated with type 2 diabetes (Jain et al., 2010). One of the roles of mercaptopyruvate, which is produced by the breakdown of L-cysteine (Kanehisa and Goto, 2000), is as an intermediate in the production of hydrogen sulphide (Nasi et al., 2020). The importance of mercaptopyruvate in the association between cysteine metabolism and steady state GD at baseline in the present work provides further evidence of this degradation pathway in glucoregulation.

Glycine was also identified as another metabolite of importance in the association with rates of GD at baseline. Glycine has previously been identified as a serum biomarker of insulin sensitivity in older adults (Lustgarten et al., 2014). Additionally, plasma glycine levels are elevated following interventions that improve insulin sensitivity, such as exercise (Glynn et al., 2016), and correlated positively with rate of GD in healthy adults (Wang-Sattler et al., 2012). Serum glycine levels have been associated with a change in the plasma mRNA expression of 5-aminolevulinate synthase 1 (Wang-Sattler et al., 2012), a mitochondrial enzyme involved in the haem biosynthesis pathway. Haem increases mitochondrial activity through its role in the electron transfer chain (Ogura et al., 2011). The correlation between plasma abundance of glycine and GD at baseline in the present study could therefore provide a link between mitochondrial function and glucose disposal.

3.4.4.3. Sphingolipids

Sphingolipids are the major lipid species found in skeletal muscle (Sokolowska and Blachnio-Zabielska, 2019) and the skeletal muscle sphingomyelin signalling pathway is reported to be an important factor in determining the development of insulin resistance (Straczkowski et al., 2004). Sphingomyelin content in human skeletal muscle is related to total ceramide content, which is unsurprising given the function of sphingomyelin in the ceramide biosynthesis pathway (Bikman and Summers, 2011).

Ceramides have previously been linked to decreased sensitivity of skeletal muscle to insulin. Under normal conditions fatty acids (such as sphingomyelin) enter the ceramide biosynthesis pathway when a cell's energy requirements are met, preventing their use in fat oxidation. Accumulation of ceramides, such as that seen in skeletal muscle tissue of type 2 diabetics (Broskey et al., 2018), can suppress carbohydrate oxidation and promote fat oxidation leading to insulin resistance (Summers et al., 2019). One proposed mechanism is that the accumulation of ceramides within muscle can inhibit the transmission of insulin signals through the Akt signalling cascade leading to a failure in insulin mediated glucose uptake (Powell et al., 2003). Ceramide plasma abundance at baseline in the present study was correlated with GD in the steady state. These data therefore align with the current literature and support a role for ceramides and the sphingomyelin pathway in the regulation of insulin-mediated GD. Of note, glycine, sphingomyelin, and ceramide were also identified in pathways correlated with rates of steady-state fat or carbohydrate oxidation. Given GD, fat and carbohydrate oxidation are all known to be regulated by circulatory insulin and glucose concentrations, the overlap between these metabolites is unsurprising.

3.4.4.4. Correlation with lean body mass

Whole-body lean mass is the largest sink for GD, and therefore is important in the regulation of glucose homeostasis. For example, LBM has been inversely associated with incident type 2 diabetes in men (Kalyani et al., 2020) and a lower LBM was observed in children and adolescents with insulin resistance compared to their insulin sensitive counterparts (Rodríguez-Córdoba et al., 2022). Likewise, LBM is a determinant of REE in adults (Deriaz et al., 1992; Müller et al., 2001). It is therefore not surprising that many of the metabolites identified to be associated with LBM at baseline were also found to be associated with REE, GD and steady-state substrate oxidation.

Correlation of metabolite abundance with outcome measures at baseline shows associations which are in line with the current literature, which demonstrates the reliability of this approach and shows that it is an appropriate method to employ to study the relationship between the change in the plasma metabolome during bed rest with concurrent changes in GD and fuel metabolism.

3.4.5. Association between the change in plasma metabolite abundance and outcome measures with bed rest

After 56 days of bed rest, fewer modules of metabolites were associated with the outcome measures. This may be reflective of the reduced diversity of the plasma metabolome as a consequence of bed rest, in line with previous literature (Sket et al., 2020). Change in LBM, REE and steady-state carbohydrate oxidation rates were not associated with the change in plasma abundance of metabolites during bed rest. It is therefore possible that disruption to insulin mediated fat oxidation and GD are the primary adaptations associated with bed rest, with the other outcome measures occurring secondary to disruption in insulin mediated metabolic pathways.

3.4.5.1. Glycerophospholipids

Change in the rate of fat oxidation during the steady-state of the insulin clamp was correlated with glycerophospholipid metabolism. It was discussed above how glycerophospholipid level and SERCA activity were related in respect to REE. However, SERCA expression is also related to oxidative efficiency (O'Donnell et al., 2009) and levels of intracellular Ca^{2+} contributes to the balance between rates of fat and carbohydrate oxidation by promoting lipolysis, which in turn promotes fat oxidation (Melanson et al., 2003), and activating glycogen phosphorylase, which leads to glycogenolysis and hyperglycaemia (Tammineni et al., 2020). It was previously shown that muscle mRNA expression of ATP2A1, which encodes SERCA, was increased after 56 days bed rest (Shur et al., 2022) adding further support that chronic bed rest is associated with increased cellular free calcium availability.

PE and 1- acyl-Sn-glycero-3-phosphocholine are constituents of plasma membranes. It has been suggested that the lipid composition of plasma membranes is influential in the development of insulin resistance (Ferrara et al., 2021; Wolfgang, 2021). It is therefore possible that the decrease in plasma abundance of PE and 1- acyl-Sn-glycero-3-phosphocholine reflects a change in membrane lipid composition induced by bed rest, which contributed to the blunting of the insulin mediated suppression of fat oxidation with BR. In keeping with this, IPA predicted the upregulation of fat oxidation following bed rest (Figure 3.7, Shur et al. 2022).

Finally, the role of glycerophospholipids in the shift in fuel oxidation may also relate to an adaptation in mitochondrial function. PE is abundant in the inner mitochondrial membrane (Tasseva et al., 2013). Recently it was proposed that PE facilitates the entry of pyruvate into the mitochondrion to regulate membrane flexibility and, furthermore, that low mitochondrial PE availability was associated with poor mitochondrial

pyruvate uptake in vitro and in murine models (Siripoksup et al., 2022), suggesting a shift away from carbohydrate oxidation to fat oxidation. The importance of PE in the correlation of glycerophospholipid metabolism and change in the rate of fat oxidation during steady-state in the insulin clamp suggests a similar mechanism may occur in humans and that aberrant glycerophospholipid metabolism, in particular change in the abundance of PE, may act as a primary signal for a shift in mitochondrial fuel utilisation.

3.4.5.2. Amino acid metabolism

Change in steady-state GD with bed rest was correlated with several pathways related to amino acid metabolism. Plasma concentrations of amino acids have previously been used as biomarkers of insulin resistance. For example, greater concentrations of tyrosine have been associated with increased risk of type 2 diabetes (Sanmei Chen et al., 2019) and insulin resistance (Tai et al., 2010). Likewise, increased plasma proline concentrations are associated with insulin resistance (Tai et al., 2010) and increase the risk of type 2 diabetes, regardless of age (Chen et al., 2021). Here, tyrosine and proline were both found to be important metabolites in the association of amino acid metabolic pathways and the change in GD after bed rest. Abnormal amino acid metabolism is believed to precede impaired GD (Wurtz et al., 2012). Although the precise mechanism is unknown it has been proposed that the increased abundance of amino acids inhibits the phosphorylation of IRS-1 and IRS-2, key proteins involved in the insulin signalling cascade which stimulates GD (Patti et al., 1998). Muscle mRNA expression of these proteins was not assessed in this study, so direct links cannot be made between the signalling cascade and abundance of proline or tyrosine.

L-hydroxyproline and putrescine, two breakdown products related to arginine and proline metabolism, were also highlighted as important in the association between

amino acid metabolites and the change in GD with bed rest. Putrescine is a polyamine. Polyamines are able to regulate insulin signalling via IGF-1 (Welsh, 1990) and as such have been implicated in diabetes (Fernandez-Garcia et al., 2019). The muscle mRNA expression of IGF-1 was different after bed rest (Shur et al., 2022), pointing to a mechanism by which differential abundance of putrescine could have affected the signalling action of IGF-1. Hydroxyproline is highly abundant in collagen (Chow et al., 2015). Increased collagen content is found in insulin resistant skeletal muscle indicating remodelling of the extracellular matrix (ECM) (Berria et al., 2006). One possible mechanism by which ECM remodelling contributes to the development of insulin resistance and impaired GD is by the reduction of microvascular density which acts as a physical barrier, preventing both the binding of insulin to its receptor and the transmission of signals within the cell (Williams et al., 2016; Ahmad et al., 2018). Increased muscle mRNA expression of COL6A3 was observed after bed rest (Shur et al., 2022) lending further support to the association of collagen and impaired GD. Change in abundance of hydroxyproline therefore potentially links to change in deposition of collagen within muscle and contributes to the blunting of GD by inhibiting insulin signalling.

The phenylalanine, tyrosine and tryptophan biosynthesis pathway was correlated with change in GD. Tyramine was one metabolite identified as important within this pathway. Tyramine administration in a murine model can cause large stimulation of GD, likely through peripheral monoamine oxidase activities (Morin et al., 2002) however in this study tyramine plasma abundance declined after bed rest. Such a decline in tyramine abundance may lead to low stimulation of monoamine oxidase and therefore contribute to blunted GD. Serotonin was also highlighted as an important metabolite within the tryptophan metabolism pathway. There are several possible explanations for the role of serotonin in decline in GD after bed rest. Firstly,

serotonin is a regulator of the contractile response of skeletal muscle (Takamori, 1977), potentially through interaction with myostatin (MSTN) as inhibition of MSTN increases the expression of the Tph1 enzyme, which catalyses the rate limiting step in serotonin synthesis, in skeletal muscle (Chandran et al., 2012). It was suggested that a primary signal for adaptation in fuel selection after chronic bed rest was the lack of muscle contraction per se, while the regulation of glucose uptake appeared to be dissociated from the regulation of substrate oxidation when comparing acute and chronic bed rest responses (Shur et al., 2022). The importance of serotonin in driving associations between tryptophan metabolism and rate of steady-state GD in this study also supports the view that a lack of muscle contraction is a primary component of the adaptation in GD induced by chronic bed rest. Secondly, it has been suggested that the interaction between MSTN and serotonin pathways plays role in the regulation of glucose metabolism within skeletal muscle. *Mstn-/-* mice have greater insulin sensitivity than their wild type counterparts (Zhang et al., 2011). Transcriptomics analysis of skeletal muscle following chronic bed rest found increased expression of MSTN mRNA after bed rest (Shur et al., 2022). While further research is needed to fully elucidate the mechanism of interaction the combination of transcriptomics and metabolomics data in this cohort provides further evidence to support a role for the interaction of MSTN and serotonin in the development of insulin resistance.

Dopamine was also identified as important in the correlation of the tyrosine metabolism pathway with change in GD with bed rest. Levels of dopamine in the peripheral nervous system are linked to insulin sensitivity, although the mechanism behind this association is unclear. For instance, treatment with a dopamine agonist improved insulin sensitivity of adipose tissue and whole-body metabolic profile in a murine model of type 2 diabetes (Tavares et al., 2021a). Dopamine has been proposed to regulate glucose uptake by skeletal muscle in an insulin independent manner

(Tavares et al., 2021b) however the correlation in the current data demonstrate a link between dopamine abundance and insulin-mediated GD in humans. More studies are needed to fully clarify the mechanism of action.

Finally, L-aspartate was identified as important in correlation of change in GD with the alanine, aspartate and glutamate metabolism pathway. In Section 3.3.3, L-aspartate was found to be present at a significantly different plasma abundance after bed rest which suggests overall differential metabolite abundance may be reflective of a bed rest induced reduction in GD. Circulating aspartate has previously been identified as a possible marker of insulin resistance. Plasma aspartate was inversely associated with fasting glucose (Cheng et al., 2012) and serum aspartate was associated with elevated fasting glucose levels, decreased insulin secretion, and increased risk of type 2 diabetes (Vangipurapu et al., 2019). Mechanistic studies are lacking, but the association between aspartate and insulin resistance may be due to differences in enzymatic activity of the malate-aspartate shuttle. Glucose restriction increased aspartate biosynthesis, which in turn increased activity of the malate-aspartate shuttle and a shift in substrate oxidation (Olszewski et al., 2022). It is therefore possible that differential abundance of L-aspartate after bed rest is not causative of blunted GD, but is instead reflective of an increase in aspartate biosynthesis triggered by reduced GD.

Many of the pathways significantly correlated with steady-state GD and rate of fat oxidation after bed rest were different from the pathways which were significantly correlated at baseline suggesting that bed rest induced a significant shift in normal metabolic homeostasis. Importantly, identifying correlations between plasma metabolite abundance and measures of whole body and muscle metabolism and metabolic function suggests that systemic changes in the plasma metabolome are reflective of physiological adaptations and highlight the potential of plasma as a proxy

in studies of human metabolism. Irrespective of this point, it is clear that metabolomics in combination with human physiology brings unprecedented granularity and novel insight to research progression.

Chapter 4. Changes in the plasma metabolome in response to resistance exercise with ageing in healthy volunteers

4.1. Background

4.1.1. Changes in skeletal muscle associated with ageing

Sarcopenia is the unintentional loss of muscle mass, quality, strength or performance associated with increasing age (Cruz-Jentoft et al., 2019). Sarcopenia directly impairs locomotory function, increases risk of disability and mortality rates (Mcleod et al., 2019), and is associated with severely reduced self-reported quality of life scores which cannot be explained by social factors such as gender, years of education or marital status (Veronese et al., 2022). Sarcopenia is also associated with increased healthcare costs. It has been reported that the total annual cost of hospitalisation for individuals with sarcopenia in the United States was $40.4 billion between 1994 and 2004 representing 4.12% of the United States' total health expenditure (Goates et al., 2019) and in the United Kingdom the mean annual cost for healthcare per person with muscle weakness was reported as £4,592 resulting in approximately £2.5 billion excess costs for health and social care (Pinedo-Villanueva et al., 2018).

Despite an appreciation for the social and clinical consequences of sarcopenia and heavy investment by multiple pharmaceutical companies, there have been no successful clinical translations of drugs which counteract the loss of muscle mass and strength (Kwak and Kwon, 2019; Feike et al., 2021). At present the most effective method of managing sarcopenia is by mitigating, but not completely preventing, the loss of muscle mass and strength through increased physical activity, in particular through the use of RET (Law et al., 2016) which prevents the loss of skeletal muscle mass by providing skeletal muscle with anabolic signals that promote MPS which leads to a positive protein balance and therefore muscle hypertrophy (Pasiakos, 2012).

4.1.2. The influence of resistance exercise on protein turnover

In the postabsorptive state, skeletal muscle protein is the primary source of amino acids (Argilés et al., 2016). In order to maintain a steady-state concentration of amino acids in the postabsorptive state, proteins in skeletal muscle are catabolised and the resulting amino acids are released into the vasculature for use in critical processes such as energy production or gluconeogenesis in other tissues including the liver, brain and kidneys (Carbone and Pasiakos, 2019). The catabolism of proteins and subsequent release of amino acids results in a negative protein balance within skeletal muscle which, in healthy individuals, is corrected for by the stimulation provided by feeding. When an adult individual consumes adequate daily protein but does not exercise muscle mass remains unchanged as the stimulation of MPS from feeding is transient and cannot build a positive net protein balance on its own. RET provides anabolic signals to skeletal muscle which dramatically increase MPS to rates that are sustained for up to 48 hours (Miller et al., 2005; Churchward-Venne et al., 2012). MPB is also elevated following exercise in order to provide amino acids to support the increase in MPS, however the provision of exogenous EAAs after exercise attenuates MPB and further stimulates MPS causing net protein balance to become positive (Phillips et al., 1997; Burd et al., 2009). The positive net protein balance leads to an increase in muscle mass and strength through the process of hypertrophy. It is suggested that short lasting but high intensity muscle contractions caused by RET cause the balance of protein turnover in skeletal muscle to shift in favour of MPS by the activation of the mammalian target of rapamycin (mTOR) pathway (Endo et al., 2020), although the mechanisms of skeletal muscle adaptation are not completely defined.

4.1.2.1. Age-related blunting of adaptations to resistance exercise training

The benefits of RET in older individuals are well documented. Maximal motor unit discharge rates increased 49% in older adults following a 6 week resistance exercise

intervention (Kamen and Knight, 2004) representing an increase in force produced by the muscle. 12 weeks of RET elicited improvements in five repetition-maximum (RM) scores of leg extension (44.6%) and leg curl (44.9%) (Wood et al., 2001). In addition, RET has been shown to be effective at reducing mortality risk across all age groups (Nilsson et al., 2020). However, the hypertrophic response of skeletal muscle to RET is blunted in older adults compared to young individuals. For instance, while 1RM increased by 35% in young men and 25.3% in older men with no significant difference between the groups, average change in maximal voluntary contraction (MVC) across all joint angles improved in young (21%) but not older (6.3%) men (Brook et al., 2016). Likewise, muscle thickness of the vastus lateralis (VL) improved by 8.1% in young men but only 5% in older men, and VL fibre length improved in young men (5.1%) but not older men (0.8%). The discrepancies in skeletal muscle adaptations were underlaid by differences in rates of MPS and phosphorylation of P70S6K1, an activator of mTORC1 associated with hypertrophy (Brook et al., 2016). 12 weeks of RET blunted the expression of REDD1, an inhibitor of mTOR signalling, by 80% in young but not older women (Greig et al., 2011). The differential expression of REDD1 was proposed as an explanation for the age-related differences in improvements in quadriceps volume (6.2% in young versus 2.5% in older women) and strength (27% in young versus 16% in older women).

These data suggest that the blunted hypertrophic response in older adults may be linked to expression of regulators of the mTOR pathway, however the associations are not well established. Given the versatility of mTOR regulators (Bai and Jiang, 2010) it is difficult to achieve a complete profiling of their expression using traditional analytical approaches. Furthermore, the response to exercise is complex and likely multifactorial. Metabolomics is capable of simultaneously monitoring hundreds of

metabolites (Lv et al., 2022) making it a powerful technique in the study of complex conditions such as the adaptive response of skeletal muscle to RET.

4.1.3. Metabolomics in the study of adaptations to resistance exercise training

Metabolomics has previously been used to study adaptations to endurance exercise in adults (Lewis et al., 2010) but recent evidence suggests that long term resistance and endurance exercise training induce distinct metabolic adaptations to the same exercise test. Cycling to exhaustion resulted in lower plasma concentrations of branched chain amino acids in resistance trained athletes than endurance trained, sprint trained or untrained individuals, while endurance athletes had higher CPT1-ratios than other groups (Schranner et al., 2021). Wider differences in the metabolic response to exercise testing between groups were not established as the study used a targeted metabolomics kit which assessed amino acids and lipids, however it is likely that more discrepancies in the exercise response would be identified with an untargeted approach. To understand the mechanisms underlying the age-related blunting of the hypertrophic response it is therefore important to study adaptations in the plasma metabolome specific to RET.

While most of the literature has focused solely on endurance exercise (Schranner et al., 2020) there is growing interest in applying metabolomics to specifically study adaptations to resistance exercise. Berton et al (2016) identified 13 metabolites with significant changes over time following resistance exercise in healthy young men. Metabolites which responded rapidly to exercise were largely related to the anaerobic system and energy metabolism pathways while those with significant changes occurring up to 1 hour after the end of exercise were linked to anabolic processes and muscular recovery. In their comprehensive profiling of the plasma metabolome, Morville et al. (2020) demonstrated that one hour of resistance exercise resulted in

significant changes to the expression of 93 metabolites either immediately following exercise cessation or over the course of 3 hours. The metabolites belonged to a range of classes, with lipids and nucleotides downregulated following exercise and amino acids upregulated. Finally, 46 metabolites in skeletal muscle were altered by 5 weeks RET and were linked to a wide range of metabolic functions including those involved in muscle growth (Gehlert et al., 2022). However, these studies only investigated young, healthy, and relatively well-trained men and therefore there is no appreciation for the impact of age on the metabolic response to RET or how the metabolic response may relate to the blunting of functional improvements of skeletal muscle in older individuals.

It is known that metabolomics can be used to identify metabolites that act as markers of decline in metabolic health related to the development of sarcopenia in both the muscle and plasma metabolomes. For example, differences in plasma concentration of EAAs, glutamine and tyrosine were identified between frail and non-frail elderly individuals (Adachi et al., 2018). Likewise, 37 serum amino acids and their derivatives were informative of physical frailty and sarcopenia in individuals over 70 years old. However, both of these studies were targeted, focussing specifically on amino acid profile and therefore did not investigate the wider metabolism affected by age, and neither compared amino acid profile to young individuals. Differences in frail and non-frail older individuals in the muscle metabolome were similar to those of healthy older and young individuals, with most metabolites relating to mitochondrial respiration, oxidation and muscle tissue turnover (Fazelzadeh et al., 2016b). The same study demonstrated that RET in older individuals led to adaptations in muscle amino acid metabolism and acylcarnitine level, however the younger group did not undergo the exercise intervention and therefore potential age related blunting of metabolic adaptation could not be investigated (Fazelzadeh et al., 2016b). This study also used a

targeted approach and therefore potentially misses out on important insights in adaptations to both ageing and resistance exercise. Using an untargeted approach, 81 metabolites indicative of widespread metabolic changes were identified as significantly altered from baseline to follow up in a 5 year longitudinal study (Johnson et al., 2019) however the mean age at baseline was 59 and there was no evaluation of similar 5 year changes in young individuals. Although the current literature lacks an evaluation of the effect of age on the exercise response it does demonstrate that both the metabolic changes associated with ageing and the response to RET can be detected with a metabolomics approach. Metabolomics may therefore be used to identify and explain differences in the adaptive response to resistance exercise between young and older adults.

Recently it was shown that 20 weeks of RET led to hypertrophic responses in skeletal muscle in young individuals which were blunted with increasing age in both men and women (Phillips et al., 2017). Markers of metabolic health, such as insulin sensitivity assessed by fasting glucose concentration and homeostasis model of insulin resistance (HOMA-IR) score, plasma cholesterol and plasma triglycerides, were assessed before and after resistance exercise intervention. While resistance exercise was able to mitigate the age-related increase in HOMA-IR observed at baseline it was not able to combat the age associated elevation of plasma triglycerides (Phillips et al., 2017). The differences in the biochemical profile associated with age before and after 20 weeks of RET suggest that metabolism is impacted differentially by resistance exercise with advancing age. From the same cohort of participants, a panel of metabolites were identified as predictors of ageing at baseline from a skeletal muscle tissue biopsy using an untargeted metabolomics approach (Wilkinson et al., 2020). However evaluation of the metabolome using untargeted techniques before and after RET has not yet been conducted.

Metabolomics analysis of muscle tissue provides a direct readout of metabolic changes that may underlie the ageing process. However, muscle biopsies are an invasive procedure which require highly trained individuals to perform and can lead to complications, including severe discomfort or infection (Cotta et al., 2021). In contrast the collection of plasma is minimally invasive and easier to achieve, particularly in functionally limited older populations such as individuals with sarcopenia (Wilson et al., 2018). Although Fazelzadeh and colleagues concluded that plasma metabolites should not be used in assessment of muscle metabolism (Fazelzadeh et al., 2016b) others suggest the plasma metabolome provides an accurate readout of muscle health. For instance, a concordance between the plasma metabolome and skeletal muscle transcriptome was observed in type 1 diabetic individuals with several pathways, including lipid and carbohydrate metabolism, showing similar directional changes during insulin deprivation (Dutta et al., 2012). A later study found plasma metabolites were correlated with skeletal muscle tissue, including several species of phospholipid and triglyceride, and concluded that the plasma metabolome could be used as a proxy for studying tissue metabolites (Wu et al., 2022). In addition, Chapter 3 of this thesis demonstrated that assessment of differential metabolite abundance before and after 56 days of bed rest informed on adaptations in substrate oxidation and insulin sensitivity at the level of skeletal muscle and therefore lends further support to the use of plasma as a proxy for skeletal muscle tissue in studies of human metabolism. As biopsies may not always be viable, especially in older adults with functional limitations, identifying markers of ageing and the adaptive response to resistance exercise in plasma would be beneficial.

Much of the previous metabolomics work has focused either on young individuals or old individuals with few comparisons between the ages, especially in regard to adaptations to RET. In this study, a fully characterised patient cohort of healthy adults

completed a supervised, controlled exercise intervention and reported age-related blunting of skeletal muscle hypertrophy and other improvements relating to metabolic health. In addition, a defined panel of biomarkers for ageing in the muscle metabolome were identified, demonstrating the ability of untargeted metabolomics to classify participant cohorts by age in this study. However our understanding of age-related adaptations to resistance exercise in the metabolome is still lacking and it is unknown whether the metabolites which were informative of age in the muscle metabolome are reflected in the more easily accessible plasma. The aims of this chapter are therefore as follows:

1. To identify metabolites important in the classification of samples by age in the plasma metabolome at baseline and to compare the plasma and muscle metabolomes at baseline to determine whether plasma biomarkers of ageing are an accurate reflection of metabolic changes within skeletal muscle tissue
2. To investigate the adaptive response to resistance exercise in the plasma metabolome in young and older individuals, and to evaluate the differences in plasma markers of resistance exercise between the groups to determine the impact of ageing on the plasma metabolic response to RET

4.2. Methods

4.2.1. Study design

This work utilised samples collected as part of a published volunteer intervention study (Phillips et al., 2017) conducted at the University of Nottingham. This study was reviewed and approved by the University of Nottingham Medical School Ethics Committee (D/2/2006) and complied with the Declaration of Helsinki. All subjects gave written informed consent to participate in the study prior to inclusion after all procedures and risks were explained. The original study design is as follows:

Healthy young (n = 11, 25±4 years), middle-aged (n = 10, 50±4 years), and older (n = 10, 70±4 years) men and women were recruited for a RET intervention study. All subjects performed activities of daily living but did not participate in routine exercise and were well matched for baseline lean mass. Exclusion criteria included metabolic, respiratory or cardiovascular disorders; overt muscle wasting (>1 SD below age norms); or other signs and symptoms of ill health.

Participants underwent 20 weeks whole-body RET, completing 3 supervised sessions of approximately 60 minutes per week. For the first 4 weeks of training, intensity was increased from 40% to 60% 1RM. For the remaining 16 weeks, intensity was set at 70% 1RM with multiple sets of 12 repetitions and 2 minutes of rest between sets. A total of 8 exercises (seated chest press, latissimus pull down, seated lever row, leg extension, leg curl, leg press, back extension, and ab curl) were performed in each session using the same number of repetitions. Assessments of 1RM were made every 4 weeks to ensure the intensity of the training was correct.

Prior to starting RET and following the final training session, two experimental visits were performed. Subjects refrained from exercise for 72 hours period to each visit and arrived in an overnight fasted state. Body composition was measured by dual-energy X-ray absorptiometry (DEXA; Lunar Prodigy II, GE Medical Systems, Chalfont St Giles,

UK). A catheter was then inserted into the antecubital vein of one arm for primed, continuous infusion of [1,2-$^{13}C_2$] leucine tracer (Cambridge Isotopes Ltd, Newtown Unthank, UK). A baseline blood sample was drawn from the antecubital vein for measures of plasma insulin and glucose, and serum cholesterol and triglycerides. For metabolomics, 4 ml venous blood was collected in EDTA-coated collection tubes at each visit and plasma was separated and immediately stored at -80°C until further analysis. Biopsies of VL tissue were taken under sterile conditions at 0, 120 and 250 minutes of tracer infusion using the conchotome biopsy technique. Muscle was snap-frozen in liquid nitrogen before storage at -80°C. Fractional synthetic rate (FSR) of myofibrillar protein was calculated from the incorporation of tracer into VL at 120 minutes.

Due to limitations in laboratory equipment size, plasma samples were randomly sorted into 2 batches and prepared in an identical manner. Metabolites were extracted from plasma according to the protocol detailed in Section 2.3. Separation of metabolites within samples via liquid chromatography was performed according to the parameters detailed in Section 2.4 and acquisition of data by tandem mass spectrometry was performed according to the protocol in Section 2.5.

4.2.2. Data pre-processing and statistical analysis

Data pre-processing was performed in R using the parameters detailed in Section 2.6. For statistical analysis, data for each polarity and ionisation mode were analysed separately. All analysis was performed using inhouse R scripts using R version 4.1. Scripts are available in Appendix 2.

4.2.2.1. Comparison of groups by age at baseline

Firstly, to identify metabolites informative of age, samples were grouped by time and comparisons were made between young, middle-aged, and older individuals at baseline. Secondly, under the assumption that metabolite abundance in the middle-

aged group would fall between the young and older groups (Wilkinson et al., 2020) the middle-aged group was removed and comparisons were made between only the young and older groups.

Data was centred and scaled to perform principal component analysis (PCA) and partial least squares discriminant analysis (PLS-DA) validated by *k*-fold cross validation using the mixOmics package (Le Cao et al., 2016). Model accuracy was determined by percentage classification error. Variable importance to classification in PLS-DA was determined by VIP score. All features with a VIP score greater than 1 were retained for further analysis. Significance in differential abundance between older and young groups was determined by Student's t-test adjusted for false discovery rate (FDR) using the Benjamini-Hochberg procedure when $p_{adj}<0.05$ (Benjamini and Hochberg, 1995). To demonstrate that metabolite abundance in the middle-aged group fell between the young and older groups, the middle-aged group was then included and significance in differential abundance between all age groups was determined by one-way ANOVA.

4.2.2.1. Comparison of groups by age after resistance exercise training

The same approach was taken to identify metabolites significantly different between plasma collected after RET in younger and older groups. The middle-aged group was again removed under the expectation that metabolite abundance would fall between the two extremes of age. Data was centred and scaled to perform PCA and PLS-DA validated by *k*-fold cross validation. Model accuracy was determined by percentage classification error. The dataset was reduced using VIP>1 and significance was determined using Student's t-test for young vs older comparison. As before, to demonstrate that metabolite abundance in the middle-aged group fell between older and young groups the middle group was then included in analysis and one-way ANOVA was used to determine significance in differential metabolite abundance between all age groups, adjusted for FDR.

4.2.2.1. Pre-post analyses of the influence of age on the metabolic response to resistance exercise training

To study the effect of increasing age in response to RET, baseline and post-intervention samples were compared within each age group using PCA and PLS-DA. Due to high error when the PLS-DA model was validated, a linear mixed effect model was next fitted to the data to find differential metabolite abundance. Linear models can test for variability of metabolite abundance in high dimensionality data (Filzmoser and Nordhausen, 2020). Age and time of collection were fixed effects. Participant ID was a random effect to account for subject specific variation. Contrast matrices were set up to evaluate differences in metabolite abundance at the baseline and post-intervention timepoints within each age group, and to evaluate which metabolites responded differently over time in the old group relative to the young group. Empirical Bayes moderated t-tests were performed to obtain p-values (Smyth, 2004). FDR was accounted for using the Benjamini-Hochberg procedure. Metabolites were deemed significantly different between comparisons when FDR<0.05. Analysis was performed using the limma package (Ritchie et al., 2015).

Finally, to assess the overall similarities between baseline and post-intervention datasets for each group, the Spearman correlation coefficient for the abundance each metabolic feature at baseline and after resistance exercise was determined using the corrplot package (Wei and Simko, 2021).

4.2.3. Prediction of functional activity of metabolites important in classification

Metabolites deemed important in classification by age at baseline or after training were further assessed for functional relevance. Metabolites were putatively identified using the R package metID (Shen, Wu, et al., 2022) which utilises m/z and MS^2 spectra matching from public metabolomics databases (HMDB, KEGG, MoNA, and MassBank) to identify metabolite features. Mass tolerance was set at 5ppm.

Common compound names of identified features were taken from HMDB and mapped to metabolic pathways by over representation analysis (ORA) using MetaboAnalyst version 5.0 (Pang et al., 2021). ORA provides a pathway impact score, which is calculated as the sum of the importance measures of the matched metabolites normalised by the importance measures of all matched and unmatched metabolites in each pathway (Xia and Wishart, 2011). Pathway impact score represents an estimate of the importance of each pathway relative to the global metabolic network (Liu et al., 2019). Pathways with impact score > 0.1 were considered to be the most relevant in ageing, in keeping with current literature (Guo and Tao, 2018; Liu et al., 2019).

4.3. Results

4.3.1. Physiological adaptations to resistance exercise

The physiological adaptations to RET are reported in Phillips et al. (2017), however for clarity a summary is presented here. Although significant gains in whole body strength and muscle quality were observed in young, middle-aged, and older groups after 20 weeks of RET ($p<0.001$ for both measures), only the young group demonstrated significant improvements in whole-body hypertrophy ($p<0.0001$) and relative skeletal mass index ($p<0.05$) in response to RET. Additionally, the young group showed significant improvements in whole-body lean mass and relative skeletal mass index compared to middle-aged and older individuals (lean mass, $p<0.01$; skeletal mass index, $p<0.05$). Although there were no differences in fasted and rested FSR before or after RET between age groups, feeding and acute resistance exercise enhanced FSR significantly only in the young group ($p<0.05$) which may account for the differences in hypertrophy.

Prior to training, HOMA-IR and fasting glucose level were significantly higher in the older group compared to the young ($p<0.05$ for both measures) representing lower insulin sensitivity. Following RET the older group reported significant improvements in HOMA-IR ($p<0.05$) such that there were no significant age-related differences in HOMA-IR after training. While there were no significant differences in plasma levels of triglycerides or total, LDL or HDL cholesterol between age groups before RET, there was a significant relationship seen between advancing age and LDL before RET and RET did not induce significant differences in LDL cholesterol. There was also a significant relationship between age and triglycerides after RET, indicating age-related differences in the metabolism.

4.3.2. Metabolomic analysis of skeletal muscle tissue

In the same cohort of patients, biopsies of skeletal muscle tissue were taken at baseline to investigate biomarkers of ageing (Wilkinson et al., 2020). A summary of

these findings is presented here. An untargeted metabolomics approach was undertaken and the random forest algorithm was used to identify a subset of metabolites most informative of age in skeletal muscle tissue. The top 10 metabolites for each polarity and ion mode, as determined by variable importance, were selected and putatively identified. Several identified metabolites were already known to be associated with ageing, lending support to this approach. For example, androgen steroids decreased in abundance in the older group which is in line with current literature. In addition, metabolite network generation showed generation of subnetworks around phosphocreatine, androgen metabolism, histamine and lysophospholipid metabolism, pointing to role for these metabolites in human muscle ageing.

4.3.3. Multivariate analysis of groups at baseline

Having demonstrated that an untargeted metabolomics approach is appropriate for classifying samples by age and can identify metabolites most informative of age in skeletal muscle tissue, the next step was to test whether a similar approach could be applied to a more easily accessible tissue such as plasma. Initial analysis at baseline using PCA showed no separation between age group. After fitting the PLS-DA model, better clustering of samples based on age was observed. However when the model was validated error rates of approximately 40% were seen in all ionisation modes and polarities. The model was therefore found to be overfitted and the classification was not reliable.

After removal of the middle age group so that only the extremes of age would be represented, clustering of older and young samples remained poor with PCA but there was improved clustering of samples when a PLS-DA separation model was applied allowing for the classification of samples by age (Figure 4.1). Cross validation of this model showed classification error improved in all ionisation modes and polarities.

After filtering by VIP score, a total of 111 polar metabolites (54 negative and 57 positive) and 926 non-polar metabolites (327 negative and 599 positive) were found to be informative of age and were retained for further analysis.

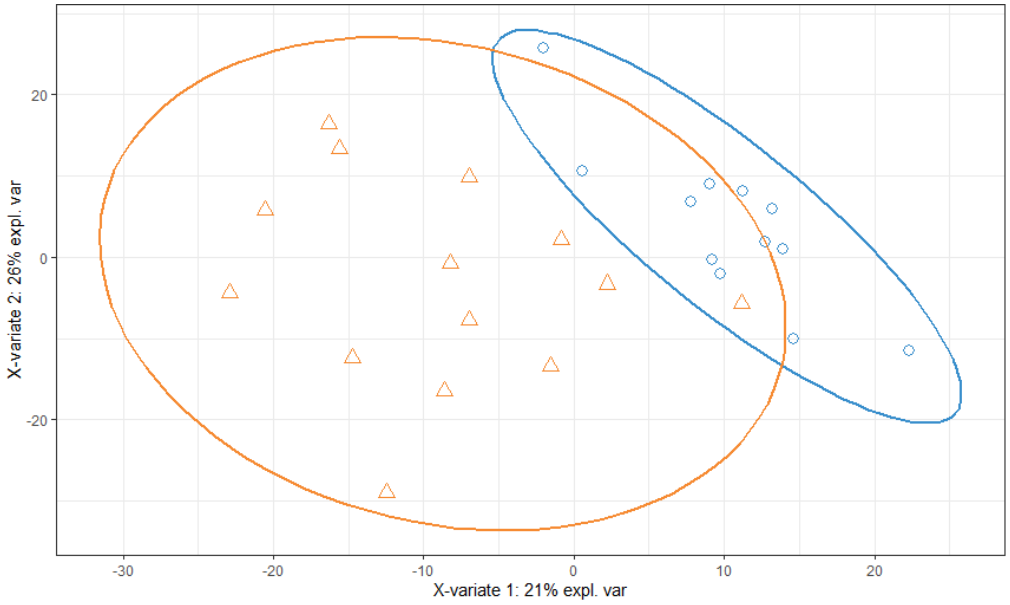

Figure 4.1 Separation of age groups at baseline using multivariate statistical approaches following removal of middle-aged group

Representative plot of partial least squares discriminant analysis (PLS-DA) with 95% confidence intervals showing similarity in abundance of all metabolites detected in the fasting, rested state at baseline between healthy young (orange triangle) and older (blue circle) individuals in non-polar negative data. Using PLS-DA, separation of older and young groups was observed, allowing classification of samples by age.

4.3.3.1. Identification of metabolites informative of age at baseline

Annotation by metID putatively identified 81 unique polar metabolites (38 negative and 43 positive) and 514 unique non-polar metabolites (167 negative and 347 positive) within a mass tolerance of 5ppm.

The baseline plasma abundance of androgen related metabolites was found to be disturbed with ageing (Figure 4.2). Previously, a number of metabolites related to androgen steroid metabolism declined in abundance with age in skeletal muscle tissue (Wilkinson et al., 2020) and thus the plasma is accurately reflecting muscle level adaptations to age. Most notably, dehydroepiandrosterone (DHEA) sulphate

decreased significantly in the older group ($p<0.001$). Androsterone, another androgen related metabolite, decreased between older and young groups, although not significantly ($p=0.056$). Furthermore, 24-hydroxycalcitriol, a metabolite of vitamin D_3, tended to decline in abundance in the older group ($p=0.073$).

The plasma abundance of several species of lipid metabolites were different between young and older groups. For example, significant increases in plasma level of sphingolipid metabolite glucosylceramide (d18:1/16:0) and the ether lipid metabolite lysoPA(P-16:0e/0:0) ($p<0.001$ and $p=0.03$, respectively) with age were observed, as was a significant decrease in plasma DG(18:0e/2:0/0:0) ($p<0.001$) (Figure 4.3). ORA also found that other sphingolipid and ether metabolites were involved in pathway disturbances between young and older groups, although they did not change significantly within the plasma individually (for all metabolites, $p>0.05$) (Figure 4.4 and Figure 4.5).

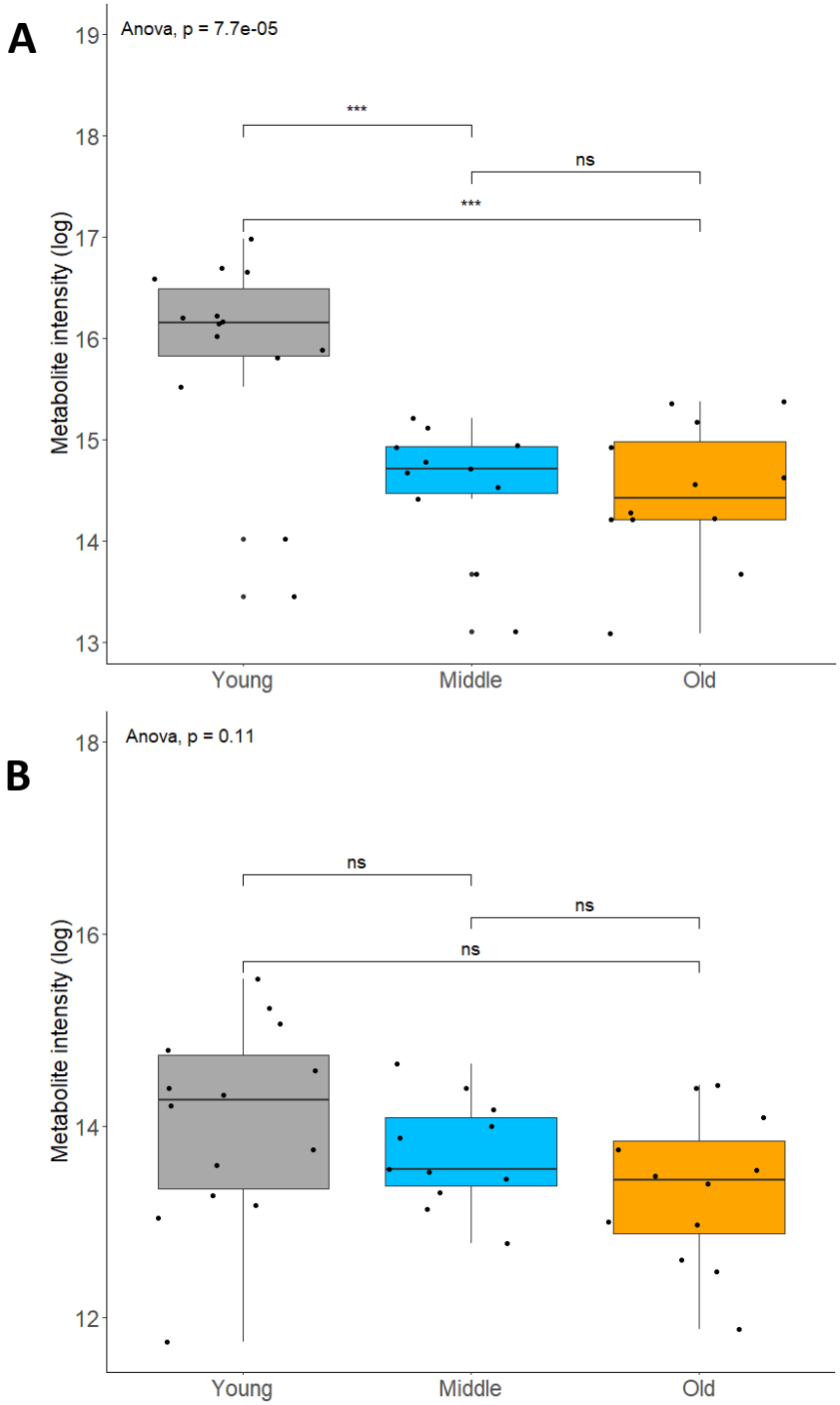

Figure 4.2 Plasma abundance of androgen steroid metabolites in young, middle-aged and older individuals at baseline

Boxplots showing log transformed abundance of (A) DHEA sulphate and (B) androsterone in the fasting, rested plasma metabolome in healthy young (Young), middle-aged (Middle) and older individuals (Old) prior to beginning RET. Plasma level of DHEA sulphate decreased significantly between young and middle-aged and young and older individuals. Plasma level of androsterone decreased between young and older individuals but the decline was not significant ($p>0.05$).

***$p<0.001$

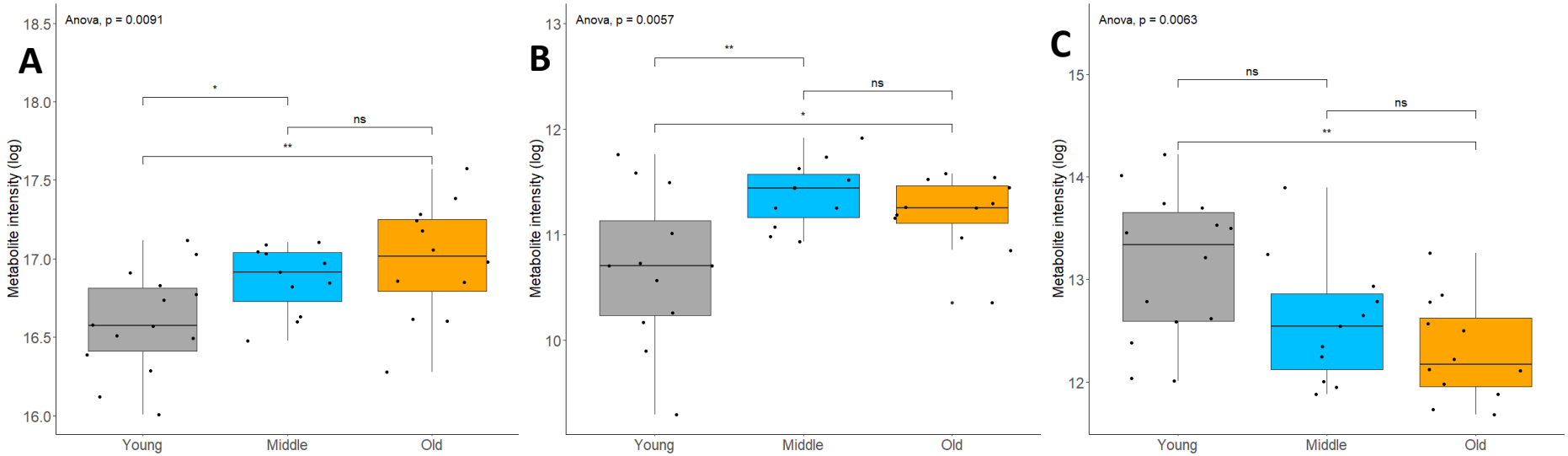

Figure 4.3 Plasma abundance of sphingolipid and ether metabolites in young, middle-aged and older individuals at baseline

Boxplots showing log transformed abundance and (A) glucosylceramide (d18:1/16:0), (B) lysoPA(P-16:0e/0:0), and (C) DG(18:0e/2:0/0:0) in the fasting, rested plasma metabolome in healthy young (Young), middle-aged (Middle) and older individuals (Old) prior to beginning RET. Plasma levels of glucosylceramide (d18:1/16:0) and lysoPA(P-16:0e/0:0) increased significantly between young and older individuals while DG(18:0e/2:0/0:0) decreased significantly between young and older individuals.

*p<0.05, **p<0.01

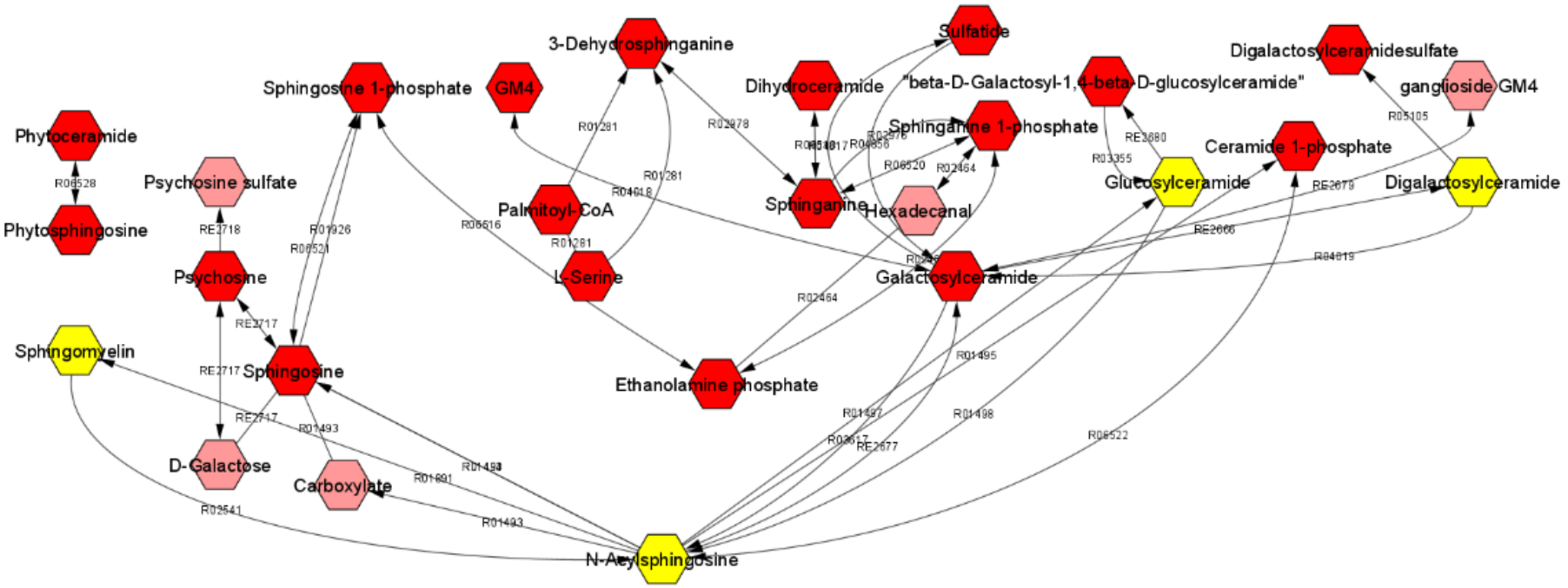

Figure 4.4 Output of over representation analysis mapping metabolites to sphingolipid metabolism pathways

Putative metabolite identification and over representation analysis (ORA) found sphingolipid metabolism pathways were different between healthy older and young individuals (pathway impact score > 0.1) in the fasted, rested state prior to RET. Metabolites highlighted in yellow were identified as most important in pathway analysis.

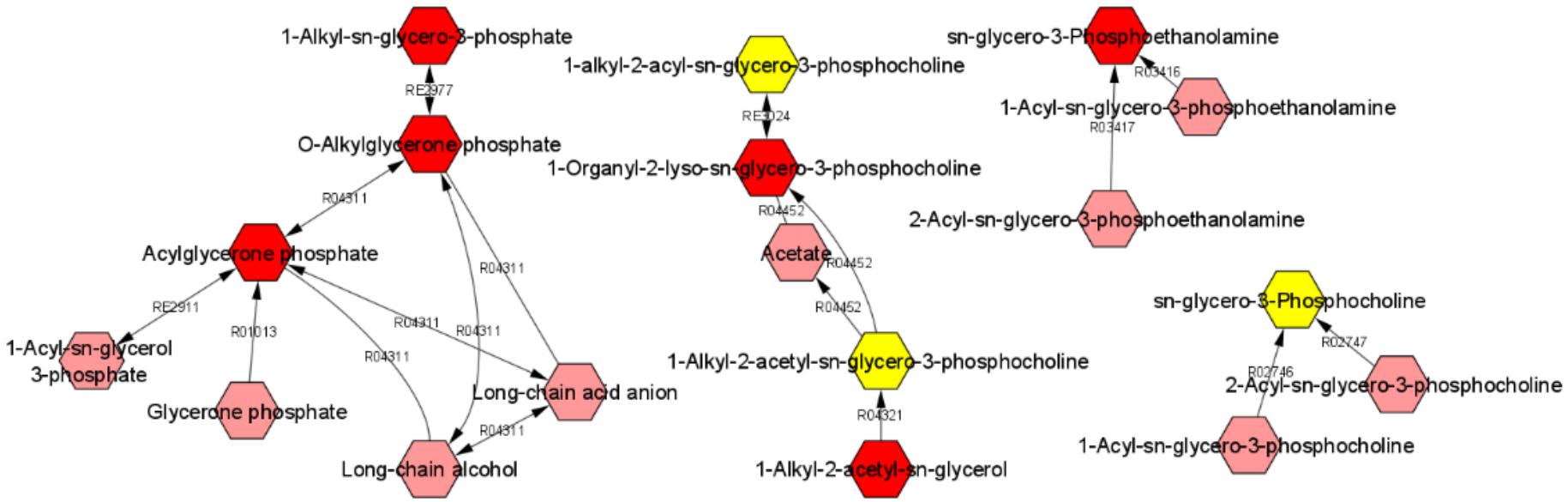

Figure 4.5 Output of over representation analysis to map metabolites to biological pathways involved in differences in ether metabolites with ageing baseline

Putative metabolite identification and over representation analysis found that ether metabolism pathways were different (pathway impact score > 0.1) between healthy young and older individuals in the fasting, rested state prior to RET. Metabolites highlighted in yellow were identified as most important in pathway analysis.

Finally, ORA identified 24 pathways involved in the separation of samples by age, of which 10 had impact score > 0.1. Among these pathways, five were involved in lipid metabolism. The major pathway disturbed between older and young participants was linoleic acid metabolism, with the most influential changes mapped to a significant decrease in the plasma level of the metabolite 13-L-hydroperoxylinoleic acid (13(S)-HPODE) ($p<0.01$) (Figure 4.6).

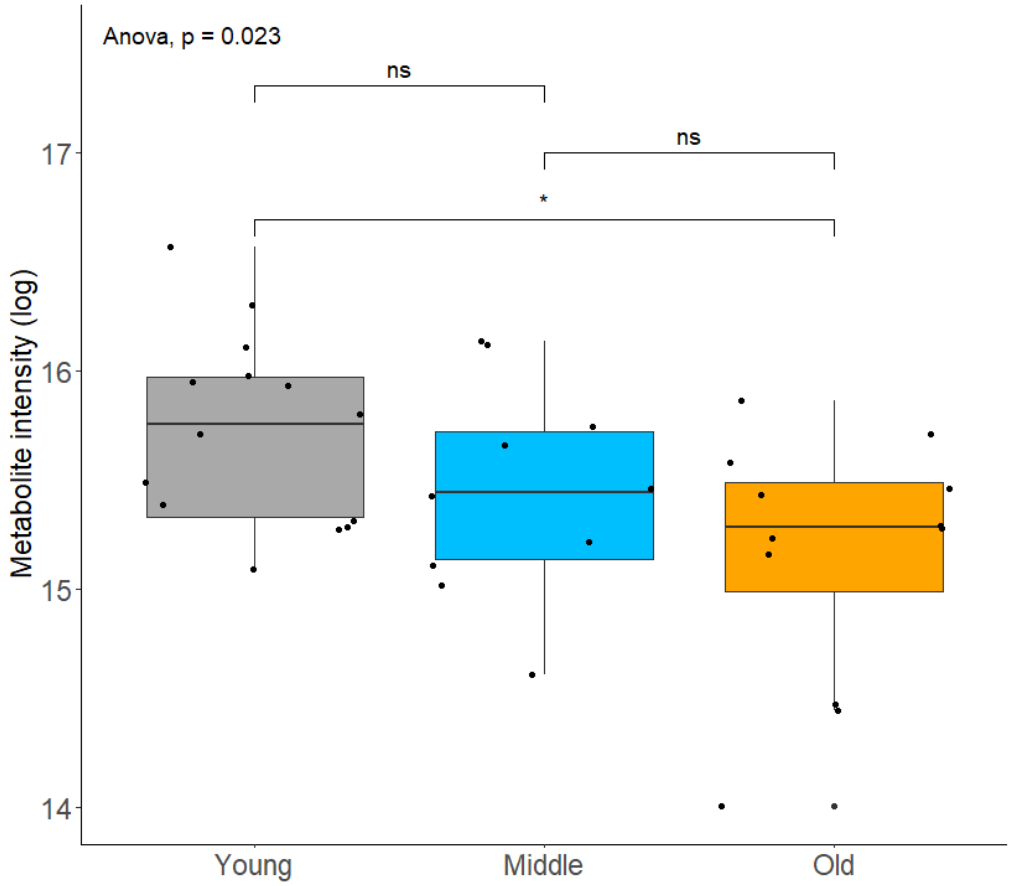

Figure 4.6 Plasma abundance of 13(S)-HPODE in young, middle-aged and older individuals at baseline

Boxplot showing log transformed abundance of 13-L-hydroperoxylinoleic acid (13(S)-HPODE), a metabolite involved in linoleic acid metabolism, in the fasting, rested plasma metabolome between healthy young (Young), middle-aged (Middle) and older individuals (Old) prior to beginning RET. Plasma level decreased significantly between young and older age groups.

*$p<0.05$

4.3.4. Multivariate analysis of groups post-intervention

Similarly to baseline analysis, PCA plots of post-intervention samples showed poor separation when the middle age group was included and although clustering improved with PLS-DA classification error remained very high. When the middle group was removed from analysis, classification error of PLS-DA was reduced and samples could be classified as young or older (Figure 4.7). After filtering by VIP score a total of 127 polar metabolites (63 negative and 64 positive) and 901 non-polar metabolites (335 negative and 566 positive) were retained for further analysis.

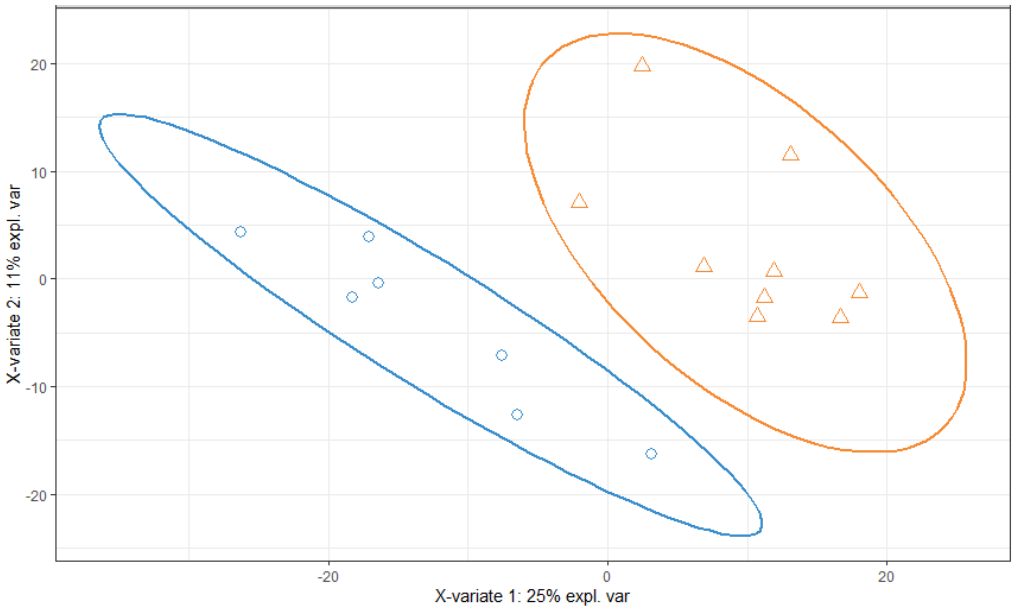

Figure 4.7 Separation of old and young age groups after RET using PLS-DA

Representative plot of partial least squares-discriminant analysis (PLS-DA) separation models with 95% confidence intervals showing similarity in abundance of all metabolites detected in the fasting, rested state after 20 weeks RET between healthy young (orange triangle) and older (blue circle) individuals in non-polar negative data. Clustering of samples by age was improved from previous PLS-DA model which included the middle-aged group.

4.3.4.1. Comparison to baseline plasma metabolome

Metabolite identification found 329 unique metabolites involved in the separation of young and older groups were overlapping between baseline and post-training

samples. ORA showed that many metabolic pathways involved in driving separation of samples by age were similar in the baseline and post-intervention samples (Figure 4.8).

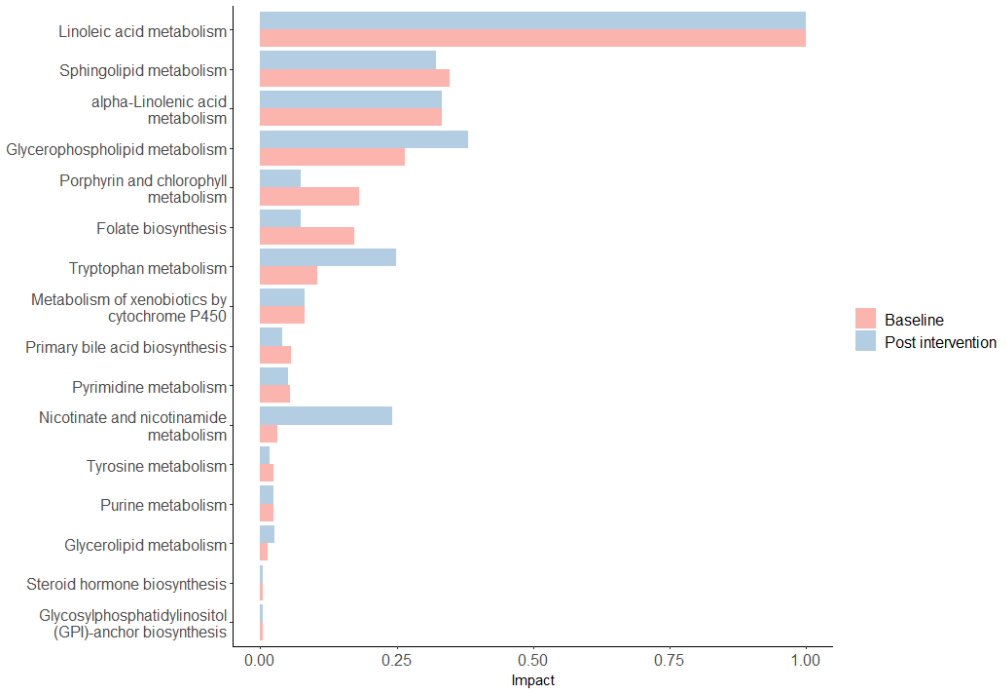

Figure 4.8 Bar graph showing similarity of pathway impact scores between baseline and post-intervention samples

Impact scores of pathways which were identified by over representation analysis as different between the healthy young and older groups at baseline were compared to impact scores of the same pathways after 20 weeks RET. Many pathways had similar impact scores before and after resistance training. Linoleic acid metabolism had the largest impact score between ages at both timepoints.

For instance, linoleic acid metabolism had the strongest impact in classifying groups by age at both baseline and after resistance exercise, although the mechanisms differed slightly. At baseline, differences in the pathway were mapped to a decline in the plasma abundance of a breakdown product of linoleic acid, however after exercise, differences were mapped to a significant decrease in linoleic acid itself ($p<0.01$) (Figure 4.9).

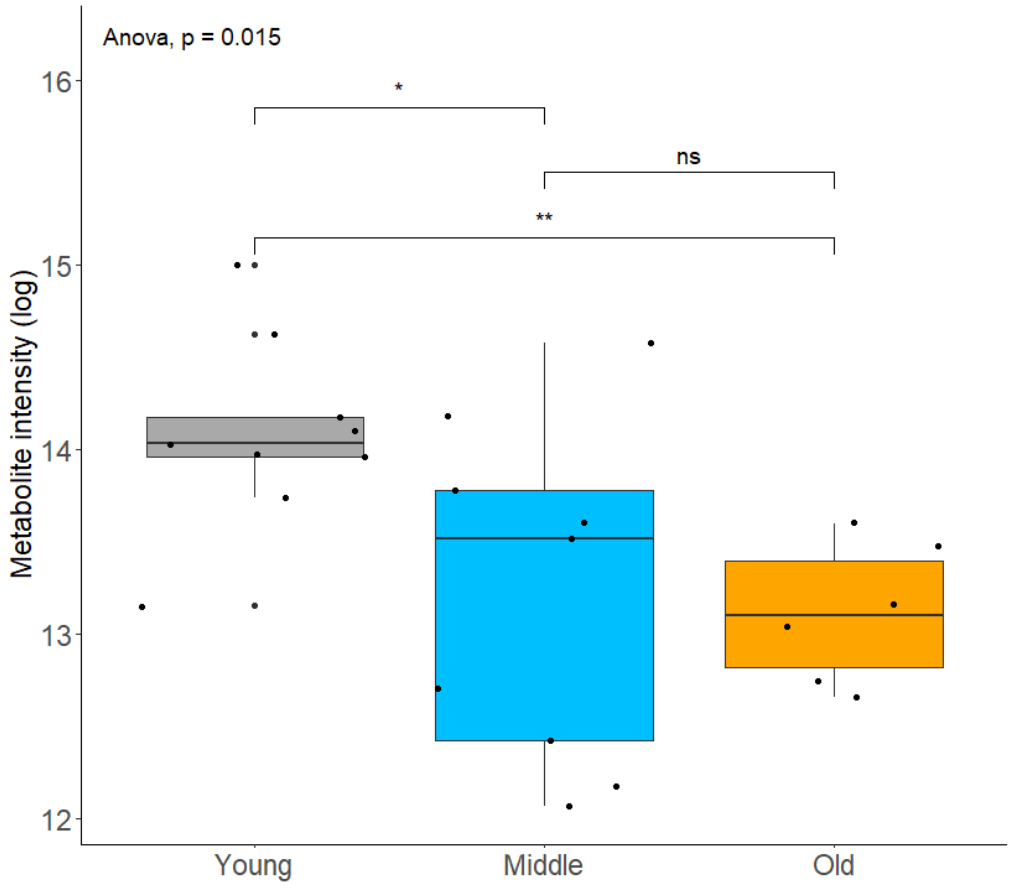

Figure 4.9 Plasma abundance of linoleic acid in young, middle-aged and older individuals after resistance exercise training

Boxplot showing log transformed abundance of linoleic acid in the fasting, rested plasma metabolome between healthy young (Young), middle-aged (Middle) and older (Old) individuals after completing 20 weeks supervised RET. Plasma levels of linoleic acid decreased significantly between young and middle, and young and older age groups.

*p<0.05, **p<0.01

Similar impact scores at baseline and after resistance exercise were also seen in sphingolipid metabolism, purine metabolism, pyrimidine metabolism and steroid hormone biosynthesis pathways. In particular, the pattern of decline in plasma metabolite abundance of DHEA sulphate and androsterone with ageing was similar to baseline, although interestingly the decline was significant for both metabolites after resistance exercise ($p<0.001$ and $p<0.01$, respectively) (Figure 4.10). These data therefore suggest that, although some precise pathways may differ, the overall plasma

metabolomic profile of ageing remains similar to baseline despite the exercise intervention.

However, a large increase in the impact score of nicotinate and nicotinamide metabolism after resistance exercise was observed. This impact was mapped to the presence of two precursors of the essential energy metabolite nicotinamide adenine dinucleotide (NAD+), diamino-NAD+ and nicotinamide D-ribonucleotide (NMN) (Figure 4.11), although their plasma metabolite abundance was not significantly different between the young and older groups ($p=0.18$ and $p=0.4$, respectively).

An increase in the impact score of glycerophospholipid metabolism to 0.38 after resistance exercise was also noted when compared to its baseline score of 0.26. Of the five metabolites identified as involved in the pathway by ORA, significant increases in the plasma abundance of phosphatidate ($p=0.024$) and phosphatidylethanolamine (PE) ($p=0.046$) were observed in the older group (Figure 4.12).

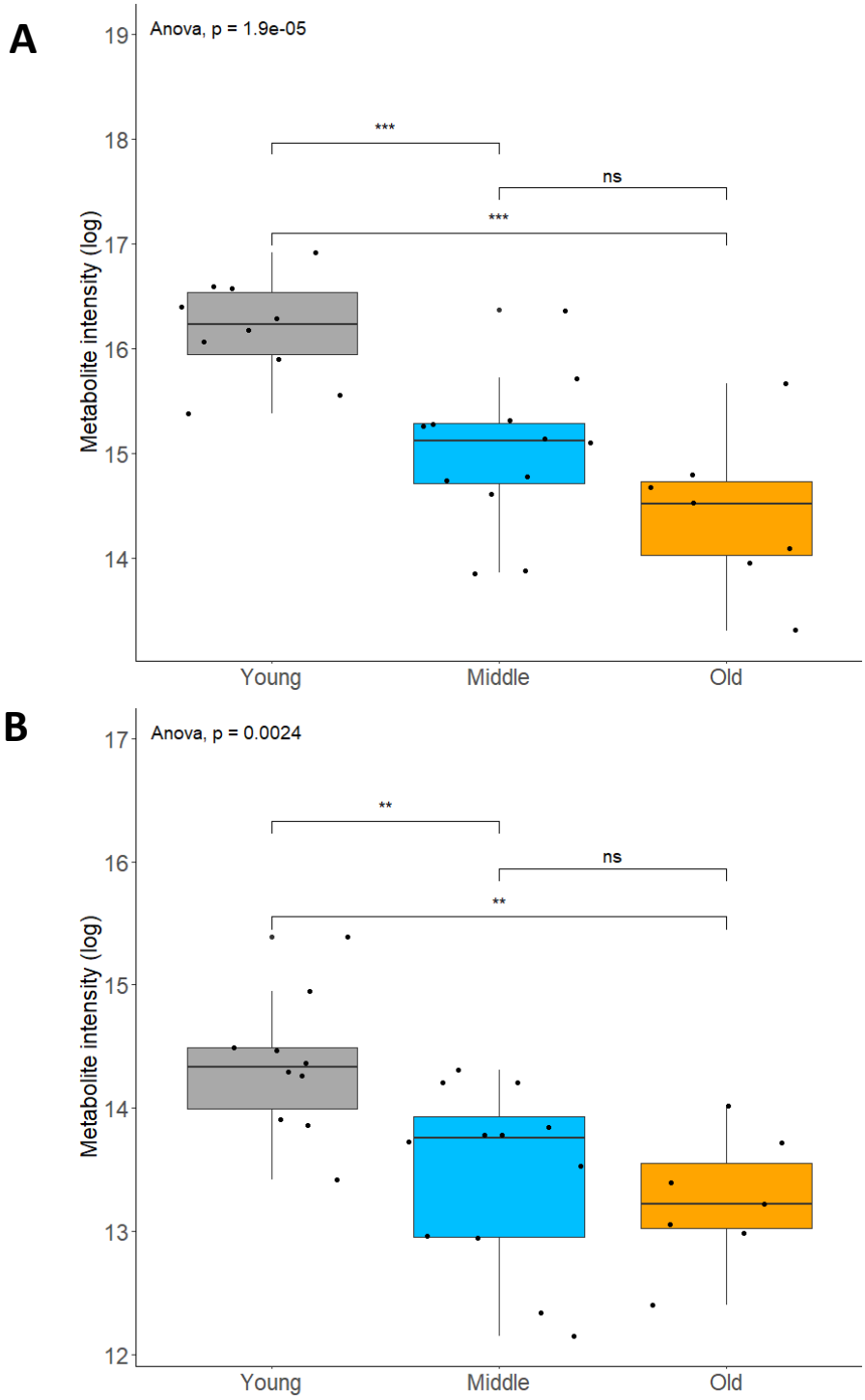

Figure 4.10 Plasma abundance of androgen steroid metabolites in young, middle-aged and older individuals after resistance exercise training

Boxplots showing differences in log transformed abundance of (A) DHEA sulphate and (B) androsterone in the fasting, rested plasma metabolome between healthy young, middle-aged and older individuals after 20 weeks RET. Plasma abundance of DHEA sulphate and androsterone decreased significantly between young and middle-aged, and young and older individuals.

**p<0.01, ***p<0.001

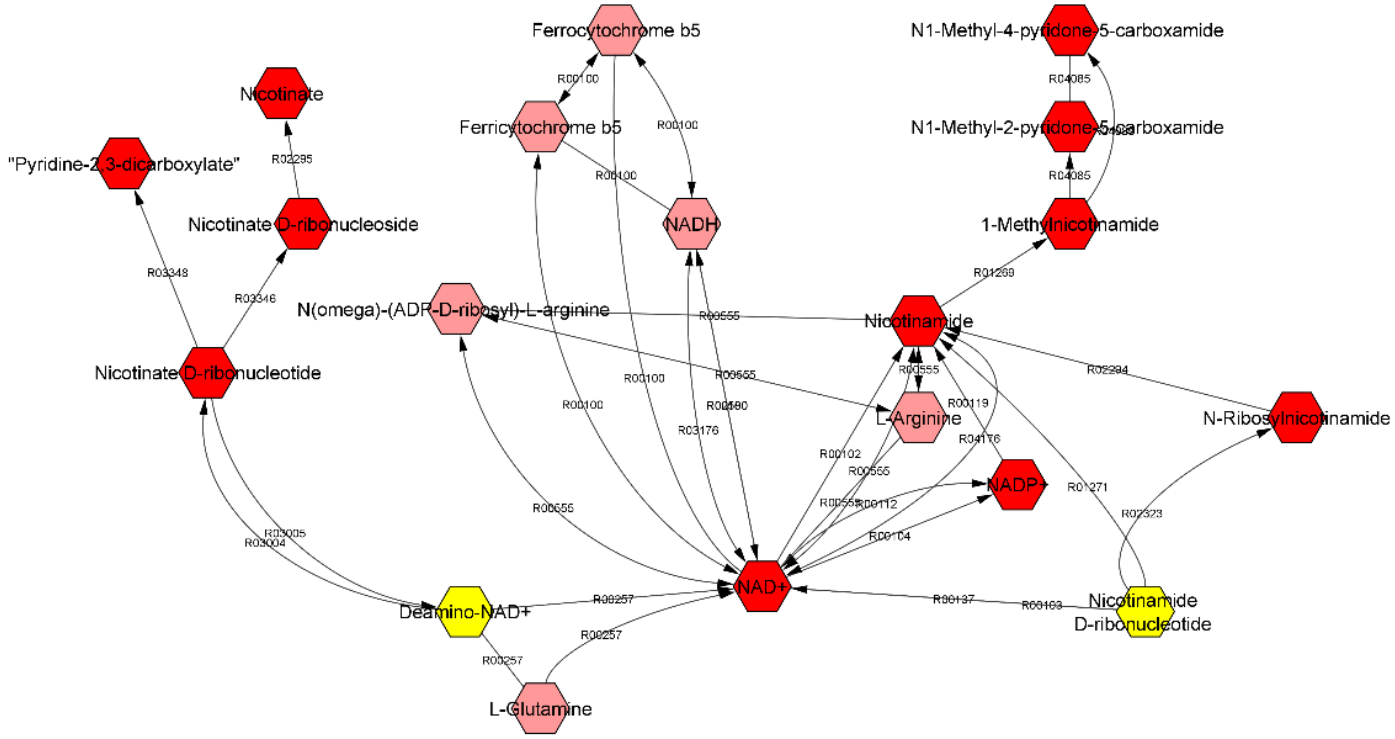

Figure 4.11 Output of over representation analysis to map metabolites to biological pathways involved in differences in nicotinate and nicotinamide metabolism with ageing after resistance exercise training

Putative metabolite identification and over representation analysis found that nicotinate and nicotinamide metabolism pathways were different (pathway impact score > 0.1) between healthy young and older individuals after 20 weeks RET in the fasted, rested state. The impact score of the nicotinate and nicotinamide metabolism pathway increased from 0.03 at baseline to 0.24 after RET. Metabolites highlighted in yellow were deemed important in driving pathway impact in ageing by over representation analysis.

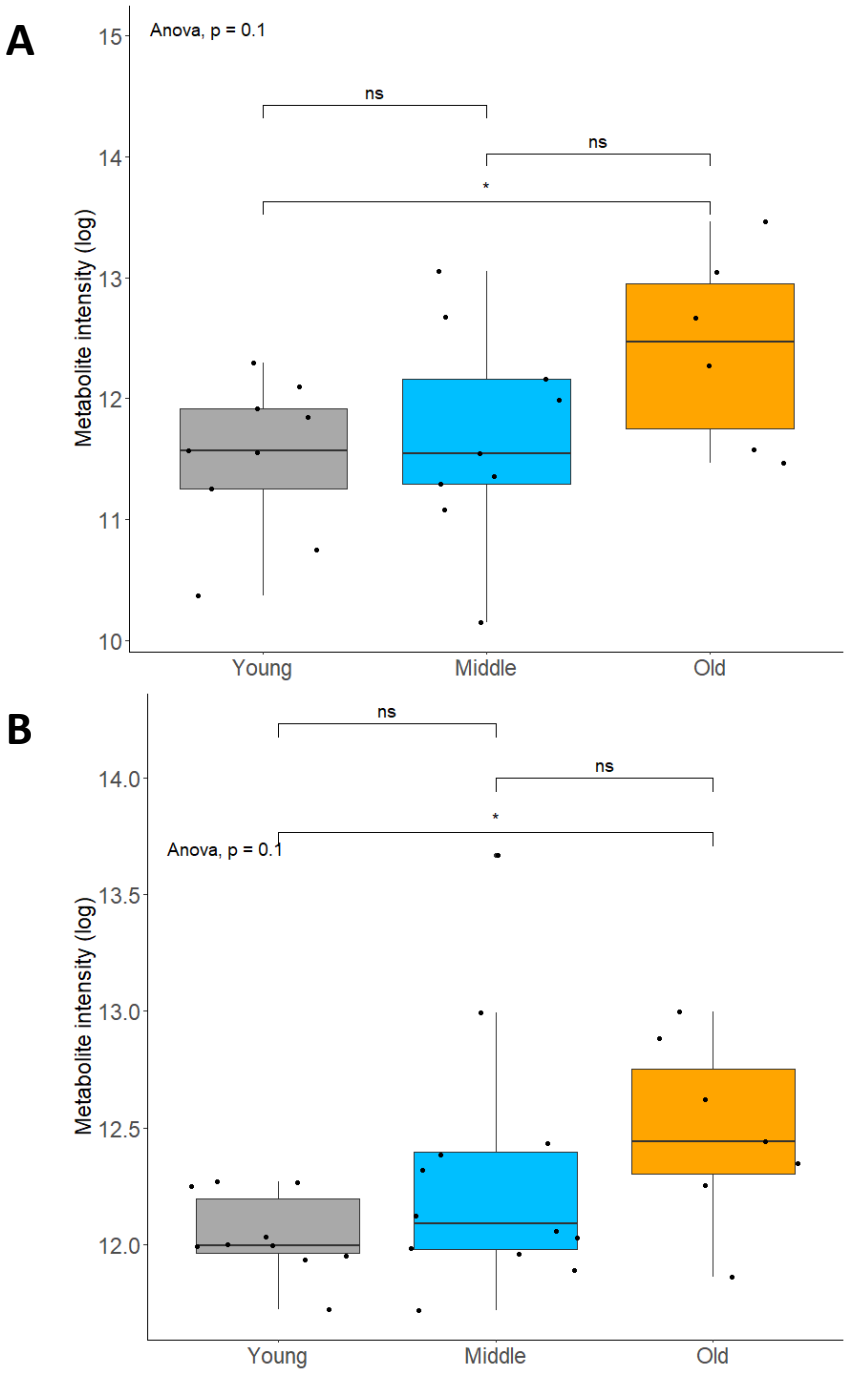

Figure 4.12 Differences in plasma abundance of glycerophospholipids between age groups after resistance exercise training

Boxplots showing differences in log transformed abundance of (A) phosphatidylethanolamine and (B) phosphatidate in the fasting, rested plasma metabolome between healthy young, middle-aged and older individuals after 20 weeks RET. Plasma level increased significantly between young and older individuals for both metabolites.

*p<0.05

4.3.5. Within age group time course analysis

No real differences were seen in metabolites important in classification of samples by age at either pre- or post-exercise intervention, therefore confirmatory analysis to see if this was reflected from a pre-to-post intervention standpoint was next performed. To identify metabolites specifically changed by RET, the samples were grouped by age and formed three separate datasets for analysis. Firstly, for each age group, baseline and post-intervention samples were compared using PLS-DA. However, validation of the PLS-DA model returned high error rates for all ages (Figure 4.13).

Fitting a linear mixed effect model is an alternative approach to testing variability of metabolite abundance in high dimensionality time course data (Filzmoser and Nordhausen, 2020), therefore a linear mixed effect model was fitted to each data matrix using participant ID as a random effect to control for subject specific variation at baseline which may be a confounding factor. However, no significant differences in metabolite abundance were found. Pre-post analysis of metabolites also found that no metabolites were significantly altered by resistance exercise in the old group relative to the young (Figure 4.14).

To confirm pre-post analysis findings, a correlation matrix of all detected metabolite features was constructed. Correlation of abundance values at baseline and post-intervention for each metabolite showed high levels of correlation in all age groups (Figure 4.15). Collectively, these data suggest that 20 weeks RET has little to no impact on the fasting, resting plasma metabolome regardless of age.

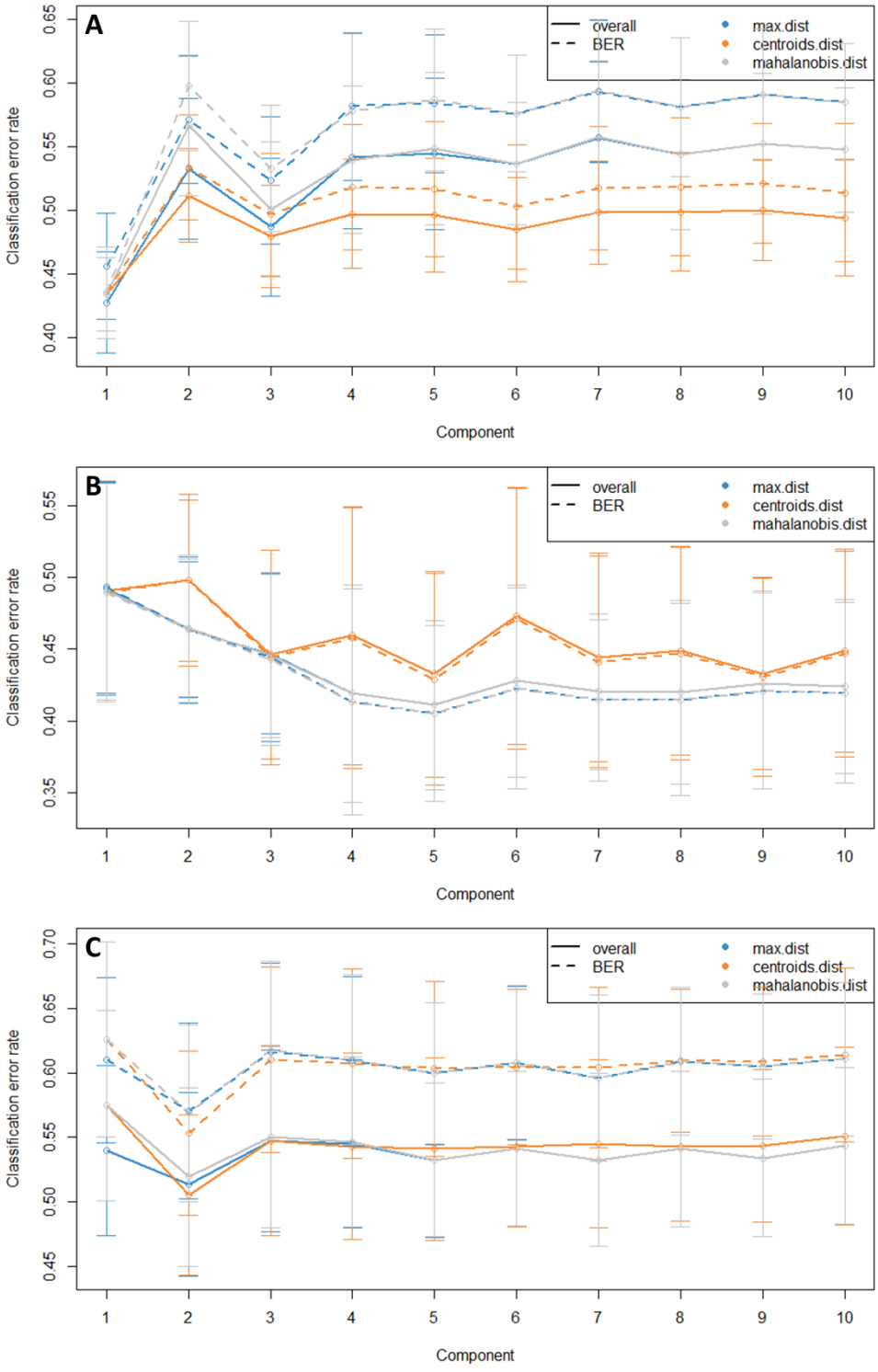

Figure 4.13 Representative plots of classification error of PLS-DA separation model for classification of samples by time

Representative example of classification error following k-fold cross validation of PLS-DA models of separation by timepoint for (A) young, (B) middle-aged, and (C) older individuals from the non-polar negative dataset. Overall maximum distance error was high (>40%) for all age groups, indicating that the separation model would be overfitted if applied to the data.

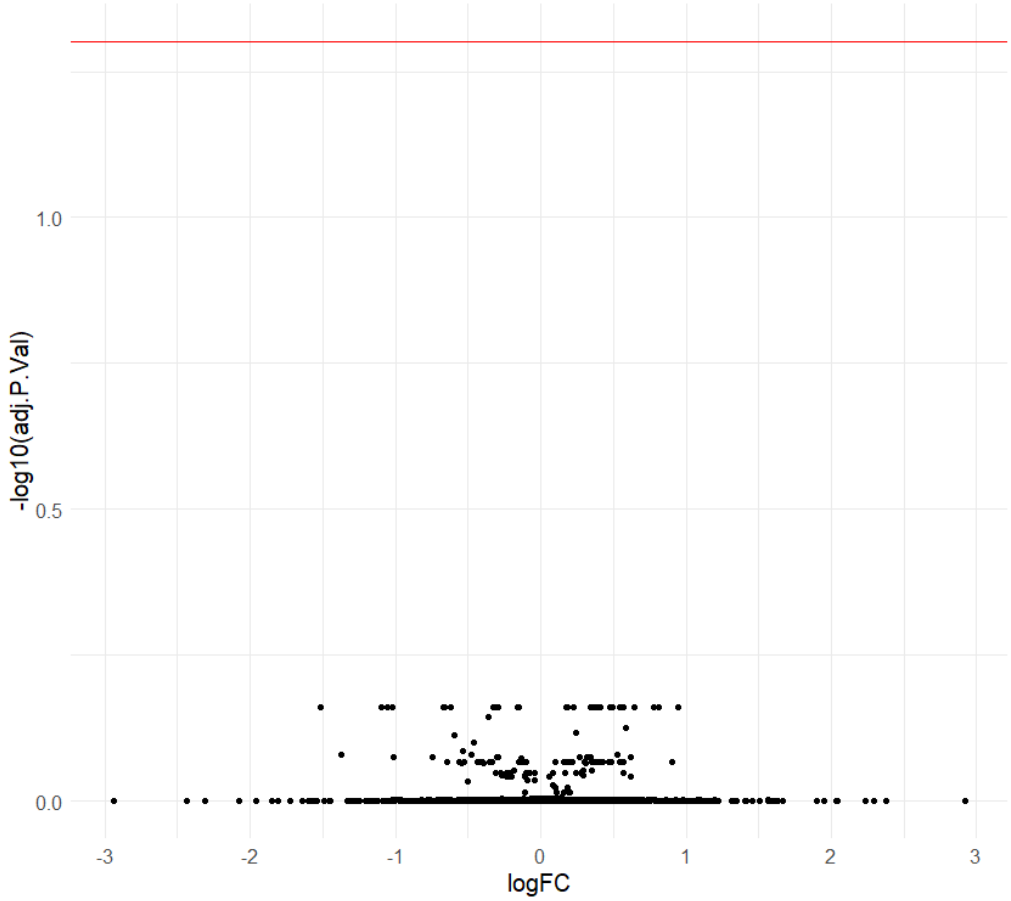

Figure 4.14 Differential abundance of metabolites before and after resistance exercise training in older group relative to young group

Volcano plot showing metabolites which are significantly different in abundance after 20 weeks RET in the older group relative to the young group. Each plotted point represents one metabolite. The x axis shows log fold change of metabolite abundance. The y axis shows -log10 p-value adjusted for false discovery rate (FDR) by the Benjamini-Hochberg method. The red line shows the threshold of FDR<0.05. No metabolites were significantly different in the older group relative to the young group after RET.

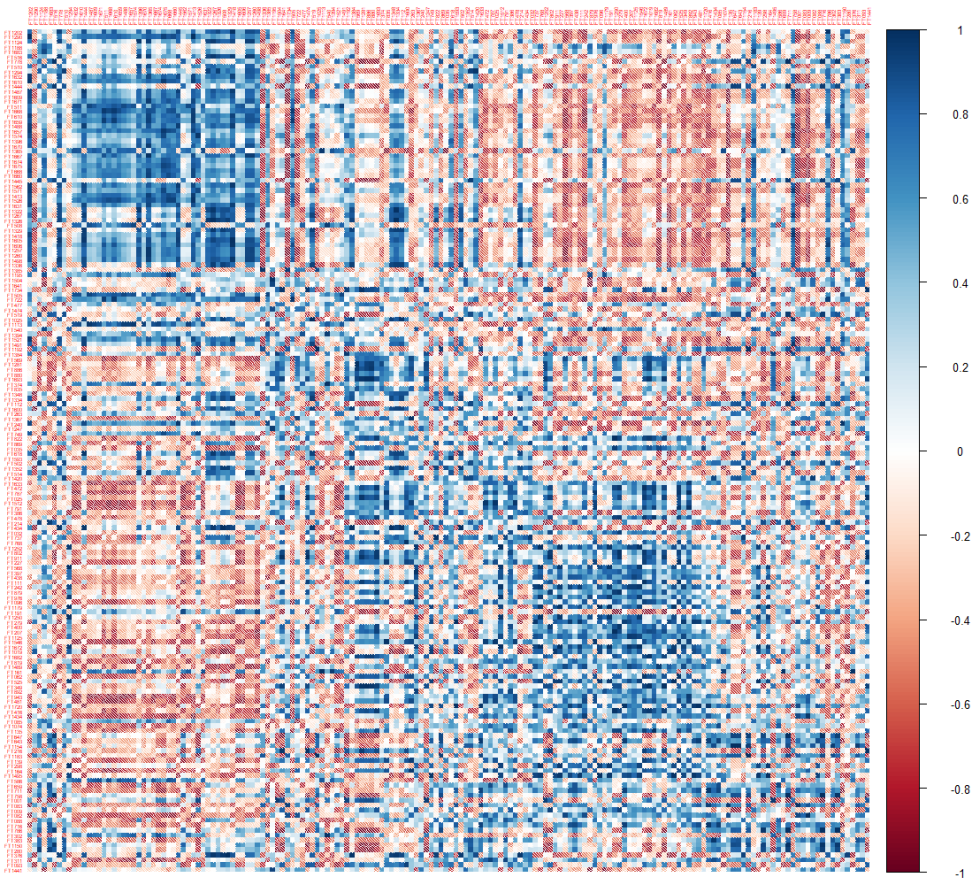

Figure 4.15 Correlation matrix of baseline and post-intervention metabolite abundance

Representative example of correlation between baseline and post-intervention samples for older individuals in the polar negative dataset. Correlation across the whole dataset was high, indicating large amounts of similarity between the baseline and post-intervention fasting, rested plasma metabolomes. Similar degrees of correlation were seen for other ion modes and polarities between age groups.

4.4. Discussion

This chapter demonstrates the ability of untargeted metabolomics to detect differences in the fasting plasma metabolome that reflect the effect of ageing between healthy young and older adults within skeletal muscle. Plasma metabolites which were significantly different between age groups at baseline were similar to the markers of ageing previously identified within the muscle metabolome, suggesting that the plasma metabolome reflects age-related adaptations within muscle. However, many of the metabolic pathways driving separation remained the same following a 20-week RET intervention. Furthermore, paired expression analysis found no significant differences in metabolite abundance in young, middle-aged, or older adults after training. Collectively, these data suggest that RET does not lead to systemic adaptations within the metabolome regardless of age.

4.4.1. Comparison of the ageing plasma and muscle metabolomes

4.4.1.1. Androgen steroid metabolism

In previous work, androgen steroid metabolites were prominent in the metabolic signature of ageing within muscle (Wilkinson et al., 2020). In the present study the plasma abundance of DHEA sulphate declined significantly with age and the plasma abundance of androsterone showed a tendency to decrease with age. It is well established that testosterone level declines with age in both men and women (Harman et al., 2001; Feldman et al., 2002; Fabbri et al., 2016). This decline has been associated with reduced muscle mass and strength (Horstman et al., 2012), increased incidence of comorbidities (Stanworth and Jones, 2008) and increased risk of all-cause mortality (Bhasin, 2021). Therefore, the observed decline in plasma abundance of androgen steroids in this study provides plausible support for an untargeted metabolomics approach to study the physiology of ageing. Importantly, these data also provide

evidence to suggest the plasma metabolome provides an accurate reflection of physiological changes occurring within skeletal muscle as a consequence of ageing.

Additionally, plasma levels of 24-hydroxycalcitrol, a metabolite of vitamin D_3, tended to decrease with age in this study. Although vitamin D is not directly related to androgens the current literature supports an association between vitamin D deficiency and deficiency in serum testosterone and androgen metabolism in men (Wehr et al., 2010). Like testosterone, vitamin D is a steroid hormone derived from cholesterol (Cutolo et al., 2014; Chu et al., 2021), which may explain this association as cholesterol metabolism is known to be altered with increasing age (Morgan et al., 2016; Nunes et al., 2022). Additionally, it is well known that vitamin D metabolism acts as a regulator of skeletal muscle health (Bollen et al., 2022). Low serum vitamin D_3 levels are consistently associated with reduced grip strength (Haslam et al., 2014; Mendoza-Garces et al., 2021), physical function (Rejnmark, 2011; Maroon et al., 2013), and an increased risk of sarcopenia (Vissier et al., 2003; Luo et al., 2021; Yoo et al., 2021). Vitamin D also appears to have a role as a regulator of muscle mass as dietary vitamin D supplementation improved cross sectional areas of the thigh and tibialis anterior muscles in haemodialysis patients (Gordon et al., 2008), and a significant association between low vitamin D levels and low skeletal muscle was observed in men and women under 65 years old (Marantes et al., 2012). A decline in the plasma abundance of a vitamin D_3 breakdown product with age in the present study therefore lends support to the current literature and points to a role for the metabolism of vitamin D_3 in the physiology of skeletal muscle deconditioning in ageing.

4.4.1.2. Phospholipids

Lipid metabolites were also identified as markers of ageing within skeletal muscle (Wilkinson et al., 2020). In this study ORA found several pathways related to lipid

metabolism were disturbed between age groups at baseline. Several lipid metabolites were tentatively identified as phospholipid species. Phospholipids are key components of membranes, acting both as structural compounds which regulate physiochemical properties of membranes and as regulators of cellular processes including interaction with proteins to control signalling pathways between and within cells (Harayama and Riezman, 2018). Phospholipids are particularly abundant in the inner and outer mitochondrial membranes and disturbances to phospholipid composition of these membranes have been linked to reduced mitochondrial content and function (Mejia and Hatch, 2016). Ether lipids also make up significant component of subcellular membranes, including the mitochondrial membrane (Schooneveldt et al., 2022), and were noted to increase in plasma abundance with age in this study. It is known that ageing is associated with a decline in mitochondrial content and oxidative capacity (Short et al., 2005; Crane et al., 2010). The observed differences in the plasma abundance of phospholipid and ether lipid metabolites in this study may therefore reflect the disruption of the mitochondrial membrane as a consequence of age related mitophagy. Phosphocreatine was previously identified as perturbed in ageing muscle (Wilkinson et al., 2020) providing more evidence of the impairment of fuel metabolism pathways. While phosphocreatine was not identified here as a plasma marker of ageing, fumarate, an intermediate of the citric acid cycle, decreased in plasma abundance from young to older participants at baseline which reflects dysregulation to energy production pathways characteristic of ageing.

Recent evidence also suggests that plasma ratios of PC and lysoPC metabolites play a role in longevity, possibly through interaction with chromatin (Papsdorf and Brunet, 2018), and serve as accurate biomarkers of ageing (S. Kim et al., 2014; Pradas et al., 2019). In the present study, there were alterations in the plasma level of several PC and lysoPC metabolites, with increased abundance of lysoPC(O-18:0) and

PC(20:0/22:4(7Z,10Z,13Z,16Z)), and decreased lysoPC(15:0) identified by ORA as important in driving metabolic pathway disruption in ageing, providing support to the current literature and pointing to a role for phospholipids in the age-related adaptations of skeletal muscle.

4.4.1.3. Sphingolipids

There were also changes in the plasma metabolome of several sphingolipids. Sphingolipids are essential in many aspects of cellular homeostasis, including as components of cellular membranes and in signalling (Hannun and Obeid, 2018). Sphingolipids have been identified as markers of ageing. For example, levels of sphingolipids within mouse tissue significantly with age (Wu et al., 2007) and an increase in sphingolipid enzymatic activity was observed in rat tissues (Sacket et al., 2009). In humans, sphingolipid levels were associated with longevity (Montoliu et al., 2014) and comorbidities of age, such as obesity (Turpin et al., 2014), atherosclerosis (Jiang et al., 2000) and Alzheimer's disease (Mielke et al., 2012). The precise role of sphingolipids in adaptations in skeletal muscle associated with ageing is unclear but it has been suggested that dysregulation of sphingolipid metabolism in ageing may be related to cellular senescence (Montoliu et al., 2014) as the increase in sphingolipids leads to an accumulation of ceramides within tissues which in turn has a detrimental effect on maximum life span. In this study there was a significant increase in several ceramide metabolites in the older group relative to the young group, suggesting an association between elevation in plasma levels of ceramides and the physiology of ageing.

4.4.1.4. Linoleic acid metabolism

Finally, the pathway with the largest impact in classification of samples by age at baseline was linoleic acid metabolism. There was a significant decline in the

abundance of 13(S)-HPODE, a primary product of the linoleic acid metabolism pathway (Paley and Karp, 2021), with ageing. The linoleic acid metabolism pathway is known to be involved in mitochondrial oxidative phosphorylation. Dietary supplementation of linoleic acid leads to an increase in mitochondrial metabolites in a mouse model (Maekawa et al., 2019), therefore the present decrease in linoleic acid may provide further evidence to the decline in mitochondrial oxidative capacity and dysregulation of energy production with ageing, however without correlation to measures of oxidative capacity within the muscle in this study the association remains speculative, which should be acknowledged as a limitation to this study.

4.4.2. Changes in the ageing plasma metabolome induced by resistance exercise training

Putative metabolite identification and ORA showed that the ageing plasma metabolome was largely unchanged by 20 weeks RET although after training a greater number of metabolites were identified by PLS-DA as important in classifying samples by age than at baseline, potentially due to greater mobility of metabolites following exercise although this did not occur to a great enough degree as to be significant.

4.4.2.1. Linoleic acid metabolism

ORA found that linoleic acid metabolism remained the pathway with the highest impact score when classifying samples by age. Steroid hormone biosynthesis also showed a similar impact in baseline and post-intervention samples, although there were slight differences in the plasma metabolite profile when pathways were investigated further. For instance, at baseline disturbances to linoleic acid metabolism were primarily linked to a decline in the plasma abundance of 13(S)-HPODE, a breakdown product of linoleic acid, while after intervention pathway disturbances were mapped to linoleic acid itself. This discrepancy may be explained by the highly dynamic nature of the metabolome. Although samples were collected in the fasted,

rested state at baseline and post-intervention, it is possible that day-to-day variation may have an impact on metabolic profile. However, given that the same pattern of decrease was seen in linoleic acid and 13(S)-HPODE, the outcome of pathway disturbances at baseline and after RET are likely to be similar.

4.4.2.2. Androgen steroid metabolism

There was also a difference in the profile of androgen steroids. While a decline in plasma abundance in androgen steroids was seen with age at both baseline and after intervention, the decline in androsterone was only significant after exercise training. This may reflect the attenuated capacity for the production of androgen steroids through RET with age. There is some disagreement in the current literature over whether androgen steroids are affected by exercise. While Ahtiainen et al. found mean androgen receptor mRNA and protein expression did not change after 21 weeks RET in either young or older men, indicating no change in androgen concentration as a consequence of exercise (Ahtiainen et al., 2003), Keizer and colleagues reported an increase in plasma DHEA sulphate after endurance exercise (Keizer et al., 1989) and Tremblay et al. observed an increase in plasma androgen level in response to resistance exercise in healthy, younger men (Tremblay et al., 2004). Here, the larger decline in androsterone plasma abundance after resistance exercise when compared to baseline suggests that the increase in androgen level following exercise may be blunted by ageing. However, it should also be considered that, as with linoleic acid, the differences in abundance may be reflective of the dynamic nature of the metabolome.

4.4.2.3. Glycerophospholipid metabolism

Despite the overall ORA output being very similar to the baseline analysis, there were some differences which indicate the ageing plasma metabolome may be affected in

some way by RET. The increase in the impact score of glycerophospholipid metabolism after resistance exercise when compared to baseline was mapped to significant increases in the plasma abundance of phosphatidate and PE. Both are highly flexible metabolites with roles in numerous metabolic pathways, such as the biosynthesis of components of biological membranes or as intermediates in glycolysis (Kanehisa and Goto, 2000), which makes identifying the specific mechanisms underlying the shift in pathway impact more complex and as physiological outcome measures were not assessed in this study the precise role of these metabolites in the exercise response is still unclear. However, it is possible that the overall increase in plasma abundance of these metabolites may represent a greater mobilisation of lipids following RET in older individuals.

4.4.2.4. Nicotinate and nicotinamide metabolism

The most notable change was the increase in impact score of the nicotinate and nicotinamide pathway, which is involved in the production of the coenzyme NAD+ and its subsequent roles in several metabolic processes, most notably as a critical metabolite in mitochondrial energy production through redox homeostasis (Chini et al., 2017). There is a growing body of evidence which points to a reduction in NAD+ as a major feature of both normal and sarcopenic ageing (Okabe et al., 2019), although data from human trials is lacking. In murine and cell culture models, the reduction has been observed in many tissues including skeletal muscle (Fang et al., 2017). Here, the plasma abundance of metabolites related to NAD+ tended to decline with age, although no significant differences were observed. Although the reduction in plasma abundance of these metabolites was non-significant, the large increase in the impact score of the nicotinate and nicotinamide pathway as a classifier of ageing suggests that even small changes in metabolite abundance can have a large influence on the plasma metabolome and therefore the ageing phenotype, and that small differences should

not be immediately disregarded. The decline in NAD+ metabolites and the greater pathway influence may point to a shift in energy metabolism as a consequence of RET that is impacted by age.

Overall, some changes in the fasting, rested plasma metabolome after RET suggest that 20 weeks of exercise intervention may primarily have an impact on pathways relating to energy metabolism. However, despite the minor differences in metabolite profile within influential metabolic pathways the large similarities in output of metabolite identification and pathway ORA between baseline and post-intervention samples also suggest the plasma metabolites characteristic of age are largely unchanged by 20 weeks RET.

4.4.3. Time course analysis of exercise induced metabolomic changes

To confirm the similarities between baseline and post-intervention samples, time course analysis of each age group was conducted. This confirmatory analysis also suggested that the plasma metabolome is largely unaffected by RET as no significant differences were found in any group when baseline and post-intervention samples were compared. This may be due to length of the intervention. It is possible that an extended period of training, for example several years, is required to induce detectable shifts in systemic metabolism. Alterations in 20 metabolites were found to persist for 8 days after a bout of high intensity concentric-eccentric exercise, however the subjects were well trained athletes (Dünnwald et al., 2022) suggesting that to see a sustained metabolic response to exercise long term training is required. It should also be considered that Dünnwald et al. collected baseline samples under simulated normobaric hypoxic conditions, while day 8 was collected under normal conditions which may account for some differences in the metabolome. In the present study,

plasma collection was conducted under identical test conditions, eliminating this potential variation in the metabolome.

Alternatively, lack of differential metabolites may also relate to the study design. Plasma was collected in a fasted, rested state 72 hours after the participants' last bout of exercise. Given the temporal nature of MPS and MPB rates in response to anabolic signals from exercise (Atherton and Smith, 2012) and the lack of change in basal FSR before and after RET observed previously in the same cohort (Phillips et al., 2017), it is not unreasonable to suggest that adaptations in the metabolome may be similarly regulated, occurring in minutes not days. The temporal nature of metabolite expression following exercise is supported by the current literature. For instance, studies which show differences in the plasma metabolome following resistance exercise involve the collection of samples immediately following the cessation of exercise (Berton et al., 2016; Morville et al., 2020; Gehlert et al., 2022). In addition, time course profiling revealed many metabolites significantly impacted by RET returned to or approached pre-intervention levels over a recovery period of 240 minutes (Morville et al., 2020). Moreover, in a 24-week endurance exercise intervention in untrained individuals when plasma was collected 48 hours after completion of exercise, the fasting plasma metabolome showed no difference between exercise and control groups, and only 7 metabolites were different between baseline and post-intervention in the exercise group (Brennan et al., 2018). It is likely that the number of significantly different metabolites would reduce with increasing time. Therefore, to fully understand the changes to the metabolome induced by RET and the effect of age on the response of skeletal muscle to resistance exercise, it may be necessary to collect plasma immediately following cessation of exercise.

Chapter 5. Plasma response to aerobic exercise training and detraining in healthy young individuals

5.1. Background

5.1.1. Adaptations in metabolism associated with aerobic exercise training

A predominant adaptation in metabolism linked with submaximal aerobic exercise training (AET) is a change in substrate selection during exercise. At a moderate training intensity, there is a decreased utilisation of carbohydrate substrates in oxidation which is compensated for by a proportional increase in fat oxidation (Ramadoss et al., 2022). Maximal rates of fat oxidation occur at exercise intensities of approximately 65% VO_2^{PEAK} (Achten and Jeukendrup, 2003).

Another major physiological adaptation to submaximal AET is the increase in endurance capacity of skeletal muscle, defined as the ability of an individual to sustain an activity for extended periods of time relative to their baseline capacity (Gibala et al., 2006). It has been suggested that this improvement is underpinned by the well documented change in substrate selection in oxidation which is suggested to increase skeletal muscle oxidative capacity. For instance, AET at 65% VO_2^{PEAK} was shown to ameliorate the reductions in fat and carbohydrate oxidation rates associated with obesity and improve muscular endurance in obese individuals (Pérez-Martin et al., 2001). In non-obese, older adults, AET at the same intensity increased capacity for fat oxidation from 15.03 to 19.29 µmol/min/kg fat free mass (Pruchnic et al., 2004). Thirty-one days of 60% VO_2^{PEAK} AET induced a 10% increase in total fat oxidation which was linked to a 63% increase in intramuscular triglyceride oxidation and a 16% decrease in glycogen oxidation (Phillips et al., 1996). As these changes occurred prior to increased maximal mitochondrial enzyme activity, it suggests that changed substrate utilisation precedes improvements in mitochondrial activity and thus oxidative capacity.

Beyond oxidative capacity, AET is also associated with improved glucose handling in healthy adults. Increases in the coefficient of glucose tolerance between 4 and 19 minutes (83.9%) and between 10 and 30 minutes (90.6%) after glucose bolus, glucose effectiveness at zero insulin (76.02%), and basal insulin effectiveness (134.3%) were observed in healthy young men and women after AET at 85% VO_2^{PEAK} (Brun et al., 1995). Subsequent investigations have confirmed 60% VO_2^{PEAK} AET is also linked to improved glucose handling (Phillips et al., 1996; Carter et al., 2001). Submaximal AET may therefore be a potential therapeutic intervention for the treatment of muscle deconditioning, which is associated with shift in skeletal muscle oxidation (Chopard et al., 2009) and glucose tolerance (Q. Wang et al., 2019).

5.1.2. Metabolomics in the study of the response to aerobic exercise training

Recent work has demonstrated that increased aerobic physical activity is linked to adaptations in the plasma metabolome. Rats that underwent five days of aerobic exercise training a week for 6 weeks reported elevations in purine metabolism and greater metabolic flexibility compared to their sedentary counterparts (Starnes et al., 2017), reflecting improvements in the ability to adapt to demands on energy expenditure. In humans, changes in plasma levels of amino acids, fatty acids and carbohydrates have also been reported following aerobic exercise (Schranner et al., 2020), representing the beneficial impacts of exercise on key pathways involved in maintenance of skeletal muscle metabolic health including the TCA cycle, ketogenesis, and gluconeogenesis. Plasma collected immediately after endurance exercise in middle-aged individuals demonstrated that the acute metabolic response to running or cycling reflected rapid changes in substrate utilisation of skeletal muscle, glycolysis, lipolysis and amino acid catabolism (Lewis et al., 2010), however participants were well trained which may affect the response as metabolomic changes in response to the same exercise stimuli differ between trained and untrained individuals (Mukherjee

et al., 2014). Another study found cycling to exhaustion lead to significant increases or decreases in the plasma abundance of 50 metabolites in resistance trained, endurance trained, sprint trained and untrained individuals, including several species of acylcarnitine and ratios of spermidine/putrescine and serotonin/tryptophan (Schranner et al., 2021). However, this study used a targeted metabolomics kit which measured only amino acids and lipids therefore potential insight into the adaptive response of the wider metabolism was missed.

Conversely to the benefits in glucose handling and oxidative capacity in skeletal muscle discussed above that are conferred by regular physical activity, undergoing periods where skeletal muscle does not receive sufficient stimuli leads to the loss of exercise-induced adaptations in the muscle, referred to as detraining. Detraining is associated with a reduction in the capacity of skeletal muscle for oxidation of fatty acids (Laye et al., 2009) and is linked to reduced skeletal muscle function. For example, 3 months of detraining following 9 months of exercise led to a 7.57% decline in the distance travelled in a six minute walk test (Leitao et al., 2019), indicating reduced muscle function. In young female athletes, an 87% reduction in training intensity for one month caused a significant decrease in jump height from 0.48 to 0.44m (Dai et al., 2012), suggesting reduced function of skeletal muscle occurs even after physical activity is reduced without complete cessation of exercise training. The impact of complete immobilisation on whole-body and skeletal muscle specific metabolism is outlined in Chapter 3 but there is also evidence to suggest simply reducing physical activity without absolute disuse has a similarly negative effect on the plasma metabolome. When older individuals underwent a short-term period of step reduction, 8 plasma metabolites were found to undergo significant changes in plasma circulation (Saoi et al., 2019) including carnitines and their sulphate derivatives, oxoproline, and creatine which overall reflected adaptations in muscle energy

metabolism in response to reduced physical activity. A limited assessment of the plasma metabolic profile after 6 months and 1 year of detraining following a period of exercise intervention found declines in plasma glucose, TAG, cholesterol, HDL-c and LDL-c alongside an increase in free insulin, suggesting an overall decline in metabolic health (Rossi et al., 2017), however this study focussed specifically on established clinical markers and did not investigate the potential mechanisms underlying the reduction in metabolic health associated with adaptation to detraining. Similarly, improvements in insulin sensitivity and HDL-c after 4 months of aerobic interval training relapsed after only 1 month of detraining (Mora-Rodriguez et al., 2014), but the underlying mechanisms were not discussed and a full assessment of the metabolome was not carried out. As such, while there is increasing interest in applying metabolomics to study the exercise training response (Khoramipour et al., 2022) and the potential of metabolomics in understanding physiological adaptations to physical inactivity is clear (Saoi et al., 2019), the response of the plasma metabolome to detraining following a period of exercise intervention is relatively understudied.

In a previously published volunteer intervention study (Latimer et al., 2021), 8 weeks of AET at 65% VO_2^{PEAK} in a healthy young cohort induced a significant increase in mitochondrial DNA copy number ($p<0.001$) which declined following the period of exercise withdrawal where participants resumed habitual physical activity ($p<0.001$). Mitochondrial maximal rates of ATP production (MAPR) increased from baseline with AET for three substrate combinations (palmitate $p=0.003$; glutamate and succinate $p=0.008$; and glutamate and malate $p=0.011$) before returning to baseline values after the exercise withdrawal period (palmitate, $p=0.016$; glutamate and succinate, $p<0.001$; glutamate and malate, $p=0.003$), indicating a strong response in mitochondrial efficiency to both AET and exercise withdrawal in healthy young individuals.

In Chapter 4 of this thesis it was shown that a 20-week RET intervention had no significant effect on the plasma metabolome in healthy young or older individuals, however it was hypothesised that the type of exercise is likely to be influential in dictating metabolomic adaptations and therefore AET may induce differences in the plasma metabolome reflective of known physiological adaptations. In Chapter 3, it was demonstrated that metabolic signatures identified by untargeted metabolomics reflected muscle level adaptations to chronic bed rest. It is therefore reasonable to suggest a similar approach can be employed to identify plasma markers of metabolic dysregulation following exercise withdrawal which may influence the observed adaptations in skeletal muscle. The aims of this chapter are therefore as follows:

1. To determine whether the response of the plasma metabolome to 8 weeks of AET is reflective of physiological adaptations in healthy young individuals, and to identify metabolites most influential in driving metabolic adaptations to 8 weeks of AET
2. To determine whether there is a detraining response in the plasma metabolome following 4 weeks of exercise withdrawal, and to identify metabolites most influential in driving metabolic adaptations to 4 weeks of exercise withdrawal
3. To determine the relationship between changes in the plasma metabolome with relevant physiological outcome measures previously associated with adaptations to AET in healthy young individuals

5.2. Methods

5.2.1. Study design

This study involved retrospective analysis of samples collected as part of a volunteer intervention study (Latimer et al., 2021) which was conducted at the Universities of Leicester and Nottingham, UK (Clinical Trials Register: ISRCTN10906292). The study was approved by the NHS National Research Ethics Service. All participants provided written informed consent. The original study design is as follows:

COPD patients (n=19, 60-80 years), healthy controls age matched to COPD (HO, n=10) and young healthy controls (HY, n=10, 18-35 years) were recruited to an 8-week submaximal AET intervention followed by 4 weeks of exercise withdrawal. In this chapter, only HY was used in analysis. Participants were required to have normal lung function (FEV1/FVC > 0.7, FEV1 > 80%) and were excluded for any respiratory diagnosis. Individuals who participated in exercise exceeding 150 minutes/week at moderate intensity were excluded. Subjects were also excluded if: they had a medical condition associated with metabolic disturbances, inflammation, or impaired muscle function; they were receiving corticosteroid medication; they were receiving anticoagulation therapy or had a condition causing impaired clotting; they were a current smoker. Baseline subject characteristics are provided in Table 5.1.

Baseline assessments were performed over three visits. On the first visit, body composition was acquired by dual energy X-ray absorptiometry (DEXA, Lunar Prodigy II, GE Healthcare, Buckinghamshire, UK) and participants underwent a familiarisation incremental cycling cardiopulmonary exercise test (CPET) on an electromagnetically braked cycle ergometer (Lode Corival, Groningen, The Netherlands). After three minutes unloading pedalling, workload increased progressively at a rate between 5W/min and 20W/min for a test of 8-12 minutes duration. VO_2^{PEAK} was monitored using a metabolic cart (Medisoft, Sorrines, Belgium). The second visit took place a

minimum of 48 hours after the first and participants completed a second incremental CPET to verify the preceding test. At the third visit, muscle biopsy samples were obtained from the vastus lateralis (VL) muscle of the dominant leg using a needle micro-biopsy technique. Four passes were performed. Each pass harvested approximately 20mg VL tissue. Approximately 40mg muscle tissue was weighed for mitochondrial function and content measurements. The remaining tissue was snap frozen and stored in liquid nitrogen for assessment of DNA and mRNA expression analysis.

Submaximal exercise testing consisted of 30 minutes of continuous cycling at 65% of the workload corresponding to the participant's highest VO_2^{PEAK} achieved in either of the baseline tests. Continuous monitoring of respiratory exchange ratio (RER) was performed throughout the test using a metabolic cart (Ergocard Professional, Medisoft, Sorinnes, Belgium) and an average was reported for the steady-state period. Training intensity was reset after 4 weeks. At the end of week 8, participants resumed their habitual physical activity levels. Incremental and submaximal tests were separated by at least 30 minutes of rest time.

Fasted and rested venous blood samples were drawn at baseline, 1 week post baseline, after 4 weeks of exercise, after 8 weeks of exercise, and post detraining. Plasma and serum were separated and stored immediately at -80°C until further analysis. Plasma samples were randomly sorted into 4 batches and prepared in an identical manner. Metabolites were extracted from plasma according to the protocol detailed in Section 2.3. Separation of metabolites within samples via liquid chromatography was performed according to the parameters detailed in Section 2.4 and acquisition of data by tandem mass spectrometry was performed according to the protocol in Section 2.5.

Table 5.1 Baseline subject characteristics. Data are presented as mean±SD unless otherwise stated. Percentage predicted values are calculated from normal values. FEV1: forced expiratory volume in 1s; FVC: forced vital capacity; RV: residual volume; TLC: total lung capacity; TLCO: transfer factor for the lung of carbon monoxide; BMI: body mass index; FFMI: fat-free mass index; QMVC: quadriceps maximum voluntary contraction. Table from Latimer et al. (2021).

	HY (n=10)
Age, years	28±5
Female, n	6
FEV_1, % pred	112.6±20.6
FEV_1/FEV, %	81.6±9.3
RV, % pred	107.9±48.9
TLC, % pred	107.6±15.0
RV/TLC, %	26.8±9.7
T_{LCO}, % pred	95.6±13.9
Smoking history, n	
Current smoker	0
Never smoker	10
Ex-smoker	0
BMI, kg/m^2	26.0±7.6
FFMI, kg/m^2	16.5±2.8
QMVC isometric strength, Nm	162.8±72.5
Step count, 8-h average per day	6180±3449 (n=9)

5.2.2. Data pre-processing and statistical analysis

Data pre-processing was performed in R using the parameters detailed in Section 2.6. For statistical analysis, data for each polarity and ionisation mode were analysed separately. All analysis of metabolomics data was performed using inhouse R scripts using R version 4.1. Scripts are available in Appendix 2. Following processing and filtering of metabolomics data, analysis of differential metabolite abundance from baseline at 1 week, 4 weeks and 8 weeks after starting AET, and following 4 weeks of exercise withdrawal (week 12 of the study) was performed by fitting a linear mixed effect model to each data matrix. Group and time were fixed effects while participant ID was a random effect to control for subject specific variation over the course of the study. P-values were obtained for each contrast by Empirical Bayes moderated t-tests adjusted for false discovery rate (FDR). Metabolites were deemed significantly different between comparisons when FDR<0.05.

Total lean mass, exercise steady-state RER, and VO_2^{PEAK} were provided from Latimer et al. (2021) and assessed for normality using Shapiro-Wilk tests. Within group changes across time were tested using one-way repeated measures ANOVA with post-hoc pairwise comparisons adjusted for FDR using the Benjamini-Hochberg method.

5.2.3. Prediction of functional activity of differentially expressed metabolites

Metabolites were putatively identified using metID (Shen, Wu, et al., 2022) utilising publicly available metabolomics databases. Mass tolerance was set at 5ppm. Common compound names of identified features were taken from HMDB and mapped to metabolic pathways by over representation analysis (ORA) using MetaboAnalyst 5.0 (Pang et al., 2021). Pathways with an impact score greater than 0.1 were retained.

5.2.4. Correlation of metabolomic and physiological outcome data

Correlation of metabolite expression with outcome measures of VO_2^{PEAK} and RER during submaximal steady-state exercise at 65% VO_2^{PEAK} was assessed by weighted correlation network analysis (WGCNA) (Langfelder and Horvath, 2008). Metabolic modules with weak correlations ($r<|0.5|$) to outcome measures were discarded and network analysis was performed on the remaining metabolite modules to determine their functional relevance.

5.3. Results

5.3.1. Physiological adaptations to aerobic exercise training

Exercise intervention and withdrawal had no impact on total lean mass ($p>0.05$). Significant changes in VO_2^{PEAK} (Figure 5.1) and exercise steady-state RER (Figure 5.2) were observed after 8 weeks of AET (VO_2^{PEAK}, $p<0.01$; steady-state RER, $p<0.001$) and after 4 weeks of exercise withdrawal (VO_2^{PEAK}, $p<0.05$; steady-state RER, $p<0.001$) relative to their baseline values. No significant differences between VO_2^{PEAK} or exercise steady-state RER were observed between weeks 8 AET and 4 weeks of exercise withdrawal ($p>0.05$).

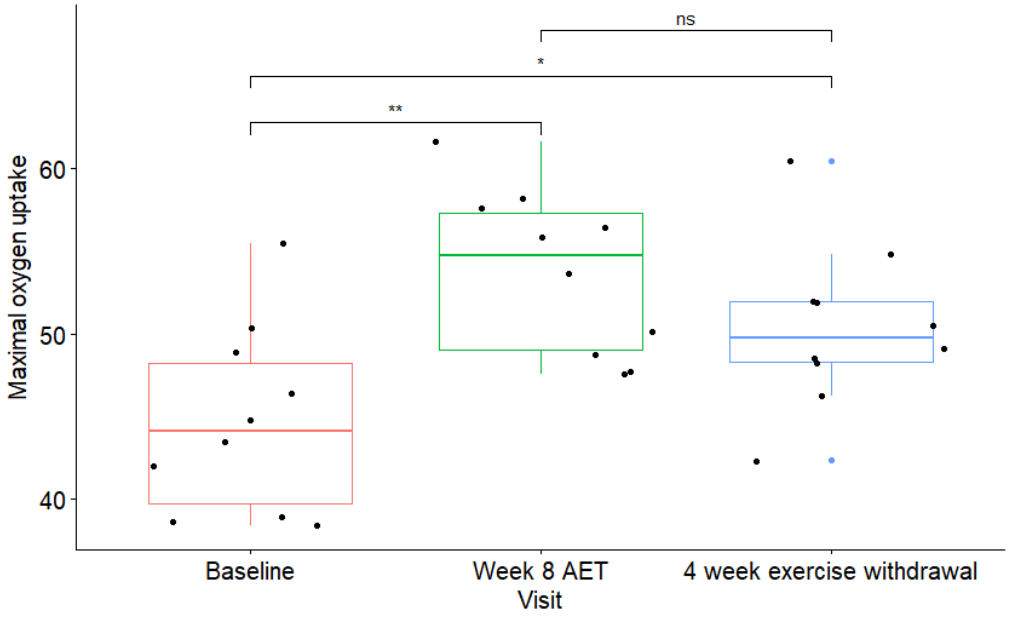

Figure 5.1 Peak oxygen uptake at baseline, after 8 weeks aerobic exercise training and 4 weeks exercise withdrawal

Change in peak oxygen uptake (VO_2^{PEAK}) after 8 weeks aerobic exercise training and 4 weeks of exercise withdrawal in healthy young adults. There was a significant increase in VO_2^{PEAK} at week 8 AET and 4 weeks exercise withdrawal relative to baseline value, however there was no difference in value of VO_2^{PEAK} between week 8 and exercise withdrawal timepoints. Boxplots represent the spread of data. Each circle represents one participant and shows precise distribution of data within groups.

*p<0.05, **p<0.01

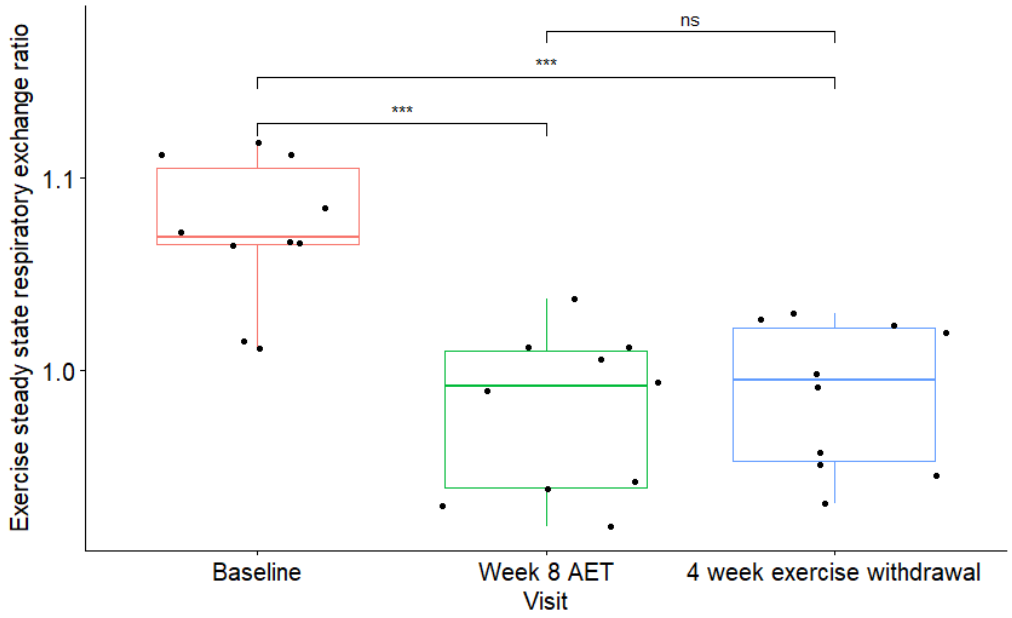

Figure 5.2 Submaximal steady-state exercise respiratory exchange ratio at baseline, after 8 weeks aerobic exercise training and 4 weeks exercise withdrawal

Change in steady state respiratory exchange ratio at 65% VO_2^{PEAK} after 8 weeks aerobic exercise training and 4 weeks of exercise withdrawal in healthy young adults. There was a significant decrease in respiratory exchange ratio at 8 weeks AET and 4 weeks exercise withdrawal relative to baseline value, however there was no difference in value of respiratory exchange ratio between week 8 AET and exercise withdrawal timepoints. Boxplots represent the spread of data. Each circle represents one participant and shows precise distribution of data within groups.

***p<0.001

5.3.2. Differential metabolite abundance

A total of 108 metabolites were present at a significantly different abundance ($p<0.05$) compared to baseline after either 1 week, 4 weeks or 8 weeks of AET or 4 weeks of exercise withdrawal. Of these, 22 were significantly different after 1 week of AET (Figure 5.3A), 14 were significantly different after 4 weeks AET (Figure 5.3B), 21 were significantly different after 8 weeks AET (Figure 5.3C), and 51 were significantly different after 4 weeks exercise withdrawal (Figure 5.4).

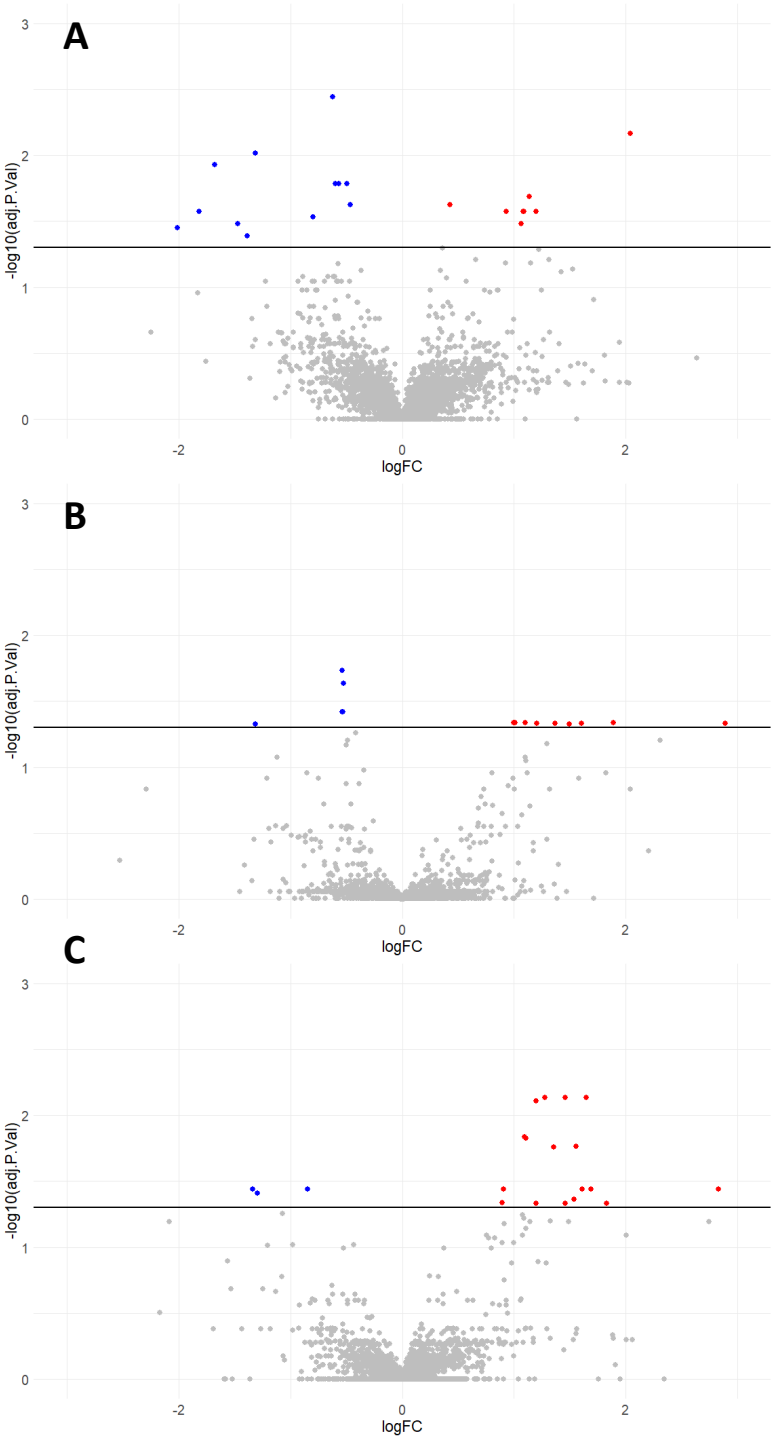

Figure 5.3 Differential metabolite abundance following exercise training

Comparison of metabolite abundance between baseline and following (A) 1, (B) 4 and (C) 8 weeks of aerobic exercise training (AET) in healthy young participants. The x axis shows log fold change of metabolite abundance. The y axis shows -log10 p-value adjusted for false discovery rate by the Benjamini-Hochberg method. The black line shows the threshold of FDR<0.05. Each plotted point represents a metabolite (blue, significantly downregulated; red, significantly upregulated; grey, not significantly different between timepoints).

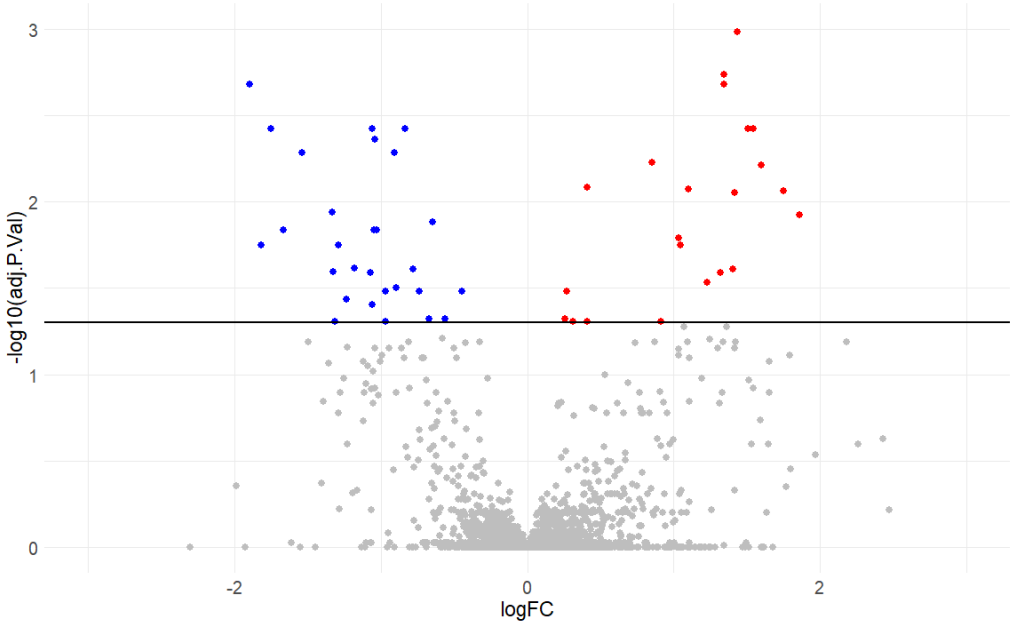

Figure 5.4 Differential metabolite abundance between baseline and 4 weeks detraining

Comparison of metabolite abundance between baseline and after 4 weeks of exercise withdrawal following aerobic exercise training in healthy young participants. The x axis shows log fold change of metabolite abundance. The y axis shows -log10 p-value adjusted for false discovery rate by the Benjamini-Hochberg method. The black line shows the threshold of FDR<0.05. Each plotted point represents a metabolite (blue, significantly downregulated; red, significantly upregulated; grey, not significantly different between timepoints).

5.3.3. Identification of metabolites

Metabolites affected by 1, 4 and 8 weeks of AET were within the same class of molecule, suggesting a consistent metabolic response to AET in all individuals (Figure 5.5). The most common metabolite classes at all timepoints were identified as organooxygen compounds, prenol lipids, carboxylic acids and their derivatives, and fatty acyls.

In contrast to the consistent response during AET, after exercise withdrawal there was a greater variety of metabolite classes identified, suggesting exercise withdrawal may have a more widespread impact than AET (Figure 5.6). In particular, there were an increased number of metabolite classes related to xenobiotics, with several metabolites identified as solely exogenous. This may reflect the importance of the diet

in dictating substrate utilisation in energy production during periods of reduced physical activity.

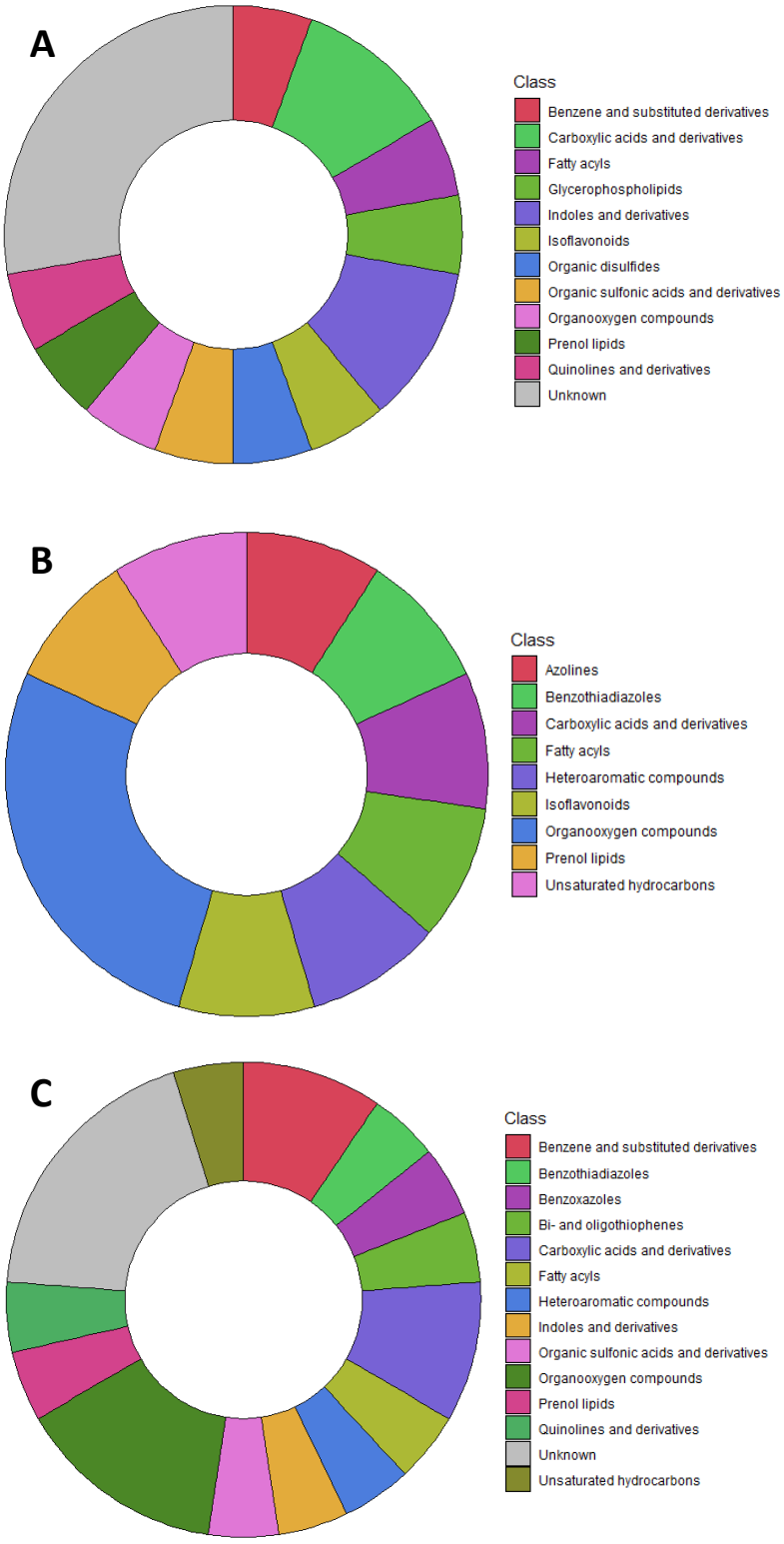

Figure 5.5 Classes of metabolites significantly different after exercise training

Donut charts showing classes of metabolites present at significantly different plasma levels after (A) 1, (B) 4 and (C) 8 weeks of aerobic exercise training compared to baseline values in healthy young individuals. Classes are represented as a percentage of the number of metabolites changed in abundance from baseline.

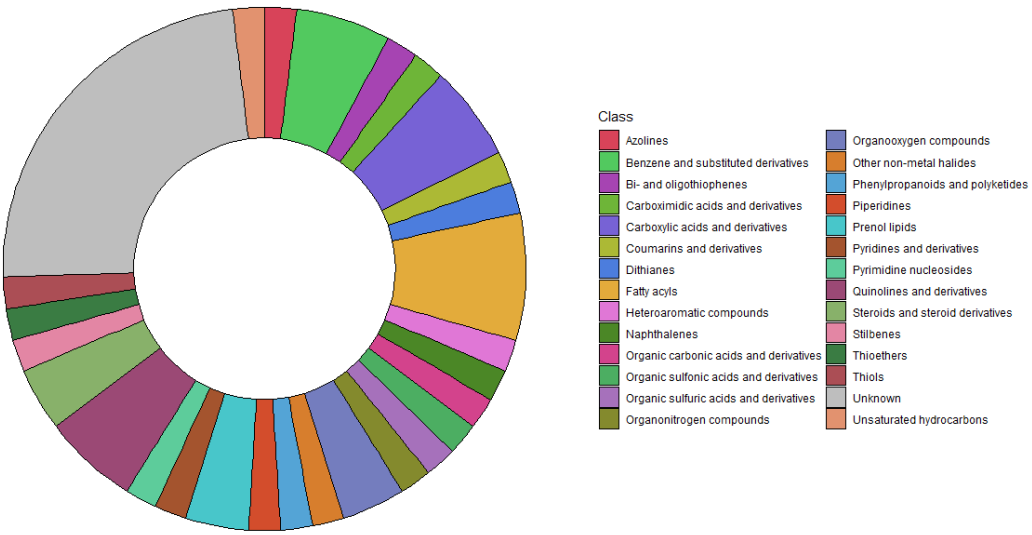

Figure 5.6 Metabolite classes significantly different after 4 weeks exercise withdrawal

Donut chart showing classes of metabolites present at significantly different plasma levels after 4 weeks exercise withdrawal compared to baseline values in healthy young individuals. Classes are represented as a percentage of the number of metabolites changed in abundance from baseline.

5.3.4. Correlation of plasma metabolite abundance with physiological adaptations

Having demonstrated that there was an observable response in the plasma metabolome over 8 weeks AET and 4 weeks of exercise withdrawal, the next aim of this chapter was to integrate metabolomic and physiological data by identifying which metabolites were associated with previously defined physiological adaptations in cardiorespiratory fitness in response to AET and exercise withdrawal. Firstly, associations between baseline measures of metabolite abundance and physiological outcomes were assessed (Table 5.2). Next, associations between change in metabolite abundance and change in physiological outcomes at week 8 (Table 5.3) and week 12 (Table 5.4) were made. WGCNA correlation indicated high degrees of association between metabolic modules and measurements of VO_2^{PEAK} and exercise steady-state RER. To clarify which metabolites were important in driving association and their biological roles, metabolite identification and pathway analysis were performed on modules which were associated with at least one measure of adaptation.

Table 5.2 Table containing metabolic modules of metabolite abundance at baseline which are correlated (r>|0.5|) with measures of exercise steady-state respiratory exchange ratio (RER) and maximal oxygen uptake (VO_2^{PEAK}) at baseline. P-values of correlation are included for reference but no correlations were significant (p<0.05). Over representation analysis was applied to metabolites within each module to identify relevant metabolic pathways (impact score > 0.1).

Module	Correlation with outcome measure	Coefficient	p-value	Pathway	Impact score
Yellow	RER	-0.77	0.1	Glycerolipid metabolism	0.33
Green		0.7	0.2	Caffeine metabolism	0.69
				beta-Alanine metabolism	0.50
				Biotin metabolism	0.20
				Arginine and proline metabolism	0.11
				Glycerophospholipid metabolism	0.10
Green-yellow	RER	-0.74	0.1	Arginine biosynthesis	0.12
	VO_2^{PEAK}	-0.54	0.3	Glycerophospholipid metabolism	0.22
				Sphingolipid metabolism	0.37
Midnight blue	RER	-0.51	0.4	Glycerophospholipid metabolism	0.20
				Sphingolipid metabolism	0.27
Yellow	RER	-0.64	0.2	Glycerophospholipid metabolism	0.25
	VO_2^{PEAK}	-0.81	0.1		
Dark green	RER	0.73	0.2	Glycerophospholipid metabolism	0.2
Dark turquoise	RER	0.96	0.01	Sphingolipid metabolism	0.27
Orange	VO_2^{PEAK}	-0.86	0.06	Sphingolipid metabolism	0.35
				alpha-Linolenic acid metabolism	0.33
				Glycerophospholipid metabolism	0.22
				Arginine biosynthesis	0.12
				Phosphatidylinositol signalling system	0.11
Magenta	VO_2^{PEAK}	0.69	0.2	Glycerophospholipid metabolism	0.26

				Nicotinate and nicotinamide metabolism	0.23
				Pentose and glucuronate interconversions	0.14
Dark grey	RER	-0.64	0.4	Glycerophospholipid metabolism	0.20
				Sphingolipid metabolism	0.18
				Pentose and glucuronate interconversions	0.14
Grey60	VO_2^{PEAK}	0.95	0.05	Propanoate metabolism	0.27
				Pentose and glucuronate interconversions	0.14
				Glycerophospholipid metabolism	0.11
Light cyan	RER	0.95	0.05	Pentose and glucuronate interconversions	0.14
	VO_2^{PEAK}	0.76	0.2		
Purple	RER	-0.63	0.4	Pentose and glucuronate interconversions	0.14
	VO_2^{PEAK}	-0.6	0.4		
Salmon	VO_2^{PEAK}	-0.52	0.5	Glycerophospholipid metabolism	0.22
				Pentose and glucuronate interconversions	0.14
Dark turquoise	RER	-0.77	0.2	Glycerophospholipid metabolism	0.25
	VO_2^{PEAK}	-0.61	0.4		

Table 5.3 Table containing metabolic modules of change in metabolite abundance after 8 weeks aerobic exercise training which are correlated (r>|0.5|) with change in measures of exercise steady-state respiratory exchange ratio (RER) and maximal oxygen uptake (VO_2^{PEAK}) after 8 weeks aerobic exercise training. Over representation analysis was applied to metabolites within each module to identify relevant metabolic pathways (impact score > 0.1).
*Correlation p<0.05

Module	Correlation with outcome measure	Coefficient	p-value	Pathway	Impact score
Turquoise	Change in RER	0.65	0.5	Caffeine metabolism	0.69
	Change in VO_2^{PEAK}	0.96	0.1	Phenylalanine, tyrosine and tryptophan biosynthesis	0.50
				beta-Alanine metabolism	0.40
				Glycerolipid metabolism	0.34
				Tyrosine metabolism	0.15
				Sulphur metabolism	0.13
				Arginine and proline metabolism	0.11
Blue	Change in RER	0.76	0.4	Glycine, serine and threonine metabolism	0.35
				Biotin metabolism	0.20
				Glycerophospholipid metabolism	0.20
				Pyrimidine metabolism	0.18
				Aminoacyl-tRNA synthesis	0.17
				beta-Alanine metabolism	0.10
Black	Change in RER	1	0.004*	Phenylalanine, tyrosine and tryptophan biosynthesis	0.50
	Change in VO_2^{PEAK}	-0.55	0.4	Phenylalanine metabolism	0.36
Yellow	Change in RER	0.62	0.4	Arginine and proline metabolism	0.11
	Change in VO_2^{PEAK}	-0.84	0.2		
Light cyan	Change in RER	-0.54	0.3	Sphingolipid metabolism	0.27

	Change in VO_2^{PEAK}	0.59	0.3	Nicotinate and nicotinamide metabolism	0.23
				Glycerophospholipid metabolism	0.22
				Pantothenate and CoA biosynthesis	0.18
				Fatty acid degradation	0.12
Grey60	Change in VO_2^{PEAK}	-0.83	0.08	Sphingolipid metabolism	0.37
				Glycerophospholipid metabolism	0.26
Dark green	Change in RER	0.85	0.07	Glycerophospholipid metabolism	0.20
Dark red	Change in VO_2^{PEAK}	0.73	0.2	Arginine biosynthesis	0.12
Yellow	Change in RER	-0.55	0.3	Glycerophospholipid metabolism	0.22
	Change in VO_2^{PEAK}	0.78	0.1	Pentose and glucuronate interconversions	0.14
				Arginine biosynthesis	0.12
				Phosphatidylinositol signalling system	0.11
Brown	Change in RER	0.78	0.07	Glycerophospholipid metabolism	0.20
				Pentose and glucuronate interconversions	0.14
Green	Change in VO_2^{PEAK}	-0.78	0.07	Sphingolipid metabolism	0.22
				Pentose and glucuronate interconversions	0.14
Blue	Change in RER	-0.84	0.04*	Glycerophospholipid metabolism	0.26
	Change in VO_2^{PEAK}	0.52	0.3	Pentose and glucuronate interconversions	0.14
Red	Change in RER	-0.77	0.08	Propanoate metabolism	0.27
				Glycerophospholipid metabolism	0.22
				Pentose and glucuronate interconversions	0.14

Table 5.4 Table containing metabolic modules of change in metabolite abundance after 4 weeks exercise withdrawal which are correlated (r>|0.5|) with change in measures of exercise steady-state respiratory exchange ratio (RER) and maximal oxygen uptake (VO_2^{PEAK}) after 4 weeks of exercise withdrawal. Over representation analysis was applied to metabolites within each module to identify relevant metabolic pathways (impact score > 0.1).
*Correlation p<0.05

Module	Correlation with outcome measure	Coefficient	p-value	Pathway	Impact score
Blue	Change in RER	0.83	0.4	Caffeine metabolism	0.69
	Change in VO_2^{PEAK}	0.97	0.1	Phenylalanine, tyrosine and tryptophan biosynthesis	0.50
				Pyrimidine metabolism	0.22
				Biotin metabolism	0.20
				Tyrosine metabolism	0.15
				Sulphur metabolism	0.13
				Arginine and proline metabolism	0.11
				Glycerolipid metabolism	0.10
Yellow	Change in VO_2^{PEAK}	-0.81	0.4	Caffeine metabolism	0.69
	Change in RER	-0.97	0.2	beta-Alanine metabolism	0.40
Brown	Change in RER	0.78	0.2	Phenylalanine, tyrosine and tryptophan biosynthesis	0.50
				Phenylalanine metabolism	0.36
				Alanine, aspartate and glutamate metabolism	0.16
Turquoise	Change in RER	0.72	0.3	Arginine and proline metabolism	0.11
	Change in VO_2^{PEAK}	-0.74	0.3		
Red	Change in RER	-0.76	0.1	Glycerophospholipid metabolism	0.10
	Change in VO_2^{PEAK}	0.78	0.1		
Green yellow	Change in RER	-0.5	0.4	Sphingolipid metabolism	0.35

				Glycerophospholipid metabolism	0.22
				Arginine biosynthesis	0.12
Dark green	Change in RER	0.77	0.1	Glycerophospholipid metabolism	0.31
	Change in VO_2^{PEAK}	-0.51	0.4	Sphingolipid metabolism	0.31
Light green	Change in RER	0.78	0.1	Glycerophospholipid metabolism	0.26
Brown	Change in RER	-0.77	0.01*	Glycerophospholipid metabolism	0.25
Dark turquoise	Change in RER	0.52	0.4	Propanoate metabolism	0.27
				Pentose and glucuronate interconversions	0.14
				Glycerophospholipid metabolism	0.10
Blue	Change in RER	-0.62	0.3	Pentose and glucuronate interconversions	0.14
	Change in VO_2^{PEAK}	0.61	0.3	Glycerophospholipid metabolism	0.11

At baseline many modules were correlated with both VO_2^{PEAK} and exercise steady-state RER (r>|0.5|). Additionally, pathways involved in correlation were similar across all modules. The most common pathway in correlations at baseline was glycerophospholipid metabolism, with 6 modules correlated with exercise steady-state RER and 7 modules correlated with VO_2^{PEAK} being linked to glycerophospholipid metabolism by ORA (impact score > 0.1). Important metabolites were similar between modules. Phosphatidylethanolamine (PE), phosphatidylcholine (PC), phosphatidylserine (PS), 1-acyl-sn-glycero-3-phosphocholine, and sn-glycero-3-phosphocholine were repeatedly found to be important in correlations of metabolic modules with VO_2^{PEAK} and exercise steady-state RER. Exercise steady-state RER was also linked to sphingolipid metabolism in 4 modules. VO_2^{PEAK} was also linked to sphingolipid metabolism in two modules (impact score > 0.1). Glucosylceramide, digalactosylceramide, sphingosine-1-phosphate, sphingomyelin and ceramide were all

found to be important in associations with both RER and VO_2^{PEAK}. Galactosylceramide was also found to be important in the association with exercise steady-state RER but not with VO_2^{PEAK}. Pentose and glucuronate interconversions were linked to VO_2^{PEAK} in 5 modules and exercise steady-state RER in 3 modules (impact score > 0.1). In all modules, plasma abundance of β-D-glucuronside was important in the pathway.

Glycerophospholipid metabolism, pentose and glucuronate interconversions and sphingolipid metabolism all remained associated with VO_2^{PEAK} and exercise steady-state RER in correlations between change in metabolite abundance and change in outcome measures after 8 weeks AET (impact score > 0.1). Glycerophospholipid metabolism was associated with change in exercise steady-state RER in 6 modules and with VO_2^{PEAK} in 4 modules, with importance again mapped to plasma abundance of PE, PC, PS, 1-acyl-sn-glycero-3-phosphocholine, and sn-glycero-3-phosphocholine. Sphingolipid metabolism was associated with change in exercise steady-state in 4 modules and with VO_2^{PEAK} in 2 modules. Like glycerophospholipid metabolism, influential metabolites in driving pathway association were the same as at baseline with the addition of sulphatide which was associated with change in VO_2^{PEAK}. Pentose and glucuronate interconversions were associated with change in exercise steady-state in 3 modules and with VO_2^{PEAK} in 5 modules with importance again mapped to the plasma abundance of β-D-glucuronside.

There was also an increase in the association of amino acid metabolism pathways with outcome measures after 8 weeks AET. Although at baseline arginine and proline metabolism pathways were associated with exercise steady-state RER and VO_2^{PEAK} and remained associated here (for all, impact score > 0.1), with L-argininosuccinate and L-ornithine identified as important in driving associations, at the 8 week timepoint a wider range of amino acid metabolism pathways were involved in correlations. First,

the phenylalanine, tyrosine and tryptophan biosynthesis pathway was found to be associated with both change in exercise steady-state RER and change in VO_2^{PEAK} in 2 modules (impact score 0.5 for both). Influential metabolites in association were identified as L-tyrosine and L-phenylalanine. L-tyrosine was also found to be influential in the association of tyrosine metabolism with both change in RER and change in VO_2^{PEAK} alongside 3-fumarylpyruvate (impact score 0.15). Similarly, L-phenylalanine was highlighted as important in the association of phenylalanine metabolism with change in exercise steady-state RER and VO_2^{PEAK} in 1 module (impact score 0.36). Glycine, serine and threonine metabolism was linked to change in exercise steady-state RER in 1 module (impact score 0.35). Influential metabolites within this pathway were identified as L-serine, creatine, carbon dioxide, dimethylglycine, and betaine.

Changes in similar metabolic pathways were associated with changes in outcome measures after 4 weeks of exercise withdrawal. Glycerophospholipid metabolism was associated with change in exercise steady-state RER in 6 modules and change in VO_2^{PEAK} in 3 modules (impact score > 0.1). Sphingolipid metabolism was associated with change in exercise steady-state RER in 2 modules and change in VO_2^{PEAK} in 1 module (impact score > 0.1). Pentose and glucuronate interconversions were associated with change in exercise steady-state RER in 2 modules and change in VO_2^{PEAK} in 1 module (impact score > 0.1). Influential metabolites in the pathways were found to be the same as in previous associations, with PE, PC, PS, 1-acyl-sn-glycero-3-phosphocholine, and sn-glycero-3-phosphocholine important in glycerophospholipid metabolism, β-D-glucuronside important in pentose and glucuronate interconversions, and glucosylceramide, digalactosylceramide, sphingosine-1-phosphate, sphingomyelin, ceramide and galactosylceramide important in sphingolipid metabolism. Amino acid metabolism pathways remained associated with change in exercise steady-state RER and VO_2^{PEAK}. Phenylalanine, tyrosine and

tryptophan biosynthesis, phenylalanine metabolism and tyrosine metabolism were associated with exercise steady-state RER in 2 modules and with VO_2^{PEAK} in 1 module (for all modules, impact score > 0.1). Influential metabolites were again identified as L-tyrosine and L-phenylalanine, but L-adrenaline was also identified as influential in the tyrosine metabolism pathway which was not found after 8 weeks AET. Arginine and proline metabolism pathways were again linked to exercise steady-state RER and VO_2^{PEAK} (for all associations, impact score > 0.1) and influential metabolites were identified as L-argininosuccinate and L-ornithine. Finally, the alanine, aspartate and glutamate metabolism pathway was associated with change in exercise steady-state RER for the first time (impact score 0.16). Influential metabolites within the pathway were identified as 2-oxoglutarate and L-glutamine.

5.4. Discussion

The main finding of this chapter is that there is an observable response to AET and subsequent exercise withdrawal in the plasma metabolome of healthy young individuals. In Chapter 4 of this thesis, it was shown that RET had no effect on the rested, fasting plasma metabolome in healthy young individuals. In contrast, these data support a role for AET and exercise withdrawal as a modulator of the plasma metabolome. It is possible that AET has a more immediate and systemic effect on metabolic health than RET, suggesting that exercise type is influential in dictating the plasma metabolic response. Furthermore, through correlation of metabolite abundance and measures of cardiorespiratory fitness, this chapter demonstrates that the plasma metabolome is reflective of adaptations to AET at the skeletal muscle level and provides complementary information to previously published work (Latimer et al., 2021).

5.4.1. Classification of metabolites impacted by exercise training intervention

5.4.1.1. Fatty acyls

Putative identification of metabolites significantly impacted by at least 1 week of AET demonstrated that there was a shift in lipid profile with AET. Many metabolites with differential abundance at 1, 4 and 8 weeks of AET were identified as fatty acyls (Figures 5.10-12). For example, there was an increase in plasma abundance of (±)-sulfobutanedioic acid at 4 weeks of AET followed by a decline in (±)-2-Hydroxy-4-(methylthio)butanoic acid after 8 weeks of AET. Both belong to a subclass of fatty acyls called thia fatty acids, suggesting that length of exercise period has differential effects on the same metabolite subclasses within the metabolome. Thia fatty acids can have profound effects on lipid metabolism, including modulating mitochondrial beta oxidation (Dyroy et al., 2006) and can reportedly promote a cardioprotective plasma profile (Berge et al., 2002). The difference in metabolite abundance may therefore

relate to a potential regulatory impact on lipid metabolism which contributes to a shift in substrate oxidation favouring lipids over carbohydrates that is reflected in the decline of exercise steady-state RER previously reported (Latimer et al., 2021). Different metabolites were affected by different lengths of exercise, likely reflective of the diverse roles of lipids in the exercise response including in substrate oxidation.

5.4.1.2. Phospholipids

There was also a significant decrease in the plasma abundance of PE 22:0/P-18:1(11Z) after 1 week of AET. PE has diverse roles in the metabolism, including in membrane fusion and as a substrate in many metabolic pathways (Vance and Tasseva, 2013). PE content in the mitochondrial membrane is therefore influential in maintaining mitochondrial biogenesis and rates of mitochondrial respiration. There is also mounting evidence to suggest that mitochondrial PE content impacts mitochondrial membrane dynamics and fluidity, although the exact mechanism still remains unclear (Grapentine and Bakovic, 2020). It is therefore possible that the observed reduction in PE 22:0/P-18:1(11Z) reflects an increased uptake of lipids in skeletal muscle mitochondria to positively modulate substrate oxidation as reflected by decreased exercise steady-state RER which suggest that submaximal exercise training leads to a greater proportion of lipids oxidised at the same intensity compared to baseline measures. Supporting this, metabolites in modules correlated with exercise steady-state RER after 8 weeks AET were mapped to glycerolipid and glycerophospholipid metabolism pathways. Moreover, the number of metabolic markers of AET which can be linked to lipid oxidation in the mitochondria mirrors previous work which shows a significant increase in mitochondrial ATP production in response to palmitate after 8 weeks AET (Latimer et al., 2021).

5.4.1.3. Carboxylic acids and derivatives

Finally, metabolism of carboxylic acids and derivatives was disrupted at all timepoints during AET. After 1 week there was an increase in plasma abundance of iminoaspartic acid and a decrease in glutaminylthreonine. Iminoaspartic acid is produced by the breakdown of aspartate and used as a substrate in the production of NAD, a major component of energetic and signalling pathways (Kanehisa and Goto, 2000). The relationship between physical activity and NAD is well established, with exercise leading to increases in NAD levels in skeletal muscle that can ameliorate age-related declines in muscle function by increasing expression of mitochondrial proteins relating to ATP production (de Guia et al., 2019). Increased plasma abundance of iminoaspartic acid may therefore relate to increased production of NAD for use in oxidative phosphorylation. Glutaminylthreonine is consumed in the glutamyl cycle as part of the mechanism of glutathione biosynthesis (Paley and Karp, 2021). Glutathione plays a crucial role in maintaining homeostasis and whole-body health including as a vital metabolite in maintenance of mtDNA (Pizzorno, 2014). In addition, glutathione depletion has been implicated in the loss of skeletal muscle function with ageing (Julius et al., 1994) and chronic degenerative diseases associated with muscle wasting (Ballatori et al., 2009). The observed decline in plasma abundance of glutaminylthreonine may relate to its increased use in glutathione biosynthesis and indicates the beneficial impact of exercise on glutathione to maintain muscle function.

In addition, phenylalanine was significantly elevated from baseline after 4 and 8 weeks of AET. Ingestion of L-phenylalanine promotes fat oxidation during exercise (Ueda et al., 2017). The present increase in plasma phenylalanine may relate to the shift to favour lipid oxidation as a source of energy in response to increased energetic demands brought about by AET, in keeping with evidence from Latimer et al. (2021)

which showed a significant increase in mitochondrial ATP production in response to palmitate.

5.4.2. Effect of exercise withdrawal on the plasma metabolome

Many metabolites which were significantly impacted by 1, 4 or 8 weeks AET were identified as belonging to the same metabolite classes. In comparison, a greater variety of metabolites were affected by the detraining period (Figure 5.13). It is possible that while the individual metabolites may differ, AET induces responses in similar metabolic pathways at each timepoint to promote a consistent metabolic profile which reflects whole-body and skeletal muscle specific adaptations to AET and promotes a healthier phenotype in young, untrained individuals. As such, returning to a more sedentary lifestyle may disrupt the newly established metabolic equilibrium resulting in large disruption to metabolic processes and the variety of metabolite classes impacted.

However, several metabolites were affected in the same way during AET and after exercise withdrawal. For instance, plasma abundance of phenylalanine was significantly elevated from baseline at both week 8 and week 12. (±)-Sulfobutanedioic acid was elevated at week 4 and week 12. As discussed above, both metabolites can be linked to regulation of fat oxidation. This suggests that, although there are changes in metabolism indicating a general decline in adaptations in the metabolism associated with greater whole-body health following exercise withdrawal, some benefits conferred by AET may be maintained during this withdrawal period. This also supports the hypothesis that exercise type is influential in dictating whole-body and muscle level adaptations in the metabolome in response to increased activity as no benefits from RET were maintained after refraining from exercise for only 72 hours (as discussed in Chapter 4). Benefits in the metabolism being maintained during the

exercise withdrawal period is also in line with the lack of significant difference in either exercise steady-state RER or VO_2^{PEAK} between the 8- and 12-week timepoints. However, assessment of plasma abundance of glycerophospholipid metabolites which were correlated with change in exercise steady-state RER and VO_2^{PEAK} (discussed further in Section 5.4.3) indicated that plasma abundance was more similar to the baseline value after 4 weeks of exercise withdrawal than after 8 weeks AET. This suggests the benefits in the metabolism may not be maintained for periods of detraining longer of 4 weeks which may then lead to observable reductions in VO_2^{PEAK} and exercise steady-state RER.

5.4.3. Integration of metabolomic and physiological outcome datasets

WGCNA correlations were able to link metabolite abundance and measures of VO_2^{PEAK} and exercise steady-state RER which were previously shown to be impacted by AET. Importantly, these results suggest that the plasma mirrors the response within skeletal muscle, providing a view of muscle level adaptations to AET without requiring a tissue biopsy. This is in line with previous findings from Chapter 4, which show plasma and metabolome biomarkers of ageing mirror each other, and in agreement with recent literature indicating a positive correlation between the levels of plasma and muscle metabolites (Wu et al., 2022). Correlations were assessed at baseline, after 8 weeks of AET and after 4 weeks of exercise withdrawal. At each timepoint there was a large overlap in metabolic pathways associated with exercise steady-state RER and VO_2^{PEAK}. The metabolome is therefore mirroring previously established correlations between RER and other indicators of physical fitness, including VO_2^{PEAK}, which were found in healthy men regardless of training condition (Ramos-Jiménez et al., 2008).

5.4.3.1. Correlations between metabolite abundance and outcome measures at baseline

Correlation between metabolite abundance and measures of exercise steady-state RER and VO_2^{PEAK} at baseline provides insight into the metabolic processes that dictate measures of physical fitness in untrained individuals. Multiple modules of metabolites were linked glycerophospholipid metabolism, sphingolipid metabolism, and pentose and glucuronate interconversion pathways (Table 5.1).

5.4.3.2. Glycerophospholipids

Associations between glycerophospholipid metabolism and rates of fat oxidation were observed in young men after bed rest in Chapter 3, pointing to a role for mitochondrial lipids in the physiological response to sedentary behaviour. The correlation of glycerophospholipid metabolism with physiological adaptations to both exercise and sedentary behaviour suggests that the regulation of mitochondrial function is key to maintaining skeletal muscle health and warrants further investigation as a potential therapeutic target for preventing the loss of muscle mass. In Chapter 3 and in the present chapter, PE was identified as an important metabolite in the association between outcome measures and metabolomics data. However, while bed rest seemed to induce a decline in plasma abundance of many PE species and some PE species were found to decrease in abundance after a bout of AET at baseline, other PE species increased in abundance following AET. This suggests that, rather than specific PE metabolites influencing fat oxidation, improvement in muscle oxidative capacity actually relates to the ratio of glycerophospholipid species present within the muscle, with some species promoting a healthier muscle oxidative state. Disruption to this ratio, such as that seen in response to chronic bed rest, may cause a decline in oxidative capacity.

5.4.3.3. Sphingolipids

Sphingolipids are found as components of cell membranes (Holthuis et al., 2001) and modulate cell signalling pathways including those involved in the growth, differentiation and regeneration of skeletal muscle cells (Tan-Chen et al., 2020). This is not the first study to find associations between sphingolipids and exercise intervention. Muscle sphingosine, sphingospine-1-phosphate and ceramide concentrations increased with a bout of submaximal exercise before decreasing in a recovery period in athletes and untrained individuals (Bergman et al., 2016). A decrease in plasma concentration of sphingomyelin and ceramides was associated with improvement in VO_2^{PEAK} over a 6 month period of AET and RET intervention (Saleem et al., 2020). It is suggested that the lipotoxic accumulation of ceramides within skeletal muscle occurs as a consequence of incomplete fatty acid oxidation (Koves et al., 2008). The association of sphingolipid metabolism with exercise steady-state RER may therefore relate to the increased reliance on lipids as a substrate in oxidation during exercise. It has also been suggested that the change in concentration of muscle sphingolipids may be related to the improved insulin sensitivity associated with chronic exercise (Bergman et al., 2016). As insulin sensitivity was not assessed in this study this association cannot be definitively validated but this may be of interest to investigate further.

5.4.3.4. Pentose and glucuronate interconversion pathways

The pentose and glucuronate interconversions pathway occurs parallel to glycolysis and relates to the metabolism of carbohydrates as substrates in oxidation (Moisá et al., 2013). Although submaximal exercise is typically associated with the preferential use of lipids as oxidative substrates (Purdom et al., 2018) there is also an increase in carbohydrate oxidation (Romijn et al., 1993). The correlation of pentose and glucuronate interconversions with the outcome measures may reflect this increase in

carbohydrate oxidation. However, ORA found that the metabolite important in driving the association of the pentose and glucuronate interconversion pathway with exercise steady-state RER and VO_2^{PEAK} was β-D-glucuronide, an intermediate in the production of D-glucuronate. This conversion mainly occurs in the liver (Bock and Kohle, 2005). Although it is possible β-D-glucuronide was released from the liver for use in carbohydrate oxidation in skeletal muscle and that this association therefore reflects organ crosstalk in the exercise response, it also demonstrates that while many changes in the plasma metabolome in response to AET reflect muscle level adaptations others are indicative of systemic changes which should be considered when viewing the metabolomic response to AET with a focus on skeletal muscle.

As associations between measures of exercise steady-state RER and VO_2^{PEAK} in skeletal muscle and plasma metabolite abundance in glycerophospholipid and sphingolipid metabolism pathways could be found at baseline it was deemed likely that adaptations in skeletal muscle as a consequence of 8 weeks AET and 4 weeks exercise withdrawal would also be associated with the plasma metabolome.

5.4.3.5. Correlations between change in metabolite abundance and outcome measures after exercise training and exercise withdrawal

Glycerophospholipid metabolism, sphingolipid metabolism and pentose and glucuronate interconversion pathways which were associated with outcome measures at baseline were also found to be associated with change in exercise steady-state RER and VO_2^{PEAK} after 8 weeks AET (Table 5.2) and after 4 weeks exercise withdrawal (Table 5.3), further demonstrating the role of these metabolites in dictating the exercise response, although as discussed above the pentose and glucuronate interconversion pathway may be more indicative of organ crosstalk that influences the exercise response than specific adaptations in skeletal muscle.

In addition to these associations, many correlations between amino acid metabolism and change in exercise steady state RER and VO_2^{PEAK} were observed after 8 weeks AET (Table 5.2).

5.4.3.6. Arginine and proline metabolism

Arginine and proline metabolism was associated with both outcome measures after 8 weeks AET. L-ornithine and L-arginosuccinate, two non-proteinogenic amino acids, were identified as influential in this pathway. Ingestion of L-ornithine supplements has previously been linked to reduced muscle fatigue during AET (Demura et al., 2010). Exercise interventions can lead to the accumulation of ammonia within skeletal muscle. When ammonia is produced by the deamination of AMP it prevents the resynthesis of ATP during exercise (Rusip et al., 2018), inhibiting oxidative phosphorylation and leading to muscle fatigue. L-ornithine facilitates the release of ammonia from skeletal muscle resulting in lower muscle fatigue and therefore the importance of L-ornithine in the association of arginine and proline metabolism with exercise steady-state RER and VO_2^{PEAK} may relate to improvements in oxidative phosphorylation with exercise. In a separate study, dietary supplementation of L-ornithine promoted lipid metabolism during an endurance exercise intervention in healthy young volunteers (Sugino et al., 2008). In the present study the observed decrease in RER indicates a higher capacity for lipid oxidation. The association of L-ornithine and exercise steady-state RER therefore provides further evidence to support a role for L-ornithine in the modulation of fuel oxidation in physiological adaptation to AET.

5.4.3.7. Glycine, serine and threonine metabolism

L-ornithine and L-arginosuccinate can also both be used as precursors in the creatine biosynthesis pathway (Haines et al., 2011). Creatine was identified as an important

metabolite in the association of the glycine, serine and threonine metabolism pathway with change in exercise steady-state RER. This highlights the interactivity of the metabolome and the metabolic response to AET. Approximately 95% of creatine in the body is stored within skeletal muscle (Haines et al., 2011). Creatine is commonly used as an anabolic supplement to improve muscle mass and strength (Cooper et al., 2012) but is also linked to normal skeletal muscle metabolism. For instance, creatine is involved in maintaining the intracellular availability of ATP (Clark, 1997) and decreased ATP content has been linked to decreased creatine in acute skeletal muscle wasting in critical illness (Puthucheary et al., 2018) implying an association between decreased oxidative capacity and decreased creatine content which supports the association between creatine and change in exercise steady-state RER observed here. However, it should be considered that decreased oxidative capacity and creatine content in critical illness may simply reflect the increase in dead muscle fibres linked to ICU admission (Formenti et al., 2019).

Other important metabolites in the serine, glycine and threonine pathway were putatively identified as L-serine, dimethylglycine, betaine, and carbon dioxide. Serine is important in regeneration and proliferation of skeletal muscle by regulating muscle progenitor cells (Thalacker-Mercer et al., 2020) indicating its importance in the maintenance of skeletal muscle. Dietary supplementation of serine reduced fatigue during submaximal aerobic exercise (Tsuda et al., 2019) providing support in the current literature that serine in some way relates to the adaptive response to exercise, although its precise role is not clear as arginine and valine were also supplemented in the study and may have anti-fatiguing effects. Serine has also been linked to pyruvate metabolism (Chaneton et al., 2012), giving it a role in carbohydrate oxidation which provides further support for its association with change in exercise steady-state RER, and to sphingolipid synthesis (Hwang et al., 2017), further highlighting the interactive

nature of the metabolome in the response to AET. Finally, serine acts as a precursor in the biosynthesis of glycine, as do betaine and dimethylglycine (Kanehisa and Goto, 2000). Glycine is also essential for skeletal muscle regeneration (Thalacker-Mercer et al., 2020) and was previously noted as important in physiological adaptations associated with chronic bed rest in Chapter 3. These results suggest that similar metabolic pathways may be disturbed in adaptive responses to muscle disuse and increased activity, potentially identifying pathways which may be utilised in therapeutic interventions to mitigate muscle deconditioning.

L-tyrosine was another metabolite identified with change in exercise steady-state RER and was also associated with change in VO_2^{PEAK}. L-tyrosine treatment in rodents has been shown to reduce deficits in locomotor activity associated with ageing (Brady et al., 1980) suggesting that tyrosine has beneficial effects on muscle strength and function. Improvements in stamina and body strength in nemaline myopathy patients were seen after dietary L-tyrosine supplementation in a pilot study (Ryan et al., 2008) suggesting tyrosine may have a similar role in muscle strength in humans. A larger study demonstrated that dietary tyrosine supplementation was associated with a 15% increase in exercise time to exhaustion (Tumilty et al., 2011) further supporting a role for tyrosine in the exercise response. While these studies only investigate supplementation of tyrosine, the beneficial response to tyrosine supplementation suggests that there is an intrinsic role for tyrosine in the exercise response. It is possible that the concentration of tyrosine naturally produced from exercise may not be enough to induce changes in strength by itself but given the association of tyrosine with both outcome measures in this study it is possible that adaptation in oxidation mechanisms and increased oxygen uptake may precede improvements in muscle strength in adaptation to AET.

The associations with amino acid metabolism and adaptations to AET and exercise withdrawal also demonstrate that correlation analysis is complementary to the output from differential abundance analysis. L-phenylalanine was identified as important in the associations of phenylalanine metabolism and phenylalanine, tyrosine and tryptophan biosynthesis pathways with change in exercise steady-state RER and VO_2^{PEAK} after 8 weeks AET and 4 weeks exercise withdrawal. As discussed in Section 5.4.1, plasma abundance of phenylalanine was significant increased after AET and remained elevated after exercise withdrawal. This provides evidence to validate the use of differential abundance analysis to find markers of change in the plasma which are relevant to intramuscular adaptations to an exercise intervention. The potential of physiological and metabolomic integration has been explored in Chapter 3 but the associations in this chapter lend further support to the importance of integrative approaches in understanding physiological adaptations.

Chapter 6. Metabolomic analysis of plasma following aerobic exercise in COPD patients and age matched healthy controls

6.1. Background

6.1.1. Chronic obstructive pulmonary disease

Chronic obstructive pulmonary disease (COPD) is the second most common lung condition in the UK, affecting roughly 9% of adults over the age of 70 (Snell et al., 2016). It is also the fourth leading cause of death worldwide, accounting for approximately 4.8% of global deaths (Raherison and Girodet, 2009). COPD patients commonly exhibit abnormal skeletal muscle characteristics compared to age-matched healthy counterparts (Jaitovich and Barreiro, 2018), including altered fibre type composition, lower cross-sectional area (CSA) (Jakobsson and Jorfeldt, 1990), dysregulated protein turnover (Jagoe and Engelen, 2003), and reduced maximal activities of oxidative enzymes (Polkey, 2002). Such adaptations influence the muscle metabolic response to exercise stimuli and contribute to the development of exercise intolerance, which is commonly reported in COPD patients. While exercise intolerance is potentially worsened by symptoms associated with decreased lung function such as breathlessness, evidence suggests ventilatory limits contribute to exercise intolerance without being the sole cause. For example, 19% of a COPD patient cohort reported leg discomfort as the primary reason for stopping exercise (Guenette et al., 2014). In addition, both single and double lung transplants restored respiratory function but not exercise tolerance or maximum work rate at either 3 months or 1 to 2 years after transplant (Williams et al., 1992).

Despite some variation in patient response (de Brandt et al., 2018; Ward et al., 2020), it is generally recognised that improvements in exercise tolerance, muscle strength and quality of life can be induced by AET interventions in COPD patients (Vogiatzis et al., 2005). For example, 8 weeks AET increased endurance exercise time from 8.8

minutes at baseline to 20.8 minutes after intervention, and 6 minute walk distance increased from 388 to 414 meters in the COPD patient cohort (Mador et al., 2004). Likewise, a 3 month period of walking at a rating of perceived dyspnoea of 3-5 on the Borg categorical scale increased 6 meter walk distance by 48.2 meters and decreased time to rise from a chair by 5 seconds in COPD patients (Berry et al., 2018). However, the physiological mechanisms underlying these improvements are not well defined. In addition, studies investigating the effect of AET on COPD often compare patients undertaking exercise to a control group of sedentary COPD patients rather than including age-matched healthy controls. As such the impact of COPD on the response of skeletal muscle to exercise is relatively understudied. Recent work has demonstrated that whole-body and muscle specific mitochondrial adaptations in response to 8 weeks AET at 65% VO_2^{PEAK} were not observed in older COPD patients, in contrast to age matched and healthy young (HY) controls at the same exercise intensity (Latimer et al., 2021). In addition, the observed response to AET was blunted in the healthy older (HO) group relative to HY. Chapter 5 of this thesis demonstrated that changes in the plasma metabolome in response to AET in the HY group were representative of muscle level adaptations in respiratory exchange ratio (RER) and VO_2^{PEAK}. It is hypothesised that a similar approach may be able to characterise adaptations to AET in older individuals and in COPD patients.

6.1.2. Metabolomic adaptations to submaximal aerobic exercise training

In addition to characterising the exercise response to 65% VO_2^{PEAK} AET in Chapter 5, metabolomics has been employed to investigate adaptations to submaximal exercise in the literature. A targeted study found extended periods of AET at an intensity of 70% VO_2^{PEAK} in 50-60 year olds was associated with change in plasma indicators of glycogenolysis, change in fuel substrate mobilisation, and differences in plasma abundance of purine metabolites and tricarboxylic acid intermediates (Lewis et al.,

2010). As only targeted metabolomics was used, there may be further changes in the metabolome not identified by Lewis and colleagues. Importantly, the participants were trained marathon runners which is highly likely to impact on their metabolic response to AET. When the urinary metabolomic response to a ramped VO_2^{PEAK} test was assessed in trained cyclists and untrained controls, differences were seen between pre- and post-exercise timepoints in urinary creatinine, citrate, TMAO and glycine (Mukherjee et al., 2014). However, there were also measurable differences in urinary metabolites involved in energy metabolism, lipid metabolism, insulin signalling and cardiovascular function found between the groups after exercise (Mukherjee et al., 2014). Previous work in this thesis demonstrated the similarities between the plasma and skeletal muscle metabolomes, but it is unclear whether the urinary metabolome also accurately reflects adaptations within skeletal muscle as no such comparison was made. Moreover, NMR spectroscopy was employed for the metabolomics analysis, which due to its lower sensitivity (discussed in more detail in Chapter 1) may be unable to detect as many metabolites as mass spectrometry, and therefore may be an inferior approach. Additionally, in both Lewis et al. (2010) and Mukherjee et al. (2014) there was no comparison to younger individuals so insight regarding a possible blunting of the exercise adaptive response with age was missing. A later study observed differences in purine metabolism between young and older trained athletes following high intensity AET which indicated an age-related decline in ATP resynthesis during exercise (Zieliński et al., 2019). As this study only investigated purine metabolism, wider changes in the metabolism were not investigated. Additionally, the exercise test was high intensity and may elicit differences in the metabolic response to exercise than submaximal testing. However, the study of Zieliński et al. (2019) does demonstrate the potential of metabolomics in investigating the impact of age in adaptations to AET. Finally, the participants in all the studies

outlined above were healthy, and therefore insight of how AET in chronic disease impacts on the metabolome is missing. This gap in the literature presents an opportunity for novel insight. The aims of this chapter are therefore as follows:

1. To determine whether the response of the plasma metabolome to 8 weeks AET is reflective of physiological adaptations in healthy older individuals, and to identify metabolites most associated with metabolic adaptations to 8 weeks of AET
2. To determine whether any differences in the physiological responses to 8 weeks AET in COPD patients and age matched healthy controls is reflected in the plasma metabolome
3. To investigate the plasma metabolome response to AET withdrawal in COPD patients and age matched healthy controls, and identify metabolites most associated with physiological adaptation to exercise withdrawal

6.2. Methods

6.2.1. Study design

This chapter retrospectively utilised samples collected as part of a volunteer intervention study (Latimer et al., 2021), which was conducted at the Universities of Leicester and Nottingham, UK (Clinical Trials Register: ISRCTN10906292). The study was approved by the NHS National Research Ethics Service. All participants provided written informed consent. Baseline assessments, submaximal testing protocols and timepoint sampling was as described in Chapter 5. HO were required to have normal lung function (FEV1/FVC > 0.7, FEV1 > 80%) and were excluded for any respiratory diagnosis. HO individuals who participated in exercise exceeding 150 minutes/week at moderate intensity were excluded. In this thesis chapter, HY was excluded from analysis. Participant characteristics are detailed in Table 6.1.

As there were a greater number of baseline samples in the COPD group than the HO control, additional baseline plasma samples from age matched healthy controls who had previously completed a 6-week exercise training study and consented to the storage and use of their plasma in future research were provided from an in-house biobank (Brook et al., 2015) to equalise numbers and allow a more robust comparison across groups at baseline.

Plasma samples were randomly sorted into 4 batches and prepared in an identical manner. Metabolites were extracted from plasma according to the protocol detailed in Section 2.3. Separation of metabolites within samples via liquid chromatography was performed according to the parameters detailed in Section 2.4 and acquisition of data by tandem mass spectrometry was performed according to the protocol in Section 2.5.

Table 6.1 Baseline subject characteristics. Data are presented as mean±SD unless otherwise stated. Percentage predicted values are calculated from normal values. FEV1: forced expiratory volume in 1 s; FVC: forced vital capacity; RV: residual volume; TLC: total lung capacity; TLCO: transfer factor for the lung of carbon monoxide; BMI: body mass index; FFMI: fat-free mass index; QMVC: quadriceps maximum voluntary contraction. ¶: pack-year average for ex-smokers only. Table from Latimer et al. (2021).

	HO (n=10)	**COPD (n=19)**	**p-value HO versus COPD**
Age, years	70.7±5.1	70.2±5.9	0.834
Female, n	5	14	
FEV_1, % pred	98.3±9.2	55.6±16.2	<0.001
FEV_1/FEV, %	74.5±4.4	44.6±12.1	<0.001
RV, % pred	98.4±19.2	157.3±44.9	0.001
TLC, % pred	104.3±11.9	121.3±19.1	0.007
RV/TLC, %	38.4±4.2	53.5±9.4	<0.001
T_{LCO}, % pred	98.3±12.7	61.5±18.7	<0.001
Smoking history, n			
Current smoker	0	0	
Never smoker	6	0	
Ex-smoker	4	19	
Smoking, pack-years¶	18.3±21.5	38.5±15.4	0.036
BMI, kg/m^2	28.5±3.3	29.0±6.4	
FFMI, kg/m^2	18.1±1.5	17.2±2.7	
QMVC isometric strength, Nm	129.7±36.8	98.6±36.1	0.058
Step count, 8-h average per day	6007±2008 (n=9)	4021±1864	0.046

6.2.2. Data pre-processing and statistical analysis

Data pre-processing was performed in R version 4.1 using the parameters detailed in Section 2.6. For statistical analysis, data for each polarity and ionisation mode were analysed separately. All analysis of metabolomics data was performed using inhouse R scripts using R version 4.1. Scripts are available in Appendix 2.

Firstly, to assess differences in the plasma metabolome between HO and CODP groups, PCA and sPLS-DA were applied to the data using the mixOmics package (Le Cao et al., 2016). Following this, analysis of differential metabolite abundance was performed by fitting a linear mixed effect model to each data matrix with the limma package (Ritchie et al., 2015) using group and time as fixed effects and participant ID as a random effect.

For time course analysis, in-house samples were removed from the datasets. Contrasts were set up within each group comparing baseline metabolite abundance with change in abundance at weeks 1, 4 and 8 of AET and after exercise withdrawal. P-values were obtained by Empirical Bayes moderated t-tests adjusted for false discovery rate (FDR) by the Benjamini-Hochberg method. Metabolites were deemed significantly different between comparisons when FDR<0.05.

Total lean mass, RER during steady-state exercise, and VO_2^{PEAK} were provided from Latimer et al. (2021) and assessed for normality using Shapiro-Wilk tests. Within group changes across time were tested using one-way repeated measures ANOVA with post-hoc pairwise comparisons adjusted for false discovery rate (FDR) using the Benjamini-Hochberg method.

6.2.3. Metabolite identification

Metabolites were putatively identified using metID (Shen, Wu, et al., 2022). Mass tolerance was set at 5ppm. Common compound names of identified features were taken from HMDB and mapped to metabolic pathways by over representation analysis (ORA) using MetaboAnalyst 5.0 (Pang et al., 2021). Pathways with an impact score greater than 0.1 were retained.

6.2.4. Correlation of metabolomic and physiological outcome data

Correlation of metabolite expression with outcome measures of VO_2^{PEAK} and RER during submaximal steady-state exercise at 65% VO_2^{PEAK} was assessed by weighted correlation network analysis (WGCNA) (Langfelder and Horvath, 2008). Metabolic modules with weak correlations ($r<|0.5|$) to outcome measures were discarded and network analysis was performed on the remaining metabolite modules to determine their functional relevance.

6.3. Results

6.3.1. Physiological adaptations to aerobic exercise training

VO_2^{PEAK} increased significantly in HO after 8 weeks AET ($p<0.01$). No significant increase was seen after 8 weeks AET in COPD ($p>0.05$). No significant difference in change in VO_2^{PEAK} was seen in either group between baseline and 4 weeks exercise withdrawal or between 8 weeks AET and 4 weeks exercise withdrawal ($p>0.05$, Figure 6.1). The RER during steady-state exercise decreased significantly from baseline after 8 weeks AET in HO ($p<0.001$) and COPD ($p<0.05$) indicating a greater contribution of fat oxidation to energy production. The RER during steady-state remained significantly lower than baseline in HO after 4 weeks exercise withdrawal ($p<0.001$), but there was no significant difference from baseline at the same point in COPD ($p>0.05$, Figure 6.2).

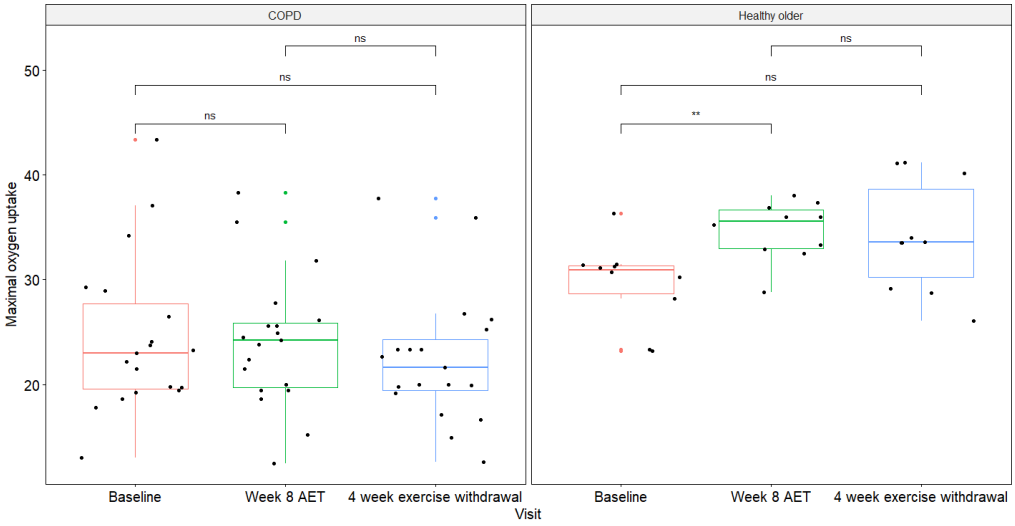

Figure 6.1 Peak oxygen uptake in COPD patients and age matched healthy controls at baseline, after 8 weeks aerobic exercise training and 4 weeks exercise withdrawal

Boxplots showing peak oxygen uptake (VO_2^{PEAK}) at baseline, after 8 weeks of aerobic exercise training (at 65% VO_2^{PEAK}) and after 4 weeks of exercise withdrawal in COPD patients and age matched healthy controls (Healthy older). Although no significant differences in VO_2^{PEAK} between time-points was seen in the COPD group, VO_2^{PEAK} increased significantly in the healthy older group at week 8. Boxplots represent the spread of data. Each black circle represents one participant and shows the specific distribution of data within groups. Outlying data points for baseline, week 8 or week 4 withdrawal measurements are shown in red, green or blue, respectively.

**p<0.01

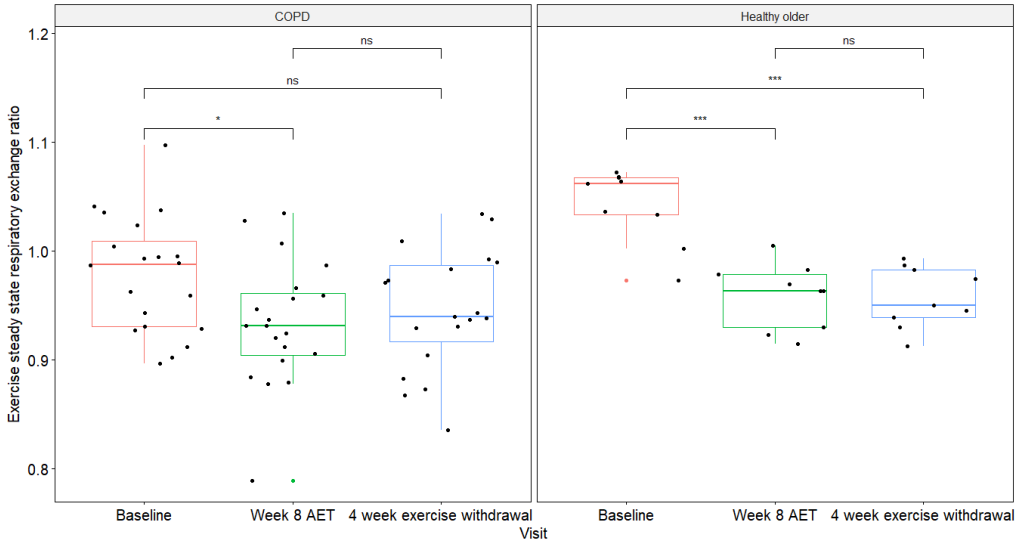

Figure 6.2 Steady-state exercise respiratory exchange ratio in COPD patients and age matched healthy controls at baseline, after 8 weeks aerobic exercise training and 4 weeks exercise withdrawal

Boxplots showing steady-state exercise respiratory exchange ratio (RER) at baseline (red), after 8 weeks of aerobic exercise training (at 65% VO2PEAK) (green) and after 4 weeks of exercise withdrawal in COPD patients and age matched healthy controls (Healthy older). A significant decrease in RER was seen at week 8 in both groups. RER was also significantly decreased after exercise withdrawal in HO but not COPD. No difference between 8 weeks AET and 4 weeks exercise withdrawal was seen in either group. Each black circle represents one participant and shows distribution of data within groups.

*p<0.05, ***p<0.001

6.3.2. Multivariate analysis of baseline samples

After filtering, a total of 2143 negatively ionised metabolites (496 polar and 1647 non-polar) and 2491 positively ionised metabolites (392 polar and 2099 non-polar) were retained at baseline. However, PCA could not distinguish between HO and COPD groups at baseline. An sPLS-DA separation model showed improved separation of groups at baseline, however cross validation showed error rates greater than 20% for all models and the separation model was therefore considered overfitted (Figure 6.3).

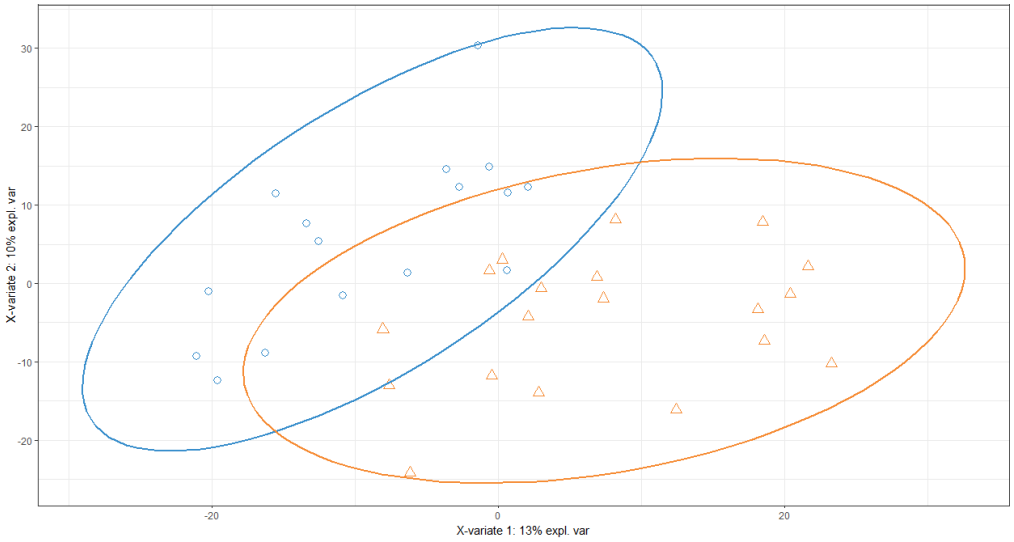

Figure 6.3 Separation of groups at baseline by sPLS-DA

Representative plot of sparse partial least squares discriminant analysis (sPLS-DA) separation model using all detected metabolites at baseline, with 95% confidence ellipses, for COPD (blue circle) and HO (orange triangle) groups in non-polar negative data. Better classification of samples by group was achieved relative to PCA, however cross-validation of the model demonstrated high error rates (>20%). High error rates indicate that the model is overfitted and thus classification cannot be considered as accurate.

6.3.3. Linear modelling

Given that PCA resulted in poor separation between groups at baseline and the sPLS-DA separation model was overfitted, an alternative approach was needed to identify classifying metabolites. A linear model can be used to test for variability of metabolite abundance between groups in high dimensionality data (Zhan et al., 2015). Following adjustment for multiple testing, significant differences ($p<0.05$) in the abundance of 65 metabolites were found between HO and COPD groups at baseline (Figure 6.4).

The linear model was then extended to compare baseline metabolite abundance with abundance after 1, 4 and 8 weeks AET and after 4 weeks exercise withdrawal (Table 6.2). A response to AET was observed in HO, with 73 metabolites present at a significantly different abundance ($p<0.05$) at either 1 week, 4 weeks or 8 weeks AET, or after 4 weeks exercise withdrawal compared to baseline. Of these, 35 were

significantly different after 1 week of AET, 35 were significantly different after 8 weeks AET and 3 were significantly different after 4 weeks exercise withdrawal. No metabolites were significantly different after 4 weeks exercise in HO. Most notably, no metabolites were found to have a significantly different expression from baseline at any point following the start of AET in COPD.

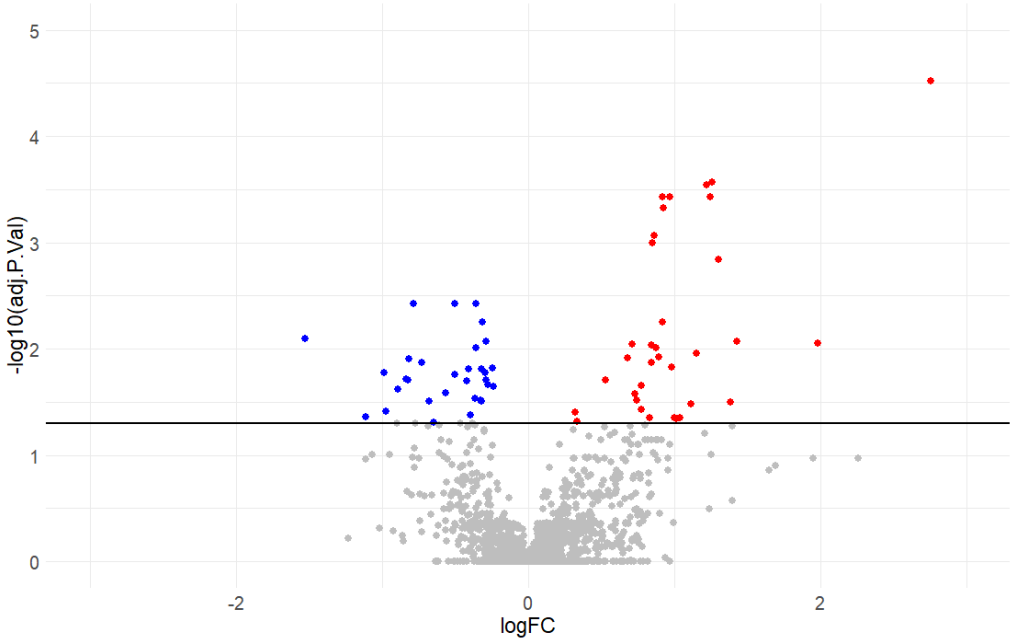

Figure 6.4 Differential metabolite abundance between groups at baseline

Comparison of metabolite abundance between COPD patients and age matched health controls. The x axis shows log fold change of metabolite abundance. The y axis shows -log10 p-value adjusted for false discovery rate by the Benjamini-Hochberg method. The black line shows the threshold of FDR<0.05. Each plotted point represents a metabolite (blue, significantly downregulated; red, significantly upregulated; grey, not significantly different between groups).

Table 6.2 Number of metabolites significantly different at at least one time point compared to the baseline value

	COPD	**Healthy Older**
HILIC negative	0	2
HILIC positive	0	20
RP negative	0	24
RP positive	0	27
TOTAL	**0**	**73**

6.3.4. Metabolite identification

At baseline, metabolites present at significantly different abundances between COPD and HO were mapped to 32 known metabolite classes. The largest known class was organooxygen compounds, followed by carboxylic acids and their derivatives (Figure 6.5).

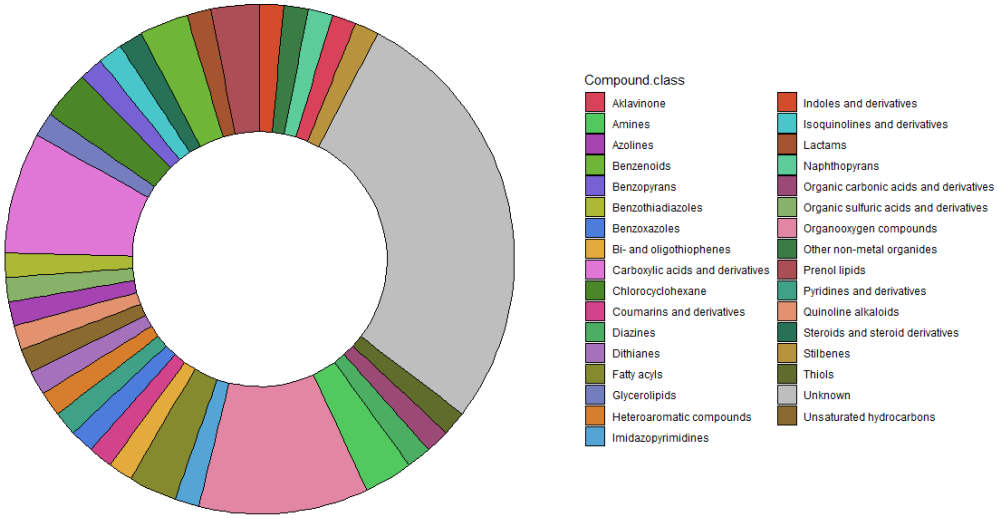

Figure 6.5 Classes of metabolites significantly different between COPD and HO groups at baseline

Donut charts showing classes of metabolites present at significantly different plasma levels when measured prior to AET intervention between COPD and HO at baseline. Classes are represented as a percentage of the number of metabolites changed in abundance.

1 week of AET induced a shift in the plasma abundance of 35 metabolites which were mapped to 16 known metabolite classes (Figure 6.6A). The largest percentage of identified classes impacted were species of lipid, most notably glycerophospholipids, prenol lipids and fatty acyls. Derivatives of carboxylic acids and steroids were also predominant in the response after 1 week. After 8 weeks AET, 18 known metabolite classes were impacted (Figure 6.6B). A greater number of metabolites were linked to carboxylic acids and their derivatives compared to after 1 week AET. An increase in the number of atty acyls, glycerophospholipids and organooxygen compounds were also seen. In contrast, after 4 weeks of exercise withdrawal only 2 metabolite classes were

impacted compared to baseline (Figure 6.7). A derivative of carboxylic acid and a bithiophene were identified as significantly different relative to baseline value. At all timepoints, there were several metabolites which could not be identified, a known limitation of untargeted metabolomics.

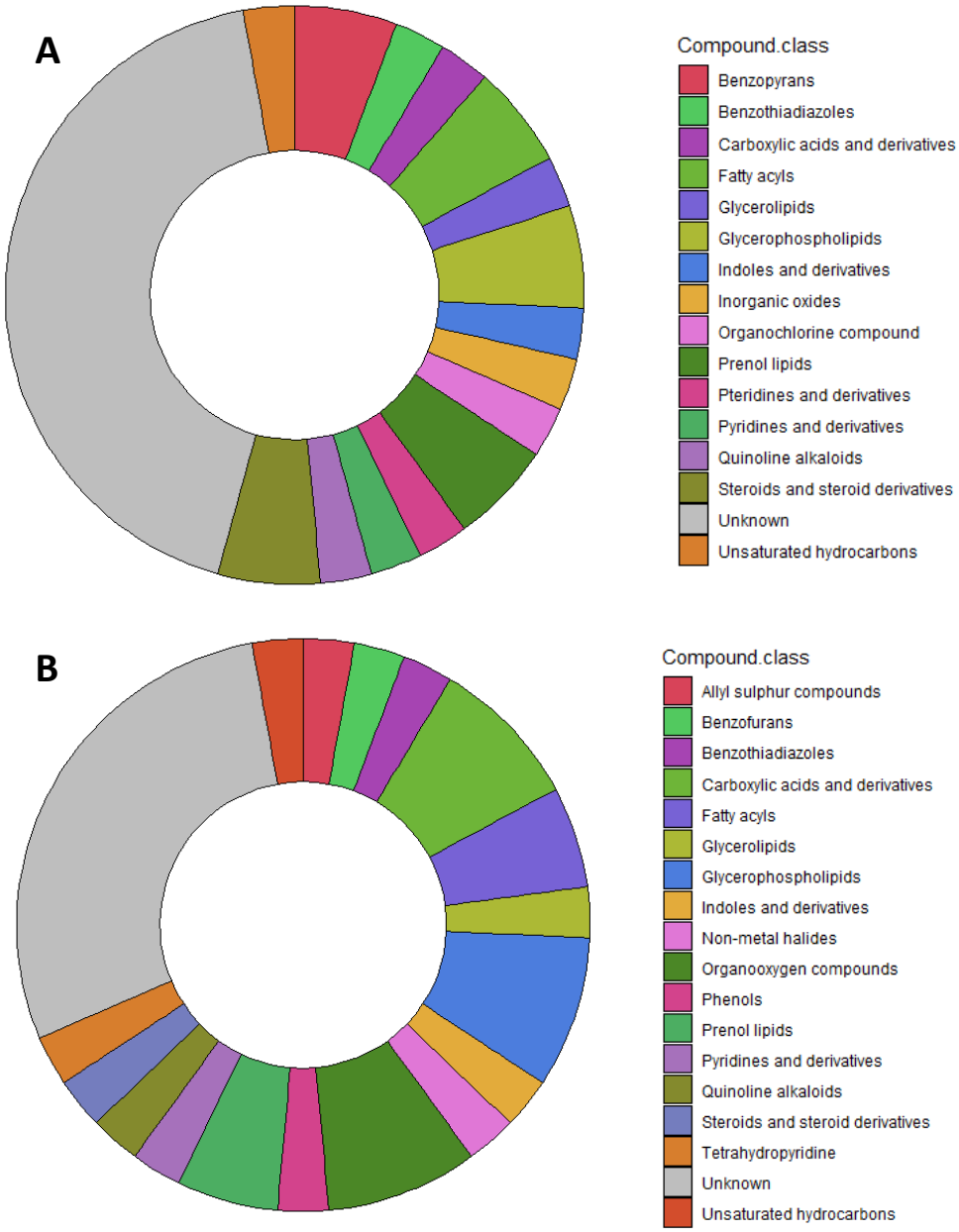

Figure 6.6 Classes of metabolites significantly different after exercise training

Donut chart showing classes of metabolites present at significantly different plasma abundance after (A) 1 week and (B) 8 weeks of aerobic exercise training intervention compared to baseline values in healthy older participants. Classes are represented as a percentage of the number of metabolites changed in abundance.

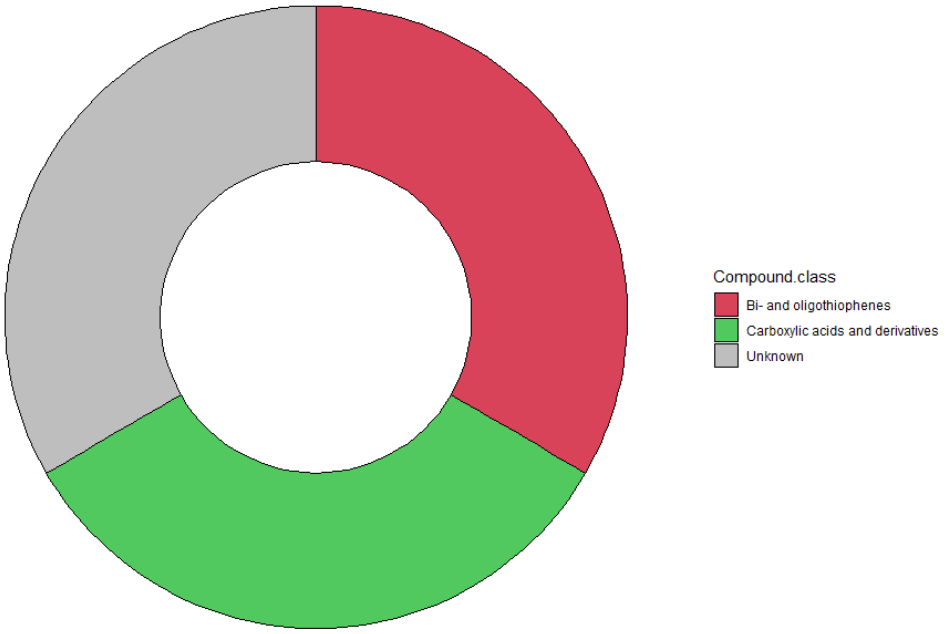

Figure 6.7 Metabolite classes significantly different after 4 weeks exercise withdrawal

Donut chart showing classes of metabolites present at significantly different plasma levels after 4 weeks exercise withdrawal compared to baseline values in healthy older participants. Classes are represented as a percentage of the number of metabolites changed in abundance.

6.3.5. Correlation analysis

Integration of metabolomics data and physiological outcome measures was performed using WGCNA to determine whether changes in the metabolome reflected skeletal muscle level adaptations. Firstly, comparisons were made between metabolite abundance and outcome measures at baseline (Table 6.3). Next, correlations between change in metabolite abundance and change in steady-state exercise RER and VO_2^{PEAK} at week 8 (Table 6.4) and week 12 (Table 6.5) were assessed. WGCNA correlation indicated high degrees of association between metabolic modules and measurements of VO_2^{PEAK} and steady-state exercise RER. To clarify which metabolites were important in driving association and their biological roles, metabolite identification and pathway analysis were performed on modules which were associated with at least one measure of adaptation.

Table 6.3 Table containing metabolic modules of metabolite abundance at baseline which are correlated (r>|0.5|, p<0.05) with measures of exercise steady-state respiratory exchange ratio (RER) and maximal oxygen uptake (VO_2^{PEAK}) at baseline. Over representation analysis was applied to metabolites within each module to identify relevant metabolic pathways (impact score > 0.1).

Module	Correlation with outcome measure	Coefficient	p-value	Pathway	Impact score
Turquoise	VO_2^{PEAK}	0.68	0.003	Arginine and proline metabolism	0.20
				Arginine biosynthesis	0.14
Cyan	RER	-0.53	0.006	Glycerophospholipid metabolism	0.20
				Pantothenate and CoA biosynthesis	0.18
				Fatty acid degradation	0.12

Table 6.4 Table containing metabolic modules of change in metabolite abundance after 8 weeks aerobic exercise training which are correlated (r>|0.5|, p<0.05) with change in measures of exercise steady-state respiratory exchange ratio (RER) and maximal oxygen uptake (VO_2^{PEAK}) after 8 weeks aerobic exercise training. Over representation analysis was applied to metabolites within each module to identify relevant metabolic pathways (impact score > 0.1).

Module	Correlation with outcome measure	Coefficient	p-value	Pathway	Impact score
Green	Change in RER	0.61	0.02	Arginine and proline metabolism	0.12
	Change in VO_2^{PEAK}	0.78	0.0006		
Turquoise	Change in VO2	-0.68	0.005	beta-Alanine metabolism	0.40
Red	Change in RER	-0.77	0.0008	Sphingolipid metabolism	0.31
				Glycerophospholipid metabolism	0.25
Black	Change in RER	-0.51	0.05	Sphingolipid metabolism	0.27
				Pantothenate and CoA biosynthesis	0.18
				Fatty acid degradation	0.12

Table 6.5 Table containing metabolic modules of change in metabolite abundance after 4 weeks exercise withdrawal which are correlated (r>|0.5|, p<0.05) with change in measures of exercise steady-state respiratory exchange ratio (RER) and maximal oxygen uptake (VO_2^{PEAK}) after 4 weeks of exercise withdrawal. Over representation

analysis was applied to metabolites within each module to identify relevant metabolic pathways (impact score > 0.1).

Module	Correlation with outcome measure	Coefficient	p-value	Pathway	Impact score
Brown	Change in VO_2^{PEAK}	-0.56	0.02	Phenylalanine, tyrosine and tryptophan biosynthesis	0.50
				Tyrosine metabolism	0.14
				Pyrimidine metabolism	0.13
Turquoise	Change in VO_2^{PEAK}	0.51	0.04	Caffeine metabolism	0.69
				beta-Alanine metabolism	0.40
				Glycerolipid metabolism	0.34
				Biotin metabolism	0.20
				Arginine and proline metabolism	0.11
				Pyrimidine metabolism	0.10
Grey	Change in RER	0.53	0.03	Glycine, serine and threonine metabolism	0.27
				Aminoacyl-tRNA biosynthesis	0.17
Brown	Change in VO_2^{PEAK}	-0.78	0.0006	beta-Alanine metabolism	0.40
Turquoise	Change in RER	-0.5	0.04	Glycerophospholipid metabolism	0.14
Salmon	Change in VO_2^{PEAK}	0.51	0.04	Glycerophospholipid metabolism	0.22

At baseline, VO_2^{PEAK} in HO was correlated with the polar positive turquoise module (r=0.68). Metabolites in this module were related to arginine biosynthesis (impact score 0.14) and arginine and proline metabolism (impact score 0.2). Within these pathways, influential metabolites were putatively identified as L-guanidinoacetate, L-ornithine, L-arginine, creatine, 2-oxoglutarate and urea. Steady-state exercise RER in HO at baseline was associated with the cyan module in the non-polar positive dataset (r=-0.53). Metabolites in this module were mapped to glycerophospholipid

metabolism (impact score 0.2), pantothenate and CoA biosynthesis (impact score 0.18) and fatty acid degradation (impact score 0.12) pathways. In the glycerophospholipid metabolism pathway, influential metabolites were identified as phosphatidylethanolamine (PE) and phosphatidylcholine (PC). In the pantothenate and CoA biosynthesis and fatty acid degradation pathways, the important metabolite was identified as CoA.

Similar associations were seen after 8 weeks AET in HO. Arginine and proline metabolism (impact score 0.12) remained correlated with VO_2^{PEAK} (r=0.78) but was also found to be correlated with steady-state exercise RER (r=0.61). Fewer metabolites within the pathway were important in these correlations compared to baseline. Only L-ornithine and creatine were deemed important by ORA. Glycerophospholipid metabolism (impact score 0.25), pantothenate and CoA biosynthesis (impact score 0.18) and fatty acid degradation (impact score 0.12) pathways remained associated with exercise steady-state RER. Plasma abundance of CoA increased after AET in HO. Several PE and PC species were identified in the data but there was no universal pattern of increase or decrease.

The turquoise module in the polar positive dataset was correlated with VO_2^{PEAK} after 8 weeks AET in HO (r=-0.68). Metabolites in this module were mapped to the β-alanine metabolism pathway with β-alanine identified as important within the pathway by ORA. Mean abundance of β-alanine only increased a small amount relative to baseline after 8 weeks AET, possibly indicating that only small changes in metabolite abundance is reflective of measurable physiological change. Two modules in the non-polar positive dataset which were correlated with steady-state exercise RER (red r=-0.77 and black r=-0.51) contained metabolites that were mapped to the sphingolipid metabolism pathway (impact scores 0.31 (red module) and 0.27(black module)).

Important metabolites were identified as N-acylsphingosine and sphingomyelin. Sphingolipids increased in plasma abundance after 8 weeks AET in HO.

After exercise withdrawal, β-alanine metabolism was identified in two modules in HO (impact score 0.4 for both modules), which were associated with change in VO_2^{PEAK} during exercise withdrawal (r=0.51 and r=-0.78). β-alanine was identified as important and was decreased relative to baseline abundance. Arginine and proline metabolism (impact score 0.11) was associated with change in VO_2^{PEAK} after exercise withdrawal (r=0.51). Within the pathway, L-ornithine was highlighted as influential and was found to decrease in abundance relative to baseline. Two modules associated with change in VO_2^{PEAK} (r=0.51 for both) and one module associated with change in RER (r=-0.5) in HO during exercise withdrawal were linked to glycerophospholipid metabolism (impact score > 0.1 for all associations). Metabolites important in the pathway were identified as PE, PC, phosphatidylserine (PS) and 1-acyl-sn-glycero-3-phosphocholine. Some glycerophospholipid metabolites increased in abundance relative to baseline while some decreased, suggesting that the absolute abundance is less important than the ratio of metabolites.

In addition, the glycine, serine and threonine pathway (impact score 0.27) was associated with the change in steady-state exercise RER in HO following exercise withdrawal (r=0.53). L-serine, which increased relative to baseline abundance, and betaine, which decreased relative to baseline abundance, were identified as influential within the pathway. The phenylalanine, tyrosine and tryptophan biosynthesis pathway (impact score 0.5) and tyrosine metabolism pathway (impact score 0.14) were both associated with change in VO_2^{PEAK} following exercise withdrawal (r=0.53 and r=-0.56, respectively), suggesting greater involvement of amino acids in the association of the plasma metabolome and physiological adaptations after detraining than after exercise

intervention. Within both pathways, L-tyrosine was identified as important and decreased in abundance relative to baseline.

6.4. Discussion

The main finding of this chapter is that there was an observable response to AET in the plasma metabolome of HO individuals but not in COPD patients at matched exercise intensities, which parallels the pattern of physiological and mitochondrial adaptation to AET previously reported (Latimer et al., 2021).

6.4.1. Metabolic disturbances caused by COPD at baseline

Although not a primary aim of this chapter, comparison between COPD patients and age matched healthy controls at baseline allowed for the identification of metabolites which could potentially serve as biomarkers for COPD.

6.4.1.1. Carboxylic acids and derivatives

Among the metabolites which were significantly different between groups, one of the largest classes affected was carboxylic acids and their derivatives which is indicative of dysregulated amino acid metabolism. Firstly, there was a decrease in lysine metabolism in COPD compared to HO. Plasma abundance of D-lysine and N6-N6-N6-trimethyl-L-lysine both decreased significantly in COPD patients. Previously, reduced levels of lysine in serum was associated with a greater severity of COPD (Ubhi, Riley, et al., 2012) and, although it has not been identified in humans, N6-N6-N6-trimethyl-L-lysine was significantly decreased in a rat model of COPD (Du et al., 2023). N6-N6-N6-trimethyl-L-lysine is involved in fatty acid oxidation as a precursor of carnitine biosynthesis (Paley and Karp, 2021). Recent evidence points to metabolic programming in COPD to support a reduced capacity for beta oxidation (Michaeloudes et al., 2017) and instead a higher reliance on anabolic glycolysis (Allaire et al., 2004), which may explain this disturbance. This is supported by lower steady-state exercise RER in COPD at baseline (Latimer et al., 2021).

Secondly, there was an increase in plasma abundance of phenylalanine in COPD compared to HO. These results are consistent with previous literature which shows

elevated serum and plasma phenylalanine is associated with increased disease severity in COPD patients (Ubhi, Riley, et al., 2012; Kuo et al., 2019; Kim et al., 2022). Furthermore, elevated serum phenylalanine contributed to clustering of COPD patients away from controls (Ubhi, Riley, et al., 2012), and reduced splanchnic extraction of phenylalanine was observed in COPD patients compared to age matched healthy counterparts (Jonker et al., 2017) suggesting that dysregulation of phenylalanine metabolism is a hallmark of COPD. Phenylalanine is associated with pulmonary hypertension (Tan et al., 2020), a common side effect of COPD which is associated with shorter survival and poorer clinical outcomes (Barbera et al., 2003), which may account for differences in the plasma abundance of phenylalanine between groups.

6.4.1.2. Organooxygen compounds

Another large class of metabolites significantly different between COPD and HO at baseline was organooxygen compounds, such as 2,3-diketogulonate which increased significantly in COPD. 2,3-diketogulonate is a breakdown product of ascorbate and can act as an antioxidant compound (Dewhirst and Fry, 2018). COPD is a disease with an increased oxidative burden (Domej et al., 2014). Therefore, the rise in 2,3-diketogulonate may be a protective mechanism against systemic inflammation or chronic inflammation of the airways in COPD. Some differences in the metabolome at baseline can be attributed to xenobiotic metabolism. Although exclusion criteria were selected to control for any respiratory diagnosis or comorbidities associated with metabolic disturbances, not all individual variation can be accounted for. Finally, there were a number of disturbances in other metabolite classes, such as several species of lipids, steroids and nucleotides which all may contribute to the pathogenesis of COPD, and support roles for alternative methods of substrate oxidation which may account

for decreased oxidative capacity of skeletal muscle in COPD and contribute to the noticeable difference in response to AET, discussed in the following section.

6.4.2. Exercise induced differences in the plasma metabolome

Although there was an observable response to AET in the plasma metabolome in HO, there were no differences in the plasma metabolome over 8 weeks AET in COPD patients. Importantly, this observation parallels the lack of adaptation in VO_2^{PEAK}, steady-state exercise RER and maximal rates of mitochondrial ATP production reported in this Chapter and by Latimer et al. (2021). Due to the difficulty in ascertaining true VO_2^{PEAK} in COPD patients, a higher training workload may be required in COPD patients to elicit the same response as in healthy individuals and may be an avenue for future research. Nevertheless, the absence of a metabolic response to an AET stimulus in COPD patients parallels data from the muscle mitochondrial and whole-body levels and demonstrates the strength of metabolomics as a tool for studying physiology. In addition, possible insight into the mechanism of metabolic improvement in healthy individuals is provided through the current longitudinal analysis of the plasma metabolome in age-matched controls throughout the training period.

6.4.2.1. Lipid metabolism impacted by exercise

The majority of metabolites significantly different after 1 week of AET were lipid species. In older adults, there is an increased abundance of lipids in the resting state (Wilkinson et al., 2020) and increased deposition of intramuscular fat in muscle (Crane et al., 2010). AET affects lipid mobilisation and muscle lipid utilisation, thus here it is possible that the plasma metabolome is reflecting muscular lipid composition. These findings are also complementary to the data in Latimer et al. (2021) where it was demonstrated that the muscle mitochondrial ATP production in HO increased significantly in response to palmitate, but not to glutamate and succinate or glutamate

and malate substrate combinations. The decline in steady-state exercise RER with training also reflects increased contribution of lipids to energy production. Thus, the data in this chapter provides supportive evidence to demonstrate the importance of lipid oxidation in the adaptive response to AET and provides a possible link between whole-body and muscle specific adaptations. For instance, there were significant differences in the plasma abundance of 13-hydroxy-9-methoxy-10-oxo-11-octadecenoic acid and the glycerolipids tripalmitin (TG(16:0/16:0/16:0), phosphatidylcholine (PC) 15:0/20:0, phosphatidylethanolamine (PE) 14:1(9Z)/14:1(9Z)) and lysoPC(22:5(4Z,7Z,10Z,13Z,16Z)) following 8 weeks of AET in HO. TG(16:0/16:0/16:0) is an important mediator in the metabolism of fatty acids for energy (Wishart et al., 2022). Differences in the metabolism of PCs, PEs, and lysoPCs have all previously been reported after exercise intervention (Newsom et al., 2016; S. Lee et al., 2018; Babu et al., 2022) and a significant decrease in PE 22:0/P-18:1(11Z) was noted after AET in the HY group in Chapter 5. One role of lysoPCs is as signalling mediators for oxidative stress and inflammatory responses (Law et al., 2019). Here, a decrease in plasma abundance in lysoPC(22:5(4Z,7Z,10Z,13Z,16Z)) was observed, possibly reflecting reduced oxidative stress as a consequence of an increase in oxidative capacity. Glycerophospholipids are also abundant in mitochondrial membranes, where the ratio of glycerophospholipids is influential in dictating membrane integrity and fluidity which must be maintained for mitochondrial respiration (Grapentine and Bakovic, 2020). Thus, the observed differences in plasma abundance of glycerophospholipids may reflect a change in mitochondrial lipid ratios. Altered mitochondrial lipid ratios may in turn explain the differences in lipid oxidation between COPD and HO that could contribute to the lack of observable adaptation to AET in COPD.

In addition, there was an increase in 13-hydroxy-9-methoxy-10-oxo-11-octadecenoic acid, a metabolite of linoleic acid. Linoleic acid metabolism was significantly affected by chronic bed rest, as detailed in Chapter 3. This provides evidence to suggest that this pathway is influential in muscle adaptation to change in physical activity and may potentially reflect a common mechanism underlying skeletal muscle deconditioning.

Given the number of lipid metabolites significantly impacted by at least 1 week of AET and that mitochondrial ATP production was unaffected by fatty acid substrates in COPD patients (Latimer et al., 2021), insight into the mechanisms underlying discrepancies in adaptation to AET between COPD and HO controls may lie in lipid metabolism and oxidation pathways and this should therefore be a focus of future research.

6.4.2.2. Amino acid metabolism following exercise

There was also a rise in plasma phenylalanine level from baseline at 1 week AET. The potential benefits of phenylalanine in exercise were discussed previously in Chapter 5 and related to the promotion of fat oxidation during exercise by L-phenylalanine supplementation (Ueda et al., 2017). The observed increase in plasma phenylalanine in HO may therefore be involved in the preferential use of lipids as oxidative substrates in response to increased energetic demands as a consequence of AET. This is in line with the significant increase in mitochondrial ATP production after 8 weeks AET in response to palmitate but not to glutamate and succinate or glutamate and malate (Latimer et al., 2021). After 8 weeks AET in HO, L-phenylalanine remained significantly elevated from baseline.

6.4.2.3. Metabolites changed after exercise withdrawal

Finally, after 4 weeks of exercise withdrawal, only three metabolites remained significantly different to baseline value in HO. Phenylalanine remained elevated from

baseline, possibly indicating that the plasma metabolome maintains some of the benefits conferred by AET. This is in line with the changes in plasma abundance in HY after exercise withdrawal. However, the reduced number of significantly different metabolites after withdrawal when compared to 1 or 8 weeks of AET suggests that there is a general loss of the beneficial changes to the plasma metabolome, even during a short detraining period. No lipid metabolites were significantly different after exercise withdrawal, which is in line with mitochondrial ATP production rates which returned to baseline value in HO, even in response to palmitate (Latimer et al., 2021). It is possible that decline in lipid oxidation contributes to the loss of physiological adaptations during a detraining period.

6.4.3. Correlation of metabolite abundance with outcome measures at baseline in healthy older controls

A major strength of this study is the collection of detailed data relating to physiological outcome measures of steady-state VO_2^{PEAK} and steady-state exercise RER. Correlation of physiological measurements with metabolomics data allows for a greater insight in the possible mechanisms underlying skeletal muscle adaptations to AET without the use of muscle biopsies, as demonstrated with the similar examples in Chapters 3 and 5. Although outcome measures were collected for both COPD and HO, as no metabolites were significantly different from baseline at any timepoint during the AET intervention in COPD correlation analysis was only performed on HO.

6.4.3.1. Amino acid metabolism association with maximal oxygen uptake

At baseline, steady-state VO_2^{PEAK} was associated with arginine and proline metabolism pathways (Table 6.2). Within these pathways, L-arginine, creatine, 2-oxoglutarate, L-guanidinoacetate, L-ornithine and urea were found to be important in the association. As discussed in Chapter 5, L-ornithine may relate to a fatigue response by facilitating

the release of ammonia from skeletal muscle to promote phosphorylation (Rusip et al., 2018). L-ornithine may also promote lipid oxidation (Sugino et al., 2008), indicating metabolites most associated with whole body physiological adaptations to AET are involved in lipid oxidation, aligning with the previous findings of this chapter and with mitochondrial ATP production rates (Latimer et al., 2021). 2-oxoglutarate is a rate limiting intermediate of the TCA cycle (Araújo et al., 2014), therefore the importance of 2-oxoglutarate in the association of arginine and proline metabolism with VO_2^{PEAK} may provide a direct link between arginine and proline metabolism and oxidative metabolism pathways. Finally, several meta-analyses suggest that L-arginine supplementation may increase VO_2^{PEAK} in healthy individuals (Viribay et al., 2020; Rezaei et al., 2021). L-arginine is a precursor of nitric oxide, which can increase vessel vasodilation and flow. As VO_2^{PEAK} can be limited by locomotor muscle blood flow (Saltin and Calbet, 2006), a possible mechanism linking L-arginine and VO_2^{PEAK} is that synthesis of nitric oxide from L-arginine enhances oxygen and nutrient delivery to skeletal muscle, enabling an increase in oxygen consumption. Although these studies assess dietary supplementation of L-arginine, the present data suggests arginine metabolism may promote improvements in VO_2^{PEAK} without supplementation. In addition, as there was no difference in L-arginine in COPD at the 8-week AET timepoint, disturbances to arginine and proline metabolism pathways in COPD may help explain why the COPD group did not demonstrate an improvement in VO_2^{PEAK} following 8 weeks of AET (Latimer et al., 2021).

6.4.3.2. Metabolites associated with respiratory exchange ratio

Three pathways were significantly associated with exercise steady-state RER at baseline (Table 6.2). Plasma levels of CoA were identified as influential in forming the association between RER and fatty acid degradation and pantothenate and CoA biosynthesis pathways. CoA can be related to the synthesis and degradation of fatty

acids (Leonardi and Jackowski, 2007) and therefore this association likely also links to the increase in lipid oxidation following AET, which appears to be the primary adaptive response, although it should also be considered that this association may be influenced by dietary consumption of pantothenic acid. Additionally, glycerophospholipid metabolism was identified in modules associated with steady-state exercise RER with PE and PC identified as important within the pathway. As suggested in previous chapters of this thesis, change in glycerophospholipid metabolism may relate to the ratio of mitochondrial lipids which regulates skeletal muscle metabolism in the adaptive response to change in physical activity through influencing oxidative capacity.

The association of these three pathways with steady-state exercise RER are either in line with previous findings in this thesis or highlight pathways expected to be impacted by increased energetic demand, such as in the exercise response, which lends support to this method as an analytical approach.

6.4.4. Correlation of metabolite abundance with outcome measures after aerobic exercise training and exercise withdrawal in healthy older individuals

All four pathways associated with outcome measures at baseline in HO remained associated after 8 weeks AET (Table 6.3). The same metabolites were identified as influential in the pathway in glycerophospholipid metabolism, fatty acid degradation and pantothenate and CoA biosynthesis, however in arginine and proline metabolism only L-ornithine and creatine were identified as important, which is different than at baseline. L-ornithine can be related to the biosynthesis of creatine which may relate to increased oxidative capacity through its role in maintaining intracellular availability of ATP (Clark, 1997). The relation of arginine and proline metabolism to ATP availability is further supported by the identification of creatine as an influential metabolite. In addition, while glycerophospholipid metabolism, fatty acid degradation and

pantothenate and CoA biosynthesis all remained associated with only exercise steady-state RER, arginine and proline metabolism was associated with both RER and VO_2^{PEAK}.

6.4.4.1. Associations of metabolites with change in respiratory exchange ratio

In addition to the established associations, plasma abundance of N-acylsphingosine and sphingomyelin was influential in forming an association between sphingolipid and change in steady-state exercise RER (Table 6.3). Ceramides accumulate as a consequence of incomplete fatty acid oxidation (Koves et al., 2008) which may explain this association, as the observed decline in RER represents an increased contribution of lipids as oxidative substrates. In addition, sphingolipids and ceramides have previously been noted to increase within muscle tissue following submaximal exercise (Bergman et al., 2016; Saleem et al., 2020). The present results indicate that the plasma metabolome is reflecting intramuscular adaptations.

6.4.4.2. Associations of metabolites with change in maximal oxygen uptake

Finally, β-alanine metabolism was identified as significantly associated with change in VO_2^{PEAK} after 8 weeks AET in HO. Within this pathway, change in plasma abundance of β-alanine was identified as influential. β-Alanine can be diverted to the pantothenate and CoA biosynthesis pathway or to the malonate biosynthesis pathway (Kanehisa and Goto, 2000), both of which relate to the biosynthesis and degradation of fatty acids and may therefore relate to increase in oxidative capacity as a consequence of AET. This would highlight the interactive nature of the metabolome, which was previously seen in the associations with physiological outcome measures in HY. Alternatively, β-alanine is commonly used as a performance enhancing supplement (Hobson et al., 2012) as it is converted to carnosine within skeletal muscle which acts as a buffer for

lactic acid and reduces the fatigue effect (Artioli et al., 2010), resulting in greater endurance capacity. Improvements in VO_2^{PEAK} have been associated with improvements in endurance capacity of skeletal muscle (Bartov et al., 2009). The association between β-alanine metabolism and change in VO_2^{PEAK} may therefore relate to greater endurance capacity of skeletal muscle following exercise intervention.

6.4.4.3. Metabolites associated with measures after exercise withdrawal

After 4 weeks of exercise withdrawal, arginine and proline metabolism and β-alanine metabolism remained associated with change in VO_2^{PEAK} and glycerophospholipid metabolism remained associated with change in both VO_2^{PEAK} and steady-state exercise RER, indicating that some metabolic benefits conferred by AET are maintained throughout the detraining period (Table 6.4). However, fatty acid degradation, CoA biosynthesis and sphingolipid metabolism were no longer associated with RER or VO_2^{PEAK} which indicates that not all metabolic adaptations persist following cessation of exercise. Following a longer period of detraining, associations between arginine and proline, β-alanine and glycerophospholipid metabolism pathways with outcome measures may also be lost.

6.4.5. Comparison of metabolic adaptations in healthy older and young control groups

Fewer metabolites were significantly different following 8 weeks of AET in the older group compared to the young which suggests the exercise adaptation response is blunted with age. This aligns with previously published data at the muscle mitochondrial and whole-body level (Latimer et al., 2021). However, some elements of the exercise response appear to be unaffected by age. For instance, there were similarities in the direction of change of phosphatidylethanolamine species between older and young groups. Phenylalanine was also significantly elevated following AET in

both young and older groups. L-ornithine was involved in associations with VO_2^{PEAK} and steady-state exercise RER in both age groups, suggesting the biosynthesis of creatine occurs in the AET adaptive response regardless of age. Such common mechanisms may provide possible insight into a common mechanism of adaptation in skeletal muscle metabolism following AET.

In healthy young individuals, more metabolites remained significantly different from baseline after the withdrawal period, possibly indicating that the positive effects of AET on the metabolism are lost more quickly in older individuals which may allow for the rapid development of deconditioning with age. This is in line with a greater decline in VO_2^{PEAK} in healthy older than young individuals over the 4 week detraining period (Latimer et al., 2021), and with current literature, which shows old adults (74-86 years) had a significantly poorer performance in arm curl and 6 minute walk tests following 52 weeks of detraining after a 9 week period of strength training from their baseline scores while their 'young-old' counterparts (60-73 years) returned to baseline value (Toraman, 2005). However of the 12 pathways associated with either VO_2^{PEAK} or steady-state exercise RER after exercise withdrawal in the healthy older group 9 were previously found to be associated with the same outcome measures in healthy young, suggesting that many adaptations to detraining are unaffected by age. Notably, in both groups there was a consistent association of VO_2^{PEAK} and steady-state exercise RER with amino acid metabolism after 4 weeks of exercise withdrawal. For instance, L-tyrosine was associated with VO_2^{PEAK} following exercise withdrawal regardless of age. L-tyrosine is a popular supplement in exercise and oral consumption of a L-tyrosine supplement prior to exercise was associated with a 15% increase in exercise capacity and significantly increased time to exhaustion in healthy young men and was therefore suggested to improve endurance of skeletal muscle by increasing availability for dopamine synthesis (Tumilty et al., 2011). However, others have reported no benefit

of supplementary L-tyrosine on muscle endurance or strength (Chinevere et al., 2002; Attipoe et al., 2015). Although there is interest in understanding the impact of tyrosine as a supplement on muscle strength and mass, the current literature has not focused on assessing the impact of endogenous L-tyrosine on exercise. Here, the association of L-tyrosine with VO_2^{PEAK} regardless of age provides preliminary evidence to link L-tyrosine abundance with whole body physiological adaptations to exercise.

L-serine and betaine were associated with RER after withdrawal in both age groups. Both have previously been linked to the biosynthesis of glycine, which itself was associated with skeletal muscle adaptations to bed rest in Chapter 3 of this thesis and is an essential mediator in skeletal muscle regeneration in response to injury (Thalacker-Mercer et al., 2020) where it exerts its action by increasing the activation of mTORC1 in muscle progenitor cells (Lin et al., 2020). Whether the mechanism of action of L-serine and betaine in response to exercise withdrawal is the same as their involvement in the glycine synthesis pathway for regeneration following injury is unclear, however the association of these amino acid metabolites with physiological outcome measures regardless of age indicates a potential role for amino acids in the detraining response that may be of interest to investigate in future research.

Chapter 7. General discussion

This thesis used an untargeted metabolomics approach to characterise the plasma metabolome in four studies in order to provide insight into the metabolic pathways involved in the whole-body and skeletal muscle level adaptive responses to ageing and change in physical activity. In addition, by comparison to physiological outcomes relevant to adaptations at the muscular and whole-body level this thesis has demonstrated the potential of metabolomics in an integrative approach to studying physiological adaptation to stressors. Such an approach allows insight into specific metabolic pathways most highly associated with adaptation at a whole-body level to a specific intervention and which metabolites within those pathways are most important in the association. The integration of metabolomics and physiological data is a key strength of this thesis over much of the current literature, which often focuses on the use of metabolomics in isolation from relevant participant metadata or physiological measures.

7.1.1.1. Similarities across studies

Across the four studies discussed in this thesis, plasma levels of glycerophospholipid were consistently identified as markers of adaptation. Additionally, ceramides and other sphingolipids were consistently identified as plasma markers of adaptation. Moreover, both glycerophospholipids and sphingolipids were associated with physiological endpoint measures in Chapters 3, 5 and 6. Glycerophospholipids have essential roles as components of mitochondrial membranes (Tasseva et al., 2013) and it is suggested that ceramides can accumulate due to incomplete fatty acid oxidation (Sokolowska and Blachnio-Zabielska, 2019). Additionally in Chapter 6, no metabolites were present at a significantly different abundance following AET in the COPD group indicating a failure to adapt to stimulus provided by AET at the whole-body level in COPD patients. This parallels previous results from mitochondrial functional testing

which showed no difference in mitochondrial ATP production rates in response to palmitate substrate in COPD. Overall, the consistency in the identified metabolites and metabolic pathways which are significantly disturbed by each intervention points to the regulation of mitochondrial metabolism as a primary feature of adaptation to change in physical activity or age.

7.1.1.2. The use of plasma to reflect muscle metabolism

While the plasma metabolome reflects whole body metabolism, association of plasma metabolite abundance with physiological outcome measures provides evidence to suggest that it is possible to correlate changes in the plasma metabolome with adaptions occurring within skeletal muscle. Physiological outcome measures were not available for Chapter 4, which is a limitation to that study, however a similar association between the plasma metabolome and skeletal muscle was demonstrated by comparing putative identifications of markers of ageing in the plasma with previously identified markers of ageing in the muscle metabolome (Wilkinson et al., 2020).

7.1.1.3. Novel non-annotated metabolites

Many metabolites identified in this thesis are complementary to the current literature, however in each study a number of metabolites were unidentified, representing potential novel markers of metabolic adaptation. As advances in the metabolomics field continue and databases expand, in the future it may be possible to annotate these compounds and identify new markers of adaptation.

7.1.1.4. Future directions

The consistent identification of metabolites related to mitochondrial composition and oxidation across studies, in combination with parallels to previously published functional testing data, suggests that mitochondrial respiratory activity and

maintenance of normal mitochondrial morphology may be major contributors to whole body and skeletal muscle adaptations. Interventions to maintain mitochondrial health and respiratory function may be of benefit in combating deconditioning and loss of muscle strength and mass, either by therapeutics that target mitochondria (Singh et al., 2021) or by exercise (Sorriento et al., 2021), and may therefore be of interest to investigate further.

Additionally, similar associations between mitochondrial metabolites such as glycerophospholipids and glycerolipids with measures of increased whole body lipid oxidation in Chapters 3, 5 and 6 suggest that adaptations to sedentary behaviour and submaximal exercise may occur through similar metabolic pathways. This provides preliminary evidence to suggest a linkage between muscle mRNA expression, muscle mitochondrial function, whole body physiological adaptations, and the plasma metabolome. Both hypotheses may be tested further by determining correlations between metabolomics data, muscular mRNA expression (Shur et al., 2022) and maximal rates of muscle mitochondrial ATP production (Latimer et al., 2021).

Physiological and metabolomic data in Chapter 6 also demonstrated that adaptations to AET could not be detected in the plasma metabolome of the COPD patients, in contrast to the observable response in the metabolome of age matched healthy controls. The failure to respond at the metabolomic level mirrors previously published research at the muscle mitochondrial and whole-body levels (Latimer et al., 2021). This may in part be due to ventilatory capacities of COPD patients affecting a true calculation of VO_2^{PEAK}. Therefore, an intervention of differing exercise intensities may also be of interest in this cohort as higher intensity AET may elicit similar responses to those seen in the control groups at 65% VO_2^{PEAK}.

Finally, while AET resulted in change in the abundance of plasma metabolites in healthy individuals a 20-week RET intervention did not result in observable differences in the plasma abundance of any metabolites in either healthy young or older participants. It is possible that the type of exercise intervention has an influence on the skeletal muscle exercise response. However, while participants in both studies were healthy and of comparable ages, as both studies were conducted independently there may be variations in study protocol that limit comparisons. Plasma was collected 24 hours after AET but 72 hours after RET. To fully determine whether type of exercise has an influence on metabolic adaptations, an intervention directly comparing AET and RET in healthy young and old individuals could be carried out which ensures that time of sample collection relative to finishing exercise is identical between AET and RET groups.

7.1.1.5. Limitations

There are limitations to the studies in this thesis which must be recognised. Firstly, for each study a relatively small number of participants were recruited. Small sample sizes limit the generalisability of the findings. Large scale studies recruiting hundreds of participants are required to validate these results, particularly in relation to the identification of plasma metabolites which may act as biomarkers of COPD in Chapter 6. In addition, plasma samples for each study in this thesis were provided from biobanks. Samples were previously collected by collaborators in internal and external research groups. Therefore, while sample processing and analysis could be controlled across studies, sample collection (for example, time of collection or time until quenching) and storage prior to use in this thesis could not be controlled and may introduce variation into the results. As discussed in the Introduction of this thesis, variations in sample collection and storage procedures can have large impacts on the plasma metabolic profile (Smith et al., 2020). A limitation in current untargeted

metabolomics work is the inability to identify all detected metabolic features due to the complexity and diversity of the metabolome. The poor annotation of the metabolome relative to the genome or proteome remains a drawback to a metabolomics approach but advances are continually being made in this field to permit annotation of previously unidentified metabolites (Zamboni et al., 2015). As new technologies are continually emerging to aid in metabolite identification, future research may revisit this work to annotate metabolic features which are currently unidentified. In addition, metabolites selected as markers through untargeted metabolomics cannot be definitively identified (Salek et al., 2013) and only relative changes in abundance can be measured by an untargeted approach (Gertsman and Barshop, 2018). Markers of skeletal muscle adaptation to sedentary behaviour, ageing or exercise identified by untargeted metabolomics in this thesis should next be verified and quantified by targeted work.

Bibliography

Aarøe, J., Lindahl, T., Dumeaux, V., Sæbø, S., Tobin, D., Hagen, N., Skaane, P., Lönneborg, A., Sharma, P. and Børresen-Dale, A.-L., 2010. Gene expression profiling of peripheral blood cells for early detection of breast cancer. *Breast Cancer Research*, 12(87).

Abbondante, S., Eckel-Mahan, K.L., Ceglia, N.J., Baldi, P. and Sassone-Corsi, P., 2016. Comparative Circadian Metabolomics Reveal Differential Effects of Nutritional Challenge in the Serum and Liver. *The Journal of Biological Chemistry* [Online], 291(6), pp.2812–2828. Available from: https://doi.org/10.1074/jbc.M115.681130.

Achari, A.E. and Jain, S.K., 2017. L-cysteine supplementation increases insulin sensitivity mediated by upregulation of GSH and adiponectin in high glucose treated 3T3-L1 adipocytes. *Archives of Biochemistry and Biophysics* [Online], 630, pp.54–65. Available from: https://doi.org/10.1016/j.abb.2017.07.016.

Achten, J. and Jeukendrup, A.E., 2003. Maximal Fat Oxidation during Exercise in Trained Men. *International Journal of Sports Medicine* [Online], 24(8), pp.603–608. Available from: https://doi.org/10.1055/s-2003-43265.

Adachi, Y., Ono, N., Imaizumi, A., Muramatsu, T., Andou, T., Shimodaira, Y., Nagao, K., Kageyama, Y., Mori, M., Noguchi, Y., Hashizume, N. and Nukada, H., 2018. Plasma Amino Acid Profile in Severely Frail Elderly Patients in Japan. *International Journal of Gerontology* [Online], 12(4), pp.290–293. Available from: https://doi.org/10.1016/j.ijge.2018.03.003.

Agustsson, T., Ryden, M., Hoffstedt, J., van Harmelen, V., Dicker, A., Laurencikiene, J., Isaksson, B., Permert, J. and Arner, P., 2007. Mechanism of Increased Lipolysis in

Cancer Cachexia. *Cancer Research* [Online], 67(11), pp.5531–5538. Available from: https://doi.org/10.1158/0008-5472.CAN-06-4585.

Ahmad, K., Lee, E.J., Moon, J.S., Park, S.-Y. and Choi, I., 2018. Multifacted Interweaving Between Extracellular Matrix, Insulin Resistance, and Skeletal Muscle. *Cells* [Online], 7(148). Available from: https://doi.org/10.3390/cells7100148.

Ahmed, S., Singh, D., Khattab, S., Babineau, J. and Kumbhare, D., 2018. The Effects of Diet on the Proportion of Intramuscular Fat in Human Muscle: A Systematic Review and Meta-analysis. *Frontiers in Nutrition* [Online], 5(7). Available from: https://doi.org/10.3389/fnut.2018.00007.

Ahtiainen, J.P., Pakarinen, A., Alen, M., Kraemer, W.J. and Hakkinen, K., 2003. Muscle hypertrophy , hormonal adaptations and strength development during strength training in strength-trained and untrained men. *European Journal of Applied Physiology* [Online], 89, pp.555–563. Available from: https://doi.org/10.1007/s00421-003-0833-3.

Akima, H., Ushiyama, J., Kubo, J., Fukuoka, H., Kanehisa, H. and Fukunaga, T., 2007. Effect of unloading on muscle volume with and without resistance training. *Acta Astronautica* [Online], 60, pp.728–736. Available from: https://doi.org/10.1016/j.actaastro.2006.10.006.

Alghamdi, A., Gray, A. and Watson, D., 2019. INVESTIGATION OF METABOLOMICS TECHNIQUES BY ANALYSIS OF MS PROPOLIS DATA : WHICH PRE-TREATMENT METHOD IS BETTER ? *Advances and applications in statistics*, 58, pp.13–34.

Allaire, J., Maltais, F., Doyon, J.F., Noël, M., LeBlanc, P., Carrier, G., Simard, C. and Jobin, J., 2004. Peripheral muscle endurance and the oxidative profile of the quadriceps in patients with COPD. *Thorax* [Online], 59(8), pp.673–678. Available

from: https://doi.org/10.1136/thx.2003.020636.

Alonso, A., Marsal, S. and Julià, A., 2015. Analytical methods in untargeted metabolomics: State of the art in 2015. *Frontiers in Bioengineering and Biotechnology* [Online], 3. Available from: https://doi.org/10.3389/fbioe.2015.00023.

Alto, V., 2019. *PCA: Eigenvectors and Eigenvalues* [Online]. Available from: https://towardsdatascience.com/pca-eigenvectors-and-eigenvalues-1f968bc6777a [Accessed 9 December 2022].

Van Ancum, J.M., Alcazar, J., Meskers, C.G.M., Nielsen, B.R., Suetta, C. and Maier, A.B., 2020. Impact of using the updated EWGSOP2 definition in diagnosing sarcopenia: A clinical perspective. *Archives of Gerontology and Geriatrics* [Online], 90(May), p.104125. Available from: https://doi.org/10.1016/j.archger.2020.104125.

Andreux, P.A., van Diemen, M.P.J., Heezen, M.R., Auwerx, J., Rinsch, C., Groeneveld, G.J. and Singh, A., 2018. Mitochondrial function is impaired in the skeletal muscle of pre-frail elderly. *Scientific Reports* [Online], 8(1), p.8548. Available from: https://doi.org/10.1038/s41598-018-26944-x.

Araújo, W.L., Martins, A.O., Fernie, A.R. and Tohge, T., 2014. 2-oxoglutarate: Linking TCA cycle function with amino acid, glucosinolate, flavonoid, alkaloid, and gibberellin biosynthesis. *Frontiers in Plant Science* [Online], 5(552). Available from: https://doi.org/10.3389/fpls.2014.00552.

Arentson-Lantz, E.J., English, K.L., Paddon-Jones, D. and Fry, C.S., 2016. Fourteen days of bed rest induces a decline in satellite cell content and robust atrophy of skeletal muscle fibers in middle-aged adults. *Journal of Applied Physiology* [Online], 120(8), pp.965–975. Available from:

https://doi.org/10.1152/japplphysiol.00799.2015.

Argilés, J.M., Campos, N., Lopez-Pedrosa, J.M., Rueda, R. and Rodriguez-Mañas, L., 2016. Skeletal Muscle Regulates Metabolism via Interorgan Crosstalk: Roles in Health and Disease. *Journal of the American Medical Directors Association* [Online], 17(9), pp.789–796. Available from: https://doi.org/10.1016/j.jamda.2016.04.019.

Arthur, S.T., Noone, J.M., Van Doren, B.A., Roy, D. and Blanchette, C.M., 2014. One-year prevalence, comorbidities and cost of cachexia-related inpatient admissions in the USA. *Drugs In Context* [Online], 3(212265). Available from: https://doi.org/10.7573/dic.212265.

Artioli, G.G., Gualano, B., Smith, A., Stout, J. and Lancha, A.H., 2010. Role of β-Alanine Supplementation on Muscle Carnosine and Exercise Performance. *Medicine and Science in Sports and Exercise* [Online], 42(6), pp.1162–1173. Available from: https://doi.org/10.1249/MSS.0b013e3181c74e38.

Ascenzo, D., Ascenzo, N.D., Antonecchia, E., Angiolillo, A., Bender, V., Camerlenghi, M., Xie, Q. and Costanzo, A. Di, 2022. Metabolomics of blood reveals age-dependent pathways in Parkinson's Disease. *Cell & Bioscience* [Online], 12(102). Available from: https://doi.org/10.1186/s13578-022-00831-5.

Atherton, P.J., Etheridge, T., Watt, P.W., Wilkinson, D., Selby, A., Rankin, D., Smith, K. and Rennie, M.J., 2010. Muscle full effect after oral protein: time-dependent concordance and discordance between human muscle protein synthesis and mTORC1 signaling. *The American Journal of Clinical Nutrition* [Online], 92(5), pp.1080–1088. Available from: https://doi.org/10.3945/ajcn.2010.29819.1.

Atherton, P.J., Greenhaff, P.L., Phillips, S.M., Bodine, S.C., Adams, C.M. and Lang, C.H.,

2016. Control of skeletal muscle atrophy in response to disuse: Clinical/preclinical contentions and fallacies of evidence. *American Journal of Physiology - Endocrinology and Metabolism* [Online], 311(3), pp.E594–E604. Available from: https://doi.org/10.1152/ajpendo.00257.2016.

Atherton, P.J. and Smith, K., 2012. Muscle protein synthesis in response to nutrition and exercise. *Journal of Physiology* [Online], 590(5), pp.1049–1057. Available from: https://doi.org/10.1113/jphysiol.2011.225003.

Attaway, A., Bellar, A., Dieye, F., Wajda, D., Welch, N. and Dasarathy, S., 2021. Clinical impact of compound sarcopenia in hospitalized older adult patients with heart failure. *Journal of the American Geriatrics Society* [Online], pp.1–11. Available from: https://doi.org/https://doi.org/10.1111/jgs.17108.

Attipoe, S., Zeno, S.A., Lee, C., Crawford, C., Khorsan, R., Walter, A.R. and Deuster, P.A., 2015. Tyrosine for Mitigating Stress and Enhancing Performance in Healthy Adult Humans, a Rapid Evidence Assessment of the Literature. *Military Medicine* [Online], 180(7), pp.754–765. Available from: https://doi.org/10.7205/MILMED-D-14-00594.

Aversa, Z., Costelli, P. and Muscaritoli, M., 2017. Cancer-induced muscle wasting : latest findings in prevention and treatment. *Therapeutic Advances in Medical Oncology* [Online], 9(5), pp.369–382. Available from: https://doi.org/10.1177/1758834017698643.

Babu, A.F., Csader, S., Männistö, V., Tauriainen, M.M., Pentikäinen, H., Savonen, K., Klåvus, A., Koistinen, V., Hanhineva, K. and Schwab, U., 2022. Effects of exercise on NAFLD using non-targeted metabolomics in adipose tissue , plasma , urine , and stool. *Scientific Reports* [Online], 12(6485). Available from:

https://doi.org/10.1038/s41598-022-10481-9.

Bai, X. and Jiang, Y., 2010. Key factors in mTOR regulation. *Cellular and Molecular Life Sciences* [Online], 67(2), pp.239–253. Available from: https://doi.org/10.1007/s00018-009-0163-7.Key.

Ballatori, N., Krance, S.M., Notenboom, S., Shi, S., Tieu, K. and Hammond, C.L., 2009. Glutathione dysregulation and the etiology and progression of human diseases. *Biological Chemistry* [Online], 390(March), pp.191–214. Available from: https://doi.org/10.1515/BC.2009.033.

Banerjee, P., Ghosh, S., Dutta, M., Subramani, E., Khalpada, J., Choudhury, S.R., Chakravarty, B. and Chaudhury, K., 2013. Identification of key contributory factors responsible for vascular dysfunction in idiopathic recurrent spontaneous miscarriage. *PLoS ONE* [Online], 8(11). Available from: https://doi.org/10.1371/journal.pone.0080940.

Banerjee, S. and Mazumdar, S., 2012. Electrospray Ionization Mass Spectrometry: A Technique to Access the Information beyond the Molecular Weight of the Analyte. *International Journal of Analytical Chemistry* [Online], 2012(282574). Available from: https://doi.org/10.1155/2012/282574.

Baranzini, S.E., Mudge, J., van Velkinburgh, J.C., Khankhanian, P., Khrebtukova, I., Miller, N.A., Zhang, L., Farmer, A.D., Bell, C.J., Kim, R.W., May, G.D., Woodward, J.E., Caillier, S.J., McElroy, J.P., Gomez, R., Pando, M.J., Clendenen, L.E., Ganusova, E.E., Schilkey, F.D., Ramaraj, T., Khan, O.A., Huntley, J.J., Luo, S., Kwok, P., Wu, T.D., Schroth, G.P., Oksenberg, J.R., Hauser, S.L. and Kingsmore, S.F., 2010. Genome, epigenome and RNA sequences of monozygotic twins discordant for multiple sclerosis. *Nature* [Online], 464(7293), pp.1351–1356. Available from:

https://doi.org/10.1038/nature08990.

Barbera, J.., Peinado, V.. and Santos, S., 2003. Pulmonary hypertension in chronic obstructive pulmonary disease. *European Respiratory Journal* [Online], 21, pp.892–905. Available from: https://doi.org/10.1183/09031936.03.00115402.

Barker, M. and Rayens, W., 2003. Partial least squares for discrimination. *Journal of Chemometrics* [Online], 17(3), pp.166–173. Available from: https://doi.org/10.1002/cem.785.

Bartel, J., Krumsiek, J., Schramm, K., Adamski, J., Gieger, C., Herder, C., Carstensen, M., Peters, A., Rathmann, W., Roden, M., Strauch, K., Suhre, K., Kastenmüller, G., Prokisch, H. and Theis, F.J., 2015. The Human Blood Metabolome-Transcriptome Interface. *PLoS Genetics* [Online], 11(6). Available from: https://doi.org/10.1371/journal.pgen.1005274.

Bartel, J., Krumsiek, J. and Theis, F.J., 2013. Statistical methods for the analysis of high-throughput metabolomics data. *Computational and Structural Biotechnology Journal* [Online], 4(5). Available from: https://doi.org/10.5936/csbj.201301009.

Bartle, K.D. and Myers, P., 2002. History of gas chromatography. *Trends in Analytical Chemistry*, 21(2), pp.547–557.

Bartov, D.N., Murthy, S., Kamalakkannan, G., Smith, Q., Shin, J.., Galvao, M., Burkhoff, D. and Maybaum, S., 2009. Relationship between Skeletal Muscle Function, Peak Oxygen Consumption and Cardiac Output in Patients with Chronic Heart Failure. *The Journal of Heart and Lung Transplantation* [Online], 28(2), pp.S94–S95. Available from: https://doi.org/10.1016/j.healun.2008.11.761.

Beger, R.D., Dunn, W.B., Bandukwala, A., Bethan, B., Broadhurst, D., Clish, C.B., Dasari, S., Derr, L., Evans, A., Fischer, S., Flynn, T., Hartung, T., Herrington, D., Higashi, R.,

Hsu, P.-C., Jones, C., Kachman, M., Karuso, H., Kruppa, G., Lippa, K., Maruvada, P., Mosley, J., Ntai, I., O'Donovan, C., Playdon, M., Raftery, D., Shaughnessy, D., Souza, A., Spaeder, T., Spalholz, B., Tayyari, F., Ubhi, B., Verma, M., Walk, T., Wilson, I., Witkin, K., Bearden, D.W. and Zanetti, K.A., 2019. Towards quality assurance and quality control in untargeted metabolomics studies. *Metabolomics* [Online], 15(1), p.4. Available from: https://doi.org/10.1007/s11306-018-1460-7.Submit.

Benjamini, Y. and Hochberg, Y., 1995. Controlling the False Discovery Rate : A Practical and Powerful Approach to Multiple Testing. *Journal of the Royal Statistical Society. Series B (Methodological)*, 57(1), pp.289–300.

Berdeaux, R. and Stewart, R., 2012. cAMP signaling in skeletal muscle adaptation: hypertrophy, metabolism , and regeneration. *American Journal of Physiology - Endocrinology and Metabolism* [Online], 303, pp.E1–E17. Available from: https://doi.org/10.1152/ajpendo.00555.2011.

van den Berg, R.A., Hoefsloot, H.C.J., Westerhuis, J.A., Smilde, A.K. and van der Werf, M.J., 2006. Centering, scaling, and transformations: Improving the biological information content of metabolomics data. *BMC Genomics* [Online], 7(142). Available from: https://doi.org/10.1186/1471-2164-7-142.

Berge, R.K., Skorve, J., Tronstad, K.J., Berge, K., Gudbrandsen, O.A. and Grav, H., 2002. Metabolic effects of thia fatty acids. *Current Opinion in Lipidology*, 13(3), pp.295–304.

Bergman, B.C., Brozinick, J.T., Strauss, A., Bacon, S., Kerege, A., Bui, H.H., Sanders, P., Siddall, P., Wei, T., Thomas, M.K., Kuo, M.S. and Perreault, L., 2016. Muscle sphingolipids during rest and exercise: a C18:0 signature for insulin resistance in

humans. *Diabetelogia* [Online], 59, pp.785–798. Available from: https://doi.org/10.1007/s00125-015-3850-y.

Bergouignan, A., Trudel, G., Simon, C., Chopard, A., Schoeller, D.A., Momken, I., Votruba, S.B., Desage, M., Burdge, G.C., Gauquelin-Koch, G., Normand, S. and Blanc, S., 2009. Physical inactivity differentially alters dietary oleate and palmitate trafficking. *Diabetes* [Online], 58(2), pp.367–376. Available from: https://doi.org/10.2337/db08-0263.

Berria, R., Wang, L., Richardson, D.K., Finlayson, J., Belfort, R., Pratipanawatr, T., De Filippis, E.A., Kashyap, S. and Mandarino, L.J., 2006. Increased collagen content in insulin-resistant skeletal muscle. *American Journal of Physiology - Endocrinology and Metabolism* [Online], 290, pp.E560–E565. Available from: https://doi.org/10.1152/ajpendo.00202.2005.

Berry, M.J., Sheilds, K.L. and Adair, N.E., 2018. Comparison of Effects of Endurance and Strength Training Programs in Patients with COPD. *COPD* [Online], 15(2), pp.192–199. Available from: https://doi.org/10.1080/15412555.2018.1446926.Comparison.

Berton, R., Conceição, M.S., Libardi, C.A., Canevarolo, R.R., Gáspari, A.F., Chacon-Mikahil, M.P.T., Zeri, A.C. and Cavaglieri, C.R., 2016. Metabolic time-course response after resistance exercise: A metabolomics approach. *Journal of Sports Sciences* [Online], 35(12), pp.1211–1218. Available from: https://doi.org/10.1080/02640414.2016.1218035.

Bevilacqua, M. and Bro, R., 2020. Can we trust score plots? *Metabolites* [Online], 10(7). Available from: https://doi.org/10.3390/metabo10070278.

Bhasin, S., 2021. Testosterone replacement in aging men: An evidence-based patient-

centric perspective. *Journal of Clinical Investigation* [Online], 131(4). Available from: https://doi.org/10.1172/JCI146607.

Bhatheja, R. and Bhatt, D.L., 2006. Clinical Outcomes in Metabolic Syndrome. *Journal of Cardiovascular Nursing*, 21(4), pp.298–305.

Bieler, T., Kristensen, A.L.R., Nyberg, M., Magnusson, S.P., Kjaer, M. and Beyer, N., 2022. Exercise in patients with hip osteoarthritis – effects on muscle and functional performance: A randomized trial. *Physiotherapy Theory and Practice* [Online], 38(12), pp.1946–1957. Available from: https://doi.org/10.1080/09593985.2021.1923096.

Bijlsma, A.Y., Meskers, C.G.M., Ling, C.H.Y., Narici, M., Kurrle, S.E., Cameron, I.D., Westendorp, R.G.J. and Maier, A.B., 2013. Defining sarcopenia: The impact of different diagnostic criteria on the prevalence of sarcopenia in a large middle aged cohort. *Age* [Online], 35(3), pp.871–881. Available from: https://doi.org/10.1007/s11357-012-9384-z.

Bijlsma, S., Bobeldijk, I., Verheij, E.R., Ramaker, R., Kochhar, S., Macdonald, I.A., Van Ommen, B. and Smilde, A.K., 2006. Large-scale human metabolomics studies: A strategy for data (pre-) processing and validation. *Analytical Chemistry* [Online], 78(2), pp.567–574. Available from: https://doi.org/10.1021/ac051495j.

Bikman, B.T. and Summers, S.A., 2011. Ceramides as modulators of cellular and whole-body metabolism. *The Journal of Clinical Investigation* [Online], 121(11), pp.4222–4230. Available from: https://doi.org/10.1172/JCI57144.4222.

Biolo, G., Ciocchi, B., Lebenstedt, M., Barazzoni, R., Zanetti, M., Platen, P., Heer, M. and Guarnieri, G., 2004. Short-term bed rest impairs amino acid-induced protein anabolism in humans. *Journal of Physiology* [Online], 558(2), pp.381–388.

Available from: https://doi.org/10.1113/jphysiol.2004.066365.

Bland, K.A., Kouw, I.W.K., van Loon, L.J.C., Zopf, E.M. and Fairman, C.M., 2022. Exercise-Based Interventions to Counteract Skeletal Muscle Mass Loss in People with Cancer: Can We Overcome the Odds? *Sports Medicine* [Online], 52(5), pp.1009–1027. Available from: https://doi.org/10.1007/s40279-021-01638-z.

Blomqvist, B.I., Hammarqvist, F., von der Decken, A. and Wernerman, J., 1995. Glutamine and alpha-Ketoglutarate Prevent the Decrease in Muscle Free Glutamine Concentration and Influence Protein Synthesis After Total Hip Replacement. *Metabolism*, 44(9), pp.1215–1222.

Boccard, J., Veuthey, J.-L. and Rudaz, S., 2010. Knowledge discovery in metabolomics : An overview of MS data handling. *Journal of Sepa* [Online], 33(3), pp.290–304. Available from: https://doi.org/10.1002/jssc.200900609.

Bock, K.W. and Kohle, C., 2005. UDP-Glucuronosyltransferase 1A6 : Structural, Functional, and Regulatory Aspects. *Methods in Enzymology* [Online], 400(05), pp.57–75. Available from: https://doi.org/10.1016/S0076-6879(05)00004-2.

Boehm, I., Miller, J., Wishart, T.M., Wigmore, S.J., Skipworth, R.J.E., Jones, R.A. and Gillingwater, T.H., 2020. Neuromuscular junctions are stable in patients with cancer cachexia. *The Journal of Clinical Investigation* [Online], 130(3), pp.1461–1465. Available from: https://doi.org/10.1172/JCI128411.

Bollen, S.E., Bass, J.J., Fujita, S., Wilkinson, D., Hewison, M. and Atherton, P.J., 2022. The Vitamin D/Vitamin D receptor (VDR) axis in muscle atrophy and sarcopenia. *Cellular Signalling* [Online], 96(4), p.110355. Available from: https://doi.org/10.1016/j.cellsig.2022.110355.

Bolstad, B.., Irizarry, R.., Astrand, M. and Speed, T.., 2003. A comparison of

normalization methods for high density oligonucleotide array data based on variance and bias. *Bioinformatics*, 19(2), pp.185–193.

ter Borg, S., Luiking, Y.C., van Helvoort, A., Boirie, Y., Schols, J.M.G.A. and de Groot, C.P.G.M., 2019. Low Levels of Branched Chain Amino Acids, Eicosapentaenoic Acid and Micronutrients are Associated with Low Muscle Mass, Strength and Function in Community-Dwelling Older Adults. *Journal of Nutrition, Health and Aging* [Online], 23(1), pp.27–34. Available from: https://doi.org/10.1007/s12603-018-1108-3.

Borges, E.M., 2015. Silica, Hybrid Silica, Hydride Silica and Non-Silica Stationary Phases for Liquid Chromatography. *Journal of Chromatographic Science*, 53(4), pp.580–597.

Borges, R.M., Colby, S.M., Das, S., Edison, A.S., Fiehn, O., Kind, T., Lee, J., Merrill, A.T., Merz, K.M., Metz Jr, T.O., Nunez, J.R., Tantillo, D.J., Wang, L.-P., Wang, S. and Renslow, R.S., 2020. Quantum Chemistry Calculations for Metabolomics Focus Review. *Chemical Reviews* [Online], 121(10), pp.5633–5670. Available from: https://doi.org/10.1021/acs.chemrev.0c00901.

Bowden Davies, K.A., Pickles, S., Sprung, V.S., Kemp, G.J., Alam, U., Moore, D.R., Tahrani, A.A. and Cuthbertson, D.J., 2019. Reduced physical activity in young and older adults: metabolic and musculoskeletal implications. *Therapeutic Advances in Endocrinology and Metabolism* [Online], 10(2042018819888824). Available from: https://doi.org/10.1177/2042018819888824.

Brady, K., Brown, J.W. and Thurmond, J.B., 1980. Behavioral and Neurochemical Effects of Dietary Tyrosine in Young and Aged Mice Following Cold-Swim Stress. *Pharmacology Biochemistry & Behaviour*, 12, pp.667–674.

de Brandt, J., Spruit, M.A., Hansen, D., Franssen, F.M.E., Derave, W., Sillen, M.J.H. and Burtin, C., 2018. Changes in lower limb muscle function and muscle mass following exercise-based interventions in patients with chronic obstructive pulmonary disease: A review of the English-language literature. *Chronic Respiratory Disease* [Online], 15(2), pp.182–219. Available from: https://doi.org/10.1177/1479972317709642.

Brennan, A.M., Benson, M., Morningstar, J., Herzig, M., Robbins, J., Gerszten, R.E. and Ross, R., 2018. Plasma Metabolite Profiles in Response to Chronic Exercise. *Medicine and Science in Sports and Exercise* [Online], 50(7), pp.1480–1486. Available from: https://doi.org/10.1249/MSS.0000000000001594.

Brereton, R.G. and Lloyd, G.R., 2014. Partial least squares discriminant analysis: taking the magic away. *Journal of Chemometrics* [Online], 28, pp.213–225. Available from: https://doi.org/10.1002/cem.2609.

Broadhurst, D., Goodacre, R., Reinke, S.N., Kuligowski, J., Wilson, I.D., Lewis, M.R. and Dunn, W.B., 2018. Guidelines and considerations for the use of system suitability and quality control samples in mass spectrometry assays applied in untargeted clinical metabolomic studies. *Metabolomics* [Online], 14(72). Available from: https://doi.org/https://doi.org/1007/s11306-018-1367-3.

Broadhurst, D.I. and Kell, D.B., 2006. Statistical strategies for avoiding false discoveries in metabolomics and related experiments. *Metabolomics* [Online], 2(4), pp.171–196. Available from: https://doi.org/10.1007/s11306-006-0037-z.

Brook, M.S., Wilkinson, D.J., Mitchell, W.K., Lund, J.N., Phillips, B.E., Szewczyk, N.J., Greenhaff, P.L., Smith, K. and Atherton, P.J., 2016. Synchronous deficits in cumulative muscle protein synthesis and ribosomal biogenesis underlie age-

related anabolic resistance to exercise in humans. *The Journal of Physiology* [Online], 594(24), pp.7399–7417. Available from: https://doi.org/10.1113/JP272857.

Brook, M.S., Wilkinson, D.J., Mitchell, W.K., Lund, J.N., Szewczyk, N.J., Greenhaff, P.L., Smith, K. and Atherton, P.J., 2015. Skeletal muscle hypertrophy adaptations predominate in the early stages of resistance exercise training, matching deuterium oxide-derived measures of muscle protein synthesis and mechanistic target of rapamycin complex 1 signaling. *FASEB Journal* [Online], 29(11), pp.4485–4496. Available from: https://doi.org/10.1096/fj.15-273755.

Broskey, N.T., Obanda, D.N., Burton, J.J., Cefalu, W.I. and Ravussin, E., 2018. Skeletal Muscle Ceramides and Daily Fat Oxidation in Obesity and Diabetes. *Metabolism* [Online], 82, pp.118–123. Available from: https://doi.org/10.1016/j.metabol.2017.12.012.Skeletal.

Brown, J.L., Rosa-Caldwell, M.E., Lee, D.E., Blackwell, T.A., Brown, L.A., Perry, R.A., Haynie, W.S., Hardee, J.P., Carson, J.A., Wiggs, M.P., Washington, T.A. and Greene, N.P., 2017. Mitochondrial degeneration precedes the development of muscle atrophy in progression of cancer cachexia in tumour-bearing mice. *Journal of Cachexia, Sarcopenia and Muscle* [Online], 8(6), pp.926–938. Available from: https://doi.org/10.1002/jcsm.12232.

Brown, M. and Hasser, E.M., 1996. Complexity of Age-Related Change in Skeletal Muscle. *Journal of Gerontology*, 51(2), pp.117–123.

Brun, J.., Guintrand-Hugret, R., Boegner, C., Bouix, O. and Orsetti, A., 1995. Influence of short-term submaximal exercise on parameters of glucose assimilation analyzed with the minimal model. *Metabolism*, 44(7), pp.833–840.

Bujak, R., Struck-Lewicka, W., Markuszewski, M.J. and Kaliszan, R., 2015. Metabolomics for laboratory diagnostics. *Journal of Pharmaceutical and Biomedical Analysis* [Online], 113, pp.108–120. Available from: https://doi.org/10.1016/j.jpba.2014.12.017.

Burd, N.A., Tang, J.E., Moore, D.R. and Phillips, S.M., 2009. Exercise training and protein metabolism: Influences of contraction, protein intake, and sex-based differences. *Journal of Applied Physiology* [Online], 106(5), pp.1692–1701. Available from: https://doi.org/10.1152/japplphysiol.91351.2008.

Büscher, J.M., Czernik, D., Ewald, J.C., Sauer, U. and Zamboni, N., 2009. Cross-Platform Comparison of Methods for Quantitative Metabolomics of Primary Metabolism. *Analytical Chemistry*, 81(6), pp.2134–2143.

Buszewski, B. and Noga, S., 2012. Hydrophilic interaction liquid chromatography (HILIC)--a powerful separation technique. *Analytical and Bioanalytical Chemistry* [Online], 402(1), pp.231–47. Available from: https://doi.org/10.1007/s00216-011-5308-5.

Button, K.S., Ioannidis, J.P.A., Mokrysz, C., Nosek, B.A., Flint, J., Robinson, E.S.J. and Munafò, M.R., 2013. Power failure: Why small sample size undermines the reliability of neuroscience. *Nature Reviews Neuroscience* [Online], 14(5), pp.365–376. Available from: https://doi.org/10.1038/nrn3475.

Bweir, S., Al-jarrah, M., Almalty, A., Maayah, M., Smirnova, I. V, Novikova, L. and Stehno-, L., 2009. Resistance exercise training lowers HbA1c more than aerobic training in adults with type 2 diabetes. *Diabetology & Metabolic Syndrome* [Online], 1(27). Available from: https://doi.org/10.1186/1758-5996-1-27.

Cala, M.P., Agulló-Ortuño, M.T., Prieto-García, E., González-Riano, C., Parrilla-Rubio,

L., Barbas, C., Díaz-García, C.V., García, A., Pernaut, C., Adeva, J., Riesco, M.C., Rupérez, F.J. and Lopez-Martin, J.A., 2018. Multiplatform plasma fingerprinting in cancer cachexia: a pilot observational and translational study. *Journal of Cachexia, Sarcopenia and Muscle* [Online], 9(2), pp.348–357. Available from: https://doi.org/10.1002/jcsm.12270.

Calvani, R., Picca, A., Marini, F., Biancolillo, A., Gervasoni, J., Persichilli, S., Primiano, A., Bossola, M., Urbani, A., Landi, F., Bernabei, R. and Marzetti, E., 2018. A Distinct Pattern of Circulating Amino Acids Characterizes Older Persons with Physical Frailty and Sarcopenia: Results from the BIOSPHERE Study. *Nutrients* [Online], 10(11), p.1691. Available from: https://doi.org/10.3390/nu10111691.

Cambiaghi, A., Ferrario, M. and Masseroli, M., 2017. Analysis of metabolomic data: Tools, current strategies and future challenges for omics data integration. *Briefings in Bioinformatics* [Online], 18(3), pp.498–510. Available from: https://doi.org/10.1093/bib/bbw031.

Canzler, S. and Hackermüller, J., 2020. multiGSEA: a GSEA-based pathway enrichment analysis for multi-omics data. *BMC Bioinformatics* [Online], 21(561). Available from: https://doi.org/10.1186/s12859-020-03910-x.

Cao, D., Wu, G., Yang, Z., Zhang, B., Jiang, Y., Han, Y., He, G., Zhuang, Q., Wang, Y., Huang, Z. and Xi, Q., 2010. Role of b 1-adrenoceptor in increased lipolysis in cancer cachexia. *Cancer Science* [Online], 101(7), pp.1639–1645. Available from: https://doi.org/10.1111/j.1349-7006.2010.01582.x.

Le Cao, K.-A., Rohart, F., Gonzalez, I. and Dejean, S., 2016. *mixOmics: Omics Data Integration Project. R package version 6.1.1* [Online]. Available from: https://cran.r-project.org/package=mixOmics.

Carbone, J.W. and Pasiakos, S.M., 2019. Dietary protein and muscle mass: Translating science to application and health benefit. *Nutrients* [Online], 11(5), p.1136. Available from: https://doi.org/10.3390/nu11051136.

Carter, R.N. and Morton, N.M., 2016. Cysteine and hydrogen sulphide in the regulation of metabolism: insights from genetics and pharmacology. *Journal of Pathology* [Online], 238, pp.321–332. Available from: https://doi.org/10.1002/path.4659.

Carter, S.L., Rennie, C. and Tarnopolsky, M.A., 2001. Substrate utilization during endurance exercise in men and women after endurance training. *American Journal of Physiology - Endocrinology and Metabolism* [Online], 280(6 43-6), pp.898–907. Available from: https://doi.org/10.1152/ajpendo.2001.280.6.e898.

Castro Conde, I. and de Una Alvarez, J., 2020. sgof: Multiple Hypothesis Testing. R package version 2.3.2 [Online]. Available from: https://cran.r-project.org/package=sgof.

de Castro, G.S., Simoes, E., Lima, J.D.C.C., Ortiz-Silva, M., Festuccia, W.T., Tokeshi, F., Alcântara, P.S., Otoch, J.P., Coletti, D. and Seelaender, M., 2019. Human cachexia induces changes in mitochondria, autophagy and apoptosis in the skeletal muscle. *Cancers*, 11(1264).

Chakraborty, N., Waning, D.L., Gautam, A., Hoke, A., Sowe, B., Youssef, D., Butler, S., Savaglio, M., Childress, P.J., Kumar, R., Moyler, C., Dimitrov, G., Kacena, M.A. and Hammamieh, R., 2020. Gene-Metabolite Network Linked to Inhibited Bioenergetics in Association With Spaceflight-Induced Loss of Male Mouse Quadriceps Muscle. *Journal of Bone and Mineral Research* [Online], 35(10), pp.2049–2057. Available from: https://doi.org/10.1002/jbmr.4102.

Chandran, S., Guo, T., Tolliver, T., Chen, W., Murphy, D.L. and Mcpherron, A.C., 2012.

Effects of serotonin on skeletal muscle growth. *BMC Proceedings* [Online], 6(Suppl 3), pp.2–3. Available from: https://doi.org/10.1186/1753-6561-6-S3-O3.

Chaneton, B., Hillmann, P., Zheng, L., Martin, A.C.., Maddocks, O.D.., Chokkathukalam, A., Coyle, J.E., Jankevics, A., Holding, F.P., Vousden, K.H., Frezza, C., O'Reilly, M. and Gottlieb, E., 2012. Serine is a natural ligand and allosteric activator of pyruvate kinase M2 `. *Nature* [Online], 491, pp.458–462. Available from: https://doi.org/10.1038/nature11540.

Chen, L.K., Liu, L.K., Woo, J., Assantachai, P., Auyeung, T.W., Bahyah, K.S., Chou, M.Y., Chen, L.Y., Hsu, P.S., Krairit, O., Lee, J.S.W., Lee, W.J., Lee, Y., Liang, C.K., Limpawattana, P., Lin, C.S., Peng, L.N., Satake, S., Suzuki, T., Won, C.W., Wu, C.H., Wu, S.N., Zhang, T., Zeng, P., Akishita, M. and Arai, H., 2014. Sarcopenia in Asia: Consensus report of the Asian working group for sarcopenia. *Journal of the American Medical Directors Association* [Online], 15(2), pp.95–101. Available from: https://doi.org/10.1016/j.jamda.2013.11.025.

Chen, P., Yu, Y., Tan, C., Liu, H., Wu, F., Li, H., Huang, J., Dong, H., Wan, Y., Chen, X. and Chen, B., 2016. Human metabolic responses to microgravity simulated in a 45-day 6° head-down tilt bed rest (HDBR) experiment. *Analytical Methods* [Online], 8(22), pp.4334–4344. Available from: https://doi.org/10.1039/c6ay00644b.

Chen, Sanmei, Akter, S., Kuwahara, K., Matsushita, Y., Nakagawa, T., Konishi, M., Honda, T., Yamamoto, S., Hayashi, T., Noda, M. and Mizoue, T., 2019. Serum amino acid profiles and risk of type 2 diabetes among Japanese adults in the Hitachi Health Study. *Scientific Reports* [Online], 9(7010). Available from: https://doi.org/10.1038/s41598-019-43431-z.

Chen, Shuyang, Han, C., Miao, X., Li, X., Yin, C., Zou, J., Liu, M., Li, S., Stawski, L., Zhu,

B., Shi, Q., Xu, Z., Li, C., Goding, C.R., Zhou, J. and Cui, R., 2019. Targeting MC1R depalmitoylation to prevent melanomagenesis in redheads. *Nature Communications* [Online], 10(877). Available from: https://doi.org/10.1038/s41467-019-08691-3.

Chen, T., Cao, Y., Zhang, Y., Liu, J., Bao, Y., Wang, C., Jia, W. and Zhao, A., 2013. Random forest in clinical metabolomics for phenotypic discrimination and biomarker selection. *Evidence-based Complementary and Alternative Medicine* [Online], (298183). Available from: https://doi.org/10.1155/2013/298183.

Chen, Y., Xu, J., Zhang, R. and Abliz, Z., 2016. Methods used to increase the comprehensive coverage of urinary and plasma metabolomes by MS. *Bioanalysis* [Online], 8. Available from: https://doi.org/10.4155/bio-2015-0010.

Chen, Yun, Wang, N., Dong, X., Zhu, J., Chen, Yue, Jiang, Q. and Fu, C., 2021. Associations between serum amino acids and incident type 2 diabetes in Chinese rural adults. *Nutrition, Metabolism and Cardiovascular Diseases* [Online], 31(8), pp.2416–2425. Available from: https://doi.org/10.1016/j.numecd.2021.05.004.

Cheng, S., Rhee, E.P., Larson, M.G., Lewis, G.D., Mccabe, E.L., Shen, D., Palma, M.J., Roberts, L.D., Dejam, A., Souza, A.L., Deik, A.A., Magnusson, M., Fox, C.S., Donnell, C.J.O., Vasan, R.S., Melander, O., Clish, C.B., Gerszten, R.E. and Wang, T.J., 2012. Metabolic Risk in Humans. *Circulation* [Online], 125(18), pp.2222–2231. Available from: https://doi.org/10.1161/CIRCULATIONAHA.111.067827.

Chetwynd, A.J., Dunn, W.B. and Rodriguez-Blanco, G., 2017. Collection and Preparation of Clinical Samples for Metabolomics. *Metabolomics: From Fundamentals to Clinical Applications*, [Online]. pp.19–44. Available from: https://doi.org/10.1007/978-3-319-47656-8.

Chinevere, T.D., Sawyer, R.D., Creer, A.R., Conlee, R.K. and Parcell, A.C., 2002. Effects of L-tyrosine and carbohydrate ingestion on endurance exercise performance. *Journal of Applied Physiology* [Online], 93(5), pp.1590–1597. Available from: https://doi.org/10.1152/japplphysiol.00625.2001.

Chini, E.N., Chini, C.C.S. and Tarrag, M.G., 2017. Molecular and Cellular Endocrinology NAD and the aging process : Role in life , death and everything in between. *Molecular and Cellular Endocrinology* [Online], 455, pp.62–74. Available from: https://doi.org/10.1016/j.mce.2016.11.003.

Chodzko-Zajko, W.J., Proctor, D.N., Fiatarone Singh, M.A., Minson, C.T., Nigg, C.R., Salem, G.J. and Skinner, J.S., 2009. Exercise and Physical Activity for Older Adults. *Medicine and Science in Sports and Exercise* [Online], 41(7), pp.1510–1530. Available from: https://doi.org/10.1249/MSS.0b013e3181a0c95c.

Choi, S.J., Files, D.C., Zhang, T., Wang, Z.M., Messi, M.L., Gregory, H., Stone, J., Lyles, M.F., Dhar, S., Marsh, A.P., Nicklas, B.J. and Delbono, O., 2016. Intramyocellular lipid and impaired myofiber contraction in normal weight and obese older adults. *Journals of Gerontology - Series A Biological Sciences and Medical Sciences* [Online], 71(4), pp.557–564. Available from: https://doi.org/10.1093/gerona/glv169.

Chopard, A., Hillock, S. and Jasmin, B.J., 2009. Molecular events and signalling pathways involved in skeletal muscle disuse-induced atrophy and the impact of countermeasures. *Journal of Cellular and Molecular Medicine* [Online], 13(9), pp.3032–3050. Available from: https://doi.org/10.1111/j.1582-4934.2009.00864.x.

Chow, W.Y., Bihan, D., Forman, C.J., Slatter, D.A., Reid, D.G., Wales, D.J., Farndale, R.W.

and Duer, M.J., 2015. Hydroxyproline Ring Pucker Causes Frustration of Helix Parameters in the Collagen Triple Helix. *Nature Publishing Group* [Online], 5(12556). Available from: https://doi.org/10.1038/srep12556.

Christie, A. and Kamen, G., 2006. Doublet discharges in motoneurons of young and older adults. *Journal of Neurophysiology* [Online], 95(5), pp.2787–2795. Available from: https://doi.org/10.1152/jn.00685.2005.

Chu, C., Tsuprykov, O., Chen, X., Elitok, S., Krämer, B.K. and Hoocher, B., 2021. Relationship Between Vitamin D and Hormones Important for Human Fertility in Reproductive-Aged Women. *Frontiers in Endocrinology* [Online], 12(April), p.666687. Available from: https://doi.org/10.3389/fendo.2021.666687.

Chung, D. and Keles, S., 2010. Sparse Partial Least Squares Classification for High Dimensional Data. *Statistical Applications in Genetics and Molecular Biology*, 9(1), pp.1554–1584.

Churchward-Venne, T.A., Burd, N.A. and Phillips, S.M., 2012. Nutritional regulation of muscle protein synthesis with resistance exercise: strategies to enhance anabolsim. *Nutrition and Metabolism*, 9(40).

Clark, J.F., 1997. Creatine and Phosphocreatine: A Review of Their Use in Exercise and Sport. *Journal of Athletic Training*, 32(1), pp.45–51.

Clish, C.B., 2015. Metabolomics: an emerging but powerful tool for precision medicine. *Cold Spring Harbor molecular case studies* [Online], 1(1), p.a000588. Available from: https://doi.org/10.1101/mcs.a000588.

Clore, J.N., Li, J., Gill, R., Gupta, S., Spencer, R., Azzam, A., Zuelzer, W., Rizzo, W.B., Blackard, W.G., John, N., Li, J., Gill, R., Gupta, S., Spencer, R., Azzam, A., Zuelzer, W., Rizzo, B. and Blackard, W.G., 1998. Skeletal muscle phosphatidylcholine fatty

acids and insulin sensitivity in normal humans. *American Journal of Physiology - Endocrinology and Metabolism*, 275(4), pp.E665–E670.

Coker, R.H., Hays, N.P., Williams, R.H., Xu, L., Wolfe, R.R., Evans, W.J. and Carolina, N., 2014. Bed Rest Worsens Impairments in Fat and Glucose Metabolism in Older, Overweight Adults. *Journals of Gerontology - Series A Biological Sciences and Medical Sciences* [Online], 69(3), pp.363–370. Available from: https://doi.org/10.1093/gerona/glt100.

Cooper, R., Naclerio, F., Allgrove, J. and Jimenez, A., 2012. Creatine supplementation with specific view to exercise/sports performance: an update. *Journal of the International Society of Sports Nutrition* [Online], 9(33). Available from: https://doi.org/10.1186/1550-2783-9-33.

Cotta, A., Carvalho, E., da-Cunha-Júnior, A.L., Valicek, J., Navarro, M.M., Junior, S.B., da Silveira, E.B., Lima, M.I., Cordeiro, B.A., Cauhi, A.F., Menezes, M.M., Nunes, S.V., Vargas, A.P., Neto, R.X. and Paim, J.F., 2021. Muscle biopsy essential diagnostic advice for pathologists. *Surgical and Experimental Pathology* [Online], 4(1). Available from: https://doi.org/10.1186/s42047-020-00085-w.

Crane, J.D., Devries, M.C., Safdar, A., Hamadeh, M.J. and Tarnopolsky, M.A., 2010. The effect of aging on human skeletal muscle mitochondrial and intramyocellular lipid ultrastructure. *Journals of Gerontology - Series A Biological Sciences and Medical Sciences* [Online], 65(2), pp.119–128. Available from: https://doi.org/10.1093/gerona/glp179.

Cree, M.G., Paddon-Jones, D., Newcomer, B.R., Ronsen, O., Aarsland, A., Wolfe, R.R. and Ferrando, A., 2010. Twenty-eight-day bed rest with hypercortisolemia induces peripheral insulin resistance and increases intramuscular triglycerides.

Metabolism: Clinical and Experimental [Online], 59(5), pp.703–710. Available from: https://doi.org/10.1016/j.metabol.2009.09.014.

Cruz-Jentoft, A.J., Bahat, G., Bauer, J., Boirie, Y., Bruyère, O., Cederholm, T., Cooper, C., Landi, F., Rolland, Y., Sayer, A.A., Schneider, S.M., Sieber, C.C., Topinkova, E., Vandewoude, M., Visser, M., Zamboni, M., Writing Group for the European Working Group on Sarcopenia in Older People (EWGSOP2) and EWGSOP2, T.E.G. for, 2019. Sarcopenia : revised European consensus on definition and diagnosis. *Age and Ageing* [Online], 48, pp.16–31. Available from: https://doi.org/10.1093/ageing/afy169.

Cuthbertson, D., Smith, K., Babraj, J., Leese, G., Waddell, T., Atherton, P., Wackerhage, H., Taylor, P.M. and Rennie, M.J., 2005. Anabolic signaling deficits underlie amino acid resistance of wasting, aging muscle. *FASEB Journal* [Online], 19(3), pp.422–424. Available from: https://doi.org/10.1096/fj.04-2640fje.

Cutolo, M., Paolino, S., Sulli, A., Smith, V., Pizzorni, C. and Seriolo, B., 2014. Vitamin D, steroid hormones, and autoimmunity. *Annals of the New York Academy of Sciences* [Online], 1317(1), pp.39–46. Available from: https://doi.org/10.1111/nyas.12432.

Cynober, L., 2013. *Amino Acid Metabolism* [Online]. 2nd ed. Elsevier Inc. Available from: https://doi.org/10.1016/B978-0-12-378630-2.00029-3.

Dai, B., Sorensen, C.J., Derrick, T.R. and Gillette, J.C., 2012. The effects of postseason break on knee biomechanics and lower extremity EMG in a stop-jump task : implications for ACL injury. *Journal of Applied Biomechanics*, 28(6), pp.708–717.

Dalal, S., 2019. Lipid metabolism in cancer cachexia. *Annals of Palliative Medicine* [Online], 8(1), pp.13–23. Available from:

https://doi.org/10.21037/APM.2018.10.01.

Dallmann, R., Viola, A.U., Tarokh, L., Cajochen, C. and Brown, S.A., 2012. The human circadian metabolome. *Proceedings of the National Academy of Sciences of the United States of America* [Online], 109(7), pp.2625–2629. Available from: https://doi.org/10.1073/pnas.1114410109.

Dass, C., 2007. Hyphenated separation techniques. *Fundamentals of Contemporary Mass Spectrometry*. pp.151–194.

Deans, C. and Wigmore, S.J., 2005. Systemic inflammation , cachexia and prognosis in patients with cancer. *Current Opinion in Clinical Nutrition and Metabolic Care*, 8, pp.265–269.

Deidda, M., Piras, C., Bassareo, P.P., Cadeddu Dessalvi, C. and Mercuro, G., 2015. Metabolomics, a promising approach to translational research in cardiology. *IJC Metabolic and Endocrine* [Online], 9, pp.31–38. Available from: https://doi.org/10.1016/j.ijcme.2015.10.001.

Demangel, R., Treffel, L., Py, G., Brioche, T., Pagano, A.F., Bareille, M.-P., Beck, A., Pessemesse, L., Candau, R., Gharib, C., Chopard, A. and Millet, C., 2017. Early structural and functional signature of 3-day human skeletal muscle disuse using the dry immersion model. *Journal of Physiology* [Online], 595(13), pp.4301–4315. Available from: https://doi.org/10.1113/JP273895.

Demura, S., Yamada, T., Yamaji, S., Komatsu, M. and Morishita, K., 2010. The effect of L-ornithine hydrochloride ingestion on performance during incremental exhaustive ergometer bicycle exercise and ammonia metabolism during and after exercise. *European Journal of Clinical Nutrition* [Online], 64, pp.1166–1171. Available from: https://doi.org/10.1038/ejcn.2010.149.

Deriaz, O., Fournier, G., Tremblay, A., Despres, J.-P. and Bouchard, C., 1992. Lean-body-mass before and after composition and resting energy. *The American Journal of Clinical Nutrition*, 56(5), pp.840–847.

Dewhirst, R.A. and Fry, S.C., 2018. The oxidation of dehydroascorbic acid and 2,3-diketogulonate by distinct reactive oxygen species. *Biochemical Journal*, 475, pp.3451–3470.

Dewys, W.D., Begg, C., Lavin, P.T., Band, P.R., Bennett, J.M., Cohen, M.H., Douglass, H.O., Engstrom, P.F., Ezdinli, E.Z., Horton, J., Johnson, G.J., Moertel, C.G., Oken, M.M., Perlia, C., Rosenbaum, C., Silverstein, M.N., Skeel, R.T., Sponzo, R.W. and Tormey, D.C., 1980. Prognostic Effect of Weight Loss Prior to Chemotherapy in Cancer Patients. *Clinical Studies*, 69(October), pp.491–497.

Diamandis, E.P., 2012. The failure of protein cancer biomarkers to reach the clinic: why, and what can be done to address the problem? *BMC Medicine* [Online], 10(87). Available from: https://doi.org/10.1186/1741-7015-10-87.

Dieterle, F., Ross, A., Schlotterbeck, G. and Senn, H., 2006. Probabilistic quotient normalization as robust method to account for dilution of complex biological mixtures. Application in1H NMR metabonomics. *Analytical Chemistry* [Online], 78(13), pp.4281–4290. Available from: https://doi.org/10.1021/ac051632c.

Dirks, M.L., Wall, B.T., Van De Valk, B., Holloway, T.M., Holloway, G.P., Chabowski, A., Goossens, G.H. and Van Loon, L.J., 2016. One week of bed rest leads to substantial muscle atrophy and induces whole-body insulin resistance in the absence of skeletal muscle lipid accumulation. *Diabetes* [Online], 65(10), pp.2862–2875. Available from: https://doi.org/10.2337/db15-1661.

Do, K.T., Wahl, S., Raffler, J., Molnos, S., Laimighofer, M., Adamski, J., Suhre, K.,

Strauch, K., Peters, A., Gieger, C., Langenberg, C., Stewart, I.D., Theis, F.J., Grallert, H., Kastenmüller, G. and Krumsiek, J., 2018. Characterization of missing values in untargeted MS-based metabolomics data and evaluation of missing data handling strategies. *Metabolomics* [Online], 14(128). Available from: https://doi.org/10.1007/s11306-018-1420-2.

Domej, W., Oettl, K. and Renner, W., 2014. Oxidative stress and free radicals in COPD – implications and relevance for treatment. *International Journal of Chronic Obstructive Pulmonary Disease*, 14(9), pp.1207–1224.

Dong, S., Zhan, Z.-Y., Cao, H.-Y., Wu, C., Bian, Y.-Q., Li, J.-Y. and Cheng, G.-H., 2017. Urinary metabolomics analysis identifies key biomarkers of different stages of nonalcoholic fatty liver disease. *World Journal of Gastroenterology* [Online], 23(15), pp.2771–2784. Available from: https://doi.org/10.3748/wjg.v23.i15.2771.

Druker, B.J., Talpaz, M., Resta, D.J., Peng, B., Buchdunger, E., Ford, J.M., Lydon, N.B., Kantarjian, H.M., Capdeville, R., Ohno-Jones, S. and Sawyers, C.L., 2001. EFFICACY AND SAFETY OF A SPECIFIC INHIBITOR OF THE BCR-ABL TYROSINE. *The New England Journal of Medicine*, 344(14), pp.1031–1037.

Drummond, M.J., Dickinson, J.M., Fry, C.S., Walker, D.K., Gundermann, D.M., Reidy, P.T., Timmerman, K.L., Markofski, M.M., Paddon-jones, D., Rasmussen, B.B. and Volpi, E., 2012. Bed rest impairs skeletal muscle amino acid transporter expression, mTORC1 signaling, and protein synthesis in response to essential amino acids in older adults. *American Journal of Physiology - Endocrinology and Metabolism* [Online], 203, pp.E1113–E1122. Available from: https://doi.org/10.1152/ajpendo.00603.2011.

Du, Y., Wu, J., Tian, Y., Zhang, L., Zhao, P. and Li, J., 2023. Serum metabolomics using ultra-high performance liquid chromatography–Q-Exactive tandem mass spectrometry reveals the mechanism of action of exercise training on chronic obstructive pulmonary disease rats. *Biomedical Chromatography* [Online], 37(1), pp.1–10. Available from: https://doi.org/10.1002/bmc.5507.

Dudbridge, F. and Gusnanto, A., 2008. Estimation of significance thresholds for genomewide association scans. *Genetic Epidemiology* [Online], 32(3), pp.227–234. Available from: https://doi.org/10.1002/gepi.20297.

Dunn, W.B., Broadhurst, D., Begley, P., Zelena, E., Francis-mcintyre, S., Anderson, N., Brown, M., Knowles, J.D., Halsall, A., Haselden, J.N., Nicholls, A.W., Wilson, I.D., Kell, D.B. and Goodacre, R., 2011. Procedures for large-scale metabolic profiling of serum and plasma using gas chromatography and liquid chromatography coupled to mass spectrometry. *Nature Protocols* [Online], 6(7), pp.1060–1083. Available from: https://doi.org/10.1038/nprot.2011.335.

Dunn, W.B., Lin, W., Broadhurst, D., Begley, P., Brown, M., Zelena, E., Vaughan, A.A., Halsall, A., Harding, N., Knowles, J.D., Francis-McIntyre, S., Tseng, A., Ellis, D.I., O'Hagan, S., Aarons, G., Benjamin, B., Chew-Graham, S., Moseley, C., Potter, P., Winder, C.L., Potts, C., Thornton, P., McWhirter, C., Zubair, M., Pan, M., Burns, A., Cruickshank, J.K., Jayson, G.C., Purandare, N., Wu, F.C.., Finn, J.D., Haselden, J.N., Nicholls, A.W., Wilson, I.D., Goodacre, R. and Kell, D.B., 2015. Molecular phenotyping of a UK population: defining the human serum metabolome. *Metabolomics* [Online], 11(9), pp.9–26. Available from: https://doi.org/10.1007/s11306-014-0707-1.

Dunn, W.B., Wilson, I.D., Nicholls, A.W. and Broadhurst, D., 2012. The importance of experimental design and QC samples in large-scale and MS-driven untargeted

metabolomic studies of humans. *Bioanalysis* [Online], 4(18), pp.2249–2264. Available from: https://doi.org/10.4155/bio.12.204.

Dünnwald, T., Paglia, G., Weiss, G., Denti, V., Faulhaber, M., Schobersberger, W. and Wackerhage, H., 2022. High Intensity Concentric-Eccentric Exercise Under Hypoxia Changes the Blood Metabolome of Trained Athletes. *Frontiers in Physiology* [Online], 13(June). Available from: https://doi.org/10.3389/fphys.2022.904618.

Dutta, T., Chai, H.S., Ward, L.E., Ghosh, A., Persson, X.M.T., Ford, G.C., Kudva, Y.C., Sun, Z., Asmann, Y.W., Kocher, J.P.A. and Nair, K.S., 2012. Concordance of changes in metabolic pathways based on plasma metabolomics and skeletal muscle transcriptomics in type 1 diabetes. *Diabetes* [Online], 61(5), pp.1004–1016. Available from: https://doi.org/10.2337/db11-0874.

Dyroy, E., Wergedahl, H., Skorve, J., Gudbrandsen, O.A., Songstad, J. and Berge, R.K., 2006. Thia Fatty Acids with the Sulfur Atom in Even or Odd Positions Have Opposite Effects on Fatty Acid Catabolism. *Lipids*, 41(2), pp.169–177.

Ebhardt, H.A., Degen, S., Tadini, V., Schilb, A., Johns, N., Greig, C.A., Fearon, K.C.H., Aebersold, R. and Jacobi, C., 2017. Comprehensive proteome analysis of human skeletal muscle in cachexia and sarcopenia: a pilot study. *Journal of Cachexia, Sarcopenia and Muscle* [Online], 8(4), pp.567–582. Available from: https://doi.org/10.1002/jcsm.12188.

Ejigu, B.A., Valkenborg, D., Baggerman, G., Vanaerschot, M., Witters, E., Dujardin, J.-C., Burzykowski, T. and Berg, M., 2013. Evaluation of Normalization Methods to Pave the Way Towards Large-Scale LC-MS-Based Metabolomics Profiling Experiments. *OMICS: A Journal of Integrative Biology*, 17(9), pp.473–485.

Eliuk, S. and Makarov, A., 2015. Evolution of Orbitrap Mass Spectrometry Instrumentation. *Annual Reviews of Analytical Chemistry* [Online], 8, pp.61–80. Available from: https://doi.org/10.1146/annurev-anchem-071114-040325.

Emwas, A.-H.M., 2015. The Strengths and Weaknesses of NMR Spectroscopy and Mass Spectrometry with Particular Focus on Metabolomics Research. In: J.T. Bjerrum, ed. *Metabonomics: Methods and Protocols*, [Online]. New York, NY: Springer New York, pp.161–193. Available from: https://doi.org/10.1007/978-1-4939-2377-9_13.

Endo, Y., Nourmahnad, A. and Sinha, I., 2020. Optimizing Skeletal Muscle Anabolic Response to Resistance Training in Aging. *Frontiers in Physiology* [Online], 11(874). Available from: https://doi.org/10.3389/fphys.2020.00874.

Enea, C., Seguin, F., Petitpas-Mulliez, J., Boildieu, N., Boisseau, N., Delpech, N., Diaz, V., Eugene, M. and Dugue, B., 2010. 1H NMR-based metabolomics approach for exploring urinary metabolome modifications after acute and chronic physical exercise. *Analytical and Bioanalytical Chemistry* [Online], 396, pp.1167–1176. Available from: https://doi.org/10.1007/s00216-009-3289-4.

Engskog, M.K.R., Haglo, J., Arvidsson, T. and Pettersson, C., 2016. LC – MS based global metabolite profiling : the necessity of high data quality. *Metabolomics* [Online], 12(114). Available from: https://doi.org/10.1007/s11306-016-1058-x.

Esposito, F., Mathieu-Costello, O., Wagner, P.D. and Richardson, R.S., 2018. Acute and chronic exercise in patients with heart failure with reduced ejection fraction: evidence of structural and functional plasticity and intact angiogenic signalling in skeletal muscle. *Journal of Physiology* [Online], 596(21), pp.5149–5161. Available from: https://doi.org/10.1113/JP276678.

Evans, A.M., O'Donovan, C., Playdon, M., Beecher, C., Beger, R.D., Bowden, J.A., Broadhurst, D., Clish, C.B., Dasari, S., Dunn, W.B., Griffin, J.L., Hartung, T., Hsu, P.-C., Huan, T., Jans, J., Jones, C.M., Kachman, M., Kleensang, A., Lewis, M.R., Monge, M.E., Mosley, J.D., Taylor, E., Tayyari, F., Theodoridis, G., Torta, F., Ubhi, B.K. and Vuckovic, D., 2020. Dissemination and analysis of the quality assurance (QA) and quality control (QC) practices of LC–MS based untargeted metabolomics practitioners. *Metabolomics* [Online], 16(10), p.113. Available from: https://doi.org/10.1007/s11306-020-01728-5.

Evans, W.J., Morley, J.E., Argile, J., Bales, C., Baracos, V., Guttridge, D., Jatoi, A., Kalantar-zadeh, K., Lochs, H., Mantovani, G., Marks, D., Mitch, W.E., Muscaritoli, M., Najand, A., Ponikowski, P., Rossi, F., Schambelan, M., Schols, A., Schuster, M., Thomas, D., Wolfe, R. and Anker, S.D., 2008. Cachexia : A new definition. *Clinical Nutrition* [Online], 27(6), pp.793–799. Available from: https://doi.org/10.1016/j.clnu.2008.06.013.

Fabbri, E., An, Y., Gonzalez-Freire, M., Zoli, M., Maggio, M., Studenski, S.A., Egan, J.M., Chia, C.W. and Ferrucci, L., 2016. Bioavailable testosterone linearly declines over a wide age spectrum in men and women from the Baltimore longitudinal study of aging. *Journals of Gerontology - Series A Biological Sciences and Medical Sciences* [Online], 71(9), pp.1202–1209. Available from: https://doi.org/10.1093/gerona/glw021.

Fabregat, A., Sidiropoulos, K., Viteri, G., Forner, O., Marin-Garcia, P., Arnau, V., Eustachio, P.D., Stein, L. and Hermjakob, H., 2017. Reactome pathway analysis: a high- performance in-memory approach. *BMC Bioinformatics* [Online], 18(142). Available from: https://doi.org/10.1186/s12859-017-1559-2.

Færgestad, E.M., Langsrud, Ø., Høy, M., Hollung, K., Sæbø, S., Liland, K.H., Kohler, A.,

Gidskehaug, L., Almergren, J., Anderssen, E. and Martens, H., 2009. 4.08 - Analysis of Megavariate Data in Functional Genomics. In: S.D. Brown, R. Tauler and B. Walczak, eds. *Comprehensive Chemometrics*, [Online]. Oxford: Elsevier, pp.221–278. Available from: https://doi.org/https://doi.org/10.1016/B978-044452701-1.00011-9.

Fang, E.F., Hou, Y., Demarest, T.G., Croteau, D.L., Mattson, M.P. and Bohr, V.A., 2017. NAD + in Aging : Molecular Mechanisms and Translational Implications. *Trends in Molecular Medicine* [Online], 23(10), pp.899–916. Available from: https://doi.org/10.1016/j.molmed.2017.08.001.

Fazelzadeh, P., Hangelbroek, R.W.J., Tieland, M., De Groot, L.C.P.G.M., Verdijk, L.B., Van Loon, L.J.C., Smilde, A.K., Alves, R.D.A.M., Vervoort, J., Müller, M., Van Duynhoven, J.P.M. and Boekschoten, M. V., 2016a. The Muscle Metabolome Differs between Healthy and Frail Older Adults. *Journal of Proteome Research* [Online], 15(2), pp.499–509. Available from: https://doi.org/10.1021/acs.jproteome.5b00840.

Fazelzadeh, P., Hangelbroek, R.W.J., Tieland, M., De Groot, L.C.P.G.M., Verdijk, L.B., Van Loon, L.J.C., Smilde, A.K., Alves, R.D.A.M., Vervoort, J., Müller, M., Van Duynhoven, J.P.M. and Boekschoten, M. V., 2016b. The Muscle Metabolome Differs between Healthy and Frail Older Adults. *Journal of Proteome Research* [Online], 15(2), pp.499–509. Available from: https://doi.org/10.1021/acs.jproteome.5b00840.

Fearon, K., Strasser, F., Anker, S.D., Bosaeus, I., Bruera, E., Fainsinger, R.L., Jatoi, A., Loprinzi, C., MacDonald, N., Mantovani, G., Davis, M., Muscaritoli, M., Ottery, F., Radbruch, L., Ravasco, P., Walsh, D., Wilcock, A., Kaasa, S. and Baracos, V.E., 2011. Definition and classification of cancer cachexia: An international

consensus. *The Lancet Oncology* [Online], 12(5), pp.489–495. Available from: https://doi.org/10.1016/S1470-2045(10)70218-7.

Feike, Y., Zhijie, L. and Wei, C., 2021. Advances in research on pharmacotherapy of sarcopenia. *Aging Medicine* [Online], 4(7), pp.221–233. Available from: https://doi.org/10.1002/agm2.12168.

Feldman, H.A., Longcope, C., Derby, C.A., Johannes, C.B., Araujo, A.B., Coviello, A.D., Bremner, W.J. and McKinlay, J.B., 2002. Age trends in the level of serum testosterone and other hormones in middle-aged men: Longitudinal results from the Massachusetts Male Aging Study. *Journal of Clinical Endocrinology and Metabolism* [Online], 87(2), pp.589–598. Available from: https://doi.org/10.1210/jcem.87.2.8201.

Feller, L., Khammissa, R.A.., Kramer, B., Altini, M. and Lemmer, J., 2016. Basal cell carcinoma, squamous cell carcinoma and melanoma of the head and face. *Head & Face Medicine* [Online], 12(11). Available from: https://doi.org/10.1186/s13005-016-0106-0.

Fernandez-Garcia, J.C., Delpino-Ruis, A., Samarra, I., Castellano-Castillo, D., Muñoz-Garach, A., Bernal-Lopez, M.R., Queipo-Ortuño, M.I., Cardona, F. and Ramos-Molina, B., 2019. Type 2 Diabetes Is Associated with a Different Pattern of Serum Polyamines: A Case – Control Study from the PREDIMED-Plus Trial. *Journal of Clinical Medicine* [Online], 8(71). Available from: https://doi.org/10.3390/jcm8010071.

Ferrara, P.J., Rong, X., Maschek, J.A., Verkerke, A.R.P., Siripoksup, P., Song, H., Green, T.D., Krishnan, K.C., Johnson, J.M., Turk, J., Houmard, J.A., Lusis, A.J., Drummond, M.J., Mcclung, J.M., Cox, J.E., Shaikh, S.R., Tontonoz, P., Holland, W.L. and Funai,

K., 2021. Lysophospholipid acylation modulates plasma membrane lipid organization and insulin sensitivity in skeletal muscle. *The Journal of Clinical Investigation*, 131(8), p.e135963.

Fiehn, O., 2002. Metabolomics - The link between genotypes and phenotypes. *Plant Molecular Biology* [Online], 48(1–2), pp.155–171. Available from: https://doi.org/10.1023/A:1013713905833.

Fielding, R.A., Vellas, B., Evans, W.J., Bhasin, S., Morley, J.E., Newman, A.B., van Kan, G.A., Andrieu, S., Bauer, J., Breuille, D., Cederholm, T., Chandler, U., de Meynard, C., Donini, L., Harris, T., Kannt, A., Guibert, F.K., Onder, G., Papanicolaou, D., Rolland, Y., Rooks, D., Sieber, C., Souhami, E., Verlaan, S. and Zamboni, M., 2011. Sarcopenia : An Undiagnosed Condition in Older Adults . Current Consensus Definition : Prevalence , Etiology , and Consequences . International Working Group on Sarcopenia. *Journal of the American Medical Directors Association* [Online], 12(4), pp.249–256. Available from: https://doi.org/10.1016/j.jamda.2011.01.003.

Filzmoser, P. and Nordhausen, K., 2020. Robust linear regression for high-dimensional data: An overview. *Wiley Interdisciplinary Reviews: Computational Statistics* [Online], 13(4), p.e1524. Available from: https://doi.org/10.1002/wics.1524.

Finsterer, J. and Zarrouk-Mahjoub, S., 2018. Biomarkers for Detecting Mitochondrial Disorders. *Journal of Clinical Medicine* [Online], 7(16). Available from: https://doi.org/10.3390/jcm7020016.

Formenti, P., Umbrello, M., Coppola, S., Froio, S. and Chiumello, D., 2019. Clinical review: peripheral muscular ultrasound in the ICU. *Annals of Intensive Care* [Online], 9(57). Available from: https://doi.org/10.1186/s13613-019-0531-x.

Fovet, T., Guilhot, C., Stevens, L., Montel, V., Delobel, P., Roumanille, R., Sempor, M.-Y., Freyssenet, D., Py, G., Brioche, T. and Chopard, A., 2021. Early Deconditioning of Human Skeletal Muscles and the Effects of a Thigh Cuff Countermeasure. *International Journal of Molecular Sciences*, 22(12064).

Fry, C.S. and Rasmussen, B.B., 2011. Skeletal muscle protein balance and metabolism in the elderly. *Current Aging Science*, 4(3), pp.260–268.

Fukagawa, N.., Minaker, K.., Rowe, J.., Goodman, M.., Matthews, D.., Bier, D.. and Young, V.., 1985. Insulin-mediated Reduction of Whole Body Protein Breakdown. *Journal of Clinical Investigation*, 76(December), pp.2306–2311.

Fukai, K., Harada, S., Iida, M., Kurihara, A., Takeuchi, A., Kuwabara, K., Sugiyama, D., Okamura, T., Akiyama, M., Nishiwaki, Y., Oguma, Y., Suzuki, A., Suzuki, C., Hirayama, A., Sugimoto, M., Soga, T., Tomita, M. and Takebayashi, T., 2016. Metabolic Profiling of Total Physical Activity and Sedentary Behavior in Community- Dwelling Men. *PLoS ONE* [Online], 11(10), p.e0164877. Available from: https://doi.org/10.1371/journal.pone.0164877.

Gadara, D., Coufalikova, K., Bosak, J., Smajs, D. and Spacil, Z., 2021. Systematic Feature Filtering in Exploratory Metabolomics: Application toward Biomarker Discovery. *Analytical Chemistry* [Online], 93, pp.9103–9110. Available from: https://doi.org/10.1021/acs.analchem.1c00816.

Galgani, J.E., Moro, C. and Ravussin, E., 2008. Metabolic flexibility and insulin resistance. *American Journal of Physiology - Endocrinology and Metabolism* [Online], 295, pp.1009–1017. Available from: https://doi.org/10.1152/ajpendo.90558.2008.

Ganna, A., Fall, T., Salihovic, S., Lee, W., Lind, L., Pawitan, Y. and Ingelsson, E., 2016.

Large-scale non-targeted metabolomic profiling in three human population-based studies. *Metabolomics* [Online], 12(4). Available from: https://doi.org/10.1007/s11306-015-0893-5.

Garber, K., 2016. No longer going to waste. *Nature Biotechnology*, 34(5), pp.458–461.

Garlick, P.J. and Grant, I., 1988. Amino acid infusion increases the sensitivity of muscle protein synthesis in vivo to insulin. *Biochemical Journal*, 254(2), pp.579–584.

Gehlert, S., Weinisch, P., Romisch-Margl, W., Jaspers, R.T., Artati, A., Adamski, J., Dyar, K.A., Aussieker, T., Jacko, D., Bloch, W., Wackerhage, H. and Kastenmüller, G., 2022. Effects of Acute and Chronic Exercise on the Skeletal Muscle Metabolome. *Metabolites* [Online], 12(445). Available from: https://doi.org/10.1002/jcp.25477.

Gemmink, A., Goodpaster, B.H., Schrauwen, P. and Hesselink, M.K.C., 2017. Intramyocellular lipid droplets and insulin sensitivity, the human perspective. *Biochimica et Biophysica Acta - Molecular and Cell Biology of Lipids* [Online], 1862(10), pp.1242–1249. Available from: https://doi.org/10.1016/j.bbalip.2017.07.010.

Gertsman, I. and Barshop, B.A., 2018. Promises and Pitfalls of Untargeted Metabolomics. *Journal of Inherited Metabolic Disorders* [Online], 41(3), pp.355–366. Available from: https://doi.org/10.1007/s10545-017-0130-7.Promises.

Gibala, M.J., Little, J.P., Essen, M. Van, Wilkin, G.P., Burgomaster, K.A., Safdar, A., Raha, S. and Tarnopolsky, M.A., 2006. Short-term sprint interval versus traditional endurance training: similar initial adaptations in human skeletal muscle and exercise performance. *Journal of Physiology* [Online], 575(3), pp.901–911. Available from: https://doi.org/10.1113/jphysiol.2006.112094.

Gika, H.G., Theodoridis, G.A. and Wilson, I.D., 2008. Hydrophilic interaction and reversed-phase ultra-performance liquid chromatography TOF-MS for metabonomic analysis of Zucker rat urine. *Journal of Separation Science* [Online], 31(9), pp.1598–1608. Available from: https://doi.org/10.1002/jssc.200700644.

Gika, H.G., Wilson, I.D. and Theodoridis, G.A., 2014. LC–MS-based holistic metabolic profiling. Problems, limitations, advantages, and future perspectives. *Journal of Chromatography B* [Online], 966, pp.1–6. Available from: https://doi.org/https://doi.org/10.1016/j.jchromb.2014.01.054.

Glynn, E.L., Piner, L.W., Huffman, K.M., Slentz, C.A., Elliot-Penry, L., Abouassi, H., White, P.J., Bain, J.R., Muehlbauer, M.J., Ilkayeva, O.R., Stevens, R.D., Porter Starr, K.N., Bales, C.W., Volpi, E., Brosnan, M.J., Trimmer, J.K., Rolph, T.P., Newgard, C.B. and Kraus, W.E., 2016. Impact of combined resistance and aerobic exercise training on branched-chain amino acid turnover, glycine metabolism and insulin sensitivity in overweight adults. *Diabetologia* [Online], 58(10), pp.2324–2335. Available from: https://doi.org/10.1007/s00125-015-3705-6.

Goates, S., Du, K., Arensberg, M.B., Gaillard, T., Guralnik, J. and Pereira, S.L., 2019. Economic Impact of Hospitalizations in US Adults with Sarcopenia. *The Journal of frailty & aging* [Online], 8(2), pp.93–99. Available from: https://doi.org/10.14283/jfa.2019.10.

de Goede, O.M., Nachun, D.C., Ferraro, N.M., Gloudemans, M.J., Rao, A.S., Smail, C., Eulalio, T.Y., Aguet, F., Ng, B., Xu, J., Barbeira, A.N., Castel, S.E., Kim-Hellmuth, S., Park, Y., Scott, A.J., Strober, B.J., Consortium, Gte., Brown, C.D., Wen, X., Hall, I.M., Battle, A., Lappalainen, T., Im, H.K., Ardlie, K.G., Mostafavi, S., Quertermous, T., Kirkegaard, K. and Montgomery, S.B., 2021. Population-scale tissue transcriptomics maps long non-coding RNAs to complex disease. *Cell* [Online],

184, pp.2633–2648. Available from: https://doi.org/10.1016/j.cell.2021.03.050.

Golbraikh, A. and Tropsha, A., 2002. Beware of q2! *Journal of Molecular Graphics and Modelling*, 20, pp.269–276.

Gollnick, P.D. and Saltin, B., 1982. Significance of skeletal muscle oxidative enzyme enhancement with endurance training. *Clinical Physiology*, 2(1), pp.1–12.

Gonzalez-Covarrubias, V., Martinez-Martinez, E. and del Bosque-Plata, L., 2022. The Potential of Metabolomics in Biomedical Applications. *Metabolites*, 12(194).

Goodpaster, B.H. and Sparks, L.M., 2018. Metabolic flexibility in health and disease. *Cell Metabolism* [Online], 25(5), pp.1027–1036. Available from: https://doi.org/10.1016/j.cmet.2017.04.015.Metabolic.

Gordon, P.L., Sakkas, G.K., Doyle, J.W., Shubert, T. and Johansen, K.L., 2008. The Relationship between Vitamin D and Muscle Size and Strength in Patients on Hemodialysis. *Journal of Renal Nutrition*, 17(6), pp.397–407.

Goutman, S.A., Boss, J., Guo, K., Alakwaa, F.M., Patterson, A., Kim, S., Savelieff, M.G., Hur, J. and Feldman, E.L., 2020. Untargeted metabolomics yields insight into ALS disease mechanisms. *Journal of Neurology, Neurosurgery & Psychiatry* [Online], 91, pp.1329–1338. Available from: https://doi.org/10.1136/jnnp-2020-323611.

Granic, A., Sayer, A.A. and Robinson, S.M., 2019. Dietary patterns, skeletal muscle health, and sarcopenia in older adults. *Nutrients* [Online], 11(4), pp.1–29. Available from: https://doi.org/10.3390/nu11040745.

Grapentine, S. and Bakovic, M., 2020. Significance of bilayer-forming phospholipids for skeletal muscle insulin sensitivity and mitochondrial function. *The Journal of Biomedical Research*, 34(1), pp.1–13.

Greenhaff, P.L., Karagounis, L.G., Peirce, N., Simpson, E.J., Hazell, M., Layfield, R., Wackerhage, H., Smith, K., Atherton, P., Selby, A. and Rennie, M.J., 2008. Disassociation between the effects of amino acids and insulin on signaling, ubiquitin ligases, and protein turnover in human muscle. *American Journal of Physiology - Endocrinology and Metabolism* [Online], 295(3), pp.595–604. Available from: https://doi.org/10.1152/ajpendo.90411.2008.

Greig, C.., Gray, C., Rankin, D., Young, A., Mann, V., Noble, B. and Atherton, P.., 2011. Blunting of adaptive responses to resistance exercise training in women over 75 y. *Experimental Gerontology* [Online], 46(11), pp.884–890. Available from: https://doi.org/10.1016/j.exger.2011.07.010.

Grevendonk, L., Connell, N.., McCrum, C., Fealy, C.., Bilet, L., Bruls, Y.M.., Mevenkamp, J., Schrauwen-Hinderling, V.., Jörgensen, J.., Moonen-Kornips, E., Schaart, G., Havekes, B., de Vogel-van den Bosch, J., Bragt, M.C.., Meijer, K., Schrauwen, P. and Hoeks, J., 2021. Impact of aging and exercise on skeletal muscle mitochondrial capacity, energy metabolism, and physical function. *Nature Communications* [Online], 12(4773). Available from: https://doi.org/10.1038/s41467-021-24956-2.

Groenwold, R.H.H., Goeman, J.J., Le Cessie, S. and Dekkers, O.M., 2021. Multiple testing: when is many too much? *Methodology Editorial*, 184(2), pp.11–14.

Gromski, P.S., Muhamadali, H., Ellis, D.I., Xu, Y., Correa, E., Turner, M.L. and Goodacre, R., 2015. A tutorial review: Metabolomics and partial least squares-discriminant analysis - a marriage of convenience or a shotgun wedding. *Analytica Chimica Acta* [Online], 879, pp.10–23. Available from: https://doi.org/10.1016/j.aca.2015.02.012.

Gromski, P.S., Xu, Y., Kotze, H.L., Correa, E., Ellis, D.I., Armitage, E.G., Turner, M.L. and Goodacre, R., 2014. Influence of Missing Values Substitutes on Multivariate Analysis of Metabolomics Data. *Metabolites* [Online], 4, pp.433–452. Available from: https://doi.org/10.3390/metabo4020433.

Gu, Z. and Wang, J., 2013. Systems biology CePa: an R package for finding significant pathways weighted by multiple network centralities. *Bioinformatics* [Online], 29(5), pp.658–660. Available from: https://doi.org/10.1093/bioinformatics/btt008.

Guenette, J.A., Chin, R.C., Cheng, S., Dominelli, P.B., Raghavan, N., Webb, K.A., Neder, J.A. and O'Donnell, D.E., 2014. Mechanisms of exercise intolerance in Global Initiative for Chronic Obstructive Lung Disease grade 1 COPD. *European Respiratory Journal* [Online], 44(5), pp.1177–1187. Available from: https://doi.org/10.1183/09031936.00034714.

de Guia, R.M., Agerholm, M., Nielsen, T.S., Consitt, L.A., Søgaard, D., Helge, J.W., Larsen, S., Brandauer, J., Houmard, J.A. and Treebak, J.T., 2019. Aerobic and resistance exercise training reverses age-dependent decline in NAD + salvage capacity in human skeletal muscle. *Physiological Reports* [Online], 7(12), p.e14139. Available from: https://doi.org/10.14814/phy2.14139.

Di Guida, R., Engel, J., Allwood, J.W., Weber, R.J.M., Jones, M.R., Sommer, U., Viant, M.R. and Dunn, W.B., 2016. Non-targeted UHPLC-MS metabolomic data processing methods: a comparative investigation of normalisation, missing value imputation, transformation and scaling. *Metabolomics* [Online], 12(5), pp.1–14. Available from: https://doi.org/10.1007/s11306-016-1030-9.

Guijas, C., Montenegro-Burke, J.R., Warth, B., Spilker, M.E. and Siuzdak, G., 2018.

Metabolomics activity screening for identifying metabolites that modulate phenotype. *Nature Biotechnology* [Online], 36(4), pp.316–320. Available from: https://doi.org/10.1038/nbt.4101.

Guiochon, G. and Guillemin, C.L., 1990. Gas chromatography. *Review of Scientific Instruments* [Online], 61(11), pp.3317–3339. Available from: https://doi.org/10.1063/1.1141631.

Guo, Y.S. and Tao, J.Z., 2018. Metabolomics and pathway analyses to characterize metabolic alterations in pregnant dairy cows on D 17 and D 45 after AI. *Scientific Reports* [Online], 8(1). Available from: https://doi.org/10.1038/s41598-018-23983-2.

Haines, R.J., Pendleton, L.C. and Eichler, D.C., 2011. Argininosuccinate synthase: at the center of arginine metabolism. *International Journal of Biochemistry and Molecular Biology*, 2(1), pp.8–23.

Hamburg, N.M., McMackin, C.J., Huang, A.L., Shenouda, S.M., Widlansky, M.E., Schulz, E., Gokce, N., Ruderman, N.B., Keaney, J.F. and Vita, J.A., 2007. Physical inactivity rapidly induces insulin resistance and microvascular dysfunction in healthy volunteers. *Arteriosclerosis, Thrombosis, and Vascular Biology* [Online], 27(12), pp.2650–2656. Available from: https://doi.org/10.1161/ATVBAHA.107.153288.

Hannun, Y.A. and Obeid, L.M., 2018. Sphingolipids and their metabolism in physiology and disease. *Nature Reviews Molecular Cell Biology* [Online], 19(3), pp.175–191. Available from: https://doi.org/10.1038/nrm.2017.107.

Harayama, T. and Riezman, H., 2018. Understanding the diversity of membrane lipid composition. *Nature Reviews Molecular Cell Biology* [Online], 19(5), pp.281–296. Available from: https://doi.org/10.1038/nrm.2017.138.

Harman, S.M., Metter, E.J., Tobin, J.D., Pearson, J. and Blackman, M.R., 2001. Longitudinal effects of aging on serum total and free testosterone levels in healthy men. *Journal of Clinical Endocrinology and Metabolism* [Online], 86(2), pp.724–731. Available from: https://doi.org/10.1210/jcem.86.2.7219.

Hasin, Y., Seldin, M. and Lusis, A., 2017. Multi-omics approaches to disease. *Genome Biology* [Online], 18(83). Available from: https://doi.org/10.1186/s13059-017-1215-1.

Haslam, A., Johnson, M.A., Hausman, D.B., Cress, M.E., Houston, D.K., Davey, A. and Poon, L.W., 2014. Journal of Nutrition in Gerontology and Geriatrics Vitamin D Status Is Associated With Grip Strength in Centenarians. *Journal of Nutrition in Gerontology and Geriatrics* [Online], 33(1), pp.35–46. Available from: https://doi.org/10.1080/21551197.2013.867825.

Hawley, J.A. and Lessard, S.J., 2008. Exercise training-induced improvements in insulin action. *Acta Physiologica* [Online], 192, pp.127–135. Available from: https://doi.org/10.1111/j.1748-1716.2007.01783.x.

van der Heeft, E., Bolck, Y.J.., Beumer, B., Nijrolder, A.W.J.., Stolker, A.A.. and Nielen, M.W.., 2009. Full-Scan Accurate Mass Selectivity of Ultra-Performance Liquid Chromatography Combined with Time-of-Flight and Orbitrap Mass Spectrometry in Hormone and Veterinary Drug Residue Analysis. *Journal of the American Society of Mass Spectrometry* [Online], 20(3), pp.451–463. Available from: https://doi.org/10.1016/j.jasms.2008.11.002.

Hinkley, J.M., Cornnell, H.H., Standley, R.A., Chen, E.Y., Narain, N.R., Greenwood, B.P., Bussberg, V., Tolstikov, V. V., Kiebish, M.A., Yi, F., Vega, R.B., Goodpaster, B.H. and Coen, P.M., 2020. Older adults with sarcopenia have distinct skeletal muscle

phosphodiester, phosphocreatine, and phospholipid profiles. *Aging Cell* [Online], 19(6), p.e13135. Available from: https://doi.org/10.1111/acel.13135.

Hobson, R.M., Saunders, B., Ball, G., Harris, R.C. and Sale, C., 2012. Effects of β-alanine supplementation on exercise performance: a meta-analysis. *Amino Acids* [Online], 43, pp.25–37. Available from: https://doi.org/10.1007/s00726-011-1200-z.

Hoffman, J.M., Soltow, Q.A., Li, S., Sidik, A., Jones, D.P. and Promislow, D.E.L., 2014. Effects of age, sex, and genotype on high-sensitivity metabolomic profiles in the fruit fly, Drosophila melanogaster. *Aging Cell* [Online], 13(4), pp.596–604. Available from: https://doi.org/10.1111/acel.12215.

de Hoffmann, E. and Stroobant, V., 2001. *Mass Spectrometry Principles and Applications*.

Holthuis, J.C.., Pomorski, T., Raggers, R.J., Sprong, H. and van Meer, G., 2001. The Organizing Potential of Sphingolipids in Intracellular Membrane Transport. *Physiological Reviews*, 81(4), pp.1689–1723.

Hong, A.-R., Hong, S.-M. and Shin, Y.-A., 2014. Effects of Resistance Training on Muscle Strength, Endurance , and Motor Unit According to Ciliary Neurotrophic Factor Polymorphism in Male College Students. *Journal of Sports Science and Medicine*, 13(9), pp.680–688.

Hong, S., Chang, Y., Jung, H., Yun, K.E., Shin, H. and Ryu, S., 2017. Relative muscle mass and the risk of incident type 2 diabetes: A cohort study. *PLoS ONE*, 12(11).

Horgan, R.P. and Kenny, L.C., 2011. 'Omic' technologies: genomics, transcriptomics, proteomics and metabolomics. *The Obstetrician & Gynaecologist* [Online], 13(3), pp.189–195. Available from: https://doi.org/10.1576/toag.13.3.189.27672.

Horstman, A.M., Dillon, E.L., Urban, R.J. and Sheffield-Moore, M., 2012. The role of androgens and estrogens on healthy aging and longevity. *Journals of Gerontology - Series A Biological Sciences and Medical Sciences* [Online], 67(11), pp.1140–1152. Available from: https://doi.org/10.1093/gerona/gls068.

Hrydziuszko, O. and Viant, M.R., 2012. Missing values in mass spectrometry based metabolomics: An undervalued step in the data processing pipeline. *Metabolomics* [Online], 8, pp.161–174. Available from: https://doi.org/10.1007/s11306-011-0366-4.

Huang, H., Sun, Z., Pan, H., Chen, M., Tong, Y., Zhang, J., Chen, D., Su, X. and Li, L., 2016. Serum metabolomic signatures discriminate early liver inflammation and fibrosis stages in patients with chronic hepatitis B. *Scientific Reports* [Online], 6(30853). Available from: https://doi.org/10.1038/srep30853.

Huber, W., von Heydebreck, A., Sultmann, H., Poustla, A. and Vingron, M., 2002. Variance stabilization applied to microarray calibration and to the quantification of differential. *Bioinformatics*, 18(Suppl 1), pp.S96–S104.

Huh, Y. and Son, K.Y., 2022. Association between total protein intake and low muscle mass in Korean adults. *BMC Geriatrics* [Online], 22(319). Available from: https://doi.org/10.1186/s12877-022-03019-1.

Hung, A.H., Liang, T., Sukerkar, P.A. and Meade, T.J., 2013. High Dynamic Range Processing for Magnetic Resonance Imaging. *PLOS ONE* [Online], 8(11), p.e77883. Available from: https://doi.org/10.1371/journal.pone.0077883.

Hwang, S., Gustafsson, H.T., Sullivan, C.O., Bisceglia, G., Huang, X., Klose, C., Schevchenko, A., Dickson, R.C., Cavaliere, P., Dephoure, N. and Torres, E.M., 2017. Serine-dependent Sphingolipid Synthesis Is a Metabolic Liability of

Aneuploid Cells. *Cell Reports* [Online], 21(13), pp.3807–3818. Available from: https://doi.org/10.1016/j.celrep.2017.11.103.Serine-dependent.

Iannuzzi-Sucich, M., Prestwood, K.M. and Kenny, A.M., 2002. Prevalence of sarcopenia and predictors of skeletal muscle mass in healthy, older men and women. *Journals of Gerontology - Series A Biological Sciences and Medical Sciences* [Online], 57(12), pp.772–777. Available from: https://doi.org/10.1093/gerona/57.12.M772.

Ibebunjo, C., Chick, J.M., Kendall, T., Eash, J.K., Li, C., Zhang, Y., Vickers, C., Wu, Z., Clarke, B.A., Shi, J., Cruz, J., Fournier, B., Brachat, S., Gutzwiller, S., Ma, Q., Markovits, J., Broome, M., Steinkrauss, M., Skuba, E., Galarneau, J.-R., Gygi, S.P. and Glass, D.J., 2013. Genomic and Proteomic Profiling Reveals Reduced Mitochondrial Function and Disruption of the Neuromuscular Junction Driving Rat Sarcopenia. *Molecular and Cellular Biology* [Online], 33(2), pp.194–212. Available from: https://doi.org/10.1128/MCB.01036-12.

Inns, T.B., Bass, J.J., Hardy, E.J.O., Wilkinson, D.J., Stashuk, D.W., Atherton, P.J., Phillips, B.E. and Piasecki, M., 2022. Motor unit dysregulation following 15 days of unilateral lower limb immobilisation. *Journal of Physiology* [Online], 600(22), pp.4753–4769. Available from: https://doi.org/10.1113/JP283425.

Jackman, S.R., Wallis, G.A., Yu, J., Philp, A., Baar, K., Tipton, K.D. and Witard, O.C., 2023. Co-Ingestion of Branched-Chain Amino Acids and Carbohydrate Stimulates Myofibrillar Protein Synthesis Following Resistance Exercise in Trained Young Men. *International Journal of Sport Nutrition and Exercise Metabolism* [Online], 33(4), pp.189–197. Available from: https://doi.org/10.1123/ijsnem.2023-0015.

Jagoe, R.T. and Engelen, M.P.K.J., 2003. Muscle wasting and changes in muscle protein

metabolism in chronic obstructive pulmonary disease. *European Respiratory Journal* [Online], 22(Suppl 46), pp.52–63. Available from: https://doi.org/10.1183/09031936.03.00004608.

Jain, P., Kantarjian, H.M., Ghorab, A., Sasaki, K., Jabbour, E.J., Nogueras Gonzalez, G., Kanagal-Shamanna, R., Issa, G.C., Garcia-Manero, G., Dellasala, S., Pierce, S., Konopleva, M., Wierda, W.G., Verstovsek, S., Daver, N.G., Kadia, T.M., Borthakur, G., O'Brien, S., Estrov, Z., Ravandi, F. and Cortes, J.E., 2017. Prognostic Factors and Survival Outcomes in Patients With Chronic Myeloid Leukemia in Blast Phase in the Tyrosine Kinase Inhibitor Era: Cohort Study of 477 Patients. *Cancer* [Online], 123(22), pp.4391–4402. Available from: https://doi.org/10.1002/cncr.30864.

Jain, S.K., Bull, R., Rains, J.L., Bass, P.F., Levine, S.N., Reddy, S., McVie, R. and Bocchini Jnr, J.A., 2010. Low Levels of Hydrogen Sulfide in the Blood of Diabetes Patients and Streptozotocin-Treated Rats Causes Vascular Inflammation? *Antioxidants and Redox Signalling*, 12(11), pp.1333–1337.

Jain, S.K., Micinski, D., Huning, L., Kahlon, G., Bass, P.F. and Levine, S.N., 2014. Vitamin D and L-cysteine levels correlate positively with GSH and negatively with insulin resistance levels in the blood of type 2 diabetic patients. *European Journal of Clinical Nutrition* [Online], 68(10), pp.1148–1153. Available from: https://doi.org/10.1038/ejcn.2014.114.

Jaitovich, A. and Barreiro, E., 2018. Skeletal muscle dysfunction in chronic obstructive pulmonary disease what we know and can do for our patients. *American Journal of Respiratory and Critical Care Medicine* [Online], 198(2), pp.175–186. Available from: https://doi.org/10.1164/rccm.201710-2140CI.

Jakobsson, P.E.J. and Jorfeldt, L., 1990. Skeletal muscle metabolites and fibre types in patients with advanced chronic obstructive pulmonary disease (COPD), with and without chronic respiratory failure. *European Respiratory Journal* [Online], 57(5), pp.304–309. Available from: https://doi.org/10.1159/000195861.

Jasani, B., Donaldson, L.., Ratcliffe, J.. and Sokhi, G.., 1978. Mechanism of impaired glucose tolerance with neoplasia. *British Journal of Cancer*, 38(287), pp.287–292.

Jauhiainen, A., Madhu, B., Narita, Masako, Narita, Masashi, Griffiths, J. and Tavare, S., 2014. Normalization of metabolomics data with applications to correlation maps. *Bioinformatics* [Online], 30(15), pp.2155–2161. Available from: https://doi.org/10.1093/bioinformatics/btu175.

Jiang, M., Wang, C., Zhang, Y., Feng, Y., Wang, Y. and Zhu, Y., 2013. Sparse Partial-least-squares Discriminant Analysis for Different Geographical Origins of Salvia miltiorrhiza by 1 H-NMR-based Metabolomics. *Phytochemical Analysis* [Online], 25(1), pp.50–58. Available from: https://doi.org/10.1002/pca.2461.

Jiang, X.C., Paultre, F., Pearson, T.A., Reed, R.G., Francis, C.K., Lin, M., Berglund, L. and Tall, A.R., 2000. Plasma sphingomyelin level as a risk factor for coronary artery disease. *Arteriosclerosis, Thrombosis, and Vascular Biology* [Online], 20(12), pp.2614–2618. Available from: https://doi.org/10.1161/01.ATV.20.12.2614.

Jin, R., Banton, S., Tran, V.T., Konomi, J. V., Li, S., Jones, D.P. and Vos, M.B., 2016. Amino acid metabolism is altered in adolescents with nonalcoholic fatty liver disease - An untargeted, high resolution metabolomics study. *Journal of Pediatrics* [Online], 172, pp.14-19.e5. Available from: https://doi.org/10.1016/j.jpeds.2016.01.026.

Johnson, A.D. and Donnell, C.J.O., 2009. An Open Access Database of Genome-wide

Association Results. *BMC Medical Genetics* [Online], 10(6). Available from: https://doi.org/10.1186/1471-2350-10-6.

Johnson, C.H. and Gonzalez, F.J., 2012. Challenges and opportunities of metabolomics. *Journal of Cellular Physiology* [Online], 227(8), pp.2975–2981. Available from: https://doi.org/10.1002/jcp.24002.

Johnson, C.H., Ivanisevic, J. and Siuzdak, G., 2016. Metabolomics: beyond biomarkers and towards mechanisms. *Nature Reviews Molecular Cell Biology*, 17(7), pp.451–459.

Johnson, L.C., Parker, K., Aguirre, B.F., Nemkov, T.G., Alessandro, A.D., Johnson, S.A., Seals, D.R. and Martens, C.R., 2019. The plasma metabolome as a predictor of biological aging in humans. *GeroScience*, 41(11), pp.895–906.

Jolliffe, I.T., 1990. PRINCIPAL COMPONENT ANALYSIS: A BEGINNER'S GUIDE — I. Introduction and application. *Weather* [Online], 45(10), pp.375–382. Available from: https://doi.org/10.1002/j.1477-8696.1990.tb05558.x.

Jolliffe, I.T. and Cadima, J., 2016. Principal component analysis: a review and recent developments. *Philosophical Transactions A*, 374(20150202).

Jonker, R., Erbland, M.L., Anderson, P.J. and Engelen, M.P.K.., 2017. Effectiveness of essential amino acid supplementation in stimulating whole body net protein anabolism is comparable between COPD patients and healthy older adults. *Metabolism* [Online], 69(4), pp.120–129. Available from: https://doi.org/10.1016/j.metabol.2016.12.010.Effectiveness.

Jourdan, C., Petersen, A.-K., Gieger, C., Doring, A., Illig, T., Wang-Sattler, R., Meisinger, C., Peters, A., Adamski, J., Prehn, C., Suhre, K., Altmater, E., Kastenmuller, G., Romisch-Margi, W., Theis, F.J., Krumsiek, J., Wichmann, H.-E. and Linselsen, J.,

2012. Body Fat Free Mass Is Associated with the Serum Metabolite Profile in a Population-Based Study. *PLoS ONE* [Online], 7(6), p.e40009. Available from: https://doi.org/10.1371/journal.pone.0040009.

Julius, M., Lang, C.A., Gleiberman, L. and Harbijrg, E., 1994. GLUTATHIONE AND MORBIDITY IN A COMMUNITY-BASED SAMPLE OF ELDERLY. *Journal of Clinical Epidemiology*, 47(9), pp.1021–1026.

Kalyani, R.R., Metter, E.J., Xue, Q.-L., Egan, J.M., Chia, C.W., Studenski, S., Shaffer, N.C., Golden, S., Al-sofiani, M., Florez, H. and Ferrucci, L., 2020. The Relationship of Lean Body Mass With Aging to the Development of Diabetes. *Journal of the Endocrine Society* [Online], 4(7), pp.1–16. Available from: https://doi.org/10.1210/jendso/bvaa043.

Kamburov, A., Cavill, R., Ebbels, T.M.D., Herwig, R. and Keun, H.C., 2011. Integrated pathway-level analysis of transcriptomics and metabolomics data with IMPaLA. *Bioinformatics* [Online], 27(20), pp.2917–2918. Available from: https://doi.org/10.1093/bioinformatics/btr499.

Kamen, G. and Knight, C.A., 2004. Training-Related Adaptations in Motor Unit Discharge Rate in Young and Older Adults. *Journal of Gerontology*, 59(12), pp.1334–1338.

Kanehisa, M. and Goto, S., 2000. KEGG : Kyoto Encyclopedia of Genes and Genomes. *Nucleic Acids Research*, 28(1), pp.27–30.

Kang, H., 2013. The prevention and handling of the missing data. *Korean Journal of Anesthesiology*, 64(5), pp.402–406.

Kankainen, M., Gopalacharyulu, P., Holm, L. and Oreši, M., 2011. MPEA — metabolite pathway enrichment analysis. *Bioinformatics* [Online], 27(13), pp.1878–1879.

Available from: https://doi.org/10.1093/bioinformatics/btr278.

Karnovsky, A., Weymouth, T., Hull, T., Glenn Tarcea, V., Scardoni, G., Laudanna, C., Sartor, M.A., Stringer, K.A., Jagadish, H. V., Burant, C., Athey, B. and Omenn, G.S., 2012. Metscape 2 bioinformatics tool for the analysis and visualization of metabolomics and gene expression data. *Bioinformatics* [Online], 28(3), pp.373–380. Available from: https://doi.org/10.1093/bioinformatics/btr661.

Kase, E.T., Nikolic, N., Bakke, S.S., Bogen, K.K., Aas, V., Thoresen, G.H. and Rustan, A.C., 2013. Remodeling of Oxidative Energy Metabolism by Galactose Improves Glucose Handling and Metabolic Switching in Human Skeletal Muscle Cells. *PLoS ONE* [Online], 8(4). Available from: https://doi.org/10.1371/journal.pone.0059972.

Katajamaa, M. and Orešič, M., 2007. Data processing for mass spectrometry-based metabolomics. *Journal of Chromatography A* [Online], 1158, pp.318–328. Available from: https://doi.org/10.1016/j.chroma.2007.04.021.

Kaufmann, A. and Walker, S., 2016. Extension of the Q Orbitrap intrascan dynamic range by using a dedicated customized scan. *Rapid Communications in Mass Spectrometry* [Online], 30(2), pp.1087–1095. Available from: https://doi.org/10.1002/rcm.7530.

Kawakami, Y., Akima, H., Kubo, K., Muraoka, Y., Hasegawa, H., Kouzaki, M., Imai, M., Yoji, S., Atsuaki, G., Kanehisa, H. and Fukunaga, T., 2001. Changes in muscle size, architecture, and neural activation after 20 days of bed rest with and without resistance exercise. *European Journal of Applied Physiology*, 84, pp.7–12.

Keating, C.J., Cabrera-Linares, J.C., Parraga-Montilla, J.A., Latorre-Rom, P.A., Moreno del Castillo, R. and Garcia-Pinillos, F., 2021. Influence of Resistance Training on

Gait & Balance Parameters in Older Adults: A Systematic Review. *International Journal of Environmental Research and Public Health*, 18(1759).

Kebarle, P., 2000. A brief overview of the present status of the mechanisms involved in electrospray mass spectrometry. *Journal of Mass Spectrometry*, 35, pp.804–817.

Keizer, H., Janssen, G.M.E., Menheere, P. and Kranenburg, G., 1989. Dehydroepiandrosterone Sulfate in Previously Untrained Males and Females Preparing for a Marathon. *International Journal of Sports Medicine*, 10(3), pp.139–145.

Kell, D.B. and Oliver, S.G., 2004. Here is the evidence, now what is the hypothesis? The complementary roles of inductive and hypothesis-driven science in the post-genomic era. *BioEssays* [Online], 26(1), pp.99–105. Available from: https://doi.org/10.1002/bies.10385.

Keller, A., Stahler, C.F., Meese, E., Kappel, A., Backes, C. and Leidinger, P., 2014. *Diagnostic miRNA markers for Alzheimer*.

Kelley, D.E., Goodpaster, B., Wing, R.R. and Simoneau, J.A., 1999. Skeletal muscle fatty acid metabolism in association with insulin resistance, obesity, and weight loss. *American Journal of Physiology - Endocrinology and Metabolism* [Online], 277(6), pp.E1130-41. Available from: https://doi.org/10.1152/ajpendo.1999.277.6.e1130.

Kemp, P.R., Paul, R., Hinken, A.C., Neil, D., Russell, A. and Griffiths, M.J., 2020. Metabolic profiling shows pre-existing mitochondrial dysfunction contributes to muscle loss in a model of ICU-acquired weakness. *Journal of Cachexia, Sarcopenia and Muscle* [Online], 11(5), pp.1321–1335. Available from:

https://doi.org/10.1002/jcsm.12597.

Khadka, M., Todor, A., Maner-Smith, K.M., Colucci, J.K., Tran, V., Gaul, D.A., Anderson, E.J., Natrajan, M.S., Rouphael, N., Mulligan, M.J., McDonald, C.E., Suthar, M., Li, S. and Ortlund, E.A., 2019. The Effect of Anticoagulants, Temperature, and Time on the Human Plasma Metabolome and Lipidome from Healthy Donors as Determined by Liquid Chromatography-Mass Spectrometry. *Biomolecules*, 9(200).

Khatri, P., Sirota, M. and Butte, A.J., 2012. Ten Years of Pathway Analysis: Current Approaches and Outstanding Challenges. *PLOS Computational Biology* [Online], 8(2), p.e1002375. Available from: https://doi.org/10.1371/journal.pcbi.1002375.

Khoramipour, K., Sandbakk, Ø., Keshteli, A.H., Abbas, K., Gaeini, A.A., Wishart, D.S. and Chamari, K., 2022. *Metabolomics in Exercise and Sports: A Systematic Review* [Online]. Springer International Publishing. Available from: https://doi.org/10.1007/s40279-021-01582-y.

Kim, H., Lee, H., Kim, I., Kim, Y., Ji, M., Oh, S., Kim, D., Lee, W., Kim, S. and Paik, M., 2022. Comprehensive Targeted Metabolomic Study in the Lung, Plasma, and Urine of PPE/LPS-Induced COPD Mice Model. *International Journal of Molecular Sciences*, 23(2748).

Kim, J.H., Lim, S., Choi, S.H., Kim, K.M., Yoon, J.W., Kim, K.W., Lim, J.Y., Park, K.S. and Jang, H.C., 2014. Sarcopenia: An independent predictor of mortality in community-dwelling older Korean men. *Journals of Gerontology - Series A Biological Sciences and Medical Sciences* [Online], 69(10), pp.1244–1252. Available from: https://doi.org/10.1093/gerona/glu050.

Kim, S., Cheon, H.S., Song, J.C., Yun, S.M., Park, S.I. and Jeon, J.P., 2014. Aging-related Changes in Mouse Serum Glycerophospholipid Profiles. *Osong Public Health and Research Perspectives* [Online], 5(6), pp.345–350. Available from: https://doi.org/10.1016/j.phrp.2014.10.002.

Kloos, D.P., Lingeman, H., Niessen, W.M.A., Deelder, A.M., Giera, M. and Mayboroda, O.A., 2013. Evaluation of different column chemistries for fast urinary metabolic profiling. *Journal of Chromatography B: Analytical Technologies in the Biomedical and Life Sciences* [Online], 927, pp.90–96. Available from: https://doi.org/10.1016/j.jchromb.2013.02.017.

Kokla, M., Virtanen, J., Kolehmainen, M., Paananen, J. and Hanhineva, K., 2019. Random forest-based imputation outperforms other methods for imputing LC-MS metabolomics data : a comparative study. *BMC Bioinformatics*, 20(492).

Korostishevsky, M., Steves, C.J., Malkin, I., Spector, T., Williams, F.M.K. and Livshits, G., 2016. Genomics and metabolomics of muscular mass in a community-based sample of UK females. *European Journal of Human Genetics* [Online], 24(2), pp.277–283. Available from: https://doi.org/10.1038/ejhg.2015.85.

Koves, T.R., Ussher, J.R., Noland, R.C., Slentz, D., Mosedale, M., Ilkayeva, O., Bain, J., Stevens, R., Dyck, J.R.B., Newgard, C.B., Lopaschuk, G.D. and Muoio, D.M., 2008. Mitochondrial Overload and Incomplete Fatty Acid Oxidation Contribute to Skeletal Muscle Insulin Resistance. *Cell Metabolism* [Online], 7(1), pp.45–56. Available from: https://doi.org/10.1016/j.cmet.2007.10.013.

Kulesa, A., Krzywinski, M., Blainey, P. and Altman, N., 2015. Sampling distributions and the bootstrap. *Nature Publishing Group* [Online], 12(6), pp.477–478. Available from: https://doi.org/10.1038/nmeth.3414.

Kumar, V., Selby, A., Rankin, D., Patel, R., Atherton, P., Hildebrandt, W., Williams, J., Smith, K., Seynnes, O., Hiscock, N. and Rennie, M.J., 2009. Age-related differences in the dose-response relationship of muscle protein synthesis to resistance exercise in young and old men. *Journal of Physiology* [Online], 587(1), pp.211–217. Available from: https://doi.org/10.1113/jphysiol.2008.164483.

Kuo, W.-K., Liu, Y.-C., Hua, C.-C., Huang, C.-Y., Liu, M.-H. and Wang, C.-H., 2019. Amino Acid-Based Metabolic Indexes Identify Patients With Chronic Obstructive Pulmonary Disease And Further Discriminates Patients In Advanced BODE Stages. *International Journal of Chronic Obstructive Pulmonary Disease*, 14, pp.2257–2266.

Kwak, J.Y. and Kwon, K., 2019. Pharmacological Interventions for Treatment of Sarcopenia: Current Status of Drug Development for Sarcopenia. *Annals of Geriatric Medicine and Research*, 23(3), pp.98–104.

Kwon, Y.W., Jo, H.-S., Bae, S., Seo, Y., Song, P., Song, M. and Yoon, J.H., 2021. Application of Proteomics in Cancer : Recent Trends and Approaches for Biomarkers Discovery. *Frontiers in Medicine* [Online], 8(747333). Available from: https://doi.org/10.3389/fmed.2021.747333.

Lai, X., Bo, L., Zhu, H., Chen, B., Wu, Z., Du, H. and Huo, X., 2021. Effects of lower limb resistance exercise on muscle strength, physical fitness, and metabolism in pre-frail elderly patients: a randomized controlled trial. *BMC Geriatrics*, 21(447).

Landi, F., Liperoti, R., Russo, A., Giovannini, S., Tosato, M., Capoluongo, E., Bernabei, R. and Onder, G., 2012. Sarcopenia as a risk factor for falls in elderly individuals: Results from the ilSIRENTE study. *Clinical Nutrition* [Online], 31(5), pp.652–658. Available from: https://doi.org/10.1016/j.clnu.2012.02.007.

Lang, T., Cauley, J.A., Tylavsky, F., Bauer, D., Cummings, S. and Harris, T.B., 2010. Computed Tomographic Measurements of Thigh Muscle Cross-Sectional Area and Attenuation Coefficient Predict Hip Fracture: The Health, Aging, and Body Composition Study. *Journal of Bone and Mineral Research* [Online], 25(3), pp.513–519. Available from: https://doi.org/10.1359/jbmr.090807.

Langfelder, P. and Horvath, S., 2008. WGCNA: An R package for weighted correlation network analysis. *BMC Bioinformatics* [Online], 9(559). Available from: https://doi.org/10.1186/1471-2105-9-559.

Latimer, L.E., Constantin-Teodosiu, D., Popat, B., Constantin, D., Houchen-Wolloff, L., Bolton, C.E., Steiner, M.C. and Greenhaff, P.L., 2021. Whole-body & muscle responses to aerobic exercise training and withdrawal in ageing & COPD. *European Respiratory Journal* [Online], p.2101507. Available from: https://doi.org/10.1183/13993003.01507-2021.

Law, S.H., Chan, M.L., Marathe, G.K., Parveen, F., Chen, C.H. and Ke, L.Y., 2019. An updated review of lysophosphatidylcholine metabolism in human diseases. *International Journal of Molecular Sciences* [Online], 20(1149). Available from: https://doi.org/10.3390/ijms20051149.

Law, T.D., Clark, L.A. and Clark, B.C., 2016. Resistance Exercise to Prevent and Manage Sarcopenia and Dynapenia. *Annual Review of Gerontology and Geriatrics* [Online], 36(1), pp.205–228. Available from: https://doi.org/10.1891/0198-8794.36.205.Resistance.

Laye, M.J., Rector, R.S., Borengasser, S.J., Naples, S.P., Uptergrove, G.M., Ibdah, J.A., Booth, F.W. and Thyfault, J.P., 2009. Cessation of daily wheel running differentially alters fat oxidation capacity in liver , muscle , and adipose tissue.

Journal of Applied Physiology [Online], 106, pp.161–168. Available from: https://doi.org/10.1152/japplphysiol.91186.2008.

LeBlanc, A.D., Schneider, V.S., Evans, H.J., Pientok, C., Rowe, R. and Spector, E., 1992. Regional changes in muscle mass following 17 weeks of bed rest. *Journal of Applied Physiology* [Online], 73(5), pp.2172–2178. Available from: https://doi.org/10.1152/jappl.1992.73.5.2172.

Lee, I.-M., Shiroma, E.J., Lobelo, F., Puska, P., Blair, S.N. and Katzmarzyk, P.T., 2012. Impact of Physical Inactivity on the World's Major Non-Communicable Diseases. *Lancet* [Online], 380(9838), pp.219–229. Available from: https://doi.org/10.1016/S0140-6736(12)61031-9.Impact.

Lee, J.H., Okuno, Y. and Cavagnero, S., 2014. Sensitivity Enhancement in Solution NMR: Emerging Ideas and New Frontiers. *Journal of Magnetic Resonance* [Online], 241(4), pp.18–31. Available from: https://doi.org/10.1016/j.jmr.2014.01.005.Sensitivity.

Lee, L.C., Liong, C.-Y. and Jemain, A.A., 2018. Partial least squares-discriminant analysis (PLS-DA) for classification of high-dimensional (HD) data: a review of contemporary practice strategies and knowledge gaps. *Analyst* [Online], 143, pp.3526–3539. Available from: https://doi.org/10.1039/c8an00599k.

Lee, S., Norheim, F., Gulseth, H.L., Langleite, T.M., Aker, A., Gundersen, T.E., Holen, T., Birkeland, K.I. and Drevon, C.A., 2018. Skeletal muscle phosphatidylcholine and phosphatidylethanolamine respond to exercise and influence insulin sensitivity in men. *Scientific Reports* [Online], 8(6531). Available from: https://doi.org/10.1038/s41598-018-24976-x.

Lei, Z., Huhman, D. V. and Sumner, L.W., 2011. Mass spectrometry strategies in

metabolomics. *Journal of Biological Chemistry* [Online], 286(29), pp.25435–25442. Available from: https://doi.org/10.1074/jbc.R111.238691.

Leitao, L., Pereira, A., Mazini, M., Venturini, G., Campos, Y., Vieira, J., Novaes, J., Vianna, J., de Silva, S. and Louro, H., 2019. Effects of Three Months of Detraining on the Health Profile of Older Women after a Multicomponent Exercise Program. *International Journal of Environmental Research and Public Health*, 16(3881).

Leonardi, R. and Jackowski, S., 2007. Biosynthesis of Pantothenic Acid and Coenzyme A. *EcoSal Plus* [Online], 2(2). Available from: https://doi.org/10.1128/ecosalplus.3.6.3.4.Biosynthesis.

Leung, K.S.Y. and Fong, B.M.W., 2014. LC-MS/MS in the routine clinical laboratory: Has its time come? *Analytical and Bioanalytical Chemistry* [Online], 406, pp.2289–2301. Available from: https://doi.org/10.1007/s00216-013-7542-5.

Lewis, G.D., Farrell, L., Wood, M.J., Martinovic, M., Arany, Z., Rowe, G.C., Souza, A., Cheng, S., McCabe, E.L., Yang, E., Shi, X., Deo, R., Roth, F.P., Asnani, A., Rhee, E.P., Systrom, D.M., Semigran, M.J., Vasan, R.S., Carr, S.A., Wang, T.J., Sabatine, M.S., Clish, C.B. and Gerszten, R.E., 2010. Metabolic Signatures of Exercise in Human Plasma. *Science Translational Medicine*, 2(33), pp.33–37.

Li, B., Tang, J., Yang, Q., Cui, X., Li, S., Chen, S., Cao, Q., Xue, W., Chen, N. and Zhu, F., 2016. Performance Evaluation and Online Realization of Data- driven Normalization Methods Used in LC / MS based Untargeted Metabolomics Analysis. *Scientific Reports* [Online], 6(8). Available from: https://doi.org/10.1038/srep38881.

Li, Chun-wei, Yu, K., Shyh-chang, N., Jiang, Z., Liu, T., Ma, S., Luo, L., Guang, L., Liang, K., Ma, W., Miao, H., Cao, W., Liu, R., Jiang, L., Yu, S., Li, Chao, Liu, H., Xu, L.,

Zhang, X. and Liu, G., 2022. Pathogenesis of sarcopenia and the relationship with fat mass: descriptive review. *Journal of Cachexia, Sarcopenia and Muscle* [Online], 13(2), pp.781–794. Available from: https://doi.org/10.1002/jcsm.12901.

Li, S., Park, Y., Duraisingham, S., Strobel, F.H., Khan, N., Soltow, Q.A., Jones, D.P. and Pulendran, B., 2013. Predicting Network Activity from High Throughput Metabolomics. *PLOS Computational Biology* [Online], 9(7). Available from: https://doi.org/10.1371/journal.pcbi.1003123.

Li, S., Sullivan, N.L., Rouphael, N., Yu, T., Banton, S., Maddur, M.S., McCausland, M., Chiu, C., Canniff, J., Dubey, S., Liu, K., Tran, V.L., Hagan, T., Duraisingham, S., Wieland, A., Mehta, A.K., Whitaker, J.A., Subramaniam, S., Jones, D.P., Sette, A., Vora, K., Weinberg, A., Mulligan, M.J., Nakaya, H.I., Levin, M., Ahmed, R. and Pulendran, B., 2017. Metabolic Phenotypes of Response to Vaccination in Humans. *Cell* [Online], 169(5), pp.862–877. Available from: https://doi.org/10.1016/j.cell.2017.04.026.

Li, Y. and Li, L., 2020. Retention time shift analysis and correction in chemical isotope labeling liquid chromatography / mass spectrometry for metabolome analysis. *Rapid Communications in Mass Spectrometry* [Online], 34(S1), p.e8643. Available from: https://doi.org/10.1002/rcm.8643.

Lin, C., Han, G., Ning, H., Song, J., Ran, N., Yi, X., Seow, Y. and Yin, H.F., 2020. Glycine Enhances Satellite Cell Proliferation, Cell Transplantation, and Oligonucleotide Efficacy in Dystrophic Muscle. *Molecular Therapy* [Online], 28(5), pp.1339–1358. Available from: https://doi.org/10.1016/j.ymthe.2020.03.003.

Ling, S.M., Conwit, R.A., Ferrucci, L. and Metter, E.J., 2009. Age-Associated Changes in

Motor Unit Physiology: Observations From the Baltimore Longitudinal Study of Aging. *Archives of Physical Medicine and Rehabilitation* [Online], 90(7), pp.1237–1240. Available from: https://doi.org/10.1016/j.apmr.2008.09.565.

Liu, G., Lee, D.P., Schmidt, E. and Prasad, G.L., 2019. Pathway Analysis of Global Metabolomic Profiles Identified Enrichment of Caffeine, Energy, and Arginine Metabolism in Smokers but Not Moist Snuff Consumers. *Bioinformatics and Biology Insights* [Online], 13, pp.1–11. Available from: https://doi.org/10.1177/1177932219882961.

Liu, X. and Locasale, J.W., 2017. Metabolomics: A Primer. *Trends in Biochemical Sciences* [Online], 42(4), pp.274–284. Available from: https://doi.org/10.1016/j.tibs.2017.01.004.

Low, T.Y., Heesch, S. Van, Toorn, H. Van Den, Giansanti, P., Cristobal, A., Toonen, P., Schafer, S., Hu, N., Breukelen, B. Van, Mohammed, S., Cuppen, E., Heck, A.J.R. and Guryev, V., 2013. Resource Quantitative and Qualitative Proteome Characteristics Extracted from In-Depth Integrated Genomics and Proteomics Analysis. *Cell Reports* [Online], 5, pp.1469–1478. Available from: https://doi.org/10.1016/j.celrep.2013.10.041.

Lu, W., Bennett, B.D. and Rabinowitz, J.D., 2008. Analytical strategies for LC-MS-based targeted metabolomics. *Journal of Chromatography B: Analytical Technologies in the Biomedical and Life Sciences* [Online], 871(2), pp.236–242. Available from: https://doi.org/10.1016/j.jchromb.2008.04.031.

Lu, W., Su, X., Klein, M.S., Lewis, I.A., Fiehn, O. and Rabinowitz, J.D., 2017. Metabolite Measurement: Pitfalls to Avoid and Practices to Follow. *Annual Review of Biochemistry* [Online], 86(Jun 20), pp.277–304. Available from:

https://doi.org/10.1146/annurev-biochem-061516-044952.Metabolite.

Luo, S., Chen, X., Hou, L., Yue, J., Liu, X., Wang, Y., Xia, X. and Dong, B., 2021. The Relationship between Sarcopenia and Vitamin D Levels in Adults of Different Ethnicities: Findings from the West China Health and Aging Trend Study. *Journal of Nutrition, Health & Aging*, 25(7), pp.909–913.

Lustgarten, M.S., Price, L.L., Chale, A., Phillips, E.M. and Fielding, R.A., 2014. Branched Chain Amino Acids Are Associated With Muscle Mass in Functionally Limited Older Adults. *The journals of gerontology. Series A, Biological sciences and medical sciences* [Online], 69(6), pp.717–724. Available from: https://doi.org/10.1093/gerona/glt152.

Lv, Z., Gong, Z.-G. and Xu, Y.-J., 2022. Research in the Field of Exercise and Metabolomics: A Bibliometric and Visual Analysis. *Metabolites*, 12(542).

Mador, M.J., Bozkanat, E., Aggarwal, A., Shaffer, M. and Kufel, T.J., 2004. Endurance and strength training in patients with COPD. *Chest* [Online], 125(6), pp.2036–2045. Available from: https://doi.org/10.1378/chest.125.6.2036.

Maekawa, S., Takada, S., Nambu, H., Furihata, T., Kakutani, N., Setoyama, D., Ueyanagi, Y., Kang, D., Sabe, H. and Kinugawa, S., 2019. Linoleic acid improves assembly of the CII subunit and CIII2/CIV complex of the mitochondrial oxidative phosphorylation system in heart failure. *Cell Communication and Signaling* [Online], 17(128). Available from: https://doi.org/10.1186/s12964-019-0445-0.

Mahadevan, S., Shah, S.L., Marrie, T.J. and Slupsky, C.M., 2008. Analysis of Metabolomic Data Using Support Vector Machines. *Analytical Chemistry*, 80(19), pp.7562–7570.

Mapstone, M., Cheema, A.K., Fiandaca, M.S., Zhong, X., Mhyre, T.R., Macarthur, L.H.,

Hall, W.J., Fisher, S.G., Peterson, D.R., Haley, J.M., Nazar, M.D., Rich, S.A., Berlau, D.J., Peltz, C.B., Tan, M.T., Kawas, C.H. and Federoff, H.J., 2014. Plasma phospholipids identify antecedent memory impairment in older adults. *Nature Medicine* [Online], 20(4), pp.415–418. Available from: https://doi.org/10.1038/nm.3466.

Marantes, I., Achenbach, S.J., Atkinson, E.J., Khosla, S., Melton III, L.J. and Amin, S., 2012. Is Vitamin D a Determinant of Muscle Mass and Strength. *Journal of Bone and Mineral Research* [Online], 26(12), pp.2860–2871. Available from: https://doi.org/10.1002/jbmr.510.Is.

Maroon, J.C., Mathyssek, C.M., Bost, J.W., Amos, A., Winkelman, R., Yates, A.P., Duca, M.A. and Norwig, J.A., 2013. Vitamin D Profile in National Football League Players. *The American Journal of Sports Medicine* [Online], 43(5), pp.1241–1245. Available from: https://doi.org/10.1177/0363546514567297.

Mavers, M., Ruderman, E.M. and Perlman, H., 2009. Intracellular Signal Pathways: Potential for Therapies. *Current Rheumatology Reports*, 11(5), pp.378–385.

McClain, K.M., Moore, S.C., Sampson, J.N., Henderson, T.R., Gebauer, S.K., Newman, J.W., Ross, S., Pedersen, T.L., Baer, D.J. and Zanetti, K.A., 2020. Practice of Epidemiology Preanalytical Sample Handling Conditions and Their Effects on the Human Serum Metabolome in Epidemiologic Studies. *American Journal of Epidemiology* [Online], 190(3), pp.459–467. Available from: https://doi.org/10.1093/aje/kwaa202.

McGill, M.R., Li, F., Sharpe, M.R., Williams, C.D., Curry, S.C., Ma, X. and Jaeschke, H., 2014. Circulating acylcarnitines as biomarkers of mitochondrial dysfunction after acetaminophen overdose in mice and humans. *Archives of Toxicology* [Online],

88(2), pp.391–401. Available from: https://doi.org/10.1007/s00204-013-1118-1.

Mcleod, J.C., Stokes, T. and Phillips, S.M., 2019. Resistance exercise training as a primary countermeasure to age-related chronic disease. *Frontiers in Physiology* [Online], 10(645). Available from: https://doi.org/10.3389/fphys.2019.00645.

Mejia, E.M. and Hatch, G.M., 2016. Mitochondrial phospholipids: role in mitochondrial function. *Journal of Bioenergetics and Biomembranes* [Online], 48, pp.99–112. Available from: https://doi.org/10.1007/s10863-015-9601-4.

Melanson, E.L., Sharp, T.A., Schneider, J., Donahoo, W.T., Grunwald, G.K. and Hill, J.O., 2003. Relation between calcium intake and fat oxidation in adult humans. *International Journal of Obesity* [Online], 27(2), pp.196–203. Available from: https://doi.org/10.1038/sj.ijo.802202.

Mendez, K.M., Reinke, S.N. and Broadhurst, D.I., 2019. A comparative evaluation of the generalised predictive ability of eight machine learning algorithms across ten clinical metabolomics data sets for binary classification. *Metabolomics* [Online], 15(12). Available from: https://doi.org/10.1007/s11306-019-1612-4.

Mendoza-Garces, L., Velaquez-Alva, M.C., Cabrer-Rosales, M.F., Arrieta-Cruz, I., Gutierrez-Juarez, R. and Irigoyen-Camacho, M.E., 2021. Vitamin D Deficiency is Associated with Handgrip Strength, Nutritional Status and T2DM in Community-Dwelling Older. *Nutrients*, 13(736).

Michaeloudes, C., Kuo, C.H., Haji, G., Finch, D.K., Halayko, A.J., Kirkham, P., Chung, K.F., Barnes, P.J., Brightling, C.E., Davies, D.E., Fisher, A.J., Gaw, A., Knox, A.J., Mayer, R.J., Polkey, M., Salmon, M., Sanchez, Y., Singh, D. and Tal-Singer, R., 2017. Metabolic re-patterning in COPD airway smooth muscle cells. *European Respiratory Journal* [Online], 50(5). Available from:

https://doi.org/10.1183/13993003.00202-2017.

Michalski, A., Damoc, E., Hauschild, J.-P., Lange, O., Wieghaus, A., Makarov, A., Nagaraj, N., Cox, J., Mann, M. and Horning, S., 2011. Mass Spectrometry-based Proteomics Using Q Exactive, a High-performance Benchtop Quadrupole Orbitrap Mass Spectrometer. *Molecular and Cellular Proteomics* [Online], 10(9), p.M111.011015. Available from: https://doi.org/10.1074/mcp.M111.011015.

Michalski, A., Damoc, E., Lange, O., Denisov, E., Nolting, D., Mu, M., Viner, R., Schwartz, J., Remes, P., Belford, M., Dunyach, J.-J., Cox, J., Horning, S., Mann, M. and Makarov, A., 2012. Ultra High Resolution Linear Ion Trap Orbitrap Mass Spectrometer (Orbitrap Elite) Facilitates Top Down LC MS/MS and Versatile Peptide Fragmentation Modes. *Molecular and Cellular Proteomics* [Online], 11(3). Available from: https://doi.org/10.1074/mcp.O111.013698.

Mielke, M.M., Bandaru, V.V.R., Haughey, N.J., Xia, J., Fried, L.P., Yasar, S., Albert, M., Varma, V., Harris, G., Schneider, E.B., Rabins, P. V., Bandeen-Roche, K., Lyketsos, C.G. and Carlson, M.C., 2012. Serum ceramides increase the risk of Alzheimer disease: The Women's Health and Aging Study II. *Neurology* [Online], 79(7), pp.633–641. Available from: https://doi.org/10.1212/WNL.0b013e318264e380.

Mikines, K.J., Richter, E.A., Dela, F. and Galbo, H., 1991. Seven days of bed rest decrease insulin action on glucose uptake in leg and whole body. *Journal of Applied Physiology* [Online], 70(3), pp.1245–1254. Available from: https://doi.org/10.1152/jappl.1991.70.3.1245.

Miller, B.F., Olesen, J.L., Hansen, M., Døssing, S., Crameri, R.M., Welling, R.J., Langberg, H., Flyvbjerg, A., Kjaer, M., Babraj, J.A., Smith, K. and Rennie, M.J., 2005. Coordinated collagen and muscle protein synthesis in human patella tendon and

quadriceps muscle after exercise. *Journal of Physiology* [Online], 3, pp.1021–1033. Available from: https://doi.org/10.1113/jphysiol.2005.093690.

Miller, J., Alsheri, A., Ramage, M.I., Stephens, N.A., Mullen, A.B., Boyd, M., Ross, J.A., Wigmore, S.J., Watson, D.G. and Skipworth, R.J.E., 2019. Plasma Metabolomics Identifies Lipid and Amino Acid Markers of Weight Loss in Patients with Upper Gastrointestinal Cancer. *Cancers* [Online], 11(10), p.1594. Available from: https://doi.org/10.3390/cancers11101594.

Miller, S.G., Hafen, P.S. and Brault, J., 2020. Increased Adenine Nucleotide Degradation in Skeletal Muscle Atrophy. *International Journal of Molecular Sciences*, 21(88).

Mitchell, W.K., Williams, J., Atherton, P., Larvin, M., Lund, J. and Narici, M., 2012. Sarcopenia, dynapenia, and the impact of advancing age on human skeletal muscle size and strength; a quantitative review. *Frontiers in Physiology* [Online], 3(260). Available from: https://doi.org/10.3389/fphys.2012.00260.

Moaddel, R., Fabbri, E., Khadeer, M.A., Carlson, O.D., Gonzalez-Freire, M., Zhang, P., Semba, R.D. and Ferrucci, L., 2016. Plasma Biomarkers of Poor Muscle Quality in Older Men and Women from the Baltimore Longitudinal Study of Aging. [Online], 71(10), pp.1266–1272. Available from: https://doi.org/10.1093/gerona/glw046.

Moisá, S.J., Shike, D.W., Graugnard, D.E., Rodriguez-zas, S.L., Everts, R.E., Lewin, H.A., Faulkner, D.B., Berger, L.L. and Loor, J.J., 2013. Bioinformatics Analysis of Transcriptome Dynamics During Growth in Angus Cattle Longissimus Muscle. *Bioinformatics and Biology Insights* [Online], 7, pp.253–270. Available from: https://doi.org/10.4137/BBI.S12328.

Molnar, I. and Horvath, C., 1976. Reverse-Phase Chromatography of Polar Biological Substances: Separation of Catechol Compounds by High-Performance Liquid

Chromatography. *Clinical Chemistry*, 22(9), pp.1497–1502.

Montoliu, I., Scherer, M., Beguelin, F., DaSilva, L., Mari, D., Salvioli, S., Martin, F.P.J., Capri, M., Bucci, L., Ostan, R., Garagnani, P., Monti, D., Biagi, E., Brigidi, P., Kussmann, M., Rezzi, S., Franceschi, C. and Collino, S., 2014. Serum profiling of healthy aging identifies phospho- and sphingolipid species as markers of human longevity. *Aging* [Online], 6(1), pp.9–25. Available from: https://doi.org/10.18632/aging.100630.

Mora-Rodriguez, R., Ortega, J.., Hamouti, N., Fernandez-Elias, V.., Canete Garcio-Prieto, J., Guadalupe-Grau, A., Martin-Garcia, M., Guio de Prada, V., Ara, I. and Martinez-Vizcaino, V., 2014. Nutrition , Metabolism & Cardiovascular Diseases Time-course effects of aerobic interval training and detraining in patients with metabolic syndrome. *Nutrition, Metabolism and Cardiovascular Diseases* [Online], 24(7), pp.792–798. Available from: https://doi.org/10.1016/j.numecd.2014.01.011.

Morgan, A.., Mooney, K.., Wilkinson, S.., Pickles, N.. and Mc Auley, M.., 2016. Cholesterol metabolism : A review of how ageing disrupts the biological mechanisms responsible for its regulation. *Ageing Research Reviews* [Online], 27, pp.108–124. Available from: https://doi.org/10.1016/j.arr.2016.03.008.

Morin, N., Visentin, V., Calise, D., Marti, L., Zorzano, A., Testar, X., Valet, P., Fischer, Y. and Carpene, C., 2002. Tyramine Stimulates Glucose Uptake in Insulin-Sensitive Tissues in Vitro and in Vivo via Its Oxidation by Amine Oxidases. *The Journal of Pharmacology and Experimental Therapeutics* [Online], 303(3), pp.1238–1247. Available from: https://doi.org/10.1124/jpet.102.040592.compounds.

Morley, J.E., Abbatecola, A.M., Argiles, J.M., Baracos, V., Bauer, J., Bhasin, S.,

Cederholm, T., Stewart Coats, A.J., Cummings, S.R., Evans, W.J., Fearon, K., Ferrucci, L., Fielding, R.A., Guralnik, J.M., Harris, T.B., Inui, A., Kalantar-Zadeh, K., Kirwan, B.A., Mantovani, G., Muscaritoli, M., Newman, A.B., Rossi-Fanelli, F., Rosano, G.M.C., Roubenoff, R., Schambelan, M., Sokol, G.H., Storer, T.W., Vellas, B., von Haehling, S., Yeh, S.S. and Anker, S.D., 2011. Sarcopenia With Limited Mobility: An International Consensus. *Journal of the American Medical Directors Association* [Online], 12(6), pp.403–409. Available from: https://doi.org/10.1016/j.jamda.2011.04.014.

Morville, T., Sahl, R.E., Moritz, T., Helge, J.W. and Clemmensen, C., 2020. Plasma Metabolome Profiling of Resistance Exercise and Endurance Exercise in Humans. *Cell Reports* [Online], 33(13), p.108554. Available from: https://doi.org/10.1016/j.celrep.2020.108554.

Moses, L. and Pachter, L., 2022. Museum of spatial transcriptomics. *Nature Methods* [Online], 19, pp.534–546. Available from: https://doi.org/10.1038/s41592-022-01409-2.

Mosole, S., Carraro, U., Kern, H., Loefler, S., Fruhmann, H., Vogelauer, M., Burggraf, S., Mayr, W., Krenn, M., Paternostro-sluga, T., Hamar, D., Cvecka, J., Sedliak, M., Tirpakova, V., Sarabon, N., Musaro, A., Sandri, M., Protasi, F., Nori, A., Pond, A. and Zampieri, S., 2014. Long-Term High-Level Exercise Promotes Muscle Reinnervation With Age. *Journal of Neuropathology & Experimental Neurology*, 73(4), pp.284–294.

Mukherjee, K., Edgett, B.A., Burrows, H.W., Castro, C., Griffin, J.L., Schwertani, G., Gurd, B.J. and Funk, C.D., 2014. Whole Blood Transcriptomics and Urinary Metabolomics to Define Adaptive Biochemical Pathways of High-Intensity Exercise in 50-60 Year Old Masters Athletes. *PLoS ONE* [Online], 9(3). Available

from: https://doi.org/10.1371/journal.pone.0092031.

Müller, M.J., Illner, K., Bosy-Westphal, A., Brinkmann, G. and Heller, M., 2001. Regional lean body mass and resting energy expenditure in non-obese adults. *European Journal of Nutrition*, 40(3), pp.93–97.

Muniz, C., Martin-Marin, L., Lopez, A., Sanchez-Gonzalez, B., Salar, A., Almeida, J., Sancho, J.-M., Ribera, J.M., Heras, C., Penalver, F.J., Gomez, M., Gonzalez-Barca, E., Alonso, N., Navarro, B., Olave, T., Sala, F., Conde, E., Marquez, J.A., Cabezudo, E., Cladera, A., Garcia-Malo, M., Caballero, M.D. and Orfao, A., 2014. Contribution of cerebrospinal fluid sCD19 levels to the detection of CNS lymphoma and its impact on disease outcome. *Blood* [Online], 123(12), pp.1864–1869. Available from: https://doi.org/10.1182/blood-2013-11-537993.C.M.

Munson, B., 2006. Chemical Ionization Mass Spectrometry: Theory and Applications. *Encyclopedia of Analytical Chemistry (Applicatiosn, Theory and Instrumentation)*, [Online]. pp.1–22. Available from: https://doi.org/10.1002/9780470027318.a6004.

Muoio, D.M., 2014. Metabolic inflexibility: When mitochondrial indecision leads to metabolic gridlock. *Cell* [Online], 159(6), pp.1253–1262. Available from: https://doi.org/10.1016/j.cell.2014.11.034.

Murton, A.J., Marimuthu, K., Mallinson, J.E., Selby, A.L., Smith, K., Rennie, M.J. and Greenhaff, P.L., 2015. Obesity appears to be associated with altered muscle protein synthetic and breakdown responses to increased nutrient delivery in older men, but not reduced muscle mass or contractile function. *Diabetes*, 64(9), pp.3160–3171.

Nasi, S., Ehirchiou, D., Chatzianastasiou, A., Nagahara, N., Papapetropoulos, A.,

Bertrand, J., Cirino, G., So, A. and Busso, N., 2020. The protective role of the 3-mercaptopyruvate sulfurtransferase (3-MST)-hydrogen sulfide (H2S) pathway against experimental osteoarthritis. *Arthritis Research & Therapy*, 22(49).

Nassar, A.., Parmentier, Y., Martinet, M. and Lee, D.., 2004. Liquid Chromatography – Accurate Radioisotope Counting and Microplate Scintillation Counter Technologies in Drug Metabolism Studies. *Journal of Chromatographic Science*, 42(August), pp.348–353.

Newsom, S.A., Brozinick, J.T., Kiseljak-vassiliades, K., Strauss, A.N., Bacon, S.D., Kerege, A.A., Bui, H.H., Sanders, P., Siddall, P., Wei, T., Thomas, M., Kuo, M.S., Nemkov, T., D'Alessandro, Angelo Hansen, K.C., Perreault, L. and Bergman, B.C., 2016. Skeletal muscle phosphatidylcholine and phosphatidylethanolamine are related to insulin sensitivity and respond to acute exercise in humans. *Journal of Applied Physiology* [Online], 120, pp.1355–1363. Available from: https://doi.org/10.1152/japplphysiol.00664.2015.

Ng, T.K.S., Kovalik, J.-P., Ching, J., Chan, A.W. and Matchar, D.B., 2021. Novel metabolomics markers are associated with pre-clinical decline in hand grip strength in community-dwelling older adults. *Mechanisms of Ageing and Development* [Online], 193(111405). Available from: https://doi.org/10.1016/j.mad.2020.111405.

Nielsen, J., Christensen, A.E., Nellemann, B. and Christensen, B., 2017. Lipid droplet size and location in human skeletal muscle fibers are associated with insulin sensitivity. *American Journal of Physiology - Endocrinology and Metabolism* [Online], 313(6), pp.721–730. Available from: https://doi.org/10.1152/ajpendo.00062.2017.

Nilsson, M.I., Mikhail, A., Lan, L., Carlo, A. Di, Hamilton, B., Barnard, K., Hettinga, B.P., Hatcher, E., Tarnopolsky, M.G., Nederveen, J.P., Bujak, A.L., May, L. and Tarnopolsky, M.A., 2020. A Five-Ingredient Nutritional Supplement and Home-Based Resistance Exercise Improve Lean Mass and Strength in Free-Living Elderly. *Nutrients* [Online], 12(8). Available from: https://doi.org/10.3390/nu12082391.

Noonan, V. and Dean, E., 2000. Submaximal Exercise Testing: Clinical Application and Interpretation. *Physical Therapy*, 80(8), pp.782–807.

Norton, J.A., Maher, M., Wesley, R., White, D. and Brennan, M.F., 1984. Glucose lntolerance in Sarcoma Patients. *Cancer*, 54(12), pp.3022–3027.

Nunes, V.S., Ferreira, S. and Rocha Quintão, E.C., 2022. Cholesterol metabolism in aging simultaneously altered in liver and nervous system. *Aging*, 14(3), pp.1549–1561.

O'Donnell, J.M., Pound, K., Xu, X. and Lewandowski, E.D., 2009. SERCA1 Expression Enhances the Metabolic Efficiency of Improved Contractility in Post Ischemic Hearts. *Journal of Molecular and Cellular Cardiology* [Online], 47(5), pp.614–621. Available from: https://doi.org/10.1016/j.yjmcc.2009.08.031.SERCA1.

Odom, G., Ban, J., Liu, L., Wang, L. and Chen, S., 2022. pathwayPCA: Integrative Pathway Analysis with Modern PCA Methodology and Gene Selection.

Ogura, S.-I., Maruyama, K., Hagiya, Y., Sugiyama, Y., Tsuchiya, K., Takahashi, K., Abe, F., Tabata, K., Okura, I., Nakajima, M. and Tanaka, T., 2011. The effect of 5-aminolevulinic acid on cytochrome c oxidase activity in mouse liver. *BMC Research Notes* [Online], 4(1), p.66. Available from: https://doi.org/10.1186/1756-0500-4-66.

Okabe, K., Yaku, K., Tobe, K. and Nakagawa, T., 2019. Implications of altered NAD

metabolism in metabolic disorders. *Journal of Biomedical Science*, 26(34).

Oliver, S.G., Winson, M.K., Kell, D.B. and Baganz, F., 1998. Systematic functional analysis of the yeast genome. *Trends in Biotechnology*, 16(9), pp.373–378.

Olszewski, K., Barsotti, A., Feng, X.-J., Momcilovic, M., Liu, K.G., Kim, J.-I., Morris, K., Lamarque, C., Gaffney, J., Yu, X., Patel, J.P., Rabinowitz, J.D., Shackelford, D.B. and Poyurovsky, M. V, 2022. Inhibition of glucose transport synergizes with chemical or genetic disruption of mitochondrial metabolism and suppresses TCA cycle-deficient tumors. *Cell Chemical Biology* [Online], 29(3), pp.423–435. Available from: https://doi.org/10.1016/j.chembiol.2021.10.007.

Ose, J., Gigic, B., Lin, T., Liesenfeld, D.B., Böhm, J., Nattenmüller, J., Scherer, D., Zielske, L., Schrotz-King, P., Habermann, N., Ochs-Balcom, H.M., Peoples, A.R., Hardikar, S., Li, C.I., Shibata, D., Figueiredo, J., Toriola, A.T., Siegel, E.M., Schmit, S., Schneider, M., Ulrich, A., Kauczor, H.U. and Ulrich, C.M., 2019. Multiplatform urinary metabolomics profiling to discriminate cachectic from non-cachectic colorectal cancer patients: Pilot results from the colocare study. *Metabolites* [Online], 9(178). Available from: https://doi.org/10.3390/metabo9090178.

Ottestad, I., Ulven, S.M., Oyri, L.K.L., Sandvei, K.S., Gjevestad, G.O., Bye, A., Sheikh, N.A., Biong, A.S., Andersen, L.F. and Holven, K.B., 2018. Reduced plasma concentration of branched-chain amino acids in sarcopenic older subjects: a cross-sectional study. *British Journal of Nutrition* [Online], 120(4), pp.445–453. Available from: https://doi.org/10.1017/S0007114518001307.

Overmyer, K.A., Evans, C.R., Qi, N.R., Minogue, C.E., Carson, J.J., Chermide-Scabbo, C.J., Koch, L.G., Britton, S.L., Pagliarini, D.J., Coon, J.J. and Burant, C.F., 2015. Maximal oxidative capacity during exercise is associated with fuel selection and

dynamic changes in mitochondrial protein acetylation. *Cell Metabolism* [Online], 21(3), pp.468–478. Available from: https://doi.org/10.1016/j.cmet.2015.02.007.Maximal.

Oza, V.H., Aicher, J.K. and Reed, L.K., 2019. Random forest analysis of untargeted metabolomics data suggests increased use of omega fatty acid oxidation pathway in drosophila melanogaster larvae fed a medium chain fatty acid rich high-fat diet. *Metabolites* [Online], 9(5). Available from: https://doi.org/10.3390/metabo9010005.

Pagano, A.F., Brioche, T., Arc-Chagnaud, C., Demangel, R., Chopard, A. and Py, G., 2018. Short-term disuse promotes fatty acid infiltration into skeletal muscle. *Journal of Cachexia, Sarcopenia and Muscle* [Online], 9, pp.335–347. Available from: https://doi.org/10.1002/jcsm.12259.

Paley, S. and Karp, P.D., 2021. The BioCyc Metabolic Network Explorer. *BMC Bioinformatics* [Online], 22(208). Available from: https://doi.org/10.1186/s12859-021-04132-5.

Palmer, B.F. and Clegg, D.J., 2022. Metabolic Flexibility and Its Impact on Health Outcomes. *Mayo Clinic Proceedings* [Online], 97(4), pp.761–776. Available from: https://doi.org/10.1016/j.mayocp.2022.01.012.

Pang, Z., Chong, J., Zhou, G., De Lima Morais, D.A., Chang, L., Barrette, M., Gauthier, C., Jacques, P.É., Li, S. and Xia, J., 2021. MetaboAnalyst 5.0: Narrowing the gap between raw spectra and functional insights. *Nucleic Acids Research* [Online], 49, pp.W388–W396. Available from: https://doi.org/10.1093/nar/gkab382.

Panuwet, P., Hunter Jr, R.E., Souza, P.E.., Chen, X., Radford, S.A., Cohen, J.R., Marder, M.E., Kartavenka, K., Ryan, P.B. and Boyd Barr, D., 2016. Biological Matrix Effects

in Quantitative Tandem Mass Spectrometry-Based Analytical Methods: Advancing Biomonitoring. *Critical Reviews in Analytical Chemistry* [Online], 46(2), pp.93–105. Available from: https://doi.org/10.1080/10408347.2014.980775.Biological.

Papsdorf, K. and Brunet, A., 2018. Linking Lipid Metabolism to Chromatin Regulation in Aging. *Trends in Cell Biology* [Online], 29(2), pp.97–116. Available from: https://doi.org/10.1016/j.tcb.2018.09.004.

Pasiakos, S.M., 2012. Exercise and amino acid anabolic cell signaling and the regulation of skeletal muscle mass. *Nutrients* [Online], 4(7), pp.740–758. Available from: https://doi.org/10.3390/nu4070740.

Patti, G.J., Tautenhahn, R. and Siuzdak, G., 2012. Meta-analysis of untargeted metabolomic data from multiple profiling experiments. *Nature Protocols* [Online], 7(3), pp.508–516. Available from: https://doi.org/10.1038/nprot.2011.454.Meta-Analysis.

Patti, M.E., Landaker, E J, Kahn, C R, Patti, M.-E., Brambilla, E., Luzi, L., Landaker, Edwin J and Kahn, C Ronald, 1998. Bidirectional modulation of insulin action by amino acids. *The Journal of Clinical Investigation*, 101(7), pp.1519–1529.

Pechlivanis, A., Kostidis, S., Saraslanidis, P., Petridou, A., Tsalis, G., Mougios, V., Gika, H.G., Mikros, E. and Theodoridis, G.A., 2010. H NMR-Based Metabonomic Investigation of the Effect of Two Different Exercise Sessions on the Metabolic Fingerprint of Human Urine. *Journal of Proteome Research*, 9, pp.6405–6416.

Peluso, A., Glen, R. and Ebbels, T.M.D., 2021. Multiple-testing correction in metabolome-wide association studies. *BMC Bioinformatics* [Online], 22(1). Available from: https://doi.org/10.1186/s12859-021-03975-2.

Pérez-Martin, A., Dumortier, M., Raynaud, E., Brun, J.F., Fédou, C., Bringer, J. and Mercier, J., 2001. Balance of substrate oxidation during submaximal exercise in lean and obese people. *Diabetes & Metabolism*, 27(4 Pt 1), pp.466–474.

Perez, E.R., Knapp, J.A., Horn, C.K., Stillman, S.L., Evans, J.E. and Arfsten, D.P., 2016. Comparison of LC-MS-MS and GC-MS analysis of benzodiazepine compounds included in the drug demand reduction urinalysis program. *Journal of Analytical Toxicology* [Online], 40(3), pp.201–207. Available from: https://doi.org/10.1093/jat/bkv140.

Periat, A., Grand-Guillaume Perrenoud, A. and Guillarme, D., 2013. Evaluation of various chromatographic approaches for the retention of hydrophilic compounds and MS compatibility †. *Journal of Separation Science* [Online], 36, pp.3141–3151. Available from: https://doi.org/10.1002/jssc.201300567.

Petersen, K.F. and Shulman, G.I., 2006. Etiology of Insulin Resistance. *The American Journal of Medicine* [Online], 119(5A), pp.10S-16S. Available from: https://doi.org/10.1016/j.amjmed.2006.01.009.

Petrova, O.E. and Sauer, K., 2017. High-Performance Liquid Chromatography (HPLC)-Based Detection and Quantitation of Cellular c-di-GMP. In: K. Sauer, ed. *c-di-GMP Signaling: Methods and Protocols*, [Online]. New York, NY: Springer New York, pp.33–43. Available from: https://doi.org/10.1007/978-1-4939-7240-1_4.

Phillips, B.E., Williams, J.P., Greenhaff, P.L., Smith, K. and Atherton, P.J., 2017. Physiological adaptations to resistance exercise as a function of age. *JCI insight* [Online], 2(17). Available from: https://doi.org/10.1172/jci.insight.95581.

Phillips, S.M., Green, H.J., Tarnopolsky, M.A., Heigenhauser, G.J.F., Hill, R.E. and Grant, S.M., 1996. Effects of training duration on substrate turnover and oxidation

during exercise. *Journal of Applied Physiology* [Online], 81(5), pp.2182–2191. Available from: https://doi.org/10.1152/jappl.1996.81.5.2182.

Phillips, S.M., Tipton, K.D., Aarsland, A., Wolf, S.E. and Wolfe, R.R., 1997. Mixed muscle protein synthesis and breakdown after resistance exercise in humans. *American Journal of Physiology - Endocrinology and Metabolism*, 273(1), pp.E99-107.

Piasecki, M., Ireland, A., Piasecki, J., Stashuk, D.W., Swiecicka, A., Rutter, M.K., Jones, D.A. and McPhee, J.S., 2018. Failure to expand the motor unit size to compensate for declining motor unit numbers distinguishes sarcopenic from non-sarcopenic older men. *Journal of Physiology* [Online], 596(9), pp.1627–1637. Available from: https://doi.org/10.1113/JP275520.

Picart-Armada, S., Fernández-Albert, F., Vinaixa, M., Yanes, O. and Perera-Lluna, A., 2018. FELLA: an R package to enrich metabolomics data. *BMC Bioinformatics*, 19(538).

Pin, F., Barreto, R., Couch, M.E., Bonetto, A. and O'Connell, T.M., 2019. Cachexia induced by cancer and chemotherapy yield distinct perturbations to energy metabolism. *Journal of Cachexia, Sarcopenia and Muscle* [Online], 10(1), pp.140–154. Available from: https://doi.org/10.1002/jcsm.12360.

Pinedo-Villanueva, R., Westbury, L.D., Syddall, H.E., Sanchez-Santos, M.T., Dennison, E.M., Robinson, S.M. and Cooper, C., 2018. Health Care Costs Associated With Muscle Weakness: A UK Population-Based Estimate. *Calcified Tissue International* [Online], 104(2), pp.137–144. Available from: https://doi.org/10.1007/s00223-018-0478-1.

Pitt, J.J., 2009. Principles and Applications of Liquid Chromatography- Mass Spectrometry in Clinical Biochemistry. *The Clinical Biochemist Reviews*, 30(1),

pp.19–34.

Pizzorno, J., 2014. Glutathione! *Integrative Medicine*, 13(1), pp.8–12.

Da Poian, A., El-Bacha, T. and Luz, M.R.M.., 2010. Nutrient Utilization in Humans: Metabolism Pathways. *Nature Education*, 3(9), p.11.

Polkey, M.I., 2002. Muscle metabolism and exercise tolerance in COPD. *Chest* [Online], 121(5 SUPPL.), pp.131S-135S. Available from: https://doi.org/10.1378/chest.121.5_suppl.131S.

Powell, D.J., Hajduch, E., Kular, G. and Hundal, H.S., 2003. Ceramide Disables 3-Phosphoinositide Binding to the Pleckstrin Homology Domain of Protein Kinase B (PKB)/Akt by a PKC_--Dependent Mechanism. *Molecular and Cellular Biology* [Online], 23(21), pp.7794–7808. Available from: https://doi.org/10.1128/MCB.23.21.7794.

Pradas, I., Jové, M., Huynh, K., Puig, J., Ingles, M., Borras, C., Viña, J., Meikle, P.J. and Pamplona, R., 2019. Exceptional human longevity is associated with a specific plasma phenotype of ether lipids. *Redox Biology* [Online], 21, p.101127. Available from: https://doi.org/10.1016/j.redox.2019.101127.

Probst, P., Bischl, B. and Boulesteix, A.-L., 2018. Tunability: Importance of Hyperparameters of Machine Learning Algorithms. *arXiv preprint arX*, 1802.09596.

Pruchnic, R., Katsiaras, A., He, J., Kelley, D.E., Winters, C. and Goodpaster, B.H., 2004. Exercise training increases intramyocellular lipid and oxidative capacity in older adults. *American Journal of Physiology - Endocrinology and Metabolism* [Online], 287(5), pp.857–862. Available from: https://doi.org/10.1152/ajpendo.00459.2003.

PubChem, 2022. *PubChem Compound Summary for 1-octadecanoyl-sn-glycero-3-phosphocholine*.

Purdom, T., Kravitz, L., Dokladny, K. and Mermier, C., 2018. Understanding the factors that effect maximal fat oxidation. *Journal of the International Society of Sports Nutrition* [Online], 15(3). Available from: https://doi.org/10.1186/s12970-018-0207-1.

Puthucheary, Z.A., Astin, R., Mcphail, M.J.., Saeed, S., Pasha, Y., Bear, D.E., Constantin, D., Velloso, C., Manning, S., Calvert, L., Singer, M., Batterham, R.L., Gomez-Romero, M., Holmes, E., Steiner, M.C., Atherton, P.J., Greenhaff, P., Edwards, L.M., Smith, K., Harridge, S.D., Hart, N. and Montgomery, H.E., 2018. Metabolic phenotype of skeletal muscle in early critical illness. *Thorax* [Online], 73, pp.1–10. Available from: https://doi.org/10.1136/thoraxjnl-2017-211073.

R Core Team, 2021. *R: A language and environment for statistical computing* [Online]. Available from: https://www.r-project.org/.

Raherison, C. and Girodet, P.O., 2009. Epidemiology of COPD. *European Respiratory Review* [Online], 18(114), pp.213–221. Available from: https://doi.org/10.1183/09059180.00003609.

Ramadoss, R., Stanzione, J.R. and Volpe, S.L., 2022. A Comparison of Substrate Utilization Profiles During Maximal and Submaximal Exercise Tests in Athletes. *Frontiers in Psychology* [Online], 13(April). Available from: https://doi.org/10.3389/fpsyg.2022.854451.

Ramos-Jiménez, A., Hernández-Torres, R.P., Torres-Durán, P. V, Romero-Gonzalez, J., Mascher, D., Posadas-Romero, C. and Juárez-Oropeza, M.A., 2008. The Respiratory Exchange Ratio is Associated with Fitness Indicators Both in Trained

and Untrained Men : A Possible Application for People with Reduced Exercise Tolerance. *Clinical Medicine: Circulatory, Respiratory and Pulmonary*, 2, pp.1–9.

Redestig, H., Kobayashi, M., Saito, K. and Kusano, M., 2011. Exploring Matrix Effects and Quantification Performance in Metabolomics Experiments Using Artificial Biological Gradients. *Analytical Chemistry*, 83, pp.5645–5651.

Reimand, J., Isserlin, R., Voisin, V., Kucera, M., Tannus-lopes, C., Rostamianfar, A., Wadi, L., Meyer, M., Wong, J., Xu, C., Merico, D. and Bader, G.D., 2019. Pathway enrichment analysis and visualization of omics data using g:Profiler, GSEA, Cytoscape and EnrichmentMap. *Nature Protocols*, 14(2), pp.482–517.

Rejnmark, L., 2011. Effects of vitamin D on muscle function and performance : a review of evidence from randomized controlled trials. [Online], pp.25–37. Available from: https://doi.org/10.1177/2040622310381934.

Ren, J.L., Zhang, A.H., Kong, L. and Wang, X.J., 2018. Advances in mass spectrometry-based metabolomics for investigation of metabolites. *RSC Advances* [Online], 8(40), pp.22335–22350. Available from: https://doi.org/10.1039/c8ra01574k.

Rezaei, S., Gholamalizadeh, M., Tabrizi, R., Nowrouzi-Sohrabi, P., Rastgoo, S. and Doaei, S., 2021. The effect of L-arginine supplementation on maximal oxygen uptake: A systematic review and meta-analysis. *Physiological Reports* [Online], 9(3). Available from: https://doi.org/10.14814/phy2.14739.

Ritchie, M.E., Phipson, B., Wu, D., Hu, Y., Law, C.W., Shi, W. and Smyth, G.K., 2015. Limma powers differential expression analyses for RNA-sequencing and microarray studies. *Nucleic Acids Research* [Online], 43(7), p.e47. Available from: https://doi.org/10.1093/nar/gkv007.

Roberts, L.D., Souza, A.L., Gerszten, R.E. and Clish, C.B., 2012. Targeted metabolomics.

Current Protocols in Molecular Biology, [Online]. pp.30.2.1-30.2.4. Available from: https://doi.org/10.1002/0471142727.mb3002s98.

Rodríguez-Córdoba, D.P., Iglesia, I., Gomez-Bruton, A., Rodríguez, G., Casajús, J.A., Morales-Devia, H. and Moreno, L.A., 2022. Fat-free/lean body mass in children with insulin resistance or metabolic syndrome: a systematic review and meta-analysis. *BMC Pediatrics* [Online], 22(58). Available from: https://doi.org/10.1186/s12887-021-03041-z.

Rohen, A., Krause, J. and Cammann, K., 1990. Enzymatic photometric determination of lactate by reversible reduction of methylene blue. *Fresenius' Journal of Analytical Chemistry*, 338(2), pp.168–171.

Romijn, J.., Coyle, E.., Sidossis, L.., Gastaldelli, A., Horowitz, J.., Endert, E. and Wolfe, R.., 1993. Regulation in relation of endogenous fat and carbohydrate to exercise intensity and duration metabolism. *American Journal of Physiology - Endocrinology and Metabolism*, 265(28), pp.380–391.

Rossi, F.., Diniz, T.., Neves, L.., Fortaleza, A.C.., Inoue, D.., Buonani, C., Cholewa, J.., Lira, F.. and Freitas Jr, I.., 2017. The beneficial effects of aerobic and concurrent training on metabolic profile and body composition after detraining: a 1-year follow-up in postmenopausal women. *European Journal of Clinical Nutrition* [Online], 71(305), pp.638–645. Available from: https://doi.org/10.1038/ejcn.2016.263.

Roux, E. Le, De Jong, N., Blanc, S., Simon, C., Bessesen, D.H. and Bergouignan, A., 2021. Physiology of physical inactivity, sedentary behaviors and non-exercise activity: Insights from space bedrest model. *The Journal of Physiology* [Online]. Available from: https://doi.org/10.1113/jp281064.

Rudrappa, S.S., Wilkinson, D.J., Greenhaff, P.L., Smith, K., Idris, I. and Atherton, P.J., 2016. Human skeletal muscle disuse atrophy: Effects on muscle protein synthesis, breakdown, and insulin resistance-A qualitative review. *Frontiers in Physiology* [Online], 7(361). Available from: https://doi.org/10.3389/fphys.2016.00361.

Rudwill, F., O'Gorman, D., Lefai, E., Chery, I., Zahariev, A., Normand, S., Pagano, A.F., Chopard, A., Damiot, A., Laurens, C., Hodson, L., Canet-Soulas, E., Heer, M., Meuthen, P.F., Buehlmeier, J., Baecker, N., Meiller, L., Gauquelin-Koch, G., Blanc, S., Simon, C. and Bergouignan, A., 2018. Metabolic Inflexibility Is an Early Marker of Bed-Rest-Induced Glucose Intolerance even When Fat Mass Is Stable. *Journal of Clinical Endocrinology and Metabolism* [Online], 103(5), pp.1910–1920. Available from: https://doi.org/10.1210/jc.2017-02267.

Ruiz-Perez, D., Guan, H., Madhivanan, P., Mathee, K. and Narasimhan, G., 2020. So you think you can PLS-DA? *BMC Bioinformatics* [Online], 21(Suppl 1). Available from: https://doi.org/10.1186/s12859-019-3310-7.

Rusilowicz, M., Dickinson, M., Charlton, A., Keefe, S.O. and Wilson, J., 2016. A batch correction method for liquid chromatography – mass spectrometry data that does not depend on quality control samples. *Metabolomics* [Online], 12(56). Available from: https://doi.org/10.1007/s11306-016-0972-2.

Rusip, G., Suhartini, S.M. and Suen, A.B., 2018. Influence of exercise on plasma ammonia and urea after ingestion beverages of carbohydrate electrolyte. *Earth and Environmental Sciences*, 130(012020).

Rusli, H., Putri, R.M. and Alni, A., 2022. Recent Developments of Liquid Chromatography Stationary Phases for Compound Separation: From Proteins to

Small Organic Compounds. *Molecules*, 27(907).

Rutten, E.P.A., Engelen, M.P.K.J., Schols, A.M.W.J. and Deutz, N.E.P., 2005. Skeletal muscle glutamate metabolism in health and disease: State of the art. *Current Opinion in Clinical Nutrition and Metabolic Care* [Online], 8(1), pp.41–51. Available from: https://doi.org/10.1097/00075197-200501000-00007.

Ryan, M.M., Sy, C., Rudge, S., Ellaway, C., Ketteridge, D., Roddick, L.G., Iannaccone, S.T., Kornberg, A.J. and North, K.N., 2008. Dietary L-Tyrosine Supplementation in Nemaline Myopathy. *Journal of Child Neurology*, 23(6), pp.609–613.

Rygiel, K.A., Picard, M. and Turnbull, D.M., 2016. The ageing neuromuscular system and sarcopenia: a mitochondrial perspective. *Journal of Physiology* [Online], 594(16), pp.4499–4512. Available from: https://doi.org/10.1113/JP271212.

Saccenti, E., Hoefsloot, H.C.J., Smilde, A.K., Westerhuis, J.A. and Hendriks, M.M.W.., 2014. Reflections on univariate and multivariate analysis of metabolomics data. *Metabolomics* [Online], 10, pp.361–374. Available from: https://doi.org/10.1007/s11306-013-0598-6.

Sacket, S.J., Chung, H.Y., Okajima, F. and Im, D.S., 2009. Increase in sphingolipid catabolic enzyme activity during aging. *Acta Pharmacologica Sinica* [Online], 30(10), pp.1454–1461. Available from: https://doi.org/10.1038/aps.2009.136.

Saleem, M., Herrmann, N., Dinoff, A., Marzolini, S., Mielke, M.M., Andreazza, A., Oh, P.I., Lakshmi, S., Venkata, V., Haughey, N.J. and Lanctôt, K.L., 2020. Association Between Sphingolipids and Cardiopulmonary Fitness in Coronary Artery Disease Patients Undertaking Cardiac Rehabilitation. *Journals of Gerontology - Series A Biological Sciences and Medical Sciences* [Online], 75(4), pp.671–679. Available from: https://doi.org/10.1093/gerona/gly273.

Salek, R.M., Steinbeck, C., Viant, M.R., Goodacre, R. and Dunn, W.B., 2013. The role of reporting standards for metabolite annotation and identification in metabolomic studies. *GigaScience* [Online], 2(13). Available from: https://doi.org/10.1186/2047-217X-2-13.

Saltin, B. and Calbet, J.A.., 2006. Point: In health and in a normoxic environment, V̇o2 max is limited primarily by cardiac output and locomotor muscle blood flow. *American Journal of Physiology - Regulatory Integrative and Comparative Physiology* [Online], 290(2), pp.744–748. Available from: https://doi.org/10.1152/ajpregu.00332.2005.

Sangster, T., Major, H., Plumb, R., Wilson, A.J. and Wilson, I.D., 2006. A pragmatic and readily implemented quality control strategy for HPLC-MS and GC-MS-based metabonomic analysis. *Analyst* [Online], 131(i), pp.1075–1078. Available from: https://doi.org/10.1039/b604498k.

Saoi, M., Li, A., McGlory, C., Stokes, T., Von Allmen, M.T., Phillips, S.M. and Britz-McKibbin, P., 2019. Metabolic Perturbations from Step Reduction in Older Persons at Risk for Sarcopenia : Plasma Biomarkers of Abrupt Changes in Physical Activity. *Metabolites*, 9(7), p.134.

Sarafino, E.P. and Goldfedder, J., 1995. Genetic factors in the presence, severity, and triggers of asthma. *Archives of Disease in Childhood*, 73, pp.112–116.

Sato, S., Yoshida, R., Murakoshi, F., Sasaki, Y., Yahata, K., Kasahara, K., Nunes, J.P., Nosaka, K. and Nakamura, M., 2022. Comparison between concentric-only , eccentric-only, and concentric-eccentric resistance training of the elbow flexors for their effects on muscle strength and hypertrophy. *European Journal of Applied Physiology* [Online], 122(12), pp.2607–2614. Available from:

https://doi.org/10.1007/s00421-022-05035-w.

Scalbert, A., Brennan, L., Fiehn, O., Hankemeier, T., Kristal, B.S., van Ommen, B., Pujos-Guillot, E., Verheij, E., Wishart, D. and Wopereis, S., 2009. Mass-spectrometry-based metabolomics: limitations and recommendations for future progress with particular focus on nutrition research. *Metabolomics* [Online], 5, pp.435–458. Available from: https://doi.org/10.1007/s11306-009-0168-0.

Schiffman, C., Petrick, L., Perttula, K., Yano, Y., Carlsson, H., Whitehead, T., Metayer, C., Hayes, J., Rappaport, S. and Dudoit, S., 2019. Filtering procedures for untargeted LC-MS metabolomics data. *BMC Bioinformatics* [Online], 20(334). Available from: https://doi.org/10.1186/s12859-019-2871-9.

Schooneveldt, Y.L., Paul, S., Calkin, A.C. and Meikle, P.J., 2022. Ether Lipids in Obesity: From Cells to Population Studies. *Frontiers in Physiology* [Online], 13(841278). Available from: https://doi.org/10.3389/fphys.2022.841278.

Schranner, D., Kastenmüller, G., Schönfelder, M., Römisch-margl, W. and Wackerhage, H., 2020. Metabolite Concentration Changes in Humans After a Bout of Exercise: a Systematic Review of Exercise Metabolomics Studies. *Sports Medicine*, 6(11).

Schranner, D., Schönfelder, M., Römisch-Margl, W., Scherr, J., Schlegel, J., Zelger, O., Riermeier, A., Kaps, S., Prehn, C., Adamski, J., Söhnlein, Q., Stöcker, F., Kreuzpointner, F., Halle, M., Kastenmüller, G. and Wackerhage, H., 2021. Physiological extremes of the human blood metabolome: A metabolomics analysis of highly glycolytic, oxidative, and anabolic athletes. *Physiological Reports* [Online], 9(12). Available from: https://doi.org/10.14814/phy2.14885.

Schrimpe-Rutledge, A.C., Codreanu, S.G., Sherrod, S.D. and McLean, J.A., 2016. Untargeted Metabolomics Strategies—Challenges and Emerging Directions.

Journal of the American Society for Mass Spectrometry [Online], 27(12), pp.1897–1905. Available from: https://doi.org/10.1007/s13361-016-1469-y.

Schwanhäusser, B., Busse, D., Li, N., Dittmar, G., Schuchhardt, J., Wolf, J., Chen, W. and Selbach, M., 2011. Global quantification of mammalian gene expression control. *Nature* [Online], 473, pp.337–342. Available from: https://doi.org/10.1038/nature10098.

Seaton, M.E., Parent, B.A., Sood, R.F., Wurfel, M.M., Muffley, L.A. and Gibran, N.S., 2017. RISK OF COMPLICATED SEPSIS AFTER TRAUMA: A CANDIDATE GENE ASSOCIATION STUDY. *Shock* [Online], 47(1), pp.79–85. Available from: https://doi.org/10.1097/SHK.0000000000000708.MELANOCORTIN-1.

Shabir, G.., 2010. Development and Validation of a Reversed-phase HPLC Method for the Determination of Hydroxybenzene in a Cream Formulation. *Indian Journal of Pharmaceutical Sciences*, 72(3), pp.307–311.

Shafiee, G., Keshtkar, A., Soltani, A., Ahadi, Z., Larijani, B. and Heshmat, R., 2017. Prevalence of sarcopenia in the world: A systematic review and meta- analysis of general population studies. *Journal of Diabetes and Metabolic Disorders* [Online], 16(21). Available from: https://doi.org/10.1186/s40200-017-0302-x.

Shen, X., Wu, S., Liang, L., Chen, S., Contrepois, K., Zhu, Z.-J. and Snyder, M., 2022. metID: an R package for automatable compound annotation for LC–MS-based data. *Bioinformatics* [Online], 38(2), pp.568–569. Available from: https://doi.org/10.1093/bioinformatics/btab583.

Shen, X., Yan, H., Wang, C., Gao, P., Johnson, C.H. and Snyder, M.P., 2022. TidyMass an object-oriented reproducible analysis framework for LC-MS data. *Nature Communications* [Online], 13(4365). Available from:

https://doi.org/10.1038/s41467-022-32155-w.

Short, K.R., Bigelow, M.L., Kahl, J., Singh, R., Coenen-Schimke, J., Raghavakaimal, S. and Nair, K.S., 2005. Decline in skeletal muscle mitochondrial function with aging in humans. *Proceedings of the National Academy of Sciences of the United States of America* [Online], 102(15), pp.5618–5623. Available from: https://doi.org/10.1073/pnas.0501559102.

Shur, N.F., Simpson, E.J., Crossland, H., Chivaka, P.K., Constantin, D., Cordon, S.M., Constantin-teodosiu, D., Stephens, F.B., Lobo, D.N., Szewczyk, N., Narici, M., Prats, C., Macdonald, I.A. and Greenhaff, P.L., 2022. Human adaptation to immobilization : Novel insights of impacts on glucose disposal and fuel utilization. *Journal of Cachexia, Sarcopenia and Muscle* [Online]. Available from: https://doi.org/10.1002/jcsm.13075.

Singh, A., Faccenda, D. and Campanella, M., 2021. Pharmacological advances in mitochondrial therapy. *EBioMedicine* [Online], 65(103244). Available from: https://doi.org/10.1016/j.ebiom.2021.103244.

Siripoksup, P., Cao, G., Cluntun, A.A., Maschek, J.A., Pearce, Q., Lang, M.J., Eshima, H., Opurum, P.C., Mahmassani, Z.S., Taylor, E.B., Cox, J.E., Drummond, M.J., Rutter, J. and Funai, K., 2022. Phosphatidylethanolamine facilitates mitochondrial pyruvate entry to regulate metabolic flexibility. *bioRxiv* [Online], p.2022.11.01.514767. Available from: https://doi.org/10.1101/2022.11.01.514767.

Sket, R., Deutsch, L., Prevorsek, Z., Mekjavic, I.B., Plavec, J., Rittweger, J., Debevec, T., Eiken, O. and Stres, B., 2020. Systems View of Deconditioning During Spaceflight Simulation in the PlanHab Project: The Departure of Urine 1H-NMR

Metabolomes From Healthy State in Young Males Subjected to Bedrest Inactivity and Hypoxia. *Frontiers in Physiology* [Online], 11(December), p.532271. Available from: https://doi.org/10.3389/fphys.2020.532271.

Skipworth, R.J.E., Stewart, G.D., Dejong, C.H.C., Preston, T. and Fearon, K.C.H., 2007. Pathophysiology of cancer cachexia: Much more than host-tumour interaction? *Clinical Nutrition* [Online], 26(6), pp.667–676. Available from: https://doi.org/10.1016/j.clnu.2007.03.011.

Sleno, L. and Volmer, D.A., 2004. Ion activation methods for tandem mass spectrometry. *Journal of Mass Spectrometry* [Online], 39, pp.1091–1112. Available from: https://doi.org/10.1002/jms.703.

Smith, C.A., Want, E.J., O'Maille, G., Abagyan, R. and Siuzdak, G., 2006. XCMS: Processing mass spectrometry data for metabolite profiling using nonlinear peak alignment, matching and identification. *Analytical Chemistry*, 78, pp.779–787.

Smith, K., Barua, J.M., Watt, P.W., Scrimgeour, C.M. and Rennie, M.J., 1992. Flooding with L-[1-13C] leucine stimulates human muscle protein incorporation of continuously infused L-[1-13C] valine. *American Journal of Physiology - Endocrinology and Metabolism*, 262(3), pp.372–376.

Smith, K., Reynolds, N., Downie, S., Patel, A. and Rennie, M.J., 1998. Effects of flooding amino acids on incorporation of labeled amino acids into human muscle protein. *American Journal of Physiology - Endocrinology and Metabolism* [Online], 275(1 38-1), pp.73–78. Available from: https://doi.org/10.1152/ajpendo.1998.275.1.e73.

Smith, L., Villaret-Cazadamont, J., Claus, S.P., Canlet, C., Guillou, H., Cabaton, N.J. and Ellero-Simatos, S., 2020. Important considerations for sample collection in

metabolomics studies with a special focus on applications to liver functions. *Metabolites* [Online], 10(104). Available from: https://doi.org/10.3390/metabo10030104.

Smith, R.L., Soeters, M.R., Wust, R.C.. and Houtkooper, R.H., 2018. Metabolic Flexibility as an Adaptation to Energy. *Endocrine Reviews* [Online], 39(4), pp.489–517. Available from: https://doi.org/10.1210/er.2017-00211.

Smyth, G.K., 2004. Linear models and empirical bayes methods for assessing differential expression in microarray experiments. *Statistical Applications in Genetics and Molecular Biology* [Online], 3(1). Available from: https://doi.org/10.2202/1544-6115.1027.

Snell, N., Strachan, D., Hubbard, R., Gibson, J., Gruffydd-Jones, K. and Jarrold, I., 2016. S32 Epidemiology of chronic obstructive pulmonary disease (COPD) in the uk: findings from the british lung foundation's 'respiratory health of the nation' project. *Thorax* [Online], 71(Suppl 3), p.A20 LP-A20. Available from: https://doi.org/10.1136/thoraxjnl-2016-209333.38.

Sokolowska, E. and Blachnio-Zabielska, A., 2019. The Role of Ceramides in Insulin Resistance. *Frontiers in Endocrinology* [Online], 10(577). Available from: https://doi.org/10.3389/fendo.2019.00577.

Sorriento, D., Vaia, E. Di and Iaccarino, G., 2021. Physical Exercise: A Novel Tool to Protect Mitochondrial Health. *Frontiers in Physiology* [Online], 12(6600068). Available from: https://doi.org/10.3389/fphys.2021.660068.

Southam, A.D., Haglington, L.D., Najdekr, L., Jankevics, A., Weber, R.J.. and Dunn, W.B., 2020. Assessment of human plasma and urine sample preparation for reproducible and high-throughput UHPLC-MS clinical metabolic phenotyping.

Analyst [Online], 145, pp.6511–6523. Available from: https://doi.org/10.1039/d0an01319f.

Standley, R.A., Distefano, G., Trevino, M.B., Chen, E., Narain, N.R., Greenwood, B., Kondakci, G., Tolstikov, V. V, Kiebish, M.A., Yu, G., Qi, F., Daniel, P., Vega, R.B., Coen, P.M. and Goodpaster, B.H., 2020. Skeletal Muscle Energetics and Mitochondrial Function Are Impaired Following 10 Days of Bed Rest in Older Adults. *Journals of Gerontology: Medical Science* [Online], 75(9), pp.1744–1753. Available from: https://doi.org/10.1093/gerona/glaa001.

Stanworth, R.D. and Jones, T.H., 2008. Testosterone for the aging male; current evidence and recommended practice. *Clinical Interventions in Aging* [Online], 3(1), pp.25–44. Available from: https://doi.org/10.2147/cia.s190.

Starnes, J.W., Parry, T.L., Id, S.K.O.N., Bain, J.R., Muehlbauer, M.J., Honcoop, A., Ilaiwy, A., Christopher, P.M., Patterson, C. and Willis, M.S., 2017. Exercise-Induced Alterations in Skeletal Muscle, Heart, Liver, and Serum Metabolome Identified by Non-Targeted Metabolomics Analysis. *Metabolites* [Online], 7(40). Available from: https://doi.org/10.3390/metabo7030040.

Stephens, N.A., Skipworth, R.J.E., MacDonald, A.J., Greig, C.A., Ross, J.A. and Fearon, K.C.H., 2011. Intramyocellular lipid droplets increase with progression of cachexia in cancer patients. *Journal of Cachexia, Sarcopenia and Muscle* [Online], 2(2), pp.111–117. Available from: https://doi.org/10.1007/s13539-011-0030-x.

Straczkowski, M., Kowalska, I., Nikolajuk, A., Dzienis-straczkowska, S., Kinalska, I., Baranowski, M., Zendzian-piotrowska, M., Brzezinska, Z. and Gorski, J., 2004. Relationship Between Insulin Sensitivity and Sphingomyelin Signaling Pathway in Human. *Diabetes*, 53(17), pp.1215–1221.

Stuart, C.A., Shangraw, R.E., Prince, M.J., Peters, E.J. and Wolfe, R.R., 1988. Bed-rest-induced insulin resistance occurs primarily in muscle. *Metabolism* [Online], 37(8), pp.802–806. Available from: https://doi.org/10.1016/0026-0495(88)90018-2.

Stump, C.S., Henriksen, E.J., Wei, Y. and Sowers, J.R., 2006. The metabolic syndrome: Role of skeletal muscle metabolism. *Annals of Medicine* [Online], 38(6), pp.389–402. Available from: https://doi.org/10.1080/07853890600888413.

Sugino, T., Shirai, T., Kajimoto, Y. and Kajimoto, O., 2008. L-Ornithine supplementation attenuates physical fatigue in healthy volunteers by modulating lipid and amino acid metabolism. *Nutrition Research* [Online], 28(11), pp.738–743. Available from: https://doi.org/10.1016/j.nutres.2008.08.008.

Suiter, C.L., Paramasivam, S., Hou, G., Sun, S., Rice, D., Hoch, J.C., Rovnyak, D. and Polenova, T., 2014. Sensitivity gains, linearity, and spectral reproducibility in nonuniformly sampled multidimensional MAS NMR spectra of high dynamic range. *Journal of Biomolecular NMR* [Online], 59, pp.57–73. Available from: https://doi.org/10.1007/s10858-014-9824-4.

Summers, S.A., Chaurasia, B. and Holland, W.L., 2019. Metabolic Messengers: ceramides. *Nature Metabolism* [Online], 1(11), pp.1051–1058. Available from: https://doi.org/10.1038/s42255-019-0134-8.Metabolic.

Suryadinata, R.V., Wirjatmadi, B., Adriani, M. and Lorensia, A., 2020. Effect of age and weight on physical activity. *Journal of Public Health Research*, 9(1840), pp.187–190.

Tai, E.., Tan, M.L.., Stevens, R.., Low, Y.., Muehlbauer, M.., Goh, D.L.., Ilkayeva, O.., Wenner, B.., Bain, J.., Lee, J.J.., Lim, S.., Khoo, C.., Shah, S.. and Newgard, C.., 2010. Insulin resistance is associated with a metabolic profile of altered protein

metabolism in Chinese and Asian-Indian men. *Diabetologia* [Online], 53(4), pp.757–767. Available from: https://doi.org/10.1007/s00125-009-1637-8.

Tajiri, Y., Ph, D., Kato, T., Nakayama, H., Yamada, K. and Ph, D., 2010. Reduction of Skeletal Muscle, Especially in Lower Limbs, in Japanese Type 2 Diabetic Patients With Insulin Resistance and Cardiovascular Risk Factors. *Metabolic Syndrome and Related Disorders* [Online], 8(2), pp.137–142. Available from: https://doi.org/10.1089/met.2009.0043.

Takamori, M., 1977. Nerve, muscle, and serotonin. *Journal of Neurology, Neurosurgery & Psychiatry*, 40(1), pp.89–96.

Tammineni, E.R., Kraeva, N., Figueroa, L., Manno, C., Ibarra, C.A., Klip, A., Riazi, S. and Rios, E., 2020. Intracellular calcium leak lowers glucose storage in human muscle , promoting hyperglycemia and diabetes. *eLife*, 9, p.e53999.

Tan-Chen, S., Guitton, J., Bourron, O., Le Stunff, H. and Hajduch, E., 2020. Sphingolipid Metabolism and Signaling in Skeletal Muscle: From Physiology to Physiopathology. *Frontiers in Endocrinology* [Online], 11(8). Available from: https://doi.org/10.3389/fendo.2020.00491.

Tan, R., Li, J., Liu, F., Liao, P., Ruiz, M., Dupuis, J. and Zhu, L., 2020. Phenylalanine induces pulmonary hypertension through calcium-sensing receptor activation. *American Journal of Physiology - Lung Cellular and Molecular Physiology* [Online], 319, pp.1010–1020. Available from: https://doi.org/10.1152/ajplung.00215.2020.

Tang, D.-Q., Zou, L., Yin, X.-X. and Ong, C.N., 2016. HILIC-MS FOR METABOLOMICS: AN ATTRACTIVE AND COMPLEMENTARY APPROACH TO RPLC-MS. *Mass Spectrometry Reviews* [Online], 35, pp.574–600. Available from:

https://doi.org/10.1002/mas.

Tanner, C.M., Ottman, R., Goldman, S.M., Ellenberg, J., Chan, P., Mayeux, R. and Langston, J.W., 1999. Parkinson Disease in Twins. *Journal of the American Medical Association*, 281(4), pp.341–346.

Tantai, X., Liu, Yi, Yeo, Y.H., Praktiknjo, M., Mauro, E., Hamaguchi, Y., Engelmann, C., Zhang, P., Jeong, J.Y., Ad van Vugt, J.L., Xia, H., Deng, H., Gao, X., Ye, Q., Zhang, J., Yang, L., Cai, Y., Liu, Yixin, Liu, N., Li, Z., Han, T., Kaido, T., Sohn, J.H., Strassburg, C., Berg, T., Trebicka, J., Hsu, Y.-C., IJzermans, J.N.M., Wang, J., Su, G.L., Ji, F. and Nguyen, M.H., 2022. Effect of sarcopenia on survival in patients with cirrhosi: A meta-analysis. *Journal of Hepatology* [Online], 76(3), pp.588–599. Available from: https://doi.org/10.1016/j.jhep.2021.11.006.

Tasseva, G., Bai, H.D., Davidescu, M., Haromy, A., Michelakis, E. and Vance, J.E., 2013. Phosphatidylethanolamine Deficiency in Mammalian Mitochondria Impairs Oxidative Phosphorylation and Alters Mitochondrial Morphology. *The Journal of Biological Chemistry* [Online], 288(6), pp.4158–4173. Available from: https://doi.org/10.1074/jbc.M112.434183.

Tavares, G, Marques, D., Barra, C., Rosendo-Silva, D., Costa, A., Rodrigues, T., Gasparini, P., Melo, B.., Sacramento, J.., Conde, S.. and Matafome, P., 2021. Dopamine D2 receptor agonist, bromocriptine, remodels adipose tissue dopaminergic signalling and upregulates catabolic pathways , improving metabolic profile in type 2 diabetes. *Molecular Metabolism* [Online], 51(4), p.101241. Available from: https://doi.org/10.1016/j.molmet.2021.101241.

Tavares, Gabriela, Martins, F.O., Melo, B.F., Matafome, P. and Conde, S. V, 2021. Peripheral Dopamine Directly Acts on Insulin-Sensitive Tissues to Regulate Insulin

Signaling and Metabolic Function. *Frontiers in Pharmacology* [Online], 12(713418). Available from: https://doi.org/10.3389/fphar.2021.713418.

Teahan, O., Gamble, S., Holmes, E., Waxman, J., Nicholson, J.K., Bevan, C. and Keun, H.C., 2006. Impact of Analytical Bias in Metabonomic Studies of Human Blood Serum and Plasma. *Analytical Chemistry*, 78(13), pp.4307–4318.

Thalacker-Mercer, A., Blum, J. and Gheller, B., 2020. Serine and Glycine Are Essential for Skeletal Muscle Regeneration Following Injury. *Current Developments in Nutrition* [Online], 4(Supplement_2), p.81. Available from: https://doi.org/10.1093/cdn/nzaa040_081.

Theodoridis, G., Gika, H.G. and Wilson, I.D., 2008. LC-MS-based methodology for global metabolite profiling in metabonomics/metabolomics. *TrAC - Trends in Analytical Chemistry* [Online], 27(3), pp.251–260. Available from: https://doi.org/10.1016/j.trac.2008.01.008.

Thonusin, C., Iglayreger, H.B., Soni, T., Rothberg, A.E., Burant, C.F. and Evans, C.R., 2017. Evaluation of intensity drift correction strategies using MetaboDrift , a normalization tool for multi-batch metabolomics data. *Journal of Chromatography A* [Online], 1523, pp.265–274. Available from: https://doi.org/10.1016/j.chroma.2017.09.023.

Tognarelli, J.M., Dawood, M., Shariff, M.I.F., Grover, V.P.B., Crossey, M.M.E., Cox, I.J., Taylor-Robinson, S.D. and McPhail, M.J.W., 2015. Magnetic Resonance Spectroscopy: Principles and Techniques: Lessons for Clinicians. *Journal of Clinical and Experimental Hepatology* [Online], 5(4), pp.320–328. Available from: https://doi.org/10.1016/j.jceh.2015.10.006.

Tolstikov, V., James Moser, A., Sarangarajan, R., Narain, N.R. and Kiebish, M.A., 2020.

Current status of metabolomic biomarker discovery: Impact of study design and demographic characteristics. *Metabolites* [Online], 10(6). Available from: https://doi.org/10.3390/metabo10060224.

Toraman, N.F., 2005. Short term and long term detraining: Is there any difference between young-old and old people? *British Journal of Sports Medicine* [Online], 39(8), pp.561–564. Available from: https://doi.org/10.1136/bjsm.2004.015420.

Touw, W.G., Bayjanov, J.R., Overmars, L., Backus, L., Boekhorst, J., Wels, M. and Sacha van Hijum, A.F.T., 2013. Data mining in the life science swith random forest: A walk in the park or lost in the jungle? *Briefings in Bioinformatics* [Online], 14(3), pp.315–326. Available from: https://doi.org/10.1093/bib/bbs034.

Toyoshima, K., Nakamura, M., Adachi, Y., Imaizumi, A., Hakamada, T., Abe, Y., Kaneko, E., Takahashi, S. and Shimokado, K., 2017. Increased plasma proline concentrations are associated with sarcopenia in the elderly. *PLoS ONE* [Online], 12(9), p.e0185206. Available from: https://doi.org/10.1371/journal.pone.0185206.

Tremblay, M.S., Copeland, J.L. and Van Helder, W., 2004. Effect of training status and exercise mode on endogenous steroid hormones in men. *Journal of Applied Physiology* [Online], 96(2), pp.531–539. Available from: https://doi.org/10.1152/japplphysiol.00656.2003.

Trezzi, J.-P., Galozzi, S., Jaeger, C., Barkovits, K., Brockmann, K., Maetzler, W., Berg, D., Marcus, K., Betsou, F., Hiller, K. and Mollenhauer, B., 2017. Distinct Metabolomic Signature in Cerebrospinal Fluid in Early Parkinson ' s Disease. *Movement Disorders* [Online], 32(10), pp.1401–1408. Available from: https://doi.org/10.1002/mds.27132.

Tsedilin, A.M., Fakhrutdinov, A.N., Eremin, D.B., Zalesskiy, S.S., Chizhov, A.O., Kolotyrkina, N.G. and Ananikov, V.P., 2015. How sensitive and accurate are routine NMR and MS measurements? *Mendeleev Communications* [Online], 25, pp.454–456. Available from: https://doi.org/10.1016/j.mencom.2015.11.019.

Tsuda, Y., Yamaguchi, M., Noma, T., Okaya, E. and Itoh, H., 2019. Combined Effect of Arginine, Valine, and Serine on Exercise-Induced Fatigue in Healthy Volunteers: A Randomized, Double-Blinded, Placebo-Controlled Crossover Study. *Nutrients*, 11(862).

Tumilty, L., Davison, G., Beckmann, M. and Thatcher, R., 2011. Oral tyrosine supplementation improves exercise capacity in the heat. *European Journal of Applied Physiology* [Online], 111, pp.2941–2950. Available from: https://doi.org/10.1007/s00421-011-1921-4.

Turpin, S.M., Nicholls, H.T., Willmes, D.M., Mourier, A., Brodesser, S., Wunderlich, C.M., Mauer, J., Xu, E., Hammerschmidt, P., Brönneke, H.S., Trifunovic, A., Losasso, G., Wunderlich, F.T., Kornfeld, J.W., Blüher, M., Krönke, M. and Brüning, J.C., 2014. Obesity-induced CerS6-dependent C16:0 ceramide production promotes weight gain and glucose intolerance. *Cell Metabolism* [Online], 20(4), pp.678–686. Available from: https://doi.org/10.1016/j.cmet.2014.08.002.

Ubaida-Mohien, C., Lyashkov, A., Gonzalez-Freire, M., Tharakan, R., Shardell, M., Moaddel, R., Semba, R.D., Chia, C.W., Gorospe, M., Sen, R. and Ferrucci, L., 2019. Discovery proteomics in aging human skeletal muscle finds change in spliceosome, immunity, proteostasis and mitochondria. *eLife* [Online], 8. Available from: https://doi.org/10.7554/elife.49874.

Ubhi, B.K., Cheng, K.K., Dong, J., Janowitz, T., Jodrell, D., Tal-Singer, R., MacNee, W.,

Lomas, D.A., Riley, J.H., Griffin, J.L. and Connor, S.C., 2012. Targeted metabolomics identifies perturbations in amino acid metabolism that sub-classify patients with COPD. *Molecular BioSystems* [Online], 8(12), pp.3125–3133. Available from: https://doi.org/10.1039/c2mb25194a.

Ubhi, B.K., Riley, J.H., Shaw, P.A., Lomas, D.A., Tal-Singers, R., MacNeef, W., Griffin, J.L. and Connor, S.C., 2012. Metabolic profiling detects biomarkers of protein degradation in COPD patients. *European Respiratory Journal* [Online], 40(2), pp.345–355. Available from: https://doi.org/10.1183/09031936.00112411.

Uchitomi, R., Hatazawa, Y., Senoo, N., Yoshioka, K., Fujita, M., Shimizu, T., Miura, S., Ono, Y. and Kamei, Y., 2019. Metabolomic Analysis of Skeletal Muscle in Aged Mice. *Scientific Reports* [Online], 9(10425). Available from: https://doi.org/10.1038/s41598-019-46929-8.

Ueda, K., Sanbongi, C., Yamaguchi, M., Ikegami, S., Hamaoka, T. and Fujita, S., 2017. The effects of phenylalanine on exercise-induced fat oxidation: a preliminary , double-blind , placebo-controlled, crossover trial. *Journal of the International Society of Sports Nutrition* [Online], 14(34). Available from: https://doi.org/10.1186/s12970-017-0191-x.

Vance, J.E. and Tasseva, G., 2013. Formation and function of phosphatidylserine and phosphatidylethanolamine in mammalian cells. *Biochemical Society Transactions* [Online], 1831(3), pp.543–554. Available from: https://doi.org/10.1016/j.bbalip.2012.08.016.

Vangipurapu, J., Stancáková, A., Smith, U., Kuusisto, J. and Laakso, M., 2019. Nine Amino Acids Are Associated With Decreased Insulin Secretion and Elevated Glucose Levels in a 7.4-Year Follow-up Study of 5,181 Finnish Men. *Diabetes*

[Online], 68, pp.1353–1358. Available from: https://doi.org/10.2337/db18-1076.

Vanhoutte, G., Van De Wiel, M., Wouters, K., Sels, M., Bartolomeeussen, L., De Keersmaecker, S., Verschueren, C., De Vroey, V., De Wilde, A., Smits, E., Cheung, K.J., De Clerck, L., Aerts, P., Baert, D., Vandoninck, C., Kindt, S., Schelfhaut, S., Vankerkhoven, M., Troch, A., Ceulemans, L., Vandenbergh, H., Leys, S., Rondou, T., Dewitte, E., Maes, K., Pauwels, P., De Winter, B., Van Gaal, L., Ysebaert, D. and Peeters, M., 2016. Cachexia in cancer: what is in the definition? *BMJ Open Gastroenterology* [Online], 3(1), pp.1–11. Available from: https://doi.org/10.1136/bmjgast-2016-000097.

Venables, M.C., Achten, J. and Jeukendrup, A.E., 2005. Determinants of fat oxidation during exercise in healthy men and women: a cross-sectional study. *Journal of Applied Physiology* [Online], 98, pp.160–167. Available from: https://doi.org/10.1152/japplphysiol.00662.2003.

Verkerke, A.R.P., Ferrara, P.J., Lin, C.-T., Johnson, J.M., Ryan, T.E., Maschek, J.A., Eshima, H., Paran, C.W., Brenton, T.L., Siripoksup, P., Tippetts, T.S., Wentzler, E.J., Huang, H., Spangenburg, E.E., Brault, J.J., Villanueva, C.J., Summers, S.A., Holland, W.L., Cox, J.E., Vance, D.E., Neufer, P.D. and Funai, K., 2020. Phospholipid methylation regulates muscle metabolic rate through Ca2+ transport efficiency. *Nature Metabolism* [Online], 1(9), pp.876–885. Available from: https://doi.org/10.1038/s42255-019-0111-2.Phospholipid.

Veronese, N., Koyanagi, A., Cereda, E., Maggi, S., Barbagallo, M., Dominguez, L.J. and Smith, L., 2022. Sarcopenia reduces quality of life in the long - term : longitudinal analyses from the English longitudinal study of ageing. *European Geriatric Medicine* [Online], 13(3), pp.633–639. Available from: https://doi.org/10.1007/s41999-022-00627-3.

Verpoorte, R., Kim, H.K. and Choi, Y.H., 2022. Trivialities in metabolomics: Artifacts in extraction and analysis. *Frontiers in Molecular Biosciences* [Online], 9(972190). Available from: https://doi.org/10.3389/fmolb.2022.972190.

Vetrano, D.L., Landi, F., Volpato, S., Corsonello, A., Meloni, E., Bernabei, R. and Onder, G., 2014. Association of sarcopenia with short- and long-term mortality in older adults admitted to acute care wards: Results from the CRIME study. *Journals of Gerontology - Series A Biological Sciences and Medical Sciences* [Online], 69(9), pp.1154–1161. Available from: https://doi.org/10.1093/gerona/glu034.

Viribay, A., Burgos, J., Fernández-Landa, J., Seco-Calvo, J. and Mielgo-Ayuso, J., 2020. Effects of arginine supplementation on athletic performance based on energy metabolism: A systematic review and meta-analysis. *Nutrients* [Online], 12(1300). Available from: https://doi.org/10.3390/nu12051300.

Visscher, P.M., Brown, M.A., McCarthy, M.I. and Yang, J., 2012. Five years of GWAS discovery. *American Journal of Human Genetics* [Online], 90(1), pp.7–24. Available from: https://doi.org/10.1016/j.ajhg.2011.11.029.

Vissier, M., Deeg, D.J.. and Lips, P., 2003. Low Vitamin D and High Parathyroid Hormone Levels as Determinants of Loss of Muscle Strength and Muscle Mass (Sarcopenia): The Longitudinal Aging Study Amsterdam. *The Journal of Clinical Endocrinology & Metabolism* [Online], 88(12), pp.5766–5772. Available from: https://doi.org/10.1210/jc.2003-030604.

Vogiatzis, I., Terzis, G., Nanas, S., Stratakos, G., Simoes, D.C.M., Georgiadou, O., Zakynthinos, S. and Roussos, C., 2005. Skeletal Muscle Adaptations to Interval Training in Patients With Advanced COPD. *Chest* [Online], 128(6), pp.3838–3845. Available from: https://doi.org/10.1378/chest.128.6.3838.

Wandrag, L., Brett, S.J., Frost, G.S., Bountziouka, V. and Hickson, M., 2019. Exploration of muscle loss and metabolic state during prolonged critical illness: Implications for intervention? *PLoS ONE* [Online], 14(11), pp.6–16. Available from: https://doi.org/10.1371/journal.pone.0224565.

Wang-Sattler, R., Yu, Z., Herder, C., Messias, A.C., Floegel, A., He, Y., Heim, K., Campillos, M., Holzapfel, C., Thorand, B., Grallert, H., Xu, T., Bader, E., Huth, C., Mittelstrass, K., Doring, A., Mesinger, C., Gieger, C., Prehn, C., Roemisch-Margi, W., Carstensen, M., Xie, L., Boeing, H., Joost, H.-G., Hrabe de Angelis, M., Rathmann, W., Suhre, K., Prokisch, H., Peters, A., Meitinger, T., Roden, M., Wichmann, H.-E., Pischon, T., Adamski, J. and Illig, T., 2012. Novel biomarkers for pre-diabetes identified by metabolomics. *Molecular Systems Biology* [Online], 8(615). Available from: https://doi.org/10.1038/msb.2012.43.

Wang, Q., Jokelainen, J., Auvinen, J., Puukka, K., Keinänen-Kiukaanniemi, S., Jarvelin, M.-R., Kettunen, J., Makinen, V.-P. and Ala-Korpela, M., 2019. Insulin resistance and systemic metabolic changes in oral glucose tolerance test in 5340 individuals: an interventional study. *BMC Medicine*, 17(217).

Wang, Y., Ma, L., Zhang, M., Chen, M., Li, P., He, C., Yan, C. and Wan, J.B., 2019. A Simple Method for Peak Alignment Using Relative Retention Time Related to an Inherent Peak in Liquid Chromatography-Mass Spectrometry-Based Metabolomics. *Journal of Chromatographic Science* [Online], 57(1), pp.9–16. Available from: https://doi.org/10.1093/chromsci/bmy074.

Want, E.J., Wilson, I.D., Gika, H., Theodoridis, G., Plumb, R.S., Shockcor, J., Holmes, E. and Nicholson, J.K., 2010. Global metabolic profiling procedures for urine using UPLC–MS. *Nature Protocols* [Online], 5(6), pp.1005–1018. Available from: https://doi.org/10.1038/nprot.2010.50.

Ward, T.J.C., Plumptre, C.D., Dolmage, T.E., Jones, A. V., Trethewey, R., Divall, P., Singh, S.J., Lindley, M.R., Steiner, M.C. and Evans, R.A., 2020. Change in VO2peak in Response to Aerobic Exercise Training and the Relationship With Exercise Prescription in People With COPD A Systematic Review and Meta-analysis. *CHEST* [Online], 158(1), pp.131–144. Available from: https://doi.org/10.1016/j.chest.2020.01.053.

Wehr, E., Pilz, S., Boehm, B.O., März, W. and Obermayer-Pietsch, B., 2010. Association of vitamin D status with serum androgen levels in men. *Clinical Endocrinology* [Online], 73(2), pp.243–248. Available from: https://doi.org/10.1111/j.1365-2265.2009.03777.x.

Wei, R., Wang, J., Su, M., Jia, E., Chen, S., Chen, T. and Ni, Y., 2018. Missing Value Imputation Approach for Mass Spectrometry-based Metabolomics Data. *Scientific Reports* [Online], 8(663). Available from: https://doi.org/10.1038/s41598-017-19120-0.

Wei, T. and Simko, V., 2021. R package 'corrplot': Visualisation of a Correlation Matrix [Online]. Available from: https://github.com/taiyun/corrplot.

Welsh, N., 1990. A role for polyamines in glucose-stimulated insulin-gene expression. *Biochemical Journal*, 271(2), pp.393–397.

Wilcox, G., 2005. Insulin and Insulin Resistance. *Clinical Biochemistry Reviews*, 26(May), pp.19–39.

Wiley, V., Carpenter, K. and Wilcken, B., 1999. Newborn screening with tandem mass spectrometry: 12 months' experience in NSW Australia. *Acta Paediatrica*, 88(s432), pp.48–51.

Wilkinson, D.J., Rodriguez-Blanco, G., Dunn, W.B., Phillips, B.E., Williams, J.P.,

Greenhaff, P.L., Smith, K., Gallagher, I.J. and Atherton, P.J., 2020. Untargeted metabolomics for uncovering biological markers of human skeletal muscle ageing. *Aging* [Online], 12(13), pp.12517–12533. Available from: https://doi.org/10.18632/aging.103513.

Willforss, J., Chawade, A. and Levander, F., 2019. NormalyzerDE: Online Tool for Improved Normalization of Omics Expression Data and High-Sensitivity Differential Expression Analysis. *Journal of Proteome Research* [Online], 18, pp.732–740. Available from: https://doi.org/10.1021/acs.jproteome.8b00523.

Williams, A.S., Kang, L. and Wasserman, D.H., 2016. The Extracellular Matrix and Insulin Resistance. *Trends in Endocrinology Metabolism* [Online], 26(7), pp.357–366. Available from: https://doi.org/10.1016/j.tem.2015.05.006.The.

Williams, T.J., Patterson, G.A., McClean, P.A., Zamel, N. and Maurer, J.R., 1992. Maximal exercise testing in single and double lung transplant recipients. *American Review of Respiratory Disease* [Online], 145(1), pp.101–105. Available from: https://doi.org/10.1164/ajrccm/145.1.101.

Wilson, D., Breen, L., Lord, J.M. and Sapey, E., 2018. The challenges of muscle biopsy in a community based geriatric population. *BMC Research Notes* [Online], 11(830). Available from: https://doi.org/10.1186/s13104-018-3947-8.

Wischmeyer, P.E., Puthucheary, Z., Millán, I.S., Butz, D. and Grocott, M.P.W., 2017. Muscle mass and physical recovery in ICU: Innovations for targeting of nutrition and exercise. *Current Opinion in Critical Care* [Online], 23(4), pp.269–278. Available from: https://doi.org/10.1097/MCC.0000000000000431.

Wishart, D.S., 2019. Metabolomics for investigating physiological and pathophysiological processes. *Physiological Reviews* [Online], 99, pp.1819–1875.

Available from: https://doi.org/10.1152/physrev.00035.2018.

Wishart, D.S., Guo, A., Oler, E., Wang, F., Anjum, A., Peters, H., Dizon, R., Sayeeda, Z., Tian, S., Lee, B.L., Berjanskii, M., Mah, R., Yamamoto, M., Jovel, J., Torres-calzada, C., Hiebert-giesbrecht, M., Lui, V.W., Varshavi, Dorna, Varshavi, Dorsa, Allen, D., Arndt, D., Khetarpal, N., Sivakumaran, A., Harford, K., Sanford, S., Yee, K., Cao, X., Budinski, Z., Liigand, J., Zhang, L., Zheng, J., Mandal, R., Karu, N., Dambrova, M., Greiner, R., Gautam, V. and Schi, H.B., 2022. HMDB 5.0 : the Human Metabolome Database for 2022. *Nuclei*, 50(November 2021), pp.622–631.

Wolfgang, M.J., 2021. Remodeling glycerophospholipids affects obesity-related insulin signaling in skeletal muscle. *The Journal of Clinical Investigation*, 131(8), p.e148176.

Wood, R.H., Reyes, R., Welsch, M.A., Favaloro-sabatier, J., Sabatier, M., Lee, C.M., Johnson, L.G. and Hooper, P.F., 2001. Concurrent cardiovascular and resistance training in healthy older adults. *Medicine and Science in Sports and Exercise*, 33(10), pp.1751–1758.

Worley, B. and Powers, R., 2013. Multivariate Analysis in Metabolomics. *Current Metabolomics* [Online], 1(1), pp.92–107. Available from: https://doi.org/10.2174/2213235X11301010092.Multivariate.

Worley, B. and Powers, R., 2016. PCA as a Practical Indicator of OPLS-DA Model Reliability. *Current Metabolomics* [Online], 4(2), pp.97–103. Available from: https://doi.org/10.2174/2213235x04666160613122429.

Wu, D., Ren, Z., Pae, M., Guo, W., Cui, X., Merrill, A.H. and Meydani, S.N., 2007. Aging Up-Regulates Expression of Inflammatory Mediators in Mouse Adipose Tissue. *The Journal of Immunology* [Online], 179(7), pp.4829–4839. Available from:

https://doi.org/10.4049/jimmunol.179.7.4829.

Wu, Z.E., Kruger, M.C., Cooper, G.J.S., Sequeira, I.R., McGill, A.T., Poppitt, S.D. and Fraser, K., 2022. Dissecting the relationship between plasma and tissue metabolome in a cohort of women with obesity: Analysis of subcutaneous and visceral adipose, muscle, and liver. *FASEB journal : official publication of the Federation of American Societies for Experimental Biology* [Online], 36(7), p.e22371. Available from: https://doi.org/10.1096/fj.202101812R.

Wurtz, P., Tiainen, M., Makinen, V.-P., Kangas, A.J., Soininen, P., Saltevo, J., Keianen-Kiukaanniemi, S., Mantyselka, P., Lehtimaki, T., Laakso, M., Jula, A., Kahonen, M., Vanhala, M. and Ala-Korpela, M., 2012. Circulating Metabolite Predictors of Glycemia in Middle-Aged Men and Women. *Diabetes Care* [Online], 35(8), pp.17549–1756. Available from: https://doi.org/10.2337/dc11-1838.

Xi, P., Jiang, Z., Zheng, C., Lin, Y. and Wu, G., 2011. Regulation of protein metabolism by glutamine: Implications for nutrition and health. *Frontiers in Bioscience* [Online], 16(2), pp.578–597. Available from: https://doi.org/10.2741/3707.

Xia, J. and Wishart, D.S., 2011. MetPA: A web-based metabolomics tool for pathway analysis and visualization. *Bioinformatics* [Online], 27(13), pp.2342–2344. Available from: https://doi.org/10.1093/bioinformatics/btq418.

Xiao, Q., Moore, S.C., Keadle, S.K., Xiang, Y.-B., Zheng, W., Peters, T.M., Leitzmann, M.F., Ji, B.-T., Sampson, J.N., Shu, X.-O. and Matthews, C.E., 2016. Objectively measured physical activity and plasma metabolomics in the Shanghai Physical Activity Study. *International Journal of Epidemiology* [Online], 45(5), pp.1433–1444. Available from: https://doi.org/10.1093/ije/dyw033.

Yamada, M., Kimura, Y., Ishiyama, D., Nishio, N., Tanaka, T., Ohji, S., Otobe, Y., Koyama,

S., Sato, A., Suzuki, M., Ogawa, H., Ichikawa, T., Ito, D. and Arai, H., 2018. PLASMA AMINO ACID CONCENTRATIONS ARE ASSOCIATED WITH MUSCLE FUNCTION IN OLDER JAPANESE WOMEN. *Journal of Nutrition, Health & Aging*, 22(7), pp.819–823.

Yang, J., Zhao, X., Lu, X., Lin, X. and Xu, G., 2015. A data preprocessing strategy for metabolomics to reduce the mask effect in data analysis. *Frontiers in Molecular Biosciences* [Online], 2(FEB). Available from: https://doi.org/10.3389/fmolb.2015.00004.

Yang, Q.J., Zhao, J.R., Hao, J., Li, B., Huo, Y., Han, Y.L., Wan, L.L., Li, J., Huang, J., Lu, J., Yang, G.J. and Guo, C., 2018. Serum and urine metabolomics study reveals a distinct diagnostic model for cancer cachexia. *Journal of Cachexia, Sarcopenia and Muscle* [Online], 9(1), pp.71–85. Available from: https://doi.org/10.1002/jcsm.12246.

Yang, W., Chen, Y., Xi, C., Zhang, R., Song, Y., Zhan, Q., Bi, X. and Abliz, Z., 2013. Liquid Chromatography−Tandem Mass Spectrometry-Based Plasma Metabonomics Delineate the Effect of Metabolites' Stability on Reliability of Potential Biomarkers. *Analytical Chemistry*, 85, pp.2606–2610.

Yoo, J.-I., Chung, H.J., Kim, B.G., Jung, Y.-K., Baek, K., Song, M.-G. and Cho, M.-C., 2021. Comparative analysis of the association between various serum vitamin D biomarkers and sarcopenia. *Journal of Clinical Laboratory Analysis* [Online], 35(7), p.e23946. Available from: https://doi.org/10.1002/jcla.23946.

Yoon, M., 2016. The Emerging Role of Branched-Chain Amino Acids in Insulin Resistance and Metabolism. *Nutrients* [Online], 8(405). Available from: https://doi.org/10.3390/nu8070405.

Youdim, M.B.., Mandel, S.A., Grunblatt, E. and Riederer, P., 2007. *Diagnostic test for Parkinson's disease*.

Yu, L., Li, K. and Zhang, X., 2017. Next-generation metabolomics in lung cancer diagnosis, treatment and precision medicine: mini review. *Oncotarget* [Online], 8(70), pp.115774–115786. Available from: https://doi.org/10.18632/oncotarget.22404.

Yuan, D., Jin, H., Liu, Q., Zhang, J., Ma, B., Xiao, W. and Li, Y., 2022. Publication Trends for Sarcopenia in the World: A 20-Year Bibliometric Analysis. *Frontiers in Medicine* [Online], 9(February). Available from: https://doi.org/10.3389/fmed.2022.802651.

Zamboni, N., Saghatelian, A. and Patti, G.J., 2015. Defining the Metabolome: Size, Flux, and Regulation. *Molecular Cell* [Online], 58(4), pp.699–706. Available from: https://doi.org/10.1016/j.molcel.2015.04.021.

Zhan, X., Patterson, A.D. and Ghosh, D., 2015. Kernel approaches for differential expression analysis of mass spectrometry-based metabolomics data. *BMC Bioinformatics* [Online], 16(1), pp.1–13. Available from: https://doi.org/10.1186/s12859-015-0506-3.

Zhang, A., Sun, H. and Wang, X., 2017. Emerging role and recent applications of metabolomics biomarkers in obesity disease research. *RSC Advances* [Online], 7(25), pp.14966–14973. Available from: https://doi.org/10.1039/c6ra28715h.

Zhang, A., Sun, H., Yan, G., Wang, P. and Wang, X., 2015. Metabolomics for Biomarker Discovery: Moving to the Clinic. *BioMed Research International* [Online], 2015(354671). Available from: https://doi.org/10.1155/2015/354671.

Zhang, C., McFarlane, C., Lokireddy, S., Bonala, S., Ge, X., Masuda, S., Gluckman, P..,

Sharma, M. and Kambadur, R., 2011. Myostatin-deficient mice exhibit reduced insulin resistance through activating the AMP-activated protein kinase signalling pathway. *Diabetelogia* [Online], 54, pp.1491–1501. Available from: https://doi.org/10.1007/s00125-011-2079-7.

Zhang, J., Gonzalez, E., Hestilow, T., Haskins, W. and Huang, Y., 2009. Review of Peak Detection Algorithms in Liquid-Chromatography-Mass Spectrometry. *Current Genomics* [Online], 10(6), pp.388–401. Available from: https://doi.org/10.2174/138920209789177638.

Zhao, Q., Shen, H., Su, K.J., Tian, Q., Zhao, L.J., Qiu, C., Garrett, T.J., Liu, J., Kakhniashvili, D. and Deng, H.W., 2018. A joint analysis of metabolomic profiles associated with muscle mass and strength in Caucasian women. *Aging* [Online], 10(10), pp.2624–2635. Available from: https://doi.org/10.18632/aging.101574.

Zieliński, J., Slominska, E.M., Król-Zielińska, M., Krasiński, Z. and Kusy, K., 2019. Purine metabolism in sprint- vs endurance-trained athletes aged 20–90 years. *Scientific Reports* [Online], 9(1). Available from: https://doi.org/10.1038/s41598-019-48633-z.

Zubarev, R.A. and Makarov, A., 2013. Orbitrap Mass Spectrometry. *Analytical Chemistry*, 85, pp.5288–5296.

Appendix 1. Pre-processing and filtering of metabolomics data

```
##XCMS PREPROCESSING

library(BiocManager)

library(xcms)

library(RColorBrewer)

library(pander)

library(magrittr)

library(pheatmap)

library(SummarizedExperiment)

library(CAMERA)



setwd("D:/UroCa_eHIT/28Apr22_HILICpos/mzXML") #example files

mzXML <- dir("Samples", full.names = TRUE, recursive = TRUE)



#load raw data using readMSData method from MSnbase package

raw_data <- readMSData(files = mzXML, mode = "onDisk")



#get base peak chromatograms

bpis <- chromatogram(raw_data, aggregationFun = "max")
```

```
#define peakwidth parameters using widest and narrowest peaks

rtr <- c(8.5*60, 10.5*60)

mzr <- c(293.0981+0.01, 293.0981-0.01)



chr_raw <- chromatogram(raw_data, mz = mzr, rt = rtr)



#run chromatogram extraction

cwp <- CentWaveParam(peakwidth = c(10, 40),ppm = 20) # set parameters

xdata <- findChromPeaks(raw_data, param = cwp)



#align data

xdata <- adjustRtime(xdata, param = ObiwarpParam(binSize = 0.6))



#get base peak chromatograms

bpis_adj <- chromatogram(xdata, aggregationFun = "max")

#does the object have adjusted retention times?

hasAdjustedRtime(xdata)



##correspondence

#define the m/z slice
```

```
mzr <- c(180.05, 180.15)

#extract and plot the chromatogram

chr_mzr <- chromatogram(xdata, mz = mzr, rt = c(0, 930))

par(mfrow = c(2, 1), mar = c(1, 4, 1, 0.5))

plot(chr_mzr)

#define bandwidth paramters for peak density method

pdp <- PeakDensityParam(sampleGroups = rep(1, length(fileNames(xdata))),

                        minFraction = 0.4, bw = 10)

plotChromPeakDensity(xdata, mz = mzr, param = pdp, pch = 16, xlim = c(0, 930))



##perform the correspondence

pdp <- PeakDensityParam(sampleGroups = rep(1, length(fileNames(xdata))),

                    minFraction = 0.4, bw = 10)

xdata <- groupChromPeaks(xdata, param = pdp)



#fill missing peaks using default settings

xdata <- fillChromPeaks(xdata)



#convert XCMSnExp object to xcmsSet for use with CAMERA

xset <- as(xdata, "xcmsSet")
```

```
xsa <- annotate(xset, cor_eic_th = 0)

peaklist <- getPeaklist(xsa)

indexNA <- is.na(peaklist)

peaklist[indexNA] <- 0

is.na(peaklist) #sanity check

#write peaklist as csv file

write.csv(peaklist, "hiit_hilicpos.csv")



##FILTERING METABOLOMICS DATA

#import data from .csv file and convert to SummarizedExperiment

#load required package

library(SummarizedExperiment)

setwd("D:/UroCa_eHIT/09May22_RPneg/pmp") #set working directory for files

rpneg_all <- read.csv("data.csv",

                      row.names = 1) #load data into dataframe

rpneg <- list()

rpneg$dataMatrix <- rpneg_all #form dataMatrix



#transpose peak matrix, so features are in rows and samples in columns

rpneg$dataMatrix <- as.matrix(t(rpneg$dataMatrix))
```

```
colnames(rpneg[["dataMatrix"]]) #colnames should be sample names

row.names(rpneg[["dataMatrix"]]) #rownames should be metabolite names



#missing values in the input data are stored as 0, replace with NA

rpneg$dataMatrix[rpneg$dataMatrix == 0] <- NA



#round numbers to 5 digits

#rownames(rpneg$assay) <- round(as.numeric(rownames(rpneg$assay)), 5)

#import metadata

meta <- read.csv("sample.csv")

rpneg$sampleMetadata <- meta #store in list



#make SummarizedExperiment object combining metabolites and metadata

rpneg <- SummarizedExperiment(assays = list(rpneg$dataMatrix),

                              colData = DataFrame(rpneg$sampleMetadata))



#load required packages

library(BiocManager)

library(pmp)

library(S4Vectors)
```

```
#use summarizedExperiment. Check class:

rpneg



#check missing samples and find %

sum(is.na(assay(rpneg)))

sum(is.na(assay(rpneg)))/length(assay(rpneg))*100



##filter by QC

#apply the mv feature to filter based on QC sample Class only. Peaks must be present

in

#at least 70% of QC samples:

rpneg_filtered <- filter_peaks_by_fraction(df = rpneg,

                                           min_frac = 0.7,

                                           classes = rpneg$Group,

                                           method = "QC",

                                           qc_label = "QC")



#check missing samples again

sum(is.na(assay(rpneg_filtered)))
```

```
#filter by RSD<30%

rpneg_filtered <- filter_peaks_by_rsd(df = rpneg_filtered,

                                      max_rsd = 30,

                                      classes = rpneg$Group,

                                      qc_label = "QC")

#check missing samples again

sum(is.na(assay(rpneg_filtered)))



##filter by blank

#FC 20 is equivalent to 0.05 blank/QC ratio

#QC label means only QC samples are used to calculate comparison intensity

rpneg_blank <- filter_peaks_by_blank(rpneg_filtered,

                                     fold_change = 20,

                                     classes = rpneg_filtered$Group,

                                     blank_label = "B",

                                     qc_label = "QC",

                                     remove_peaks = TRUE,

                                     remove_samples = FALSE,

                                     fraction_in_blank = 0)
```

```
sum(is.na(assay(rpneg_blank)))


#discard blank for further analysis

rpneg_drop <- rpneg_blank[, rpneg_blank$Remove == "NO"]


sum(is.na(assay(rpneg_drop)))

##DATA NORMALISATION

#this will apply probabilistic quotient normalisation

#normalise samples to pooled QC

rpneg_norm <- pqn_normalisation(df = rpneg_drop,

                        classes = rpneg_drop$Group,

                        qc_label = "QC")


#MISSING VALUE IMPUTATION

rpneg_mv_imputed <- mv_imputation(rpneg_norm,

                         method = "knn")


##DATA SCALING

#the glog transformation algorithm stabilises variance across low and high intensity

#features
```

```
rpneg_glog <- glog_transformation(df = rpneg_mv_imputed,
                        classes = rpneg_mv_imputed$Group,
                        qc_label = "QC")


##signal correction - used for batch effect correction when samples run over several
#batches. Not always necessary
#set class, batch and sample order from m\etadata
class <- rpneg_mv_imputed$Group
batch <- rpneg_mv_imputed$Batch
order <- rpneg_mv_imputed$Order


#apply signal drift correction using QCRSC function
corrected_data <- QCRSC(df = rpneg_mv_imputed,
                    order = order,
                    batch = batch,
                    classes = class,
                    spar = 0,
                    minQC = 4)
#visual comparison of results
plots <- sbc_plot(df = rpneg_mv_imputed, corrected_data,
```

```
            classes = class,
            batch = batch,
            output = NULL,
            index = c(10, 50, 100, 150))
plots


#write files in .csv format as required
write.csv(assay(rpneg_glog), "rpneg_glog.csv")
write.csv(assay(rpneg_mv_imputed), "rpneg_mv_imputed.csv")
write.csv(assay(rpneg_blank), "rpneg_blank_filtered.csv")
write.csv(assay(rpneg_filtered), "rpneg_RSD_filtered.csv")
write.csv(assay(rpneg_norm), "rpneg_PQN.csv")
write.csv(assay(corrected_data), "rpneg_qcrsc.csv")
```

Appendix 2. Statistical analysis from Chapter 4

```
#PLS-DA

#load required packages

library(mixOmics)

library(dplyr)



#set working directory

setwd("C:/Users/mzxia1/Documents/BBSRC2/RP pos/PLS")

#load log transformed metabolite data and sample metadata

glog <- read.csv("rppos_glog.csv",

                 row.names = 1)

meta <- read.csv("meta.csv",

                 row.names = 1)



#double check samples are the same

keep_glog <- colnames(glog)

meta <- as.data.frame(meta[which(rownames(meta) %in% keep_glog),])



#combine glog data with meta data

glog <- as.data.frame(t(glog))
```

```
glog <- cbind(meta, glog)


#filter including middle group

glog_mid_pre <- glog %>%

  filter(class == "O"|class == "Y"|class == "M") %>%

  filter(timepoint == "F") #replace timepoint with L for post-intervention comparison


#set up dataframes - post-intervention comparisons

X_mid_pre <- glog_mid_pre[,4:ncol(glog_mid_pre)]

Y_mid_pre <- as.factor(glog_mid_pre$class)

#check dimensions and summary

dim(X_mid_pre); length(Y_mid_pre)

summary(Y_mid_pre)


#preliminary analysis with PCA

pca.mid.post <- pca(X_mid_pre, ncomp = 10, center = TRUE, scale = TRUE)

plot(pca.mid.post)

plotIndiv(pca.mid.post, group = glog_mid_pre$class, ind.names = FALSE,

        legend = TRUE, title = "PCA post-intervention",

        ellipse = TRUE)
```

```
#tuning parameters and numerical outputs:

# 1) determine number of components:

plsda_mid_pre <- plsda(X_mid_pre, Y_mid_pre, ncomp = 10)

set.seed(123) #for reproducibility

plsda_mid_pre_tuned <- perf(plsda_mid_pre, validation = "Mfold",

                  folds = 6, progressBar = TRUE,

                  nrepeat = 100)

plot(plsda_mid_pre_tuned,

    sd = TRUE, legend.position = "horizontal") #plot tuning



#2) final PLS-DA

plsda_mid_pre_final <- plsda(X_mid_pre, Y_mid_pre, ncomp = 2)

plotIndiv(plsda_mid_pre_final, ind.names = FALSE,

        legend = TRUE, ellipse = TRUE,

        title = "PLS-DA, postline comparison")



##testing without middle

glog_pre <- glog_mid_pre %>%

  filter(class == "O"|class == "Y")

X_pre <- glog_pre[,4:ncol(glog_pre)]
```

```
Y_pre <- as.factor(glog_pre$class)


#preliminary analysis with PCA

pca.post <- pca(X_pre, ncomp = 10, center = TRUE, scale = TRUE)

plotIndiv(pca.post, group = glog_pre$class, ind.names = FALSE,

        legend = TRUE, title = "PCA post-intervention (Old vs Young)",

        ellipse = TRUE)


#tuning parameters and numerical outputs:

# 1) determine number of components:

plsda_pre <- plsda(X_pre, Y_pre, ncomp = 9)

set.seed(123)

plsda_pre_tuned <- perf(plsda_pre, validation = "Mfold",

                  folds = 6, progressBar = TRUE,

                  nrepeat = 100)

plot(plsda_pre_tuned, col = color.mixo(1:3),

    sd = TRUE, legend.position = "horizontal")


#2) final PLS-DA

plsda_pre_final <- plsda(X_pre, Y_pre, ncomp = 4)
```

```
plotIndiv(plsda_pre_final, ind.names = FALSE,
        legend = TRUE, ellipse = TRUE,
        title = "PLS-DA, post-intervention comparison")


#get vip scores from final model
vip <- as.data.frame(vip(plsda_pre_final))
vip$mean <- rowMeans(vip)
#filter to only keep VIP > 1
vip <- vip %>%
  filter(mean > 1)
#export file of all metabolites with VIP > 1
write.csv(vip, "vip_pre_rp.csv")


#PLS-DA of baseline vs post-intervention samples by age
#example: young group
glog_young <- glog %>%
  filter(class == "Y")
X_young <- glog_young[,4:ncol(glog_young)]
Y_young <- as.factor(glog_young$timepoint)
```

```
#check dimensions and summary

dim(X_young); length(Y_young)

summary(Y_young)



#preliminary analysis with PCA

pca.young <- pca(X_young, ncomp = 10, center = TRUE, scale = TRUE)

plot(pca.young)

plotIndiv(pca.young, group = glog_young$timepoint, ind.names = FALSE,

        legend = TRUE, title = "PCA Young group",

        ellipse = TRUE)



#tuning parameters and numerical outputs:

# 1) determine number of components:

plsda_young <- plsda(X_young, Y_young, ncomp = 10)

set.seed(123)

plsda_young_tuned <- perf(plsda_young, validation = "Mfold",

                  folds = 8, progressBar = TRUE,

                  nrepeat = 100)

plot(plsda_young_tuned,

    sd = TRUE, legend.position = "horizontal")
```

```
#Correlation heatmap

#load required packages

library(dplyr)

library(corrplot)

#set working directory and load data

setwd("C:/Users/mzxia1/Documents/BBSRC2/Correlation")

rppos <- read.csv("rppos_glog.csv", row.names = 1)

rppos <- rppos[ave(1:nrow(rppos), rppos$Participant, FUN = length)>1,]



#filter data

old_last <- rppos %>%

  filter(Target == "O_L")

old_first <- rppos %>%

  filter(Target == "O_F")



#remove metadata and transpose

old_last <- old_last[,5:ncol(old_last)]

old_last <- as.data.frame(t(old_last))

old_first <- old_first[,5:ncol(old_first)]

old_first <- as.data.frame(t(old_first))
```

```
#arrange data frames in correct order

old_last$ID <- rownames(old_last)

old_last <- old_last %>%

 relocate(ID, .before = PW031L) %>%

 relocate(GS042L, .after = MJ022L) %>%

 relocate(JS019L, .after = PW031L)

old_first$ID <- rownames(old_first)

old_first <- old_first %>%

 relocate(ID, .before = PW031F)



#set up correlation matrix

cormat= matrix(0, nrow=nrow(old_first), ncol=nrow(old_last))

head(old_first);

head(old_last);

for(i in 1:nrow(old_first)){

 for(j in 1:nrow(old_last))

 {

  cormat[i,j] = cor(unlist(old_first[i,-1]), unlist(old_last[j,-1]),

                    use = "complete.obs")

 }
```

```
}

rownames(cormat) <- rownames(old_first)

colnames(cormat) <- rownames(old_first)



#plot heatmap

library(corrplot)

corrplot(cormat,

        order = "hclust",

        method = "shade",

        tl.cex = 0.5)
```

Appendix 3. Statistical analysis from Chapters 5 and 6

```
##PHYSIOLOGICAL DATA

#example of young group. Replace with old and COPD as necessary

#load required packages

library(ggpubr)

library(tidyverse)

library(broom)



####lean mass####

setwd("C:/Users/mzxia1/Documents/COPD/Chapter graphs Nov 22")

alldata <- read.csv("leanmass_young.csv")



#check normality

res <- aov(Total.Lean.Mass ~ Visit,

          data = alldata)

shapiro.test(res)



kruskal.test(Total.Lean.Mass ~ Visit, data = alldata) # data not normally distributed so

use non-parametric
```

```
####vo2 and rer young####

library(reshape2)

fitness <- read.csv("rer_vo2.csv")



rer_young <- fitness[,c(1:5)] %>%

  filter(Group== "HY")

vo2_young <- fitness[,c(1:2, 6:8)] %>%

  filter(Group == "HY")



rer_young_m <- melt(rer_young)

res.rer <- aov(value ~ variable,

               data = rer_young_m)

summary(res.rer)

shapiro.test(res.rer$residuals)



#significance difference in anova so post hoc test

pairwise.t.test(rer_young_m$value, rer_young_m$variable, paired = TRUE,

               p.adjust.method = "BH")



#same test with vo2
```

```
vo2_young_m <- melt(vo2_young)

rer.vo2 <- aov(value ~ variable,

               data = vo2_young_m)

summary(rer.vo2)

shapiro.test(rer.vo2$residuals)



#not normally distributed so need kruskal wallis

kruskal.test(value~variable, data = vo2_young_m) #still significant



pairwise.t.test(vo2_young_m$value, vo2_young_m$variable, paired = TRUE,

                p.adjust.method = "BH")



##FIT LINEAR MIXED EFFECTS MODEL

#load required packages

library(mosaic)

library(dplyr)

library(limma)

library(reshape2)

library(ggplot2)

library(statmod)
```

```
library(forcats)



setwd("D:/COPD/limma")

all_data <- read.csv("rppos_all.csv",

                     row.names = 1) #data matrix including metadata in first three columns



#for replicated time points, it is most convenient to join the experimental factors

#into one combined factor

all_data <- mutate(all_data, group_time = derivedFactor(

  "COPD_V1" = (Class == "COPD" & Timepoint == "V1"),

  "COPD_V2" = (Class == "COPD" & Timepoint == "V2"),

  "COPD_V3" = (Class == "COPD" & Timepoint == "V3"),

  "COPD_V4" = (Class == "COPD" & Timepoint == "V4"),

  "COPD_V5" = (Class == "COPD" & Timepoint == "V5"),

  "Old_V1" = (Class == "Old" & Timepoint == "V1"),

  "Old_V2" = (Class == "Old" & Timepoint == "V2"),

  "Old_V3" = (Class == "Old" & Timepoint == "V3"),

  "Old_V4" = (Class == "Old" & Timepoint == "V4"),

  "Old_V5" = (Class == "Old" & Timepoint == "V5"),

  "Young_V1" = (Class == "Young" & Timepoint == "V1"),
```

```
  "Young_V2" = (Class == "Young" & Timepoint == "V2"),
  "Young_V3" = (Class == "Young" & Timepoint == "V3"),
  "Young_V4" = (Class == "Young" & Timepoint == "V4"),
  "Young_V5" = (Class == "Young" & Timepoint == "V5"),
  method = "first",
  .default = NA
)) #see limma user's guide section 9.6 and 9.7 for more details

all_data <- all_data %>%
  relocate(group_time, .after = Timepoint) #arrange columns so all metadata is at the
start of matrix

#create required inputs for lmmsDE function
dat <- all_data[,5:ncol(all_data)] #data matrix with each row representing an
experimental sample, and each column a single metabolite
#dat contains no metadata

group_time <- factor(all_data$group_time) #factor containing combined group and
time point
group_time <- group_time %>%
  fct_relevel("COPD_V1", "COPD_V2", "COPD_V3", "COPD_V4", "COPD_V5",
```

```
        "Old_V1", "Old_V2", "Old_V3", "Old_V4", "Old_V5",
        "Young_V1", "Young_V2", "Young_V3", "Young_V4", "Young_V5") #make
sure factor levels are in the right order
sampID <- as.character(all_data$Participant) #character vector containing the
sample names
class <- as.character(all_data$Class) #character vector indicating group of each
sample
namesMetab <- colnames(dat) #metabolite column names

#prepare for linear mixed model differential expression analysis using limma
#design group * time effect model
design <- model.matrix(~0+group_time)
colnames(design) <- levels(group_time)

#block subject specific variability (baseline differences between subjects)
dupcor <- duplicateCorrelation(t(dat), design, block=sampID)

#fit linear mixed effect model
fit <- lmFit(object = t(dat), design = design, block = sampID,
        correlation = dupcor$consensus.correlation)
fit <- eBayes(fit)
```

```
#make desired contrasts between experimental conditions

cmAllTime <- makeContrasts(V1_COPD_Old = COPD_V1 - Old_V1,

                           V2_COPD_Old = COPD_V2 - Old_V2,

                           V3_COPD_Old = COPD_V3 - Old_V3,

                           V4_COPD_Old = COPD_V4 - Old_V4,

                           V5_COPD_Old = COPD_V5 - Old_V5,

                           V1_Old_Young = Old_V1 - Young_V1,

                           V2_Old_Young = Old_V2 - Young_V2,

                           V3_Old_Young = Old_V3 - Young_V3,

                           V4_Old_Young = Old_V4 - Young_V4,

                           V5_Old_Young = Old_V5 - Young_V5,

                           V1_COPD_Young = COPD_V1 - Young_V1,

                           V5_COPD = COPD_V5 - COPD_V1,

                           V4_COPD = COPD_V4 - COPD_V1,

                           V3_COPD = COPD_V3 - COPD_V1,

                           V2_COPD = COPD_V2 - COPD_V1,

                           V5_Old = Old_V5 - Old_V1,

                           V4_Old = Old_V4 - Old_V1,

                           V3_Old = Old_V3 - Old_V1,
```

```
                V2_Old = Old_V2 - Old_V1,

                V5_Young = Young_V5 - Young_V1,

                V4_Young = Young_V4 - Young_V1,

                V3_Young = Young_V3 - Young_V1,

                V2_Young = Young_V2 - Young_V1,

                levels = design)


# store names of contrast in variable

contrastNames <- names(as.data.frame(cmAllTime))


# Then compute these contrasts and moderated t-tests

fitAllTime <- contrasts.fit(fit, cmAllTime)

fitAllTime <- eBayes(fitAllTime)


# pull out up and down expression summary data

dtAllTime  <- decideTests(fitAllTime)

dESumAllTime  <- summary(dtAllTime)


#create tables of differences
```

```
topMetab <- topTable(fitAllTimepoint, coef = 1, n = Inf, adjust.method = "BH")
#replace coefficient for desired comparisons


###METABOLITE IDENTIFICATION
#data in format of ID, m/z, rt
#load required packages
library(metid)
library(dplyr)


getwd()
setwd("C:/Users/mzxia1/Documents/COPD/metID”)
#annotate with multiple databases
#set parameters - MS1 databases
param1 <- identify_metabolites_params(ms1.match.ppm = 5,
                                      rt.match.tol = 1000000,
                                      polarity = "negative",
                                      column = "hilic",
                                      candidate.num = 1,
                                      database = "hmdb_ms1_database0.0.3")
param2 <- identify_metabolites_params(ms1.match.ppm = 5,
```

```
                        rt.match.tol = 1000000,

                        polarity = "negative",

                        column = "hilic",

                        candidate.num = 1,

                        database = "kegg_ms1_database0.0.3")

#MS2 databases

param3 <- identify_metabolites_params(ms1.match.ppm = 5,

                        rt.match.tol = 1000000,

                        polarity = "negative",

                        column = "hilic",

                        candidate.num = 1,

                        database = "hmdb_database0.0.3")

param4 <- identify_metabolites_params(ms1.match.ppm = 5,

                        rt.match.tol = 1000000,

                        polarity = "negative",

                        column = "hilic",

                        candidate.num = 1,

                        database = "massbank_database0.0.3")

param5 <- identify_metabolites_params(ms1.match.ppm = 5,

                        rt.match.tol = 1000000,
```

```
                        polarity = "negative",

                        column = "hilic",

                        candidate.num = 1,

                        database = "mona_database0.0.3")

param6 <- identify_metabolites_params(ms1.match.ppm = 5,

                        rt.match.tol = 1000000,

                        polarity = "negative",

                        column = "hilic",

                        candidate.num = 1,

                        database = "orbitrap_database0.0.3")



#metabolite identification using all parameters

result <- identify_metabolite_all(ms1.data = "metab_ms1.csv",

                    ms2.data = "PooledQC_MSn_3.mzXML",

                    parameter.list = c(param1, param2, param3,

                            param4, param5, param6),

                    path = ".")



#get identification tables for results where metabolites are annotated

table1 <- get_identification_table(result[[1]],
```

```
                        type = "new") #replace result[[x]] for each table


#remove nas from table

table1 <- table1 %>%

   filter(!is.na(Compound.name)) #replace table number as necessary


#if one peak has multiple annotations, we only want the one with highest confidence

table2 <- table2 %>%

  filter(!(name %in% table1$name)) #replace table2 number as necessary


#combine tables and export

annotation_table_all <- rbind(table1, table2, table3, table4, table5, table6)

write.csv(annotation_table_all, "metab_annotation.csv")



#WGCNA

#Exaple: Base in metab data vs Base in clinical data

####DATA INPUT AND CLEANING####

setwd("C:/Users/mzxia1/Documents/COPD/Updated analysis Oct

22/Correlation/WGCNA")#set working directory
```

```
#load required packages

library(WGCNA)

library(dplyr)

options(stringsAsFactors = FALSE)



metabData <- read.csv("metabdata_v1_hilicpos.csv")



#check what is in data set

dim(metabData)

names(metabData)



#remove auxillary data if necessary and transpose expression data for further

analysis

datExpr0 <- as.data.frame(t(metabData[,-1]))

names(datExpr0) <- metabData$FeatID



#check for missing values and identification of outlier samples

gsg <- goodSamplesGenes(datExpr0, verbose = 3)

gsg$allOK
```

```
#cluster the samples to see if there are any obvious outliers

sampleTree <- hclust(dist(datExpr0), method = "average")



#plot the sample tree

sizeGrWindow(12,9) #open graphic output window of 12 by 9 inches

par(cex = 0.6)

par(mar = c(0,4,2,0))

plot(sampleTree, main = "Sample clustering to detect outliers",

    sub="", xlab = "", cex.lab = 1.5, cex.axis = 1.5,

    cex.main = 2)



#based on graph, choose height cut that will remove the outlying samples

abline(h=4.1, col = "red") #plot line to show cut

clust <- cutreeStatic(sampleTree, cutHeight = 30, minSize = 3) #determine cluster
under line

table(clust) #clust 1 contains samples we want to keep

keepSamples <- (clust == 1)

datExpr <- datExpr0[keepSamples,]



nMetabs <- ncol(datExpr)
```

```
nSamples <- nrow(datExpr)

#variable datExpr now contains expression data for network analysis



#load clinical trait data

traitData <- read.csv("clinvars.csv")

traitData <- na.omit(traitData)

dim(traitData)

names(traitData)



#make sure only same subjects are used

keepmetabs <- rownames(datExpr)

traitData <- subset(traitData, SubjectID %in% keepmetabs)

keeprows <- traitData$SubjectID

datExpr <- as.data.frame(datExpr[which(rownames(datExpr) %in% keeprows),])



traitBase <- traitData[,c(1,3,6,9)]

colnames(traitBase)[2:7] <- c("TFM", "RER", "VO2")



#form dataframe analogous to expression data that will hold the clinical traits

metabSamples <- rownames(datExpr)
```

```
traitRowsBase <- match(metabSamples, traitData$Subject)

datBase <- traitBase[traitRowsBase,-1] #so only numeric values are left

rownames(datBase) <- traitBase[traitRowsBase, 1]



collectGarbage()



#re-cluster samples

sampleTree2 <- hclust(dist(datExpr), method = "average")

#convert traits to a colour representation: white means low, red means high, grey
means missing entry

traitColours <- numbers2colors(datBase, signed = FALSE)

#plot the sample dendogram and colours underneath

sizeGrWindow(12,9) #open graphic output window of 12 by 9 inches

par(cex = 0.6)

plotDendroAndColors(sampleTree2, traitColours,

                    groupLabels = names(datBase),

                    main ="Sample dendogram and trait heatmap")



####NETWORK CONSTRUCTION AND MODULE DETECTION####

#choose set of soft-threshold powers
```

```
powers <- c(c(1:10), seq(from=12, to=20, by=2))
#call network topology analysis function
sft <- pickSoftThreshold(datExpr, powerVector=powers, verbose=5)
#plot the results
sizeGrWindow(9,5)
par(mfrow =c(1,2))
cex1=0.9
#scale free topology fit index as a function of the soft-thresholding power
plot(sft$fitIndices[,1], -sign(sft$fitIndices[,3])*sft$fitIndices[,2],
    xlab="Soft Threshold (power)",ylab="Scale Free Topology Model Fit,signed
R^2",type="n",
    main = paste("Scale independence"))
text(sft$fitIndices[,1], -sign(sft$fitIndices[,3])*sft$fitIndices[,2],
    labels=powers,cex=cex1,col="red")
#this line corresponds to using an R2 cutoff of h
abline(h=0.9, col = "red")
#mean connectivity as a function of the soft-tresholding power
plot(sft$fitIndices[,1], sft$fitIndices[,5],
    xlab="Soft Threshold (power)",ylab="Mean Connectivity", type="n",
    main = paste("Mean connectivity"))
```

```
text(sft$fitIndices[,1], sft$fitIndices[,5], labels=powers, cex=cex1,col="red")

#choose the lowest power for which the scale-free topology fit index curve flattens
out upon reaching a high value


#co-expression similarity and adjacency

#calculate adjacncies using soft thresholding power

softPower <- 8

adjacency <- adjacency(datExpr, power = softPower)


#topology overlap matrix (TOM) to minimise effects of noise and spurious
associations

#turn adjacency into topology overlap

TOM <- TOMsimilarity(adjacency)

dissTom <- 1-TOM


#clustering using TOM

#use hierarchical clustering to produce dendogram of metabolites

#call clustering function

metabTree <- hclust(as.dist(dissTom), method ="average")

#plot resulting clustering tree

sizeGrWindow(12,9)
```

```
plot(metabTree, xlab = "", sub="", main = "Metabolite clustering on TOM-based
dissimilarity",
    labels = FALSE, hang = 0.04)


#to get large modules, set minimum module size relatively high
minModuleSize <- 30
#module identification using dynamic tree cut
dynamicMods <- cutreeDynamic(dendro=metabTree, distM = dissTom,
                    deepSplit=2, pamRespectsDendro = FALSE,
                    minClusterSize = minModuleSize)
table(dynamicMods)#returns modules labelled largest to smallest. 0 is unassigned
features


#plot the module assignment under the gene dendogram
dynamicColors <- labels2colors(dynamicMods)
table(dynamicColors)
#plot the dendogram and colours underneath
sizeGrWindow(8,6)
plotDendroAndColors(metabTree, dynamicColors, "Dynamic Tree Cut",
            dendroLabels = FALSE, hang = 0.03,
            addGuide = TRUE, guideHang = 0.05,
```

```
                    main = "Metabolite dendrogram and module colors")


#merging of modules whose expression profiles are very similar

#calculate eigengenes

MEList <- moduleEigengenes(datExpr, colors = dynamicColors)

MEs <- MEList$eigengenes

#calculate dissimilarity of module eigengenes

MEDiss <- 1-cor(MEs)

#cluster module eigengenes

METree <- hclust(as.dist(MEDiss), method = "average")

#plot the results

sizeGrWindow(7,6)

plot(METree, main = "Clustering of module eigengenes",

    xlab = "", sub = "")


#here, choose a height cut of 0.3, corresponding to correlation of 0.7, to merge

MEDissThres <- 0.3

#plot the cut line into the dendogram

abline(h=MEDissThres, col = "red")

#call automatic merging function
```

```
merge <- mergeCloseModules(datExpr, dynamicColors, cutHeight = MEDissThres,
                           verbose = 3)
#get merged module colours
mergedColours <- merge$colors
#eigengenes of the new merged modules
mergedMEs <- merge$newMEs


#plot dendogram again with original and merged module colours underneath
sizeGrWindow(12,9)
plotDendroAndColors(metabTree, cbind(dynamicColors, mergedColours),
                    c("Dynamic Tree Cut", "Merged dynamic"),
                    dendroLabels = FALSE, hang = 0.03,
                    addGuide = TRUE, guideHang = 0.05)


#rename to moduleColours
moduleColours <- mergedColours
#construct numerical labels corresponding to the colours
colourOrder <- c("grey", standardColors())
moduleLabels <- match(moduleColours, colourOrder)-1
MEs <- mergedMEs
```

```
####RELATING MODULES TO EXTERNAL INFORMATION AND IDENTIFYING
IMPORTANT METABOLITES####

#quantify module-trait associations

#define numbers of genes and samples

#nMetabs <- ncol(datExpr)

#nSamples <- nrow(datExpr)



#recalculate MEs with colour labels

MEs0 <- moduleEigengenes(datExpr, moduleColours)$eigengenes

MEs <- orderMEs(MEs0)

moduleTraitCor <- cor(MEs, datBase, use = "p")

moduleTraitPvalue <- corPvalueStudent(moduleTraitCor, nSamples)



#colour code each association by the correlation value

sizeGrWindow(20,6)

# Will display correlations and their p-values

textMatrix = paste(signif(moduleTraitCor, 2), "\n(",

                   signif(moduleTraitPvalue, 1), ")", sep = "");

dim(textMatrix) = dim(moduleTraitCor)
```

```
par(mar = c(6, 8.5, 3, 3))

# Display the correlation values within a heatmap plot

labeledHeatmap(Matrix = moduleTraitCor,

               xLabels = names(datBase),

               yLabels = names(MEs),

               ySymbols = names(MEs),

               colorLabels = FALSE,

               colors = blueWhiteRed(50),

               textMatrix = textMatrix,

               setStdMargins = FALSE,

               cex.text = 0.5,

               zlim = c(-1,1),

               main = paste("Module-trait relationships"))



#metabolite relationship to trait and important modules quantify associations of

#individual features with trait of interest by defining metabolite significance as the

#absolute value of the correlation between the gene and the trait

#also, define a quantitative measure of module membership as correlation of

#module

#eigengene and metabolite expression profile

tfm <- as.data.frame(datBase$TFM)
```

```
names(tfm) <- "tfm"


rer <- as.data.frame(datBase$RER)
names(rer) <- "rer"


vo2 <- as.data.frame(datBase$VO2)
names(vo2) <- "vo2"


# names (colors) of the modules
modNames <-  substring(names(MEs), 3)
metabModuleMembership <- as.data.frame(cor(datExpr, MEs, use = "p"));
MMPvalue <-
as.data.frame(corPvalueStudent(as.matrix(metabModuleMembership), nSamples))
names(metabModuleMembership) = paste("MM", modNames, sep="");
names(MMPvalue) <-  paste("p.MM", modNames, sep="");


#first trait
metabTraitSignificance <-  as.data.frame(cor(datExpr, vo2, use = "p"));
MSPvalue <-  as.data.frame(corPvalueStudent(as.matrix(metabTraitSignificance),
nSamples));
names(metabTraitSignificance) <-  paste("MS.", names(vo2), sep="");
```

```
names(MSPvalue) <-  paste("p.MS.", names(vo2), sep="")

#second trait

metabTraitSignificance2 <-  as.data.frame(cor(datExpr, rer, use = "p"));

MSPvalue2 <-  as.data.frame(corPvalueStudent(as.matrix(metabTraitSignificance2),
nSamples));

names(metabTraitSignificance2) <-  paste("MS.", names(rer), sep="");

names(MSPvalue2) <-  paste("p.MS.", names(rer), sep="")

#third trait

metabTraitSignificance3 <-  as.data.frame(cor(datExpr, tfm, use = "p"));

MSPvalue3 <-  as.data.frame(corPvalueStudent(as.matrix(metabTraitSignificance6),
nSamples));

names(metabTraitSignificance3) <-  paste("MS.", names(tfm), sep="");

names(MSPvalue3) <-  paste("p.MS.", names(tfm), sep="")




#identify genes with high GS and MM

module <- "grey" #find module with high association

column <- match(module, modNames)

moduleMetabs <- moduleColours == module



sizeGrWindow(7,7)
```

```
par(mfrow = c(1,1))

verboseScatterplot(abs(metabModuleMembership[moduleMetabs, column]),

                   abs(metabTraitSignificance[moduleMetabs, 1]),

                   xlab = paste("Module Membership in", module, "module"),

                   ylab = "Metabolite significance for Base in peak oxygen uptake",

                   main = paste("Module membership vs. metabolite significance\n"),

                   cex.main = 1.2, cex.lab = 1.2, cex.axis = 1.2, col = module)

#summary output of network analysis results

#create dataframe

metabInfo0 <- data.frame(featID = metabData$FeatID,

                         moduleColor = moduleColours,

                         metabTraitSignificance,

                         MSPvalue,

                         metabTraitSignificance2,

                         MSPvalue2,

                         metabTraitSignificance3,

                         MSPvalue3)

#order modules by significance for trait

modOrder <- order(-abs(cor(MEs, vo2, use="p")))

#add module membership information in the chosen order
```

```
for (mod in 1:ncol(metabModuleMembership)){
  oldNames = names(metabInfo0)
  metabInfo0 = data.frame(metabInfo0, metabModuleMembership[,
modOrder[mod]],
                          MMPvalue[, modOrder[mod]]);
  names(metabInfo0) = c(oldNames, paste("MM.", modNames[modOrder[mod]],
sep=""),
                        paste("p.MM.", modNames[modOrder[mod]], sep=""))
}
#order metabolites in Info variable by module colour, then by TraitSignificance
metabOrder <- order(metabInfo0$moduleColor, -abs(metabInfo0$MS.vo2))
metabInfo <- metabInfo0[metabOrder,]
#write as spreadsheet
write.csv(metabInfo, file = "metabInfo_HILICpos_base.csv")
```

Appendix 4. Chromatograms

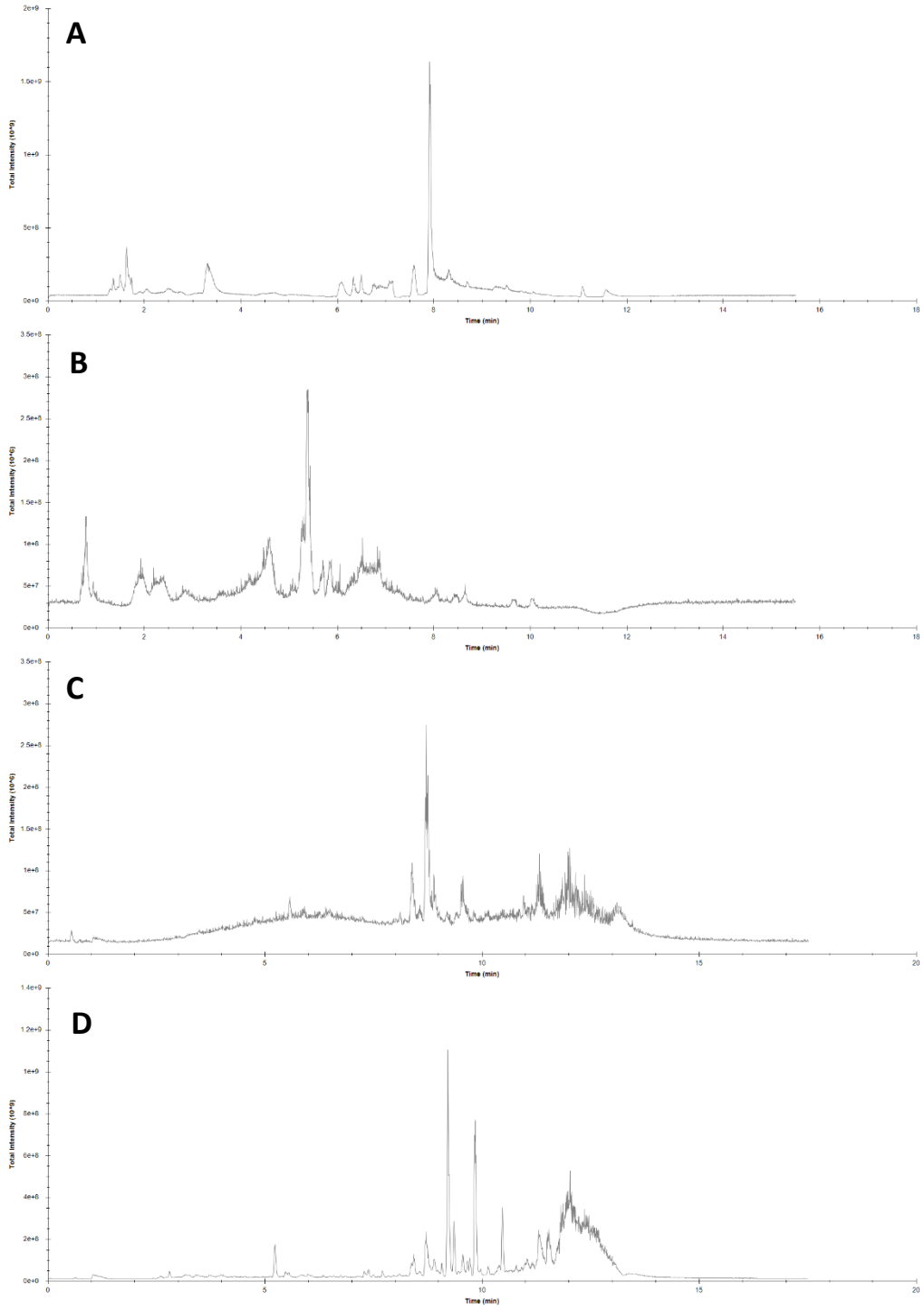

Supplementary Figure 1 Example chromatograms

Representative examples of chromatograms obtained by UHPLC-MS/MS operated in the (A) polar negative, (B) polar positive, (C) non-polar negative, and (D) non-polar positive mode.